Norwegian University of Life Sciences
Faculty of Science and Technology

Philosophiae Doctor (PhD)
Thesis 2018:20

High-throughput screening of filamentous fungi for single cell oil production by microplate cultivation and FTIR spectroscopy

High-throughput screening av mugg for oljeproduksjon ved kultivering på mikrotiterplater og FTIR-spektroskopi

Gergely Kósa

High-throughput screening of filamentous fungi for single cell oil production by microplate cultivation and FTIR spectroscopy

High-throughput screening av mugg for oljeproduksjon ved kultivering på mikrotiterplater og FTIR-spektroskopi

Philosophiae Doctor (PhD) Thesis

Gergely Kósa

Norwegian University of Life Sciences

Faculty of Science and Technology

Ås 2017

Thesis number 2018:20

ISSN 1894-6402

ISBN 978-82-575-1500-3

Doctoral thesis

Defended on 9th of March 2018

Main supervisor: Prof. Dr. Achim Kohler, Norwegian University of Life Sciences

Co-supervisors: Prof. Dr. Yngve Stenstrøm, Norwegian University of Life Sciences

Prof. Dr. Svein Jarle Horn, Norwegian University of Life Sciences

Assoc Prof. Dr. Volha Shapaval, Norwegian University of Life Sciences

Examination committee: Prof. Dr. Ganesh D Sockalingum, Université de Reims Champagne-Ardenne

Prof. Dr. Ivana Márová, Brno University of Technology

Prof. Dr. Jorge Mario Marchetti, Norwegian University of Life Sciences

Acknowledgements

The work presented in this thesis was carried out from 2014 September to 2017 December at the Norwegian University of Life Sciences (NMBU), Faculty of Science and Technology (RealTek), in the research group Biospectroscopy and Data Modelling, in collaboration with the Faculty of Chemistry, Biotechnology and Food Science (KBM), and the Norwegian Institute of Food, Fisheries and Aquaculture (Nofima AS) in Ås, Norway. The work was partially funded by the Norwegian Research Council.

First of all, I would like to thank my main supervisor Achim Kohler and co-supervisor Volha Shapaval for giving me the opportunity to start my PhD and for their guidance throughout the past 3.5 years. I am also very thankful to Boris Zimmermann for helping me in many areas during my PhD studies, including FTIR spectroscopy, data analysis and in general academic research related issues. Many thanks for Rozalia Lukacs and her husband Ferenc, who helped me in important practical issues when we arrived in Norway and because they took care of my daughter several times when I was busy with experiments. I appreciate the good time we spent together with Murat Bagciouglu and Mangesh Ramesh Avhad, and the discussions on Skype after they finished their PhD. It was also nice to have casual talks with my office mates, Maren Anna Brandsrud, Eivind Seim, Aurora Rosvoll Grøndahl and Johanne Heitmann Solheim. I also acknowledge the help and efforts of Berit Hauger Lindstad to make mine and future PhD students' life better. My gratitude goes to Nils Kristian Afseth from Nofima for all the enjoyable discussions and for letting me extend my stay at Nofima and finish experimental work. I also have to say thanks to Dimitrious Tzimorotas, John-Erik Haugen and Elin Merete Wetterhus for their suggestions and technical help with GC-FID measurements. My gratitude goes to my co-supervisor Svein Jarle Horn for being able to use the infrastructure of Bioprocess Technology and Biorefining (BTB) group. I really appreciate Dag Ekeberg's time and expertise in GC-MS measurements and for being available to discuss measurement results whenever I needed. Thanks go to Kiira Vuoristo and Line Degn Hansen for their contribution in fermentation experiments and to Aniko Varnai for her help with HPLC measurement.

Last, but not least, many thanks to my family to be with me on this journey. Andrea, Veronika, had infinite patience toward me during difficult periods. My mother also visited us on several occasions making it possible to go on holidays and finishing PhD. Without the support, encouragement, and love of my family, I could have never finished this work.

Abstract

Microorganisms have been considered for nearly a century for the production of economical and useful oils, but only in the past two or three decades they have been used commercially. These single cell oils contain high amount of polyunsaturated fatty acids (PUFA), mainly for human consumption as infant formulas and dietary supplements, although some are used for feeding farmed fish, poultry, and pigs. PUFA are critical nutrients for the prevention of several diseases, such as cardiovascular disease, diabetes, and cancer. Moreover, they contribute to the health of brain and eye. Production of the high-value PUFAs is based on the heterotrophic cultivation (usually on glucose) of various fungi and marine microorganisms. Another emerging application field of microbial oils is the production of biodiesel. Lately, there has been serious concern about first-generation biodiesel (from palm oil, rapeseed oil etc.) because of the food versus fuel debate, while second-generation biodiesel (non-edible plants, waste oil, and animal fat) might not be enough to completely substitute crude oil. Therefore, there is a rapidly-growing interest in microbial oils as sources of third-generation biodiesel. Yeast and fungi are especially interesting because they can grow on cheap substrates, such as raw glycerol or lignocellulosic waste, contributing to the development of an economically sound alternative to fossil fuels.

Establishment of a single cell oil bioprocess starts with the screening for promising production strains with high lipid yield and the desired fatty acid composition. Due to advances in molecular biology, the number of candidate strains can far exceed what is feasible with traditional shake flask approach, therefore high-throughput microtiter plate cultivation is necessary. It is also required to apply rapid, high-throughput analytical technique for the measurement of intracellular lipids. Gas chromatography-flame ionization detector (GC-FID) and gas chromatography-mass spectrometry (GC-MS) represent the typical techniques to analyze the amount and profile of fatty acids of microorganisms. However, these methods require energy-intensive and tedious procedures such as cell disruption, lipid extraction, and transesterification and thus are less applicable for high-throughput screening applications. Fourier transform infrared spectroscopy (FTIR) is a powerful, non-disruptive and high-throughput technique for measuring the chemical composition of very complex samples, such as microorganisms.

In this thesis, we investigated the screening of filamentous fungi for single cell oil production by a combined cultivation-analytical approach consisting of microtiter plate cultivation and FTIR spectroscopy. In **Paper I**, we demonstrated that highly reproducible cultivation of filamentous fungi can be achieved in the Duetz-microtiter plate system (Duetz-MTPS). We also showed that temporal changes of lipid content could be easily followed by examining of specific peaks in the FTIR spectra of fungal biomass, while for the prediction of fatty acid composition multivariate regression (PLSR) between FTIR and GC data was applied. Fatty acid groups (SAT, MUFA, PUFA), unsaturation index and main fatty acids were predicted with high precision. In **Paper II** we demonstrated that high-throughput FTIR spectroscopy can also be used to quantify substrate consumption and for the detection and quantification of extracellular metabolites in microbial screenings. Scalability of the deep-well plate cultivations to controlled stirred tank benchtop and pre-pilot scale bioreactors was

demonstrated in **Paper III**. Finally, in **Paper IV** we screened one hundred Mucoromycota fungi for single cell oil production in the established high-throughput cultivation-analytical system. Several promising strains, with high lipid content and fatty acid composition that is suitable for high-value PUFA and biodiesel production have been identified.

Based on these results, we have concluded that the Duetz-MTPS coupled with FTIR spectroscopy and multivariate data analysis, is a suitable low-cost and high-throughput platform for the screening of filamentous fungi for single cell oil production. Automation of sample preparation for FTIR spectroscopy is foreseen in the near future, in order to develop an integrated high-throughput approach for the screening of various microorganisms.

Norsk sammendrag

Mikroorganismer har i nesten et århundre blitt vurdert for produksjon av nyttige og økonomisk gunstige oljer. Men bare de siste to-tre tiårene har de blitt brukt kommersielt. Disse oljene inneholder en høy mengde flerumettede fettsyrer (PUFA), og har hovedsakelig blitt brukt til konsum som barnemat og kosttilskudd. Også noe brukes til fôring av oppdrettsfisk, fjærfe og griser. PUFA er et viktig næringsstoff for å forebygge flere sykdommer, for eksempel kardiovaskulære sykdommer, diabetes og kreft. Videre er også PUFA gunstige for hjerne og øyne. Produksjon av høyverdige PUFAer som er basert på heterotrofisk dyrking (vanligvis glukose) av ulike sopp og marine mikroorganismer. Et annet voksende bruksområde for mikrobielle oljer er produksjonen av biodiesel. Den siste tiden har de vært uttrykt bekymring rundt førstegenerasjons biodiesel (fra palmeolje, rapsolje etc.) på grunn av matressursene som denne produksjonen begrenser. Andre generasjon biodiesel (ikke spiselige planter, avfallsolje og animalsk fett) har ikke hatt potensiale til å erstatte fossil råolje full ut. Derfor er det en raskt voksende interesse for mikrobielle oljer som kilder til tredje generasjons biodiesel. Gjær og sopp er spesielt interessante siden disse kan vokse på billige substrater som rå glyserol eller lignocelluloseavfall. Dette er noe som bidrar til utviklingen av et økonomisk forsvarlig alternativ til fossile brensler.

Etablering av en bioprosess for produksjon av olje fra enkeltceller starter med en screening. Dette for å finne lovende produksjonsstammer med høyt lipidutbytte og den ønskede fettsyrekomposisjonen. På grunn av fremgangen innenfor molekylærbiologi, kan antall kandidatstammer langt overstige det som er mulig med tradisjonell rystekolbetilnærming. Derfor er det nødvendig med high-throughput kultivering på mikrotiterplater. Det er også nødvendig å anvende en hurtig, high-throughput analyseteknikk for måling av intracellulære lipider. Gasskromatografi med flammeioniseringsdetektor (GC-FID) og gasskromatografi med massespektrometri (GC-MS) representerer de tradisjonelle teknikkene for å analysere mengden og profilen til fettsyrene i mikroorganismer. Imidlertid er disse metodene energiintensive og tidkrevende prosedyrer som krever for eksempel cellebearbeidelse, lipidekstraksjon og transesterifisering. Dette er dermed mindre anvendbart for innenfor high-throughput screening. FTIR-spektroskopi (Fourier Transform Infrared Spectroscopy) er en kraftig og ikke-destruktiv med high-throughput for måling av den kjemiske sammensetning i svært komplekse prøver, som mikroorganismer.

I denne avhandlingen undersøkte vi screeningen av filamentøs sopp for oljeproduksjon ved en kombinert dyrkningsanalytisk tilnærming bestående av kultivering på mikrotiterplater og FTIR-spektroskopi. **Artikkel I** demonstrerte vi at høyt reproduserbar dyrking av filamentøs sopp kan oppnås i Duetz-mikrotiterplatesystem (Duetz-MTPS). Vi viste også at tidsmessige endringer i lipidinnholdet lett kunne følges ved å undersøke spesifikke topper i FTIR-spektrene fra soppbiomasse, mens vi kunne predikerte fettsyresammensetningen ved hjelp av multivariat regresjon (PLSR) mellom FTIR- og GC-data. Fettsyregruppene (SAT, MUFA, PUFA), grad av umettethet og hovedinnhold av fettsyrer ble spådd med høy presisjon. **Artikkel II** viste at high-throughput FTIR-spektroskopi også kan brukes til å kvantifisere i substratforbruk. Også for **deteksjon** og kvantifisering av ekstracellulære metabolitter i mikrobiell screening. Skalerbarhet ved

dyrkning i mikrotiterplater for en småskala bioreaktor og et pilotsystem ble demonstrert i **Artikkel III**. Til slutt, i **Artikkel IV**, undersøkte vi hundre Mucoromycota sopp for oljeproduksjon og det ble etablert et high-throughput dyrknings- og analysesystem. Flere lovende stammer, med høyt lipidinnhold og fettsyrekomposisjon som er egnet for høyverdig PUFA- og biodieselproduksjon, er identifisert.

Basert på disse resultatene har vi konkludert med at Duetz-MTPS kombinert med FTIR-spektroskopi og multivariate dataanalyser, er en egnet lavkostnads og high-throughput screening av filamentøs sopp for oljeproduksjon. Automatisering av prøvetillaging for FTIR-spektroskopi er planlagt i nær fremtid. Dette for å utvikle en integrert high-throughput screening av ulike mikroorganismer.

List of papers

Paper I

Kosa, Gergely; Kohler, Achim; Tafintseva, Valeria; Zimmermann, Boris; Forfang, Kristin; Afseth, Nils Kristian; Tzimorotas, Dimitrios; Vuoristo, Kiira; Horn, Svein Jarle; Mounier, Jerome; Shapaval, Volha. **Microtiter plate cultivation of oleaginous fungi and monitoring of lipogenesis by high-throughput FTIR spectroscopy**. *Microbial Cell Factories* 2017; Volume 16(1), p. 101.

Paper II

Kosa, Gergely; Shapaval, Volha; Kohler, Achim; Zimmermann, Boris. **FTIR spectroscopy as a unified method for simultaneous analysis of intra- and extracellular metabolites in high-throughput screening of microbial bioprocesses** *Microbial Cell Factories* 2017, Volume 16(1), p. 195.

Paper III

Kosa, Gergely; Vuoristo, Kiira; Horn, Svein Jarle; Zimmermann, Boris; Afseth, Nils Kristian; Kohler, Achim; Shapaval, Volha. **Scalability of oleaginous filamentous fungi and microalga cultivations from microtiter plate system to controlled stirred-tank bioreactors** (submitted) 2017

Paper IV

Kosa, Gergely; Kohler, Achim; Zimmermann, Boris; Afseth, Nils Kristian; Ekeberg, Dag; Mounier, Jerome; Shapaval, Volha. **High-throughput screening of Mucoromycota strains for single cell oil production** (Manuscript in preparation) 2017

Additional scientific contributions

Research publications

Forfang, Kristin; Zimmermann, Boris; Kosa, Gergely; Kohler, Achim; Shapaval, Volha. **FTIR spectroscopy for evaluation and monitoring of lipid extraction efficiency for oleaginous fungi**. PLoS ONE 2017; 12(1), p.e0170611.

Presentations

2017

1. Eymard, Julie Christine; Dzurendová, Simona; Kosa, Gergely; Tafintseva, Valeria; Zimmermann, Boris; Kohler, Achim; Shapaval, Volha. **FTIR spectroscopy for high-throughput screening and monitoring of Single Cell Oil production**. FTIR Spectroscopy in Microbiological and Medical Diagnostics Workshop, 19-20th October 2017, Robert-Koch Institute, Berlin, Germany

2. Shapaval, Volha; Kosa, Gergely; Zimmermann, Boris; Tafintseva, Valeria; Hovde Liland, Kristian; Forfang, Kristin; Afseth, Nils Kristian; Kohler, Achim. **FTIR spectroscopy for analyzing lipids in microbial cells**. FTIR Spectroscopy in Microbiological and Medical Diagnostics Workshop, 19-20th October 2017, Robert-Koch Institute, Berlin, Germany

3. Kosa, Gergely; Zimmermann, Boris; Ekeberg, Dag; Afseth, Nils Kristian; Kohler, Achim; Shapaval, Volha. **High-throughput screening of Mucoromycota fungi for Single Cell Oil production**. BioTech 2017 and 7th Czech-Swiss Symposium, 13-17th June 2017, Prague, Czech Republic

4. Shapaval, Volha; Kosa, Gergely; Zimmermann, Boris; Tafintseva, Valeria; Bernatova, Silvie; Samek, Ota; Kohler, Achim. **Vibrational spectroscopy for monitoring lipogenesis in microbial cells**. BioTech 2017 and 7th Czech-Swiss Symposium, 13-17th June 2017, Prague, Czech Republic

5. Shapaval, Volha; Tafintseva, Valeria; Zimmermann, Boris; Kosa, Gergely; Forfang, Kristin; Bernatova, Silvie; Samek, Ota; Kohler, Achim. **Vibrational spectroscopy for rapid, non-destructive and high-throughput analysis of lipids in microbial cells**. 13th Yeast Lipid Conference, 17-19th May 2017, Paris, France

2016

1. Kosa, Gergely; Tafintseva, Valeria; Zimmermann, Boris; Kohler, Achim; Shapaval, Volha. **Micro-cultivation of oleaginous fungi and high-throughput estimation of fatty acid profiles by FTIR spectroscopy**. European symposium on Biochemical engineering sciences (ESBES), 11-14th September 2016, Dublin, Ireland

2. Shapaval, Volha; Kosa, Gergely; Tafintseva, Valeria; Forfang, Kristin; Zimmermann, Boris; Kohler, Achim. **FTIR spectroscopy coupled with high-throughput micro-cultivation for the screening in microbial biotechnology**. 43rd Annual Conference on Yeast, 2-5th May 2016, Smolenice, Slovakia

3. Kosa, Gergely; Tafintseva, Valeria; Zimmermann, Boris; Shapaval, Volha; Kohler, Achim. **Microcultivation of Oleaginous Fungi and High-throughput Estimation of Fatty Acid Profiles by FTIR Spectroscopy**, Copenhagen School of Chemometrics 2016, 18th April-20th May 2016, University of Copenhagen, Denmark

2015

1. Kosa, Gergely; Shapaval, Volha; Kohler, Achim; Tafintseva, Valeria; Zimmermann, Boris. **HTP cultivation and measurement of SCO - PUFA production by oleaginous fungi**. Industrial mycology PhD course; 30th November – 4th December 2015, DTU, Lyngby, Denmark

2. Kosa, Gergely; Tafintseva, Valeria; Shapaval, Volha; Kohler, Achim. **Micro-cultivation of oleaginous fungi and high-throughput estimation of fatty acid profiles by FT-IR spectroscopy**. FT-IR Spectroscopy in Microbiological and Medical Diagnostics Workshop; October 15-16th 2015, Robert-Koch Institute, Berlin, Germany

3. Afseth, Nils Kristian; Måge, Ingrid; Pilat, Z; Böcker, Ulrike; Wold, Jens Petter; Shapaval, Volha; Bernatova, S; Tzimorotas, Dimitrios; Kosa, Gergely; Samek, O. **Towards quantitative lipid characterization in cellular matrices using Raman microspectroscopy?** SCIX 2015; 17th September-2th October 2015, Providence, RI, USA

Abbreviations

ALA	α-linolenic acid
ARA	arachidonic acid
ATR	attenuated total reflection
DGLA	dihomo-γ-linolenic acid
DHA	docosahexaenoic acid
EMSC	extended multiplicative signal correction
EPA	eicosapentaenoic acid
FA	fatty acid
FAME	fatty acid methyl ester
FTIR	Fourier-transform infrared spectroscopy
GLA	γ-linolenic acid
HTS	high-throughput screening
MTPS	microtiter plate system
MUFA	monounsaturated fatty acid
PCA	principal component analysis
PLSR	partial least squares regression
PUFA	polyunsaturated fatty acid
SAT	saturated fatty acid
SCO	single cell oil
TAG	triacylglycerol

Table of Contents

Aims of the thesis

The general aim of the thesis was the development and application of a high-throughput screening system for oleaginous filamentous fungi. This was achieved by combining microtiter plate cultivation and high-throughput FTIR spectroscopy. The main aim was divided into the following sub-goals:

- To test the suitability of the Duetz-microtiter plate system combined with high-throughput FTIR spectroscopy of biomass for fast screening of oleaginous fungi (**Paper I**)

- To assess high-throughput FTIR spectroscopy as a unified analytical method for the measurement of intra- and extracellular compounds in microbial screening (**Paper II**)

- To study the scalability of microplate cultivated oleaginous filamentous fungi and microalga to controlled benchtop and pre-pilot scale stirred-tank bioreactors (**Paper III**)

- To screen one hundred Mucoromycota filamentous fungi for single cell oil production in the developed high-throughput cultivation-analytical platform (**Paper IV**)

1 Introduction

1.1 Microbial lipid accumulation

In general, the microbial lipid accumulation process is based on the cultivation of an organism in excess of carbon source and under the limitation of nitrogen source. Phosphorous or sulfur limitation can have a similar effect, but nitrogen limitation is the most efficient [2]. When all necessary nutrients are present (C, H, N, O, P, S etc.) the microorganism can grow exponentially (trophophase or balanced growth phase). During this phase the carbon flux is distributed for the anabolic processes yielding carbohydrates, lipids (mainly polar, structural lipids such as sphingo- and phospholipids), nucleic acids and proteins. When nitrogen becomes depleted cells remain viable, but cannot multiply anymore (idiophase) since nitrogen is part of proteins and nucleic acids (Figure 1.1). The carbon excess in non-oleaginous species remains unutilized or it is converted into polysaccharides, while in oleaginous species the carbon is channeled toward lipid biosynthesis, resulting in the accumulation of triacylglycerol (TAG) in intracellular lipid bodies [2].

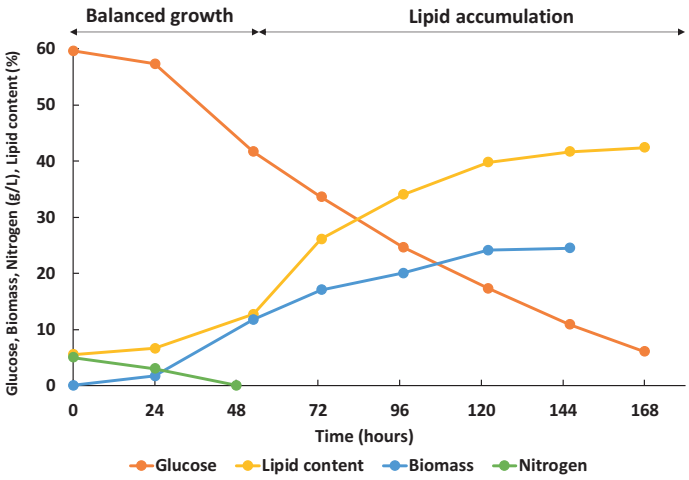

Figure 1.1 Time course of batch fermentation in microbial production of lipids (data is derived from **Paper III** in this thesis)

Microbial or single cell oil (SCO) offers several advantages when compared to animal or plant sources. First, the production capacity is higher: in plants, the lipid content is maximum 50%, while in microorganism it can be as high as 87% [3]. Secondly, microbial oils can be extracted regardless of geographical and climatic conditions - a plant is subject to bad weather, while a microorganism can be easily manipulated in a controlled environment.

Finally, the production of single cell oil requires less space, productivity is higher, and several substrates, including industrial wastes, and by-products can be utilized [4, 5].

1.2 The biochemistry of lipid accumulation in oleaginous microorganisms

Microorganisms, which have the ability to accumulate a significant amount of lipids (i.e. >20% w/w, on dry cell basis) are called oleaginous [1]. When nitrogen becomes depleted in oleaginous microorganisms the activity of adenosine monophosphate (AMP) deaminase enzyme increases approx. by a factor five in order to supply ammonium for the cells, and consequently the level of AMP decreases (Figure 1.2). The low level of AMP causes isocitrate dehydrogenase enzyme activity to drop and the citric acid (Krebs) cycle is blocked. Citrate starts to accumulate in the mitochondrion, and it is therefore exported to the cytosol. The citrate is cleaved by key-enzyme cytosolic ATP-citrate lyase (ACL) to acetyl-CoA and oxaloacetate. Acetyl-CoA is used for fatty acid (FA) biosynthesis, while oxaloacetate is converted to malate by malate dehydrogenase (MDH). The malate is a counter-ion in the citrate efflux system. For the synthesis of highly reduced fatty acids reductant agent is also necessary. More specifically, CH_3COO^- acetate has to be reduced to $–CH_2CH_2–$ units in order to create the fatty acid chain. For example, 16 moles of NADPH is needed for the synthesis of stearic acid (C18) [5]. The reductant nicotinamide adenine dinucleotide phosphate (NADPH) is provided by the malic enzyme (ME). ACL and ME enzymes thought to be physically attached to the fatty acid synthase (FAS) protein [6]. The main function of FAS is to catalyze the synthesis of palmitate (C16:0, a long-chain saturated fatty acid) from acetyl-CoA and malonyl-CoA, in the presence of NADPH. The fatty acids are esterified with glycerol into triacylglycerol (TAG) in the endoplasmic reticulum into fatty acid droplets (cells become ‘obese’). Other lipid compounds include free fatty acids, neutral lipids (such as monoacylglycerols, diacylglycerols, and steryl-esters), sterols and structural membrane components (polar fractions, e.g. phospholipids, sphingolipids, glycolipids) [7]. If cells are starving, then the reserved material (TAG) in the cells will be mobilized as a source of carbon and energy.

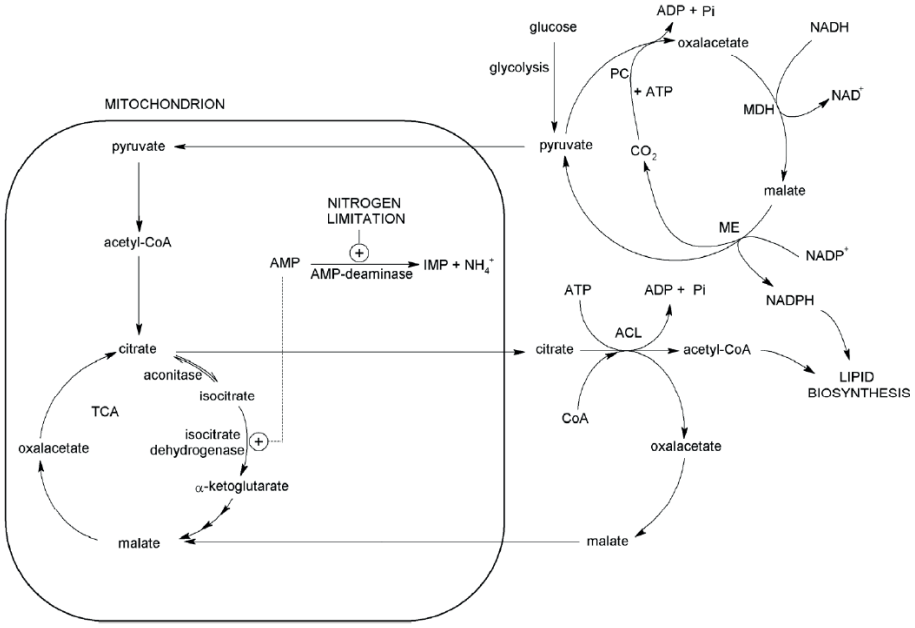

Figure 1.2 Lipid biosynthesis from excess of citrate as a consequence of nitrogen limitation. Adapted by Rossi *et al.*, 2011 [2] from Ratledge, 2004 [8]

Since the ACL enzyme complex does not exist in non-oleaginous species, in case of nitrogen limitation the accumulated citric acid will be excreted or will lead to polysaccharide (glycogen, glucans, mannans) accumulation. Bacteria, in general, do not produce triacylglycerols, but produce poly-β-hydroxybutyrates and -alkanoates as storage polymers [8].

Studies indicate that the maximum content of lipid is species dependent. Some microorganisms are able to accumulate 70% to 80% of their biomass as lipids, while others have a much lower limit (Table 1.1). It is likely that the gene that regulates the synthesis of malic enzyme (ME) controls the maximum lipid content. In some species the synthesis of ME is switched off shortly after nitrogen exhaustion, therefore NADPH is not available for fatty acid synthesis [8].

When the growth of microorganisms is carried out on hydrophobic substrates (i.e. oils and fats) the process is called *ex novo* lipid accumulation. Lipid accumulation from hydrophobic substrates is a growth-associated process, and in contrast to the *de novo* process described above, it is independent of nitrogen exhaustion from the medium. Cells produce extracellular lipase enzymes in order to break down TAGs to fatty acids and glycerol, which can be transported inside the cells. Fatty acids are then either used for growth needs, or they serve as a substrate for intracellular biotransformations. Fatty acids with different profiles (in both extra- and intracellular lipids), that did not previously exist in the medium, can be produced [7].

Table 1.1 Oil content of some microorganisms

Species	Culture conditions	Lipid content (%DW)	Reference
Microalgae			
Chlorella sp.	Phototrophic	33-66	[9]
Dunaliella sp.	Phototrophic	12-30	[10]
Neochloris oleabundans UTEX #1185	Phototrophic	19-56	[11]
Crypthecodinium cohnii	Ethanol	40	[12]
S. limacinum SR 21	Glycerol/Glucose	70	[13]
Yeasts			
Lipomyces starkeyi	Glucose and xylose	61	[14]
Rhodosporidium toruloides Y4	Glucose (fed-batch)	68	[15]
Trichosporon fermentans	Glucose	62	[16]
Cryptococcus curvatus	Glycerol	25	[17]
Yarrowia lipolytica	Stearin	52	[18]
Filamentous fungi (molds)			
Cunninghamella echinulata	Xylose	58	[19]
Aspergillus oryzae A-4	Cellulose	18	[20]
Mortierella alpina	Glucose	55	[21]
Mucor circinelloides WJ11	Glucose	36	[22]
Mortierella isabellina	Glucose	50-55	[23]
Rhizopus stolonifer LGAM (9)1	Glucose	28	[24]
Bacteria			
Acinetobacter baylyi ADP1(mutant)	Sodium gluconate and glycerol	12	[25]
Nocardia globerula 432	Pristine and acetate	50	[26]
Streptomyces coelicolor TR0958 (mutant)	Glucose	83	[27]

1.3 PUFA synthesis in microorganisms

After the synthesis of palmitic acid (C16:0) or oleic acid (C18:0) by FAS, the carbon chain is further elongated and desaturated by different enzymes (Figure 1.3). Fatty acid desaturase enzymes (FADs) insert double bonds at specific locations in the fatty acid carbon chain while elongase enzymes extend the chain in two-carbon increments [28]. The fatty acids, which are produced in the highest abundance is dependent on the genetic make-up of the species. Mammals (including humans) lack delta-12 and delta-15 desaturase enzymes, making linolenic acid (LA) and α-linolenic acid (C18:3n3, ALA) dietary essential fatty acids [29]. PUFA synthesis from LA and ALA by FADs in human results with only a small proportion of C20 PUFAs with more than 4 double bonds, meaning that EPA and DHA are conditionally essential fatty acids. More specifically, it was found that only 5-10% of C18 FAs are converted to EPA and less than one percent of ALA is transformed to DHA in the human body [29]. In yeasts, oleic (C18:1), linoleic (C18:2), palmitic (C16:0) and palmitoleic (C16:1) are the main fatty acids. If produced, the content of ALA usually does not exceed 10%. Plants also do not produce longer than C18 PUFAs (long-chain PUFAs, LCPUFAs). Only in fungi and microalga the amount of polyunsaturated fatty acids (PUFA) are above 20%. Therefore, most attention is given to these organisms for the production of high-value nutraceutical and pharmaceutically relevant fatty acids [8].

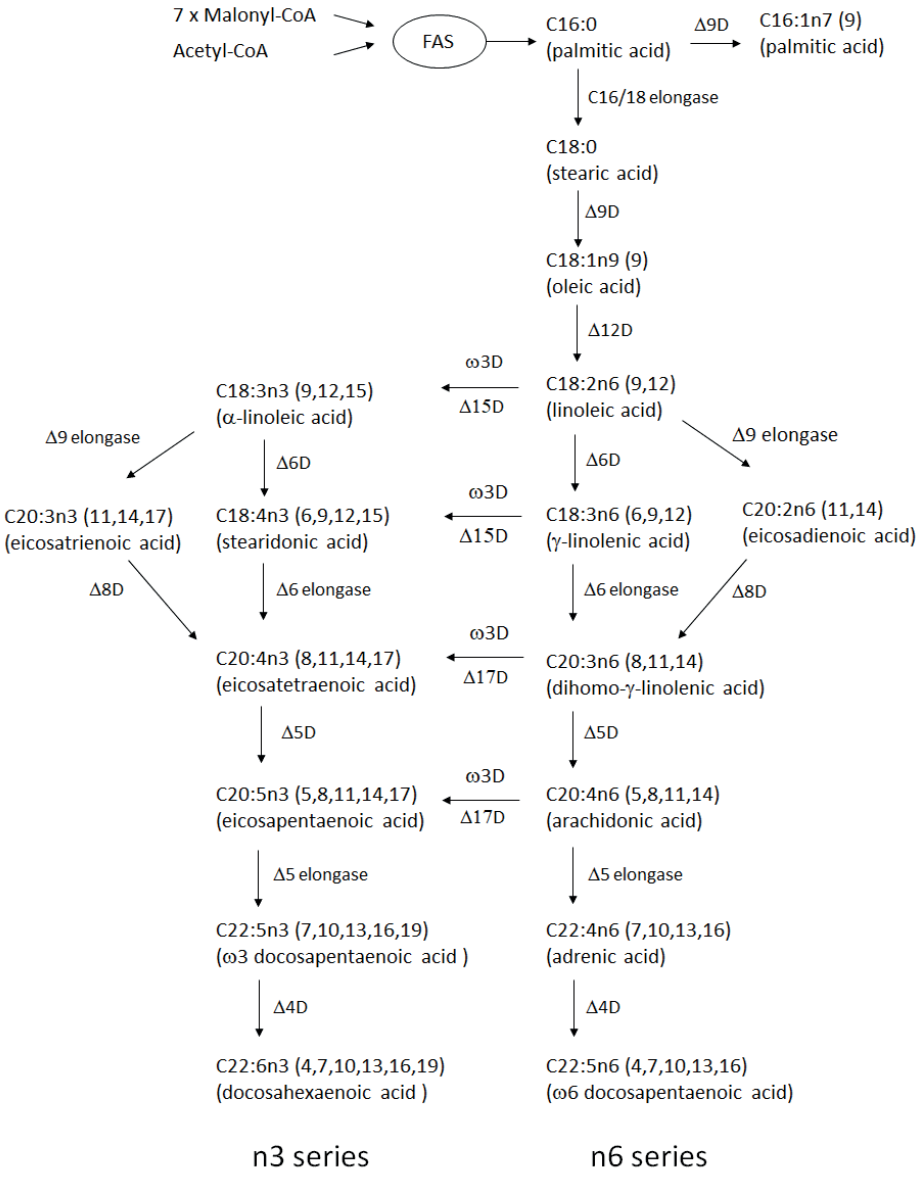

Figure 1.3 Pathways for the formation of PUFA in microorganisms. FAS: fatty acid synthase, D: desaturase, Δ: position of double bond from carboxylic end. Adapted from Ratledge, 2004, Lee *et al.*, 2016 and Ruiz-López *et al.* 2012 [8, 29, 30]

It should be noted that a different, polyketide-like PUFA biosynthesis system has been characterized for PUFA production in marine prokaryotic and eukaryotic microorganisms (e.g. *Schizochytrium* sp.) [8, 28]. However, the description of this system is beyond the scope of this thesis.

1.4 Microbial production of high-value polyunsaturated fatty acids

Single Cell Oil (SCO) designed for human consumption was named similarly to Single Cell Protein (SCP) in order to avoid mentioning the source of the oil, which might be difficult to accept by consumers. Especially fungal or mold oil could sound unsafe, although yeast or algal oil seems to be more acceptable [1]. After the unsuccessful commercialization of both SCP and SCO (in the form of cocoa butter substitutes) due to their low value, single cell oil technology development was focused on the production of long-chain PUFAs with applications in human health, as nutraceuticals, pharmaceuticals and pharmaceutical precursors [28] (Table 1.2).

Since polyunsaturated fatty acids (PUFAs) are essential components of higher eukaryotes, single cell oils are now widely accepted. There is a growing awareness of the health benefits of PUFAs, such as γ-linolenic acid (GLA), arachidonic acid (ARA), docosahexaenoic acid (DHA) and eicosapentaenoic acid (EPA). Omega-3 (or n-3) polyunsaturated fatty acids (PUFAs) have become increasingly important as nutritional and pharmaceutical ingredients. Global consumption was 21 900 t in 2012 and it is forecasted to reach 135 500 t in 2025 (16% annual growth from 2015 to 2025) (Figure 1.4). The traditional source of omega-3 FAs (EPA, DHA) is fish oil. However, it has several disadvantages compared to microalgae oil: fish oil is contaminated by chemicals which are mainly accumulated in lipid bodies (hydrophobic), it has a fish odor, and it cannot be used by vegetarians. Moreover, DHA is always accompanied with EPA, which is contraindicated in infant formula [4].

Table 1.2 Fatty acid profiles of commercially produced SCOs. Adapted from Ratledge, 2013 [1]

	Main fatty acids (% of total)													
	14:0	16:0	16:1	18:0	18:1	18:2	18:3n3	**18:3n6**	20:3n6	**20:4n6**	**20:5n3**	22:5n6	**22:6n3**	22:0+24:0
Microorganism								**GLA**		**ARA**	**EPA**		**DHA**	
Mucor circinelloides [a]	1	23	1	6	39	10	0.2	**18**	-	**-**	**-**	-	**-**	1
Mortierella alpina (DSM)[b]	-	8	-	11	14	7	-	**4**	4	**49**	**-**	-	**-**	-
Mortierella alpina (Cargill)[c]	-	7.5	-	6	9	6	-	**2.5**	4	**43**	**-**	-	**-**	12.5
Crypthecodinium cohnii [d]	20	18	2	<0.5	15	-	-	**-**	-	**-**	**-**	-	**40**	-
Schizochytrium sp.[e]	8	22	<0.5	0.5	1	-	-	**-**	-	**-**	**-**	17	**41**	-
Ulkenia sp.[f]	3	30	<0.5	1	-	-	-	**-**	-	**-**	**-**	11	**44**	-
Yarrowia lipolytica [g]	-	25	1	1	6	18	2.5	**-**	2	<1	**56**	-	**-**	-

[a] J & E Sturge (UK) (1985-1990)

[b] DSM (Netherlands)

[c] Cargill/Wuhan (China)

[d] Martek/DSM (USA)

[e] Martek/DSM (USA)

[f] Lonza (Switzerland)

[g] Du Pont (USA)

Gamma-linolenic acid (GLA, 18:3n6) was the first commercially produced microbial oil from *Mucor circinelloides*. GLA is a dietary supplement for the alleviation of premenstrual tension and for the improvement of various skin conditions [1]. Commercial production of GLA-SCO began in 1985 and finished in 1990 (J. & E. Sturge, UK). The process was carried out in 220 m^3 stirred fermenters. The cultivation took 72–96 hours with a yield of biomass at about 60 $kg \cdot m^{-3}$ and the oil content of the cells were at approx. 25%, containing 18-19% GLA in the oil. During the six years of production around 30 tons were produced and sold in encapsulated form. The cost of microbial production of GLA, however, proved to be too high in order to reach sufficient profit margin (mainly due to the cost of glucose substrate and purification steps). Currently, GLA is produced by the company DSM from plant sources, such as evening primrose oil or borage oil [1, 31]. In this thesis, the filamentous fungus *Mucor circinelloides* was used as a model organism in **Paper I, III**, while seven *M. circinelloides* strains have been screened in **Paper IV**.

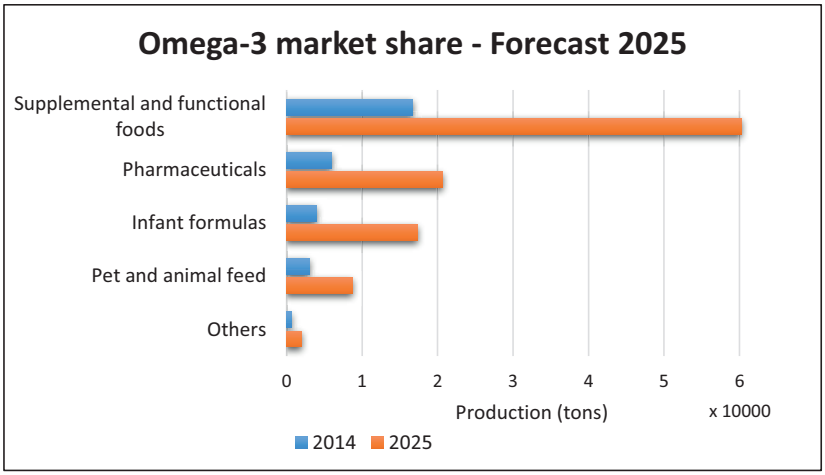

Figure 1.4 Omega-3 market volume share distributed in different sectors of industry over the last decade and its forecast to 2025. Adapted from Finco *et al.*, 2017 [4]

Arachidonic acid (ARA, C20:4n6) is produced by another filamentous fungus, *Mortierella alpina.* There is no realistic alternative source of ARA other than the biotechnological route of production [1]. ARA is the primary omega-6 fatty acid in the brain (48%). ARA is also abundant in other cells in the body and is important for proper brain development; it improves eyesight and memory in infants [31]. Adults are able to convert dietary fatty acids to ARA and DHA, however, in infants this ability is not yet fully developed, making breast milk as their only natural source of ARA and DHA. Babies who are not breastfed can obtain these important ingredients throughout infant formula products [32]. ARA also prevents the undesirable retro-conversion of DHA to EPA in infant formula. ARA production process is carried out in large bioreactors (100–150 m^3). A fermentation process of 9–10 days give the highest yields of oil. Dry biomass concentration is more than 24 g/L, the yield of oil per kg biomass is about 50% and the ARA content in the oil is between usually

40-50% [33]. 95% of commercial ARA is produced by DSM (other companies producing ARA are Cargill and Suntory). ARA and DHA in a ratio of 2:1 is sold under the name Formulaid^{TM}, and it is incorporated into infant formulas worldwide [1, 5]. In this thesis, *Mortierella alpina* was used as a model organism in **Paper III**, and three *M. alpin*a strains have been tested in the screening study (**Paper IV**).

Docosahexaenoic acid (DHA, C22:6n3) is produced mainly with two heterotrophic microalgae, a dinoflagellate *Crypthecodinium cohnii* and a stramenopile *Schizochytrium* sp. [5]. DHA is a primary structural fatty acid in the brain and retina, accounting for up to 97% of the omega-3 fatty acids in the brain and 93% in the retina. For pregnant women, DHA can help support a healthy pregnancy. For infants and children, DHA is necessary for brain and eye development. For adults, DHA contributes brain, eye, and heart health, and improves memory functions [31]. *C. cohnii* has a total fatty acid content of up to 50% and DHA corresponds to 95% of all PUFA. The purified DHA oil from *C. cohnii* is used solely for addition to infant formulas and is marketed under the trade name of life's DHA. It is currently purchased by 24 companies, covering 70% of the total world market for infant formulas [1]. *Schizochytrium* grows very fast and can reach more than 200 kg m^{-3} cell density in less than 72 h [1]. The cells contain up to 60% (w/w) oil from which at least 40% of the total fatty acids is DHA. In *Schizochytrium*, a significant amount (approximately one-third of DHA) of docosapentaenoic acid (DPA, 22:5n6) is also present, but being a natural component of human brain it does not pose any risk [1]. Beside using *Schizochytrium* oil as nutraceuticals in capsule form, it is also incorporated into different food products (mayonnaise, milk etc.) [1, 5]. In this thesis, the growth and lipid production of *Crypthecodinium cohnii* was tested in the Duetz-MTPS. The obtained results were compared to growth and lipid production in a controlled, stirred-tank benchtop bioreactor in **Paper III**.

Eicosapentaenoic acid (EPA, 20:5n3) is currently produced with a genetically modified oleaginous yeast *Yarrowia lipolytica.* EPA, together with DHA, are useful for the secondary prevention of diverse cardiac problems. EPA alone has been proposed for the treatment of various diseases: neuropsychiatric disorders, attention deficit hyperactivity, treating obesity, metabolic syndrome, non-alcoholic steatohepatitis and type-2 diabetes. EPA naturally occurs in microalgae, most of them grow only photosynthetically, therefore biomass yield is too low (3-4 $g \cdot L^{-1}$) for commercial production [1]. To achieve EPA biosynthesis in the oleaginous yeast *Yarrowia lipolytica*, 15-20 genes had to be individually introduced. In the process of DuPont, the fermentation of the GMO yeast (2 L scale) takes 6 days, resulting in 45 $g \cdot L^{-1}$ dry cell weight with 22% lipid content. The oil contains 55% EPA and is sold under the name New Harvest ^{TM} as a nutraceutical product [1]. EPA production (up to 11% of total fatty acids) was detected in *Mortierella* spp. in **Paper IV**.

1.5 Microbial lipids for biodiesel production

The rapid increase in the price of crude oil and a focus of the environmental impacts of fossil fuels have drawn interest in transportation biofuels in the last decades. One of the promising biofuels is biodiesel, which is produced from renewable biomass by transesterification of

TAGs to fatty acid methyl esters (FAMEs) or fatty acid ethyl esters (FAEEs). Environmental benefits of biodiesel include no contribution to net carbon dioxide or sulfur emission to the atmosphere, and less gaseous pollutant emission (except NO_x) [34].

First generation biodiesel is made of lipids from edible plants (palm oil, rapeseed oil, soybean oil etc.). There has been serious concern recently about the effects of the first-generation biodiesel production on disruption of food production and supply especially in the developing countries (the so-called food vs. fuel debate). Second generation biodiesel uses non-edible plants (jatropha, linseed etc.), waste or recycled oil (cooking oil, frying oil etc.) or animal fats (beef tallow, pork lard, chicken fat, fish oil etc.) as substrate [35]. However, none of the terrestrial crops are able to completely substitute crude oil [36].

An emerging alternative is the use of microbial oil from microalgae, yeast and filamentous fungi (third generation biodiesel). Sunlight-driven microalgae, that can convert CO_2 into biofuel is a promising technology, but their cultivation requires a large area, cultivation time is usually long and it depends on environmental conditions. Studies have shown that heterotrophic growth of microalgae species can lead to much higher biomass and lipid yield compared to autotrophic growth (e.g. 400 and 900% increase with *Chlorella* sp. in cell dry weight and lipid content) [36]. Utilization of oleaginous yeast and filamentous fungi for biodiesel production is a realistic option, since they can grow fast in fermenters, produce high amount of lipids, and can utilize inexpensive carbon sources, such as raw materials, by-products, and wastes, leading to significant reduction in waste and production cost (60-75% of biodiesel cost is the substrate). Techno-economic analyses show that biomass and oil generated from heterotrophic fermentation are more close to current fossil fuel cost, although it still has to be improved to become a viable alternative [36].

Biodiesel properties (such as density, viscosity, flash point, cold filter plugging point, solidifying point, heating value and iodine value etc.) are regulated by standards (ASTM Biodiesel Standard D 6751 in the US and Standard EN 14214 in Europe) and are dependent on the fatty acid composition of the lipids. Therefore, when evaluating the feasibility of microorganisms for biodiesel production, their fatty acid composition should be considered as an important indicator. Ideally, biodiesel must contain large quantities of monounsaturated fatty acids (C16:1, C18:1), small quantities of polyunsaturated fatty acids (C18:2, C18:3) as well as controlled quantities of saturated fatty acids (C16:0, C18:0). Microalgae oil is usually highly unsaturated (more than 4 double bonds). Yeasts and filamentous fungi produce lipids, which are more suitable for biodiesel purposes [36]. In addition, the fungal fatty acid composition can be adjusted by manipulating key regulators of the biosynthesis of TAGs and fatty acids [37].

In this thesis, biodiesel properties (density, viscosity, higher heating value, cetane number, iodine value) were calculated for the fungal oil in the screening study (**Paper IV**), according to the formulas in Ramírez-Verduzco et al (2002) [38].

1.6 High-throughput screening of filamentous fungi

High-throughput screening of microorganisms and cultivation conditions is an important step to develop an efficient bioprocess. In oleaginous fungi the screening purposes are two-fold: 1) the selection of best strain or mutant/transgenic line from one strain that have high lipid content, and 2) the selection of a range of culture conditions that cause the maximal lipid content of the cells, preferably with the desired fatty acid composition [39]. The majority of the screening studies with oleaginous filamentous fungi have been so far performed in shake flasks. While it is feasible to test a smaller set of fungi in shake flasks, this approach can be rather laborious and expensive in extensive screening studies due to medium cost and shaker requirement. Chatzifragkou, Buranova, Wang, Broughton, and Weete screened 15 to 150 filamentous fungi for oil production in shake flasks [40-43]. Ratledge *et al.* ran in shake flasks a comprehensive screening study (it took more than six years!) for GLA production, involving more than 300 fungi. [6]. Despite the fact that the reproducible cultivation of filamentous fungi is not an easy task, parallel cultivations are often not performed in shake flask-based screening due to time and space limitation [40, 43, 44].

Due to advances in metabolic engineering, the number of strains to be tested has increased significantly, making the throughput capacity of the shake flask cultures insufficient [45, 46]. Miniaturization of fermentations enables the screening of a high number of strains or mutant libraries in combination with different environmental factors (usually medium composition and temperature), saving process/product development time and cost [47, 48]. Microtiter plates based systems (MTPS), with either 24, 48 or 96 well plates, are the most commonly used initial screening platform in biotechnology due to their simplicity, high throughput, good reproducibility and automation possibilities [49-51]. State-of-the-art commercial MTPS and parallel microbioreactors with monitoring and control options of process parameters (pH, DO, off-gas, feeding etc.) are available now on the market. These systems however involve high investment and running cost, due to for example single use optical sensors for MTPS.

High-throughput screening is only meaningful if the results are reproducible and scalable. Scalability is not a trivial task; compared to stirred-tank bioreactors with volumetric oxygen transfer coefficients, kLa, in the range of 370-600 h^{-1}, shaken cultures only exhibit kLa's in the range of 30-60 h^{-1} due to the lack of active aeration [52]. Moreover, low volume in MTPS can lead to evaporation, while dead zones and nutrient gradients can form due to inadequate mixing. Furthermore, high surface to volume ratio can cause temperature fluctuations [53]. Single-cell microorganisms (bacteria, yeast, animal cells) have been successfully scaled up in the above mentioned state-of-the-art MTPS and micro-bioreactor systems (Biolector, Ambr 15 etc.) up to 15,000 L manufacturing scale [48, 54]. However, in case of filamentous fungi, the adherent wall growth and complex morphology make automated, reproducible and scalable cultivation even more challenging [48, 55]. Wall growth can lead to sporulation, which significantly increases the risk of cross-contamination between wells and also limits the application of optical probes. Despite the above-mentioned difficulties with filamentous microorganisms, good reproducibility results have been achieved for MTPS cultivations. Linde *et al*. demonstrated that variability of *Aspergillus*

carbonarius filamentous fungi cultivation (citric acid titer) can be reduced two and half-fold using 24-well plates compared to shake flask cultivations [56]. Similarly, Sohoni and Siebenberg showed in their studies, that cultivation of *Streptomyces coelicolor* filamentous bacterium was more reproducible in MTPS than is shake flasks (novobiocin antibiotic titer variability could be decreased from 39% to 4-9%). In addition, the performance of *S. coelicolor* in MTPS was scalable to benchtop bioreactor, which has not been achieved with shake flask cultivations [50, 57]. These results have been obtained for MTPS cultivations with the addition of glass beads that promoted mycelial growth and concomitantly decreased wall growth. Knudsen tested in his PhD thesis scalability from 48 well MTP of several filamentous fungi (nine strains from *Aspergillus*, *Penicillium*, *Taleromyces*, *Fusarium* sp.) [52]. A very similar exponential growth curve and production yields were achieved compared to 1 L fully controlled bioreactor. This has been achieved by the addition of carboxypolymethylene to the culture medium. This anionic polymer prevented pellet formation and the growth of dispersed fungi was possible to follow by online OD measurement. Nonetheless, the study utilized very low glucose concentration to remain in the linear range of OD measurement. In order to obtain fungal growth that is compatible with microplate technologies, the filamentous fungus *Chrysosporium lucknowense* was mutated to pellet growth and reduced medium viscosity [58]. Shapaval *et al.* used the Bioscreen C microcultivation system for growth and identification of 59 strains of filamentous fungi with FTIR spectroscopy [59-61]. This system was also used to test 5 *Mucor* species for lipid production on sugar and oil media [62]. In the Bioscreen-C system, 200 wells can be cultivated simultaneously in honeycomb microplates at a maximum working medium volume of 350 µl. This system offers automated optical density measurement, however, the transparent plate cover limits oxygen supply [63]. Beneyton *et al.* proposed a novel approach for high-throughput screening of filamentous fungi (7000 fungi·h^{-1} after 24 h growth phase) by using nanoliter-range, droplet-based microfluidics tools and robotic microtiter plate technology [64]. Single spores were encapsulated in ~10 nL droplets, which could be incubated and sorted based on fluorescence. The system was tested on α-amylase production by an UV-mutated *Aspergillus niger* library.

Duetz-MTPS is a simple and cheap high-throughput screening system that consists of standard microtiter plates (shallow or deep-well plates in 6, 24, 48 or 96 well format) combined with a plate cover that enables sufficient gas transfer, prohibits extensive evaporation and prevents cross-contamination between wells [65] (see Materials and Methods section as well). The system has a very high throughput (plates can be stacked in a shaker incubator), however due to lack of control options (except temperature) it is mainly used for initial strain selection based on end-point productivities [49, 50]. The Duetz-MTPS has been used successfully for screening of animal cells [45, 66, 67], single-celled and filamentous bacteria [68-70], and it has been used by several companies, such as Novozymes, Merck and Novartis, and research institutes, such as Massachusetts Institute of Technology (MIT), Technical University of Denmark (DTU), and Swiss Federal Institute of Technology (ETH) in Zurich.

The use of the Duetz-MTPS for the screening of filamentous fungi has not been sufficiently tested, due to the complex growth morphology that prevents online OD measurement and automation of the system [47]. Bills *et al.* established a screening system for antibiotics and other secondary metabolites production using heterogeneous collections of

80 fungi growing in 96-well format tested across multiple fermentation conditions. Microplates were incubated statically because many fungi completely filled the wells in a few days making agitation ineffective [71]. Khalil *et al.* used the Duetz-MTPS with 24-well plates to test the effect of different concentration of bacterial lipopolysaccharides (LPS) on secondary metabolite stimulation of 40 fungal species [72].

In this thesis, the Duetz-system with 24 deep-well plates with constant shaking was used for the screening of oleaginous fungi (**Paper I-IV**), while scalability of the cultivations of filamentous fungi and microalga to controlled, stirred-tank bioreactors was investigated in **Paper III**.

1.7 Reference methods for lipid analysis

Traditional methods for fatty acid analysis are gas chromatography-flame ionization detection (GC-FID) and gas chromatography-mass spectrometry (GC-MS). These methods provide both quantitative and qualitative data of fatty acids [73]. Other methods include gravimetric measurement, high-performance liquid chromatography (HPLC), nuclear magnetic resonance spectroscopy (NMR) and thin-layer chromatography (TLC). Generally, these methods involve the energy-intensive, time-consuming (several hours of preparation) and expensive procedures such as cell disruption, lipid extraction, and transesterification. Therefore, they are not suitable for high-throughput screening applications [73-77]. During lipid extraction, several toxic chemicals, such as organic solvents and strong acids are used. Another disadvantages of these methods are that instruments are quite expensive, and a trained technician is needed for the multi-step procedures. The estimated total cost of one TAG measurement (including equipment, manpower, and consumables) is $50 to $100 per sample [78]. Moreover, relatively high amount of biomass is needed (50-100 mg) for the analysis and due to the destructive nature of the measurement, spatial information is lost [39, 79, 80]. Despite known problems, these methods are still in routine use and any new methods should be compared to these reference methods, in particular to GC-FID or GC-MS [80].

In this thesis, GC-FID (**Paper I, III, IV**) and GC-MS (**Paper IV**) reference methods were used for total lipid content and fatty acid compositional analysis of microorganism.

1.8 Rapid analytical methods for the screening of oleaginous microorganisms

1.8.1 Biochemical and molecular methods

Eroshin *et al.*and Grantina-levina *et al.* used 0.84 g/L *aspirin* in solid agar medium (MEG or PDA) to pre-screen for ARA producing *Mortierella* and *Umbelopsis* species [81, 82]. Aspirin (acetylsalicylic acid) is a selective inhibitor of growth of ARA-producing strains. Aspirin inhibits oxygenation reactions in prostaglandin synthesis by acetylating the terminal amino

group in prostaglandin synthase, and it inhibits synthesis of ARA metabolites. *Mortierella* strains, which do not produce ARA are able to grow on media containing 0.84 g L^{-1} aspirin, but most ARA-producing strains cannot grow on such media. After this pre-screen step in the solid medium, selected candidate strains were cultivated in liquid media and fatty acid composition was determined with GC-FID and GC-MS.

Dil Raj *et al*. applied *triphenyltetrazolium chloride (TTC) staining* on *Mortierella* spp. in order to assess their ARA production capability [83]. TTC is reduced by the hydrogen atoms released from dehydrogenase enzymes of cellular respiration. Although dehydrogenase enzymes are not specific to *Mortierella* fungi, only ARA producing fungi can be stained with TTC (e.g. *Mucor* cannot be stained). There is a high correlation (r = 0.982) between staining degree (absorbance measured at 485 nm) and ARA content of mycelium. *Sudan Black B*, a non-fluorescent, relatively thermostable lysochrome (fat-soluble dye) diazo dye, is also used for staining of neutral triglycerides and lipids. For example, Kitcha *et al.* screened 889 yeast strains with Sudan Black B, and as a result, 23 strains were identified as potential lipid producers [84].

Tilay *et al.* used direct visualization *H_2O_2-plate assay* method for screening and isolation of PUFA-producing bacteria. The oxidative stability of PUFAs in growing bacteria against added H_2O_2 is a distinguishing sign between the PUFAs producers (no zone of inhibition) and non-PUFAs producers (zone of inhibition) by direct visualization. The confirmation of assay results was performed by injecting fatty acid methyl esters (FAMEs) produced by selected marine bacteria to GC-MS [85].

Broughton developed in his PhD thesis a *polymerase chain reaction (PCR) based screen* to detect the presence of VLCPUFAs (very long chain PUFAs) within fungal populations. The target gene utilized for the screening was GLELO, as it is responsible for elongating of C18:3 n6 to C20:3 n6 as well as shown to exhibit activity on the n3 substrates [44].

1.8.2 Fluorescent methods

Fluorescence-based techniques have been widely used for the screening of oleaginous microalgae [71, 86, 87], yeasts [87-92] and filamentous fungi [90, 93]. The method is based on the treatment of cells with lipophilic fluorescent stains. The sample is then excited with light at a specific wavelength (range), which results in fluorescent light emission from the stain in lipid-rich regions of the cell. Two main fluorescent dyes are commonly used for lipid staining: Nile-red and BODIPY. Nile-red is a metachromatic and lipophilic stain with color emission from deep red to strong yellow gold in hydrophobic environments [78]. Nile-red staining allows obtaining information on the lipid composition of microorganisms via the polar/neutral lipid ratio. A high correlation (R^2 up to 0.93) between PUFA content, fatty acid unsaturation index, neutral and polar lipid amount has been found between the gravimetric method and Nile-red staining [94, 95]. Neutral lipids show yellow emission (560–640 nm), while polar lipids show orange/red emission (greater than 650 nm). The disadvantages of Nile-red staining are the following: the dye does not specifically bind to lipid droplets, pigment interferes, permeation issues, fluorescence quenching, and photo-stability. BODIPY

is better than Nile-red for microscopy since it is insensitive to pH, while polarity and the green light emission is specific for lipid bodies. The disadvantages of BODIPY are the background fluorescence of the dye and its low precise for quantification [78].

The three main techniques utilizing lipophilic dyes are *fluorescent microscopy*, *spectrofluorimetry*, and *flow cytometry*. The fluorescent microscopy technique is useful for the visualization of lipid bodies (volume of lipid bodies can be estimated), but it is not a high-throughput method. Spectrofluorimetry, on the other hand, can be used in HTP format (microplate assay). Nile-red stain is more suitable for this purpose due to the self-fluorescence of BODIPY. Flow cytometry is compatible with both dyes and it is a HTP method. However, it only works for single cells (bacteria, yeasts, and algae), and is therefore not suitable for filamentous fungi.

The advantages of fluorescent methods are the following: they are relatively fast (there is no need for lipid extraction), they can be used in high-throughput screening (especially with flow cytometry), and they are suitable for quantitative measurement of lipids (R^2=0.99 correlation between gravimetric lipid content and fluorescence intensity values have been reported for single species [94, 96]). However, there are several disadvantages of the fluorescent methods as well: they need standardization, optimization (also for instrument parameters) and precision in staining is crucial for robust results. Fading of the stains is another issue. The fluorescent signal is strain specific (in microalgae the thickness of cell wall, chlorophyll content, polar membrane lipids all affect the fluorescence signal), therefore calibration to a reference method is necessary for each strain, implying that a cross-species screening is impaired. Optimal staining protocol may vary also depending on the physiological state of cells [78, 97]. In this thesis, Nile-red staining with fluorescent microscopy was used for visualization of lipid accumulation and for screening purposes (**Paper I, III, IV**).

1.8.3 Vibrational spectroscopy methods

Raman and infrared (IR) vibrational spectroscopic techniques are based on the interaction of infrared radiation with molecular vibrations (stretching and bending) that are specific to composition and structure of the measured sample. Raman spectroscopy is based on the principle of inelastic scattering of electromagnetic radiation on the measured molecules, while IR spectroscopy is an absorption-based technique. Raman and IR methods are complementary to each other. The vibrations, which lead to change in the polarizability of the molecule are Raman-active, while the molecular vibrations which lead to change in the dipole moment are IR-active. Consequently, nonpolar groups like C-C, S-S and C=C have strong Raman signals, while polar groups like C=O, N-H, and O-H give rise to strong IR bands. There are different kinds of vibrations observed in infrared as well as in Raman spectra. Vibrations observed in the CH_2 group are shown in Figure 1.5. IR spectroscopy gives information on molecular structure via frequencies of the normal modes of vibration of the molecule. For a molecule where the number of atoms is N, there are 3N-6 normal (fundamental) modes of vibrations (3N-5 for linear molecules) [98]. There are also combination and overtones of fundamental

vibrations observed in the IR spectra. The frequencies of many overtones and combination bands are mainly present in the NIR region.

The infrared segment of the electromagnetic spectrum extends from the visible to the microwave. It is conventionally specified by the ‘‘wave number’’, i.e. the number of waves per centimeter (symbolized by ‘ν’ and expressed by the unit cm^{-1}), extending from 14,000 to 10 cm^{-1} [3]. In general, infrared radiation is divided into near (NIR, ν = 14,000-4,000 cm^{-1}), middle (MIR, ν = 4,000-400 cm^{-1}) and far (FIR, ν = 400-10 cm^{-1}) infrared [99]. It has to be noted that the upper wavelength limit of the MIR region can be defined within 400-200 cm^{-1} range, depending on the author [100].

Vibrational spectroscopic techniques have advantages over traditional chemical methods since these methods are direct, fast, and non-destructive in nature. Compared to the traditional gas chromatography-based analyses, vibrational spectroscopy techniques omit cell disruption, oil extraction, and transesterification steps, hence they are easier to perform and more environmentally friendly. They have great potential for screening purposes, in particular for the high-throughput screening of oleaginous microorganisms for lipid production [76].

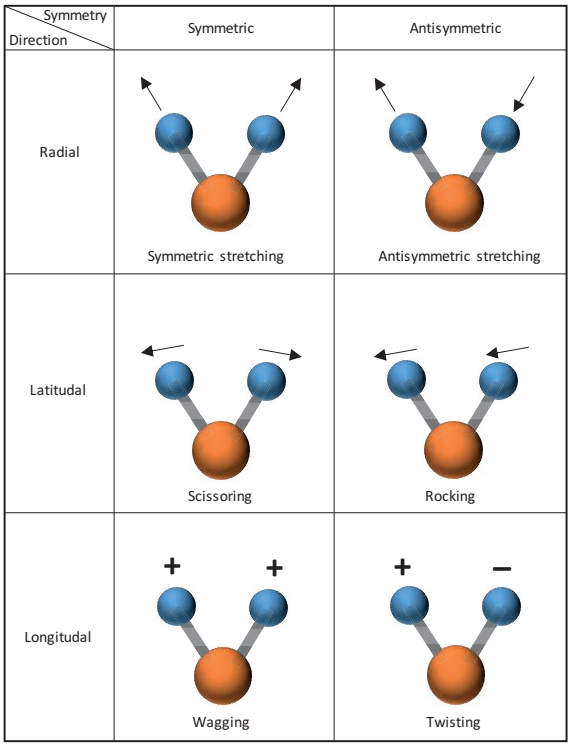

Figure 1.5. Vibrational modes in CH_2 group. Adapted from Wikipedia [101]

1.8.3.1 MIR spectroscopy

Mid-infrared spectroscopy is based on the measurement of the fundamental molecular vibrational modes. In this technique, a polychromatic infrared source (400-4000 cm^{-1}) interacts with the sample leading to either absorption, transmission or reflection of the radiation by the molecules [102]. FTIR has been successfully applied in recent years for at-line, on-line and in-situ bioprocess monitoring [103-107] for extracellular metabolites and substrates (glucose, lactic acid, ethanol, Penicillin V etc.), and for the identification of microorganism (bacteria, yeast, filamentous fungi) [59-61, 99, 102, 108, 109]. It is generally accepted that FTIR cannot fully replace a metabolic analysis like GC-MS, LC-MS, or NMR spectroscopy, but it has a high potential for screening of thousands of strains that is not possible with state-of-the-art 'wet' chemical methods [110].

The most common sampling techniques for microbial characterization are transmittance, diffuse reflectance (DRIFT), attenuated total reflectance (ATR), and micro-spectroscopy (Figure 1.6). In transmission mode, the sample is placed on one or in between two infrared-transparent plates/windows. Since water has a strong absorption in the mid-infrared spectral range, samples usually have to be dried before IR measurements in transmission mode [111]. The advantage of this method is the high signal-to-noise ratio and the inexpensive sample preparation (homogenization if needed and drying step). A disadvantage of the method is the variability in IR absorption due to different sample thickness. In DRIFT mode solid and powder samples can be analyzed, including freeze-dried biomass. Single- and multi-reflection ATR mode is based on the phenomenon of total internal reflection. The sample is in direct contact with a high refractive index crystal (diamond, zinc selenide etc.). The infrared beam generates an evanescing wave at the surface of the crystal, which penetrates to the sample. An advantage of ATR method is the compatibility with liquid, solid, film, powder samples. FTIR microscopy combines a light microscope and an FTIR spectrometer. By using this method spatially resolved chemical information can be obtained of the sample. The lateral (spatial) resolution is wavelength dependent (due to diffraction limit) and is in the range of 2-20 μm. However, such resolution is rarely achieved by a benchtop radiation source such as globar. By applying synchrotron radiation source (100-1000 fold more brilliant than benchtop infrared sources) the diffraction-limited spatial resolution can be achieved [112, 113].

In this thesis, 384-well silica plate was applied for high-throughput transmission measurement of homogenized and dried fungal biomass (**Paper I, III, IV**) and medium samples. In addition, medium samples were measured by the ATR method (single reflection on diamond crystal) (**Paper II**) (See also Materials and Methods section).

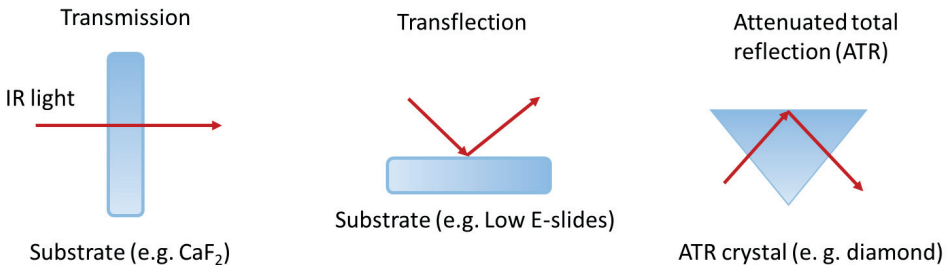

Figure 1.6 Schematic representation of the three main sampling modes for FTIR spectroscopy. Adapted from Baker *et al.* 2014 [114]

FTIR is a powerful technique for characterizing the chemical composition of very complex samples like microorganisms [102]. The spectral profile gives information about important macromolecules like proteins, lipids, nucleic acids and carbohydrates in the cells. FTIR microspectroscopy was used to monitor, compare and analyze lipid production over time in yeast [73, 92]. In addition, synchrotron FTIR micro-spectroscopy was applied for real-time in vivo measurement of single live *Thraustochytrid* cells and to obtain spatial chemical information within hyphae of *Aspergillus*, *Neurospora*, and *Rhizopus* sp [115]. Methods for total lipid content prediction in microbial biomass comprising peak height ratios, peak area and area ratios (univariate) and multivariate regression (Table 1.4). FTIR spectroscopy has been successfully applied in recent years for the prediction of fatty acid composition from pork fat [116-118], fish filet and in milk with very high precision (R^2>0.99 and low error). However, from microbial biomass only Kohler *et al.* and Shapaval *et al.* have predicted so far summed fatty acid parameters (SAT, MUFA, PUFA) [62, 110].

Temporal change in lipid content of oleaginous fungi and microalga **(Paper I, III)** and lipid content of one hundred Mucoromycota fungi **(Paper IV)** were predicted by univariate, as well as by PLSR method (multivariate). The profile of main fatty acids was predicted from oleaginous filamentous fungi versus GC-FID FAME analysis in **Paper I.**

The main regions in the FTIR spectrum of an oleaginous fungi and tentative peak assignment can be found in Figure 1.7 and in Table 1.3.

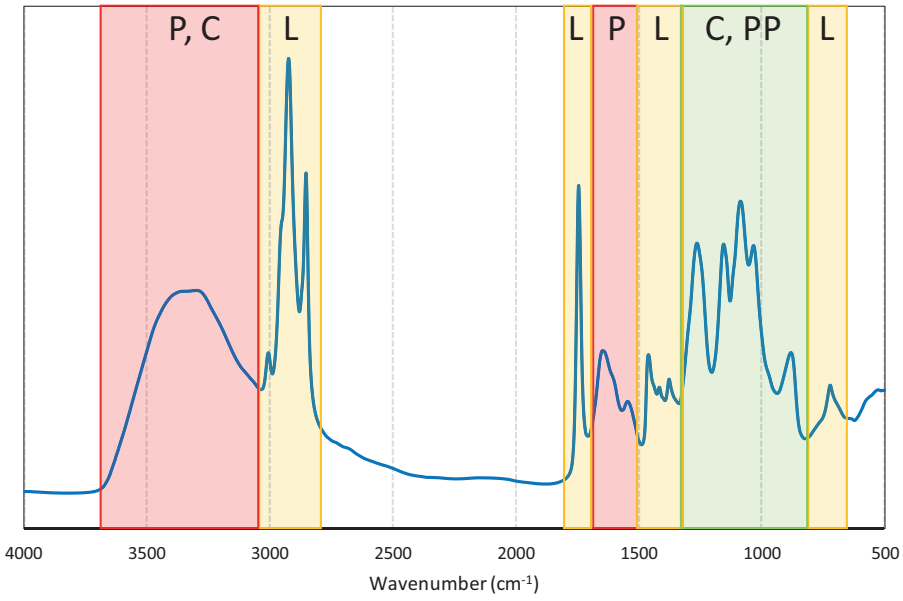

Figure 1.7 Schematic representation of the main regions in FTIR spectrum of the oleaginous filamentous fungus *Mucor circinelloides* CCM 3328. Tentative assignment of vibrational bands belonging to main biochemical constituents is indicated (P: proteins, L: lipids, C: carbohydrates, PP: polyphosphates).

Table 1.3 Tentative peak assignment in FTIR spectrum of the oleaginous filamentous fungus *Mucor circinelloides* CCM 3328. Peak frequencies have been obtained from second derivative spectra. Abbreviations: asym, antisymmetric; sym, symmetric; str, stretching; def, deformation [73, 115, 117, 119-122].

Biomolecule group	**Frequency (cm^{-1})**	**Assignment**
Lipids	3010	=C-H str
	2955	C-H str (asym) of $-CH_3$
	2925	str of $>CH_2$ of acyl chains (asym)
	2895	C–H str of -C–H methine
	2875	str of CH_3 of acyl chains (sym)
	2850	str of CH_2 of acyl chains (sym)
	1745	C=O str.
	1470	CH_2 def
	1440	CH_3 def
	1420	CH_2 def
	1380	CH_3 bending
	1155	C-O-C stretch
	725	CH_2 def
Proteins	~3300	N-H str (amide A)
	1680-1640	Amide I band (C=O str)
	1580-1520	Amide II (CONH bending)
	1610 and 1515	Benzene ring stretch in aromatic amino acids (Phe, Tyr, Trp)
	1410	Amide III band (C-N str)
Polyphosphates, Phospholipids, Nucleic acids (RNA, DNA)	1720	>C=O str
	1400	C=O str (sym) of COO^-
	1265	P=O str (asym) of $>PO_2$ phosphodiesters
	1240	$PO2^-$ str (asym)
	1095, 1080	P O str (sym) of $>PO_2$
	875	P-O-P stretching
	1600	NH_2 def
Carbohydrates (chitosan, β-1,3- and β-1,6 glucans, mannans)	~3300	O-H str
	1160, 1145, 1115, 1030, 1000, 970	C-O str, C-C str., C-O-H def. C-O-C def.

Table 1.4 (Semi)-quantitative determination of lipid content and fatty acid composition from microorganisms with FTIR spectroscopy

Microorganism	Method	Analyte	Data analysis	Range	R^2	Error	Reference
Chlamydomonas reinhardtii and *Scenedesmus subspicatus* microalgae	HTS	total lipid	Peak height ratio C=O bond (1740 cm^{-1}) and amide I (1655 cm^{-1})	Fluorescence intensity 100-2000 A.U.	0.90-0.93	n/a	Dean *et al.*, 2010 [75]
wild type and 9 mutant *Chlamydomonas Reinhardtii* microalgae	HTS	total lipid	Peak height ratio C=O bond (1740 cm^{-1}) and amid I (1655 cm^{-1})	0.2-8 DW%	0.88	n/a	Bajhaiya *et al.*, 2016 [79]
6 microalgae, 1 bacterium, 3 yeasts	dry film AgCl	total lipid (calibration with phospatidyl choline)	Peak area C–H stretching (2984-2780 cm^{-1})	0.05-0.5 mg	0.964	n/a	Pistorius *et al.*, 2008 [123]
microalga *Nannochloropsis* sp.	ATR	total lipid	Peak area C=O bond (1740 cm^{-1})	20-60 % DW	0.995	1.16% DW	Mayers *et al.*, 2013 [124]
Microalgae consortium	Dry film CaF_2	total lipid (calibration with triolein standard)	Peak area ratio C=O bond (1745 cm^{-1}) and amide I-II (1780-1480 cm^{-1})	5-30% DW	0.93	n/a	Miglio *et al.*, 2013 [122]
7 microalgae spp.	KBr pellet	total lipid	Peak area ratio C–H stretching (3000-2800 cm^{-1}) and amide I (1724-1585 cm^{-1})	10-35% DW	0.95	n/a	Meng *et al.*, 2014 [125]
4 microalgae spp.	ATR	TAG, phospholipids (calibration with trilaurin and phosphatidylcholine)	4000-500 cm^{-1} multivariate (PLS)	1-3% DW	0.907, 0.464	0.3, 0.77% DW	Laurens *et al.*, 2010 [39]
5 Mucor spp.	HTS	SAT, MUFA, PUFA	3050-700 cm^{-1} multivariate (PLS)	0.17-0.4; 0.05-0.48; 0.20-0.61	0.71; 0.78; 0.72	0.028; 0.064; 0.07	Shapaval *et al.*, 2014 [62]
21 *Saccharomyces cerevisiae* knock-out mutants	HTS	SAT, MUFA	3100-2800 + 1800-700 cm^{-1} multivariate (PLS)	0.35-0.55; 0.46-0.65	0.58	0.04-0.06	Kohler *et al.*, 2015 [110]

1.9 Multivariate data analysis

Multivariate data contain more than one measured variable per sample. A typical example is spectroscopic data, where the spectrum consists of absorbance values (collinear variables) recorded at many hundreds of wavelengths. Thus, often the number of variables is much higher than the number of samples. The FTIR spectra of biological samples are very complex and have a high-degree of collinearity because of the overlapping absorption of the main biomolecules. In order to gain significant and non-redundant information from the spectra, it is necessary to apply an appropriate multivariate analysis to process the very high-dimensional data [111]. The multivariate data, depending on the analysis, can be organized into one or more separate arrays. Two of the most common problems where chemometric methods are applied are *data exploration* and *multivariate calibration* (Figure 1.8). The goal of data exploration is to find patterns, differences and relations between objects (samples) and/or variables (wavelengths) [126]. Principal Component Analysis (PCA) is the most commonly used data exploration method for finding the underlying structure in the data. In a calibration problem, a quantitative relation has to be established between two data types (blocks) by means of a regression model. Partial Least Squares Regression (PLSR) is a standard method of choice for multivariate calibration [127].

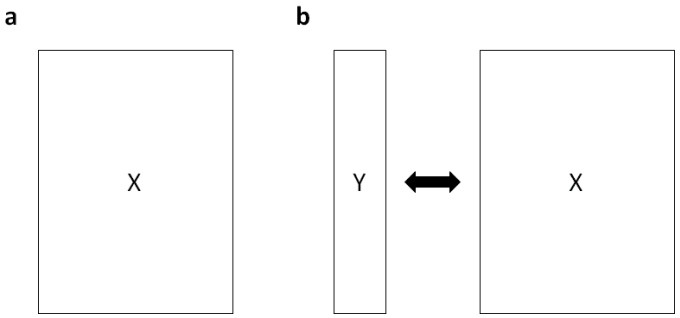

Figure 1.8 a) One 2-way X-data array for exploratory analysis (PCA) **b)** Two 2-way data arrays for the establishment of a regression model Y=f(X) (PLSR). Adapted from Ödman, 2010 [100]

1.9.1 Spectral preprocessing

It is common to mathematically transform spectral data before building calibration models. These pretreatments often help to reduce spectral variation due to the instrument (e.g. white noise) or sample variability (atmospheric CO_2 and water vapor, refractive index variation and scattering due to sample surface unevenness etc.) [39]. Multivariate regression methods, like principal components regression and partial least squares regression (PLSR), result in simpler and often better models when applying them to preprocessed data [128].

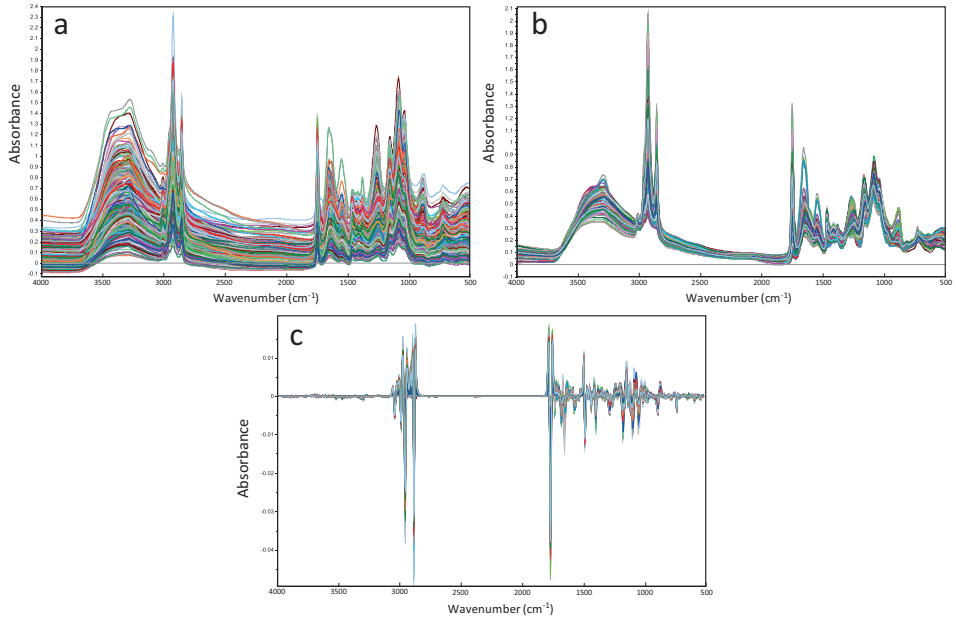

Figure 1.9 a) Raw, **b)** EMSC corrected, **c)** second-derivative FTIR spectra (N=304) of Mucoromycota fungi

Calculating derivative spectra is often the first preprocessing step, because derivatives emphasize band widths, positions, and separation, while simultaneously reducing or eliminating baseline and background effects (Figure 1.9c). For the numerical calculation of derivatives, the algorithm developed by Savitzky and Golay can be used. Very often, the second derivative of spectra is calculated, since the minima in second-derivative spectra coincide to the band peaks in the raw spectra [129].

A model-based pre-processing method, Extended Multiplicative Signal Correction (EMSC) corrects spectral effects commonly found in FTIR spectra, including (*i*) additive baseline (or interference) effects and (*ii*) multiplicative scaling effects due to path length variations, and effectively normalizes the spectra (Figure 1.9b). Consequently, the EMSC-corrected spectra present only chemically meaningful (absorption) signals, improving interpretability and accuracy of the data in both qualitative and quantitative aspects [112].

In this thesis, second-derivate (Savitzky-Golay method, second-degree polynomial, different windows sizes) and/or EMSC correction with linear and quadratic terms spectral preprocessing methods were used before PCA and PLSR analysis.

1.9.2 PCA

PCA is the most commonly used exploratory analysis technique for multivariate data. It transforms the original variables into linearly uncorrelated variables, called Principal Components (PC) (Figure 1.10). The first principal component (PC1) contains the largest possible variation in the original data and each subsequent PC contains, in order, less information than the previous one [130]. Each PC is orthogonal to each other. In PCA, the original data is transformed with the help of an orthogonal transformation to the new coordinates. However, when there is a high degree of collinearity in the data a few (A) components are sufficient to describe most of the variation in the data:

$$\boldsymbol{X} = \overline{\boldsymbol{X}} + \boldsymbol{T}_A \boldsymbol{P}_A^T + \boldsymbol{E}_A \qquad (1)$$

, where $\overline{\boldsymbol{X}}$ represents the average matrix, where in each row the column-wise average of $\boldsymbol{X}$ is repeated, $\boldsymbol{X}$ is the data matrix, $\boldsymbol{T}$ is the scores matrix, $\boldsymbol{P}$ is the loadings matrix and $\boldsymbol{E}$ is the error matrix. A refers to the number of PCA components.

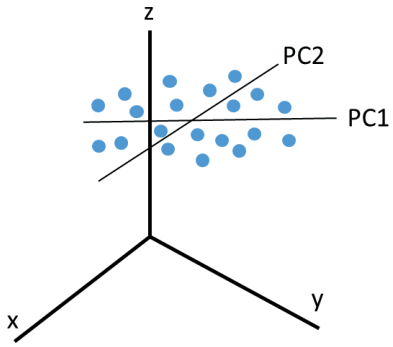

Figure 1.10 Principal components (PCs) form a new set of coordinate axes, which describes the greatest information contained in the data. Adapted from Esbensen, 2002 [131]

Each sample has a score on each PC. Scores allow to investigate sample differences or similarities in data with a high degree of collinearity and enable outlier detection as well. The loadings explain how much of the original variables contribute to the new ones in the PC coordinates. The higher the loading of a particular variable, the more it contributes to that PC.

In this thesis, PCA (**Paper I-IV**) was used to investigate the differentiation ability of FTIR spectroscopy between fungal species, cultivation temperature and time, and to analyze sample variation pattern in FTIR and GC fatty acid composition data. GC data (% of FA of the total) were divided by their standard deviation (besides mean centering) to remove scaling effect before PCA.

1.9.3 Partial Least Squares Regression

Similarly to PCA, the principle of PLSR is the transformation of a matrix $\boldsymbol{X}$ (predictor variables; e.g. FTIR spectra) and matrix $\boldsymbol{Y}$ (response variable; e.g. lipid content of biomass) into scores and loadings. However, in PLSR the aim of these decompositions is to maximize the covariance between $\boldsymbol{X}$ and $\boldsymbol{Y}$, in other words finding the latent variables in $\boldsymbol{X}$ that will best predict the latent variables in $\boldsymbol{Y}$. The PLSR method is the most common multivariate regression method since it handles multi-collinearity and gives an easily understandable graphical representation of the results (i.e. predicted versus reference plot). The PLS components are similar to principal components, but they are referred to as factors. The PLSR data representation in scores and loadings is given as

$$\boldsymbol{X} = \boldsymbol{T}_A \boldsymbol{P}_A^T + \boldsymbol{E}_A \qquad (2)$$

$$\boldsymbol{Y} = \boldsymbol{T}_A \boldsymbol{Q}_A^T + \boldsymbol{F}_A \qquad (3)$$

, where $\boldsymbol{T}$ is the score matrix, $\boldsymbol{P}$ is the loading matrix of $\boldsymbol{X}$, $\boldsymbol{Q}$ is the loading matrix of $\boldsymbol{Y}$, $\boldsymbol{E}$ and $\boldsymbol{F}$ are the error matrices. A refers to the number (rank) of PLS factors [132].

The development and validation procedure of a PLS model is shown in Figure 1.11. The data set is split into a calibration set and a validation set (test set). The calibration set is used to build the PLS model, while the purpose of the validation set is to test the final model. As it is the case in any multivariate regression modeling, model over-fitting (when noise is started to be involved in the model), by using too many PLS factors and/or too wide wavelength range, is a risk in PLS model development. The commonly used method to test for over-fitting is cross-validation, where PLS models are built on a series of subsets of the dataset and tested on the remaining data. The samples are then combined again, another group of samples are left out and new models are established. The procedure is repeated until all samples have been left out and predicted ($\widehat{\boldsymbol{Y}}_{\mathrm{CV}}$) [100]. The cross-validation performance is evaluated by expressing R^2, cross-validated squared correlation coefficient and Root Mean Square Error of Cross Validation (RMSECV, Equation 4) as a function of PLS factors.

$$RMSECV = \sqrt{\frac{\sum_{i=1}^{n}(\hat{y}-y_i)^2}{n-1}} \qquad (4)$$

y_i is the value from reference analytical method for the ith sample; $\hat{y}$ is the predicted value from the model for the same sample; n is the number of samples in each set; SD is the standard deviation in each set [124]. R^2 means the difference between true and calculated values of the cross-validation model, while $RMSECV$ represents the quality of the predictive capacity of the model and gives the approximate standard error between true and calculated values [124]. Once the number of components has been chosen (the lower the better), the final model is built using all samples in the calibration set. In the next step, the model is evaluated by test

set validation, where the samples in the validation set are predicted by the model. Root Mean Square Error of prediction (*RMSEP*, Equation 5) is calculated in a similar way as *RMSECV*.

$$RMSEP = \sqrt{\frac{\sum_{i=1}^{n}(\hat{y}-y_i)^2}{n}} \qquad (5)$$

Residual predictive deviation (*RPD*, Equation 6) is a qualitative measure for the assessment of the validation results.

$$RPD = \frac{SD}{RMSECV} \qquad (6)$$

The higher the RPD value, the closer R^2 to 1 and the smaller RMSECV and RMSEP, the better is the quality of the model. In addition, the lower the number of PLS factors the more robust is the model [39, 133].

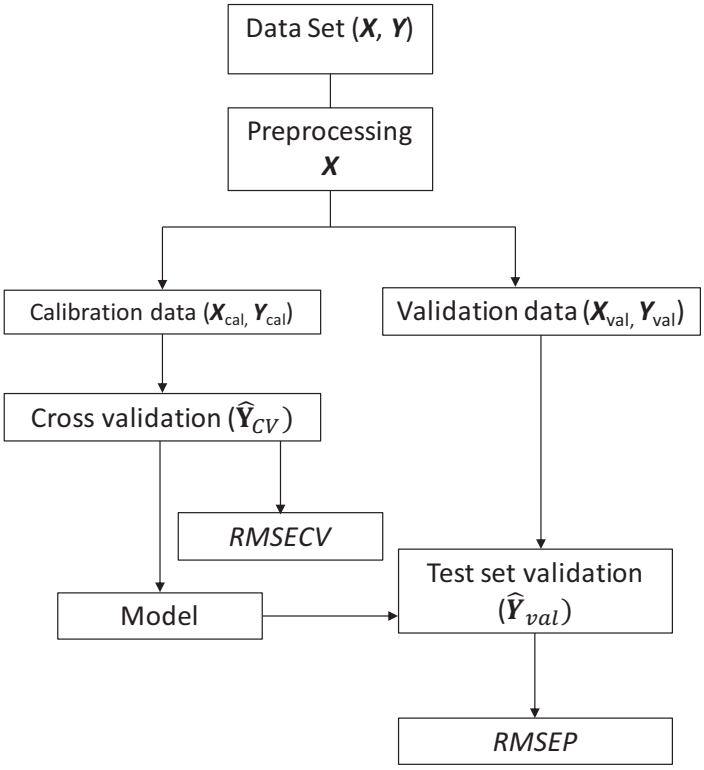

Figure 1.11 PLS model calibration and validation. In this thesis, ***X*** refers to FTIR data, ***Y*** refers to reference data (GC or HPLC). Adapted from Ödman, 2010 [100]

In **Paper I** PLSR was used to create calibration models for groups of FAs (SAT, MUFA, PUFA), unsaturation index of FAs and main individual FAs from fungal biomass. In **Paper I** and **Paper IV** total lipid content of fungal biomass, while in **Paper II** glucose and citric acid concentration of fermentation supernatant were predicted. For such models, a data set of GC or HPLC reference measurements (responses) was used as a ***Y*** matrix, which was regressed onto ***X*** matrix containing FTIR spectral data of fungal biomass and supernatant (predictors).

2 Materials and Methods

2.1 Microorganisms

Strains (Table 2.1) were purchased in the form of active mycelium in slant agar or Petri-dish, lyophilized, or in frozen state in cryovials from the following collections:

- Czech Collection of Microorganisms (CCM; Brno, Czech Republic)
- Food Fungal Culture Collection (FRR; Commonwealth Scientific and Industrial Research Organization, North Ryde, Australia)
- Norwegian School of Veterinary Science (VI; Oslo, Norway)
- Université de Bretagne Occidentale Culture Collection (UBOCC; Brest, France)
- All-Russian Collection of Microorganisms (VKM; Moscow, Russia)
- American Type Culture Collection (ATCC; VA, USA).

Selection of the strains was based on literature study. Mucoromycota fungal phylum was chosen for the screening study, due to their known ability to produce high-value PUFA (GLA, DGLA, ARA, and EPA). Most genera within Mucoromycota phylum have been already screened extensively for high-value PUFA (*Mucor*, *Cunninghamella*, *Rhizopus*, and *Mortierella*) and biodiesel (*Umbelopsis*) production, while less attention has been given so far to *Absidia*/*Lichtheimia* genus [6, 81, 82, 134]. *Crypthecodinium cohnii* dinoflagellate microalga is used to produce DHA at industrial scale (See also Chapter 1.3) [135]. In **Paper I-II** for the purpose to test the suitability of the Duetz-microplate system two Mucoromycota fungi, *Mucor circinelloides* VI 04473, *Umbelopsis isabellina* UBOCC-A-101350 and one Ascomycota fungus *Penicillium glabrum* FRR 4190 were used. In order to test the scalability of cultivations from Duetz-MTPS to stirred bioreactors, two Mucoromycota fungi, *Mucor circinelloides* VI 04473, *Mortierella alpina* ATCC 32222 and the dinoflagellate heterotrophic microalga *Crypthecodinium cohnii* ATCC 40750 were used in **Paper III**. In **Paper IV**, one hundred Mucoromycota fungi were screened in the Duetz-MTPS for single cell oil production.

Fungi were maintained in spore form in cryovials at -80 °C (1/3 vol. spore suspension + 2/3 vol. 60% glycerol) or in case of frequent use they were maintained in malt extract agar (MEA) or potato dextrose agar (PDA) in Petri-dishes (+4 °C) and were re-cultured at least monthly. The microalga *Crypthecodinium cohnii* ATCC 40750 was maintained in ATCC 2076 medium (25 °C, static) and were re-cultured weekly.

Table 2.1 List of strains that were used in this thesis. 1-101: Fungi (kingdom); 1-100: Mucoromycota, 101: Ascomycota (phyla); 1-79: Mucorales, 80-100: Mortierellales (orders); 102: Dinoflagellata (phylum)

1	*Mucor circinelloides* VI 04473	52	*Rhizopus stolonifer* VKM F-400
2	*Mucor circinelloides* CCM 8328	53	*Umbelopsis isabellina* UBOCC-A-101350
3	*Mucor circinelloides* FRR 4846	54	*Umbelopsis isabellina* UBOCC-A-101351
4	*Mucor circinelloides* FRR 5020	55	*Umbelopsis isabellina* VKM F-525
5	*Mucor circinelloides* FRR 5021	56	*Umbelopsis ramanniana* CCM F-622
6	*Mucor circinelloides* UBOCC-A-102010	57	*Umbelopsis ramanniana* VKM F-502
7	*Mucor circinelloides* UBOCC-A-105017	58	*Umbelopsis vinacea* CCM 8333
8	*Mucor flavus* CCM 8086	59	*Umbelopsis vinacea* CCM F-513
9	*Mucor flavus* VKM F-1003	60	*Umbelopsis vinacea* CCM F-539
10	*Mucor flavus* VKM F-1097	61	*Umbelopsis vinacea* UBOCC-A-101347
11	*Mucor flavus* VKM F-1110	62	*Absidia coerulea* CCM 8230
12	*Mucor fragilis* CCM F-236	63	*Absidia coerulea* VKM F-627
13	*Mucor fragilis* UBOCC-A-109196	64	*Absidia coerulea* VKM F-833
14	*Mucor fragilis* UBOCC-A-113030	65	*Absidia cylindrospora* CCM F-52T
15	*Mucor hiemalis* FRR 5101	66	*Absidia cylindrospora* VKM F-1632
16	*Mucor hiemalis* UBOCC-A-101359	67	*Absidia cylindrospora* VKM F-2428
17	*Mucor hiemalis* UBOCC-A-101360	68	*Absidia glauca* CCM 450
18	*Mucor hiemalis* UBOCC-A-109197	69	*Absidia glauca* CCM 451
19	*Mucor hiemalis* UBOCC-A-111119	70	*Absidia glauca* CCM F-444
20	*Mucor hiemalis* UBOCC-A-112185	71	*Absidia glauca* UBOCC-A-101330
21	*Mucor lanceolatus* UBOCC-A-101355	72	*Lichtheimia corymbifera* CCM 8077
22	*Mucor lanceolatus* UBOCC-A-109193	73	*Lichtheimia corymbifera* VKM F-507
23	*Mucor lanceolatus* UBOCC-A-110148	74	*Lichtheimia corymbifera* VKM F-513
24	*Mucor mucedo* UBOCC-A-101353	75	*Cunninghamella blakesleeana* CCM F-705
25	*Mucor mucedo* UBOCC-A-101361	76	*Cunninghamella blakesleeana* VKM F-993
26	*Mucor mucedo* UBOCC-A-101362	77	*Cunninghamella echinulata* VKM F-439
27	*Mucor plumbeus* CCM F-443	78	*Cunninghamella echinulata* VKM F-470
28	*Mucor plumbeus* FRR 2412	79	*Cunninghamella echinulata* VKM F-531
29	*Mucor plumbeus* FRR 4804	80	*Mortierella alpina* ATCC 32222
30	*Mucor plumbeus* UBOCC-A-109204	81	*Mortierella alpina* UBOCC-A-112046
31	*Mucor plumbeus* UBOCC-A-109208	82	*Mortierella alpina* UBOCC-A-112047
32	*Mucor plumbeus* UBOCC-A-109210	83	*Mortierella elongata* VKM F-1614
33	*Mucor plumbeus* UBOCC-A-111125	84	*Mortierella elongata* VKM F-524
34	*Mucor plumbeus* UBOCC-A-111128	85	*Mortierella gamsii* VKM F-1402
35	*Mucor plumbeus* UBOCC-A-111132	86	*Mortierella gamsii* VKM F-1529
36	*Mucor racemosus* CCM 8190	87	*Mortierella gamsii* VKM F-1641
37	*Mucor racemosus* FRR 3336	88	*Mortierella gemmifera* VKM F-1252
38	*Mucor racemosus* FRR 3337	89	*Mortierella gemmifera* VKM F-1631
39	*Mucor racemosus* UBOCC-A-102007	90	*Mortierella gemmifera* VKM F-1651
40	*Mucor racemosus* UBOCC-A-109211	91	*Mortierella globulifera* VKM F-1408
41	*Mucor racemosus* UBOCC-A-111127	92	*Mortierella globulifera* VKM F-1448
42	*Mucor racemosus* UBOCC-A-111130	93	*Mortierella globulifera* VKM F-1495
43	*Amylomyces rouxii* CCM F-220	94	*Mortierella humilis* VKM F-1494
44	*Rhizopus microsporus* CCM F-718	95	*Mortierella humilis* VKM F-1528
45	*Rhizopus microsporus* CCM F-792	96	*Mortierella humilis* VKM F-1611
46	*Rhizopus microsporus* VKM F-1091	97	*Mortierella hyalina* UBOCC-A-101349
47	*Rhizopus oryzae* CCM 8075	98	*Mortierella hyalina* VKM F-1629
48	*Rhizopus oryzae* CCM 8076	99	*Mortierella hyalina* VKM F-1854
49	*Rhizopus oryzae* CCM 8116	100	*Mortierella zonata* UBOCC-A-101348
50	*Rhizopus stolonifer* CCM F-445	101	*Penicillium glabrum* FRR 4190
51	*Rhizopus stolonifer* VKM F-399	102	*Crypthecodinium cohnii* ATCC 40750

2.1 Cultivation conditions

2.1.1 Media

Media composition for agar-based and submerged cultivations was based on literature survey and personal experience.

Malt extract agar (MEA) was prepared by dissolving 30 g malt extract (Merck, Germany), 5 g peptone (Amresco, USA) and 15 g agar powder (VWR Chemicals, Belgium) in 1 L distilled water and autoclaved at 115 °C for 10 min. Potato dextrose agar (PDA) was prepared by dissolving 39 g potato dextrose agar (VWR Chemicals, Belgium) in 1 L distilled water and autoclaved at 121 °C for 15 min. (Figure 2.1). Inoculum medium for bioreactor experiments (**Paper III**) contained 40 g/L glucose - 10 g/L YE for *M. circinelloides*, 20 g/L glucose - 10 g/L YE for *M. alpina* and ATCC 2076 medium for *C. cohnii* consisting of 4 g/L yeast extract (YE, Oxoid, England), 12 g/L glucose and 25 g/L sea salts (Sigma-Aldrich, US). Lipid production media for fungi were prepared according to the protocol described in Kavadia *et al.* [24] with modifications (g/L): glucose 50-90, yeast extract (Oxoid, England) 3-10, KH_2PO_4 7, Na_2HPO_4 2, $MgSO_4 \cdot 7H_2O$ 1.5, $CaCl_2 \cdot 2H_2O$, 0.1, trace element solution (1000x concentrated): $FeCl_3$,·6 H_2O 0.008, $ZnSO_4$,·$7H_2O$ 0.001, $CoSO_4$ $7H_2O$ 0.0001, $CuSO_4 \cdot 5H_2O$ 0.0001, $MnSO_4$ $5H_2O$ 0.0001. In case of *M. alpina* (**Paper III)**, half amount of the phosphate salts (KH_2PO_4 and Na_2HPO_4) were used. Chemicals (except yeast extract) were purchased from Merck (Germany). Liquid medium was autoclaved for 15 min at 121 °C. Glucose and trace element solution (1000x) were sterilized separately (autoclaving and filtration) and were then mixed with basic medium. The precipitation in the basic medium after autoclaving could be dissolved with cooling and mixing. For *C. cohnii* the lipid production medium consisted of 60 g/L glucose, 5 g/L YE, and 25 g/L sea salts.

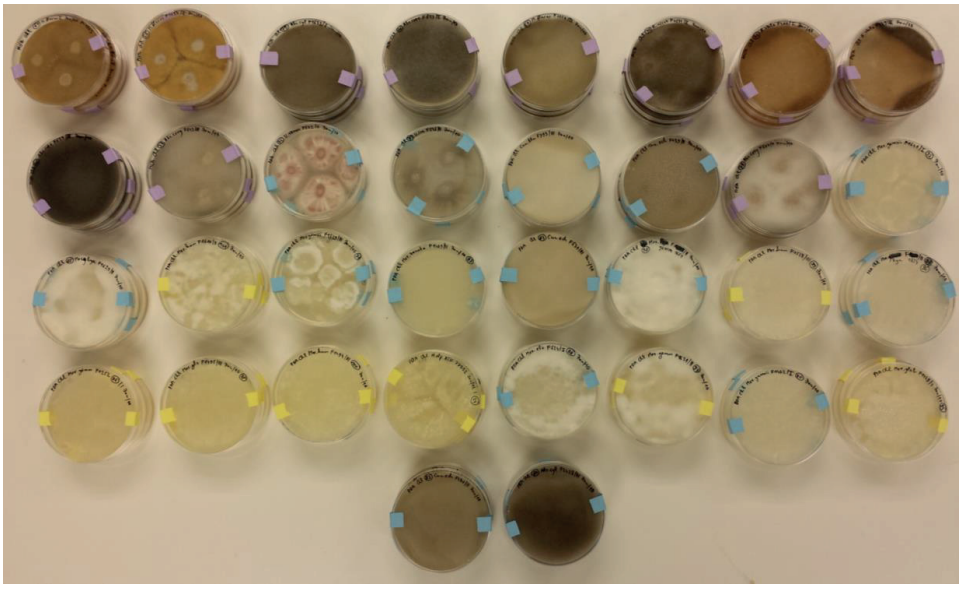

Figure 2.1 Filamentous fungi cultures on Petri-dishes with MEA and PDA media.

2.1.2 Inoculum preparation

Fungi were first cultivated in MEA or PDA for a week at 15-25 °C to obtain spores. Freeze-dried fungal strains were first rehydrated in sterile saline and suspensions were then plated on MEA or PDA plate media. Spores were collected after the addition of sterile saline on the plate with scraping off the spores with a bacteriological loop or with 'hockey stick'. Inoculums for bioreactor runs were performed in 0.5 – 2 L shake flasks with 20 v/v% filling volume. Cultivations were performed for 2-4 days at 28 °C at 100-150 rpm agitation speed on laboratory shakers: Innova 40R (Eppendorf, Germany), ISF1-X (Adolf Kühner, Switzerland), Multitron standard (Infors, Switzerland)

2.1.3 Cultivation in the Duetz-MTPS

Cultivations were performed in the Duetz-MTPS (Enzyscreen, Netherlands), consisting of 24-square, polypropylene deep well plates (11 mL total volume and 2.5 mL filling volume), low-evaporation version sandwich covers (16 µL/well/day at 30 ºC and 50% humidity and 0.7 mL/min exchange of headspace air) and extra high cover clamps (Figure 2.2). The sandwich cover has different layers: stainless steel for rigidity, microfiber filter, ePTFE filter, and the 'spongy' silicone layer to hermetically close the 'mini-reactors'. With the supplied clamp system (cross-nut and spring) ~400 N force can be exerted on the sandwich cover, which ensures good sealing and prevents cross-contamination between wells [136]. Autoclaved and dried microtiter plates were filled with 2.5 mL of sterile liquid medium by

using the Stepper 411 adjustable repeater pipette (Socorex, Switzerland). Each well was inoculated with 10-100 µL fungal spore suspension (or with 250 µL microalga suspension in **Paper III**).

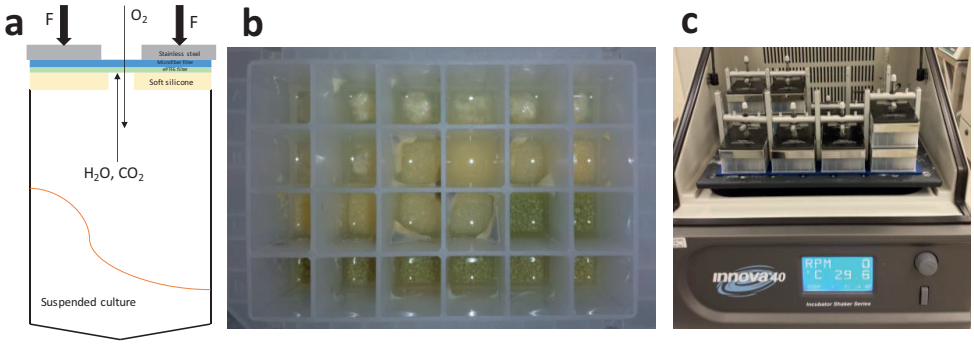

Figure 2.2 Duetz-system (Enzyscreen B.V., Netherlands) with 24 deepwell plates (11/2.5 mL) for high-throughput screening of filamentous fungi. **a)** sandwich cover layers and working principle; Figure adapted from Enzyscreen homepage [65], **b)** fungi grown in 24 deepwell MTP, **c)** Duetz-MTPs stacked on a laboratory shaker with the universal clamp system

2.1.4 Benchtop bioreactor runs

Benchtop fermentations were performed in 2.5 L total volume glass fermenter (Minifors, Infors, Switzerland) with 1.5 L working volume. Fermentation data was logged with the Iris 6 SCADA-software (Infors, Switzerland) (Figure 2.3). Vessels were equipped with two 6-blade Rushton turbines for mixing. Cultivation temperature was 28 °C. The pH was monitored with a pH probe (Mettler Toledo, Switzerland) and was kept at 6.0 for *M. circinelloides*, *M. alpina* and 6.5 for *C. cohnii* with the automatic addition of 1 M NaOH and 1 M H_2SO_4 (for fungi) or 1 M HCl (for microalga). Dissolved oxygen (DO) was monitored with polarographic oxygen sensors (Hamilton, Switzerland) and was maintained above 20% of the saturation with the automatic control of stirrer speed (300-600 rpm or 100-600 rpm for microalga). Off-gas analysis was performed with a FerMac 368 (Electrolab Biotech, UK) gas analyzer connected to the off-gas condenser of the fermenter. Cultures were aerated through a sparger at 0.5 VVM (volume/volume/minute) for fungi (0.75 L/min) or 1.0 VVM (1.5 L/min) for the microalga. Foaming was controlled via a foam sensor with five time diluted Glanapon DB 870 antifoam (Busetti, Austria).

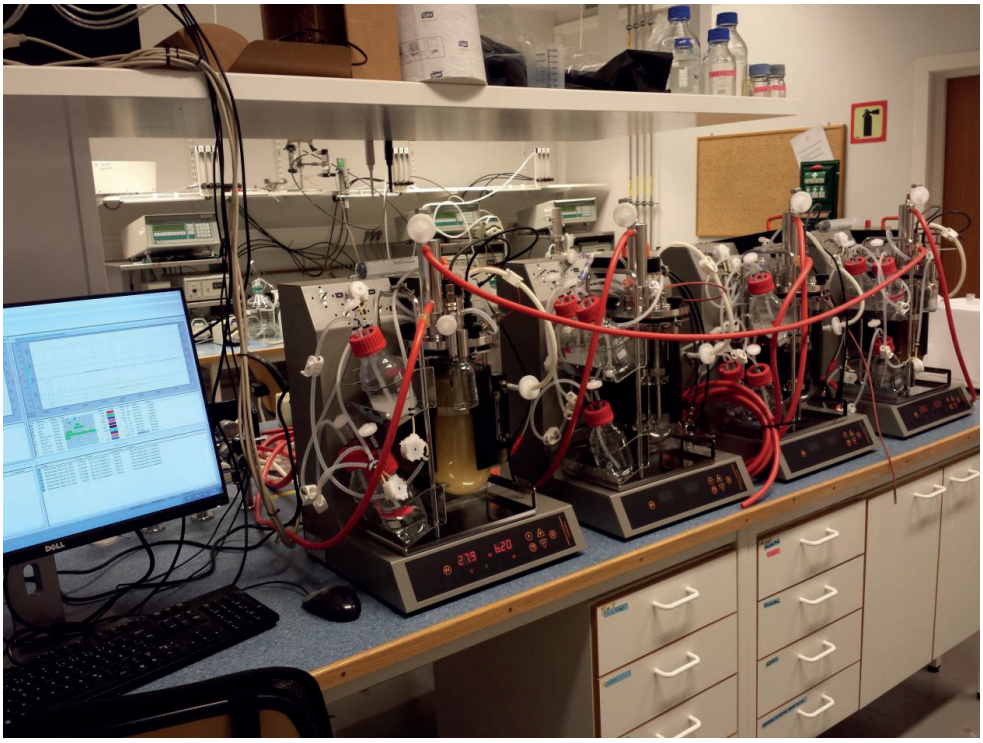

Figure 2.3 Minifors (Infors, Switzerland) benchtop fermenters (2.5 L total volume, microbial version) and Iris 6 SCADA-software for data collection.

2.1.5 Pre-pilot scale bioreactor runs

Pre-pilot scale fermentation runs were performed in a 42 L total volume stainless steel, in-situ sterilizable fermenter (Techfors-S, Infors) with working volume of 25 L (Figure 2.4). Autoclaved and in-situ sterilized media were inoculated with 4 v/v% shake flask inoculum. Glucose and trace element solutions were sterilized separately from base medium and were then combined (same in benchtop bioreactor). The fermenter was equipped with three 6-blade Rushton turbines for mixing. Cultivation temperature was 28 °C. The pH was monitored with a pH probe (Mettler Toledo, Switzerland) and was kept at 6.0 with the automatic addition of 1 M NaOH and 1 M H_2SO_4. Dissolved oxygen (DO) was monitored with a polarographic oxygen sensor (Mettler-Toledo, Switzerland) and was maintained above 20% of the saturation with the automatic control of stirrer speed (300-600 rpm). Off-gas analysis was performed with a gas analyzer (Infors, Switzerland) connected to the off-gas condenser of the fermenters. Cultures were aerated with a sparger at 0.5 VVM (12.5 L/min). Foam build-up was controlled via a foam sensor with five- time diluted Glanapon DB 870 antifoam (Busetti, Austria).

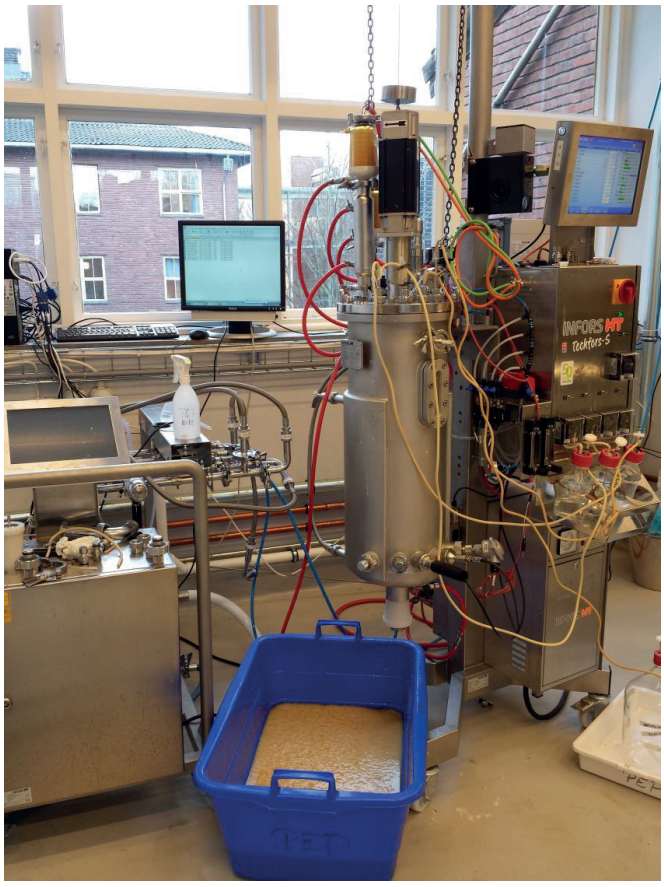

Figure 2.4 Techfors-S (Infors, Switzerland) 42 L total volume in-situ sterilizable, stainless steel bioreactor with mobile CIP (cleaning in place) unit (after harvesting the fermentation broth)

2.2 Bright-field and fluorescent microscopy

Morphology of the microorganisms was examined with a DM6000B microscope (Leica Microsystems, Germany). Microscopic pictures were obtained with an Evolution MP camera kit (Media Cybernetics, USA). A Nile-red staining solution was prepared by dissolving 1 mg Nile-red crystals (Sigma-Aldrich, USA) in 1 mL ethanol. Then, 10 µL Nile-red solution was dried onto a glass side, the biomass was added and covered with a glass coverslip. Nile-red stained samples were incubated for 1 h at 4 °C in the dark and images were captured using a 490 nm excitation/530 nm emission wavelength filter cube (Leica Microsystems, Germany). Representative micrographs of filamentous fungi from the screening study **(Paper IV)** can be seen in Figure 2.5.

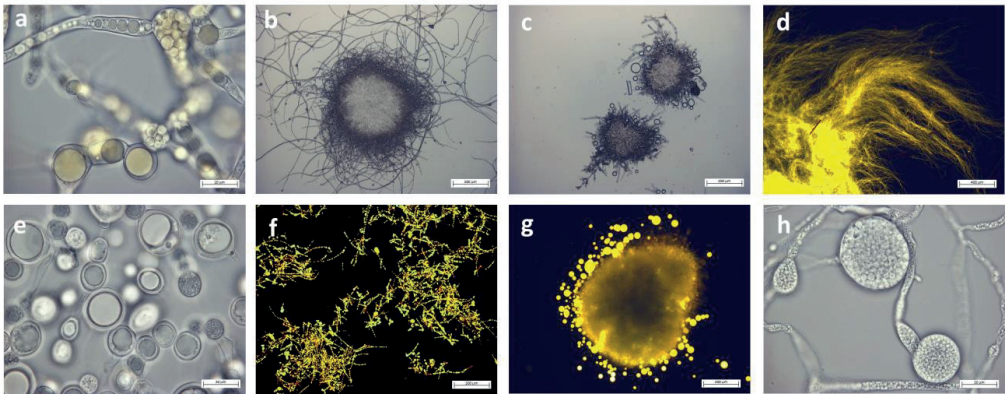

Figure 2.5 Bright-field and Nile-red stained fluorescence microphotographs. **a)** *Mucor hiemalis* UBOCC-A-101359, **b)** *Umbelopsis ramanniana* CCM F-622, **c)** *Absidia coerulea* CCM 8230, **d)** *Mortierella hyalina* VKM F-1854, **e)** *Mucor racemosus* FRR 3336, **f)** *Umbelopsis vinacea* UBOCC-A-101347, **g)** *Cunninghamella blakesleeana* VKM F-993, **h)** *Mortierella zonata* UBOCC-A-101348

2.3 Preparation of supernatant and biomass

The supernatant was separated from the fungal biomass by centrifugation 1.5 mL of the fermentation broth at 13,000 rpm for 20 min at 4 °C in an Eppendorf centrifuge. Fungal biomass was separated from the liquid by using a vacuum conical flask, a vacuum pump, and Whatman No. I filter paper (GE Whatman, USA). Fungal biomass samples of the 25 L working volume fermentations (**Paper III**) were separated by using a 75 µm aperture test sieve (Endecotts, UK). Filtered and sieved biomass was washed thoroughly with cold distilled water to remove medium components. All samples were stored at -20 °C until analysis. In case of microalga *C. cohnii*, the biomass was separated from the medium by centrifugation at

3000 rpm and it was washed once with distilled water. In the next step, the fungal and algal biomass was frozen at -20 °C and then lyophilized overnight (or longer if needed) in an Alpha 1-2 LDPlus freeze-dryer (Martin Christ, Germany) at -55 °C and 0.01 mbar pressure. The freeze-dried biomass was also used to calculate cell dry weight (CDW, g/L).

2.4 Preparation of fungal biomass for FTIR analysis

The washed fungal biomass (approx. 50 µL per sample) was homogenized in square 96-deepwell plates with 500 µL distilled water using a modular liquid handling robot with an integrated 2 mm single-pin Q55 sonicator (Qsonica, USA) (**Paper I**). The sonication was performed in a pulse regime with 15 s sonication time and 5 s washing time. Total sonication time for *U. isabellina*, *M. circinelloides*, and *P. glabrum* was 30 s, 1 min and 1.5 min, respectively. *P. glabrum* biomass cultivated at 20 °C was manually sonicated for 2 min, due to a rigid pellet structure, which was difficult to homogenize with the robotic system. In **Paper III**, approximately 10 mg of freeze-dried biomass or frozen biomass (**Paper IV)** was transferred into 2 mL screw-cap tubes containing 500 µL distilled water and 250 ± 30 mg acid-washed glass beads (800 µm, OPS Diagnostics, USA). Biomass was homogenized for 1-2 min in a FastPrep-24 high-speed benchtop homogenizer (MP Biomedicals, USA) at 6.5 m s^{-1} at +4 °C.

2.5 FTIR spectroscopy

2.5.1 Analysis of microbial biomass (HTS-XT)

FTIR analysis of the sonicated fungal biomass was performed using the High Throughput Screening eXTension (HTS-XT) unit coupled to the Vertex 70 FTIR spectrometer (both Bruker Optik, Germany) in transmission mode (Figure 2.6 a, c). From each suspension, 8 µL were transferred to an IR-light-transparent silicon 384-well microplate (Bruker Optik, Germany) in three technical replicates. Samples were dried at room temperature for approx. 2 h to form films that were suitable for FTIR analysis. The spectra were recorded in the region between 4000 and 500 cm^{-1} with a spectral resolution of 6 cm^{-1} and an aperture of 5.0 mm. For each spectrum, 64 scans were averaged. Each spectrum was recorded as the ratio of the sample spectrum to the spectrum of the empty microplate. The FTIR system was controlled with OPUS 7.5 software (Bruker Optik, Germany).

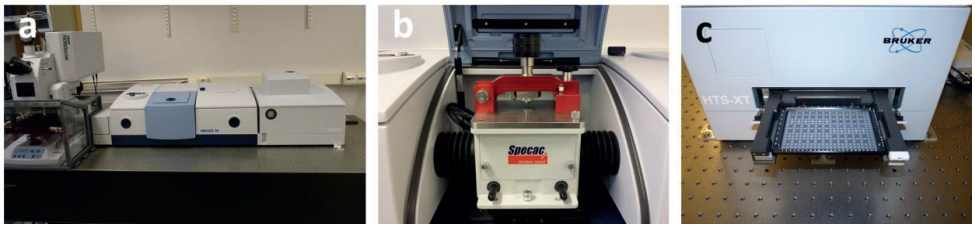

Figure 2.6 a) Vertex 70 FTIR spectrometer (middle) with High Throughput Screening eXTension (HTS-XT) unit and Hyperion 3000 FTIR microscope (left) (all Bruker Optik, Germany), **b)** High Temperature Golden Gate ATR Mk II single reflection ATR accessory (Specac, United Kingdom) mounted in the central (blue) compartment of Vertex 70, **c)** HTS-XT unit with 384-well silicon plate

2.5.2 Analysis of fermentation broth supernatant (ATR, HTS-XT)

ATR measurements were performed using a Vertex 70 FTIR spectrometer (Bruker Optik, Germany) with the single-reflection attenuated total reflectance (SR-ATR) accessory (Figure 2.6b). The ATR IR spectra were recorded with 32 scans using the horizontal SR-ATR diamond prism with 45° angle of incidence on a Specac (Slough, United Kingdom) High Temperature Golden Gate ATR Mk II. From each suspension or supernatant, 10 µL were transferred on the surface of the ATR crystal and measured in three technical replicates. Spectra were recorded in the region between 7000-600 cm^{-1} with a spectral resolution of 4 cm^{-1}. Each spectrum was recorded as the ratio of the sample spectrum to the spectrum of the empty ATR plate. Fermentation supernatant was also measured in the above described high-throughput transmission plate configuration (**Paper II**). The FTIR system was controlled with OPUS 7.5 software (Bruker Optik, Germany).

2.6 Lipid extraction

Direct transesterification was performed according to Lewis *et al.* [26] with modifications for lipid extraction from fungal biomass. 2 mL screw-cap polypropylene (PP) tubes were filled (in three technical replicates (**Paper I, III**) or three biological replicates (**Paper IV**)), with 30 ± 3 mg freeze-dried biomass, 250 ± 30 mg acid-washed glass beads (710–1180 µm diameter, Sigma-Aldrich, USA (**Paper I)** or 800 µm, OPS Diagnostics, NJ, USA, (**Paper III-IV**)) and 600 µL methanol. The fungal biomass was disrupted in a FastPrep-24 high-speed benchtop homogenizer (MP Biomedicals, USA) at 6.5 m s^{-1}, for 1 min cycle length and 6 cycles at +4 °C. The disrupted fungal biomass was transferred into glass reaction tubes by washing the PP tube with 2400 µL methanol- chloroform-hydrochloric acid solvent mixture (7.6:1:1 v/v). 0.2-1 mg (depending on the expected total lipid content of the sample) C13:0 tridecanoic acid internal standard (IS) in methanol (Sigma-Aldrich, US), and in case of *C. cohnii* samples

(**Paper III**) also 0.5 mg C23:0 tricosanoic acid IS (Larodan, Sweden) dissolved in chloroform was added to the reaction mixture. The reaction mixture was vortexed for 10 s and incubated at 90 °C for 1 h, followed by cooling to room temperature and the addition of 1 mL distilled water. The fatty acid methyl esters (FAMEs) were extracted by the addition of 2 mL hexane-chloroform (4:1 v/v) followed by 10 s vortex mixing. The reaction tubes were centrifuged at 3000 g for 10 min at 4 °C and the upper hexane phase was collected in glass tubes. The hexane–chloroform extraction was performed thrice. Subsequently, the solvent was evaporated under nitrogen at 60 °C and FAMEs were dissolved in 1.5 mL hexane containing 0.01% butylated hydroxytoluene (BHT, Sigma-Aldrich, USA). The extracted non-lipid cell compounds (insoluble in hexane) were removed after centrifugation in Eppendorf tubes at 15,000 g for 5 min at 4 °C. The FAMEs dissolved in hexane were transferred to GC vials containing a small amount of anhydrous sodium sulfate (to remove traces of water in the sample).

2.7 GC-FID fatty acid analysis

Analysis of the extracted FAMEs was performed in an HP 6890 gas chromatograph (Hewlett Packard, USA) equipped with an SGE BPX70, 60.0 m × 250 µm × 0.25 µm column (SGE Analytical Science, Australia) and flame ionization detector (FID). Helium was used as a carrier gas. The runtime was 36.3 min with an initial oven temperature of 100 °C, which was increased steadily to 220 °C (4.3 min to 170 °C, then 20 min to 200 °C and 12 min to 220 °C). The injector temperature was 280 °C and 1 µL was injected in split mode (25-50:1 split ratio). FAMEs were identified with a C4–C24 FAME standard mixture (18919-1AMP, Supelco, USA) dissolved in hexane, and then quantified by the C13:0 IS and relative response factors (RRF) of the individual FAMEs in the standard mixture. In case of *C. cohnii*, C23:0 IS was used to calculate the DHA content in the oil. Peaks were automatically integrated by the software Chemstation. Equation 7 shows the calculation of RRF for the ith fatty acid from the C4-C24 FAME mix. The concentration of each fatty acid in the FAME mix is given by the manufacturer.

$$RRF_{FA_i} = \frac{area\ FA_{i,FAME\ MIX}}{c\ FA_{i,FAME\ MIX}} \cdot \frac{c\ C13{:}O_{FAME\ MIX}}{area\ C13{:}0_{FAME\ MIX}} \quad (7)$$

After calculating RRF values for all fatty acids from the C4-C24 FAME mix, the weight of each fatty acid in the sample can be calculated according to Equation 8. The weight of added C13:0 IS to the sample is known from the concentration and volume of the prepared stock solution.

$$weight\ FA_{i,sample} = \frac{weight\ C13{:}0\ (IS)}{area\ C13{:}0\ (IS)} \cdot \frac{area\ FA_{i,sample}}{RRF_{FA_i}} \quad (8)$$

By knowing the weight of each fatty acids in the sample, the presence of these fatty acid in weight percentage can be calculated according to Equation 9. The total weight of fatty acids in the sample is corrected by the added internal standard weight.

$$\%\, FA_{i,sample} = \frac{weight\ FA_{i,sample}}{\sum weight\ FA_{i,sample} - weight\ C13{:}0\ (IS)} \quad (9)$$

Finally, the FAME content of the sample (L/X %) in weight percentage can be calculated according to Equation 10.

$$\frac{L}{X}\% = \frac{\sum weight\ FA_{i,sample} - weight\ C13{:}0\ (IS)}{weight\ of\ dry\ biomass} \quad (10)$$

Figure 2.7 shows the chromatogram of C4-C24 FAME standard, while in Figure 2.8 representative GC-FID chromatograms of filamentous fungi and microalgae FAME composition can be seen

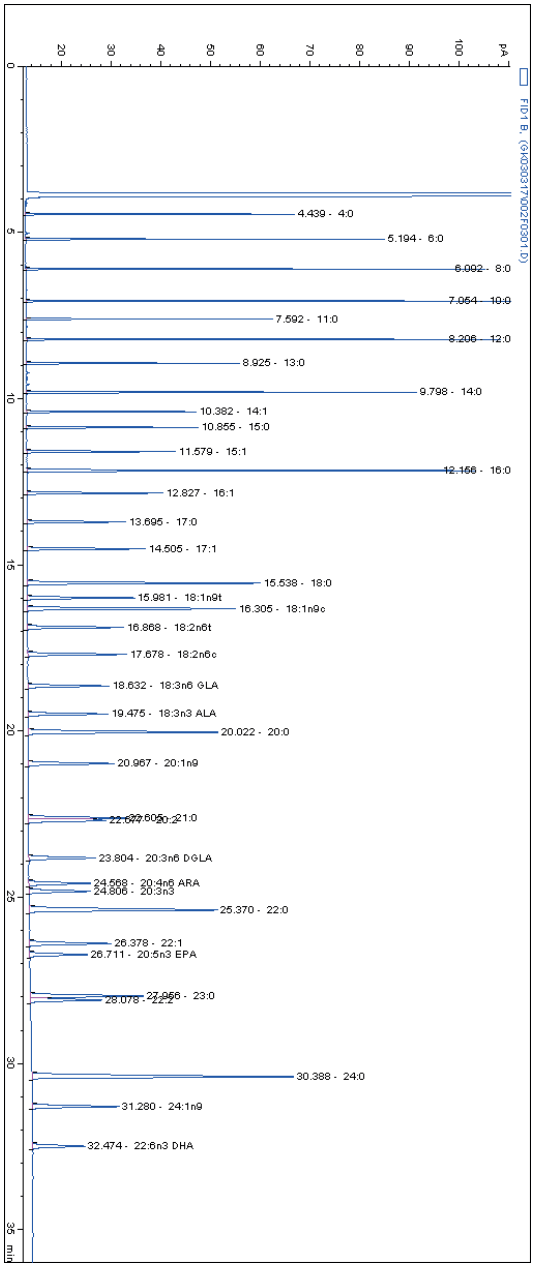

Figure 2.7 GC-FID chromatogram of C4–C24 FAME standard mixture on BPX70 column. C20:2 - C21:0 and C22:2 - C23:0 could not be fully separated (co-elution).

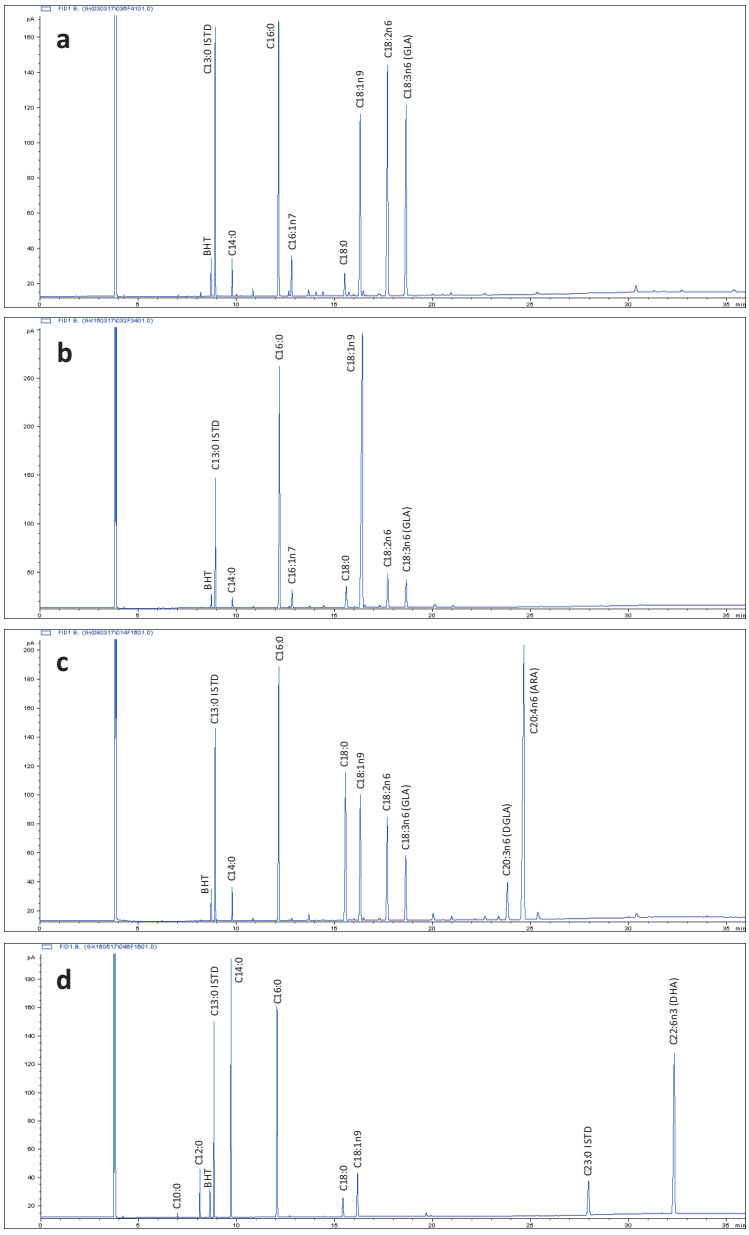

Figure 2.8 GC-FID chromatograms of fungal and microalgal oil FAME composition. **a)** *Mucor fragilis* UBOCC-A-109196, **b)** *Umbelopsis vinacea* CCM F-539, **c)** *Mortierella alpina* ATCC 32222, **d**) *Crypthecodinium cohnii* ATCC 40750. BHT: butylated hydroxytoluene (antioxidant)

2.8 GC-MS fatty acid analysis

Identification of peaks, which were present in samples, but could not be identified by the external C4 - C24 FAME mixture were performed by GC-MS (**Paper IV**). The analysis was carried out on an Agilent 6890 Series gas chromatograph (GC; Agilent, DE, USA) in combination with an Autospec Ultima mass spectrometer (MS; Micromass, England) using an EI ion source. The GC was equipped with a CTC PAL autosampler (CTC Analytics, Switzerland). Separation was carried out on a 60 m Restek column (Rtx®-2330) with 0.25 mm I.D. and a 0.2 µm film thickness of fused silica 90% biscyanopropyl/10% pylphenylcyanoprol polysiloxane stationary phase (Restek, PA, USA). For carrier gas, helium (99.99990%, from Yara, Norway) was used at 1.0 mL/min constant flow. The EI ion source was used in positive mode, producing 70 eV electrons at 250 °C. The MS was scanned in the range 40–600 m/z with 0.3 s scan time, 0.2 s interscan delay, and 0.5 s cycle time. The transfer line temperature was set at 270 °C. The resolution was 1200. A split ratio of 1/10 was used with injections of 1.0 µL sample. Identification of fatty acids was performed by comparing retention times with standards as well as MS library searches. The MassLynx version 4.0 (Waters, MA, USA) and the NIST 2014 Mass Spectral Library (Gaithersburg, MD, USA) was used. The GC oven had a start temperature of 65 °C, held for 3 min, the temperature was then raised to 150 °C (40 °C/min), held for 13 min, before being increased to 151 °C (2 °C/min) and held for 20 min, a slow increase to 230 °C (2 °C/min), held for 10 min, before a final increase to 240 °C (50 °C/min), the end temperature was held for 3.7 min.
The following fatty acids were identified with GC-MS analysis from the fungal screening study (**Paper IV**), which are not present in the C4–C24 FAME standard mixture. Retention times in GC-FID are also indicated:

- C16:2n5t, RT ~12.7 min
- 16:2n6t RT ~14.1 min
- C17:2n5 RT~15.8 min
- C18:1n7c RT~16.5 min
- C18:2n9t RT~17.3 min
- C18:4n3c (stearidonic acid, SDA) RT~20.5 min
- C17:3:n3 RT~21.3 min
- C20:2t (8,11) RT~21.3 min
- C20:3n9 RT~23.0 min (mead acid)
- C20:3n6 (5,11,14) (podocarpic acid) RT~23.4 min
- C20:4n3 (eicosatetraenoic acid, ETA) RT~26.0 min
- C22:3c (8,11,14) RT~30.0 min
- C25:0 RT~32.7 min

In addition, an oxo-derivative of C18 fatty acid was found (C18:0 9-oxo) at retention time ~35.3 min in the majority of the samples. This chemical is most likely a by-product of C18 fatty acid, which is produced during the transesterification process.

2.9 Optical density measurement

The optical density of *C. cohnii* was measured (after proper dilution) at 600 nm with a SPECTROstar Nano UV/Vis microplate reader (BMG Labtech, Germany).

2.10 Protein analysis

The protein concentration of supernatant samples was determined with a Bradford-method based colorimetric assay (Bio-Rad Protein Assay, USA) according to the microplate protocol (**Paper I**). Absorbance was measured at 595 nm with a SPECTROstar Nano UV/Vis microplate reader. A calibration curve was prepared with media containing different amount of yeast extract.

2.11 Glucose colorimetric-enzymatic assay

Quick determination of glucose concentration during cultivations were performed with the glucose oxidase/peroxidase; GOPOD assay kit (Figure 2.9) (Megazyme, Ireland). It employs high purity glucose oxidase and peroxidase and can be used for the specific measurement of D-glucose. The forming pink-red color is stable at room temperature for at least two hours after development. The assay was performed either in cuvettes or in 96 well shallow plates after 20 min incubation time at 50 °C. Absorbance values were read at 510 nm with the SPECTROstar Nano UV/Vis microplate reader.

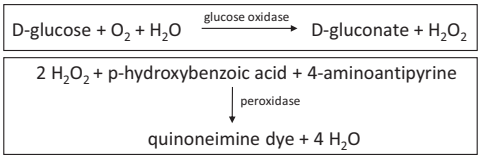

Figure 2.9 Working principle of glucose oxidase/peroxidase, GOPOD assay. Adapted from Megazyme GOPOD assay description [137]

2.12 Sugar and organic acid analysis by HPLC

Glucose and organic acids were quantified by an UltiMate 3000 UHPLC system (Thermo Scientific, USA) equipped with RFQ-Fast Acid H+8% (100 x 7.8 mm) column (Phenomenex, USA) and coupled to a refractive index (RI) detector. Samples were diluted ten times before analysis, filter sterilized and subsequently eluted isocratically at 1.0 mL min^{-1} flow rate in 6

min with 5 mM H_2SO_4 mobile phase at 85 °C column temperature. Peaks were automatically integrated with the software Chromeleon (Thermo Scientific, USA)

2.13 Data analysis

The Unscrambler, V10.3-10.5 (CAMO, Norway) and in-house written Matlab routines, R2015 (The Mathworks, USA) were used to perform the data analyses. Data analyses included spectral pre-treatment (variable selection, 2^{nd} derivative, EMSC correction), PCA and PLSR.

3 Main results and discussions

3.1 Paper I: Microtiter plate cultivation of oleaginous fungi and monitoring of lipogenesis by high-throughput FTIR spectroscopy

In **Paper I**, we introduced the Duetz-MTPS for the cultivation of filamentous fungi in combination with HTS-FTIR spectroscopy as a high-throughput analytical method for intracellular lipids. We cultured three model organisms, *Mucor circinelloides*, *Umbelopsis isabellina* and *Penillium glabrum* for 12 days under two different temperatures in order to demonstrate the suitability of the system. Lipid accumulation and fatty acid composition of the fungal biomass was measured by GC-FID reference analysis and estimated by FTIR measurements. First, the microcultivation performance was evaluated for the studied fungi based on well-to-well reproducibility. Micro-cultivations in the 24-deepwell plates showed excellent biological reproducibility on the basis of glucose consumption (pooled standard deviation = 1.1 g L^{-1} glucose) and FTIR spectral data of biomass. Fungal cultures with high biomass concentrations (up to 23 g L^{-1} CDW) and high lipid content (up to 35%) were obtained in the Duetz-MTPS on the high carbon-to-nitrogen medium. Examination of specific bands in the FTIR spectra of fungal biomass during the 12 days of fermentation resulted in lipid accumulation time profiles that were very similar to total FAME curves determined by reference GC analysis (Figure 3.1). Evaluation of the FTIR C=O ester peaks revealed smaller day-to-day variations in total lipid content than those obtained by the tedious and error-prone extraction-GC method and thus are more plausible. FTIR spectral data of biomass were calibrated versus GC fatty acid data for quantitative purposes. Summed fatty acid parameters (SAT, MUFA, PUFA, total lipid content), unsaturation index and main individual fatty acids were predicted with high precision (Table 3.1).

Growth curves, final biomass yield and fatty acid compositions obtained in Duetz-MTPS showed good agreement with previously reported results from shake flask-based cultivation [22, 23, 138]. In addition prediction of fatty acid properties from fungal biomass outperformed earlier trials [62, 110]. We concluded that cultivation in Duetz-MTPS together with HTS-FTIR spectroscopy enables the high-throughput screening of filamentous fungi for single cell oil production. Sample preparation for HTS-FTIR measurement can be fully automated to further increase the throughput of the system [139].

Table 3.1 PLS regression results between HTS-FTIR and GC fatty acid measurements (N=201). Individual fatty acids, SAT, MUFA, PUFA (wt% of total fatty acids); total lipid (wt% of biomass)

Fatty acid	Range	Mean	Standard deviation	R^{2a}	RMSECV[b]	RPD_{CV}[c]	PLS factors
C16:0	13.4-31.9	20.2	6.1	0.94	1.5	4.0	6
C18:0	2.1-14.4	6.3	3.2	0.94	0.8	4.2	6
C18:1n9	25.4-49.1	37.4	5.4	0.89	1.8	3.0	21
C18:2n6	7.6-48.1	20.8	11.5	0.96	2.3	5.0	7
C18:3n6	0.0-22.3	9.1	7.2	0.96	1.4	5.1	3
SAT	22.4-39.2	29.0	4.5	0.87	1.6	2.8	6
MUFA	27.1-52.6	40.7	5.6	0.93	1.5	3.9	21
PUFA	15.9-50.5	30.3	8.1	0.93	2.2	3.7	7
unsat. index	0.89-1.33	1.11	0.13	0.95	0.03	4.5	9
total lipid	7.9-37.1	27.8	6.1	0.86	2.3	2.6	4

[a] R^2, cross-validated squared correlation coefficient

[b] RMSECV, Root Mean Square Error of Cross Validation

[c] RPD_{CV}, Residual predictive deviation of cross-validation (standard deviation/RMSECV)

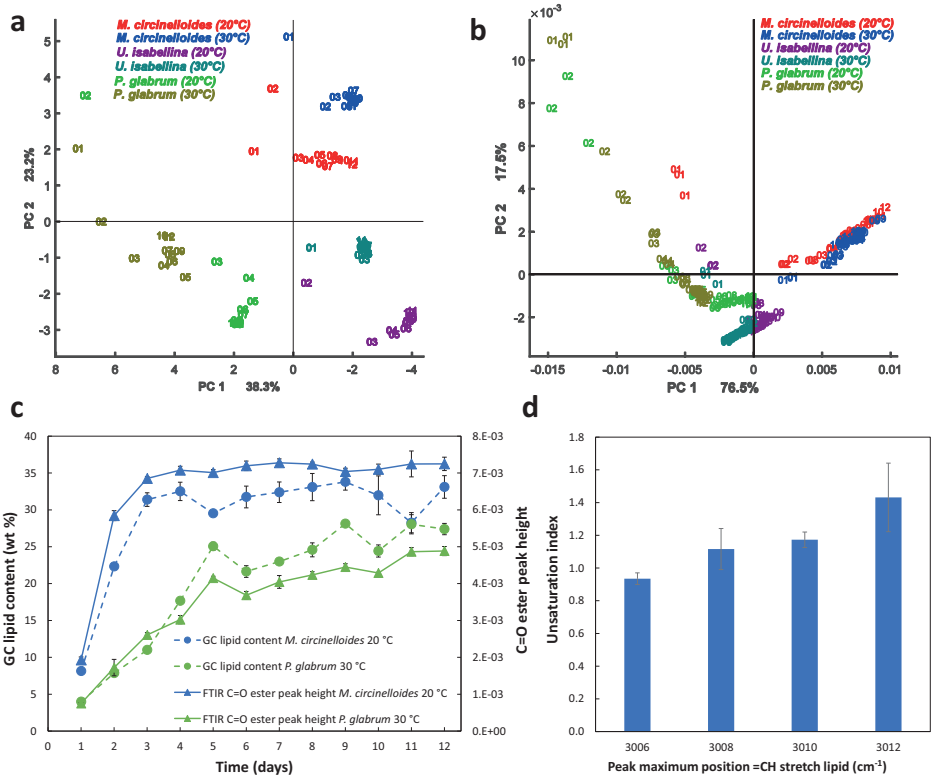

Figure 3.1 Exploratory analysis of FTIR data and comparison with GC reference data. **a)** First and second scores (PC1, PC2) in PCA of the auto-scaled GC fatty acid data, **b)** First and second scores in the (PCA) of the preprocessed FTIR spectra in the spectral range of 3100-2800 cm^{-1}, **c)** Total lipid content measured by reference GC method and followed by the C=O ester peak height from the pre-processed FTIR spectra (n=3, error bars=SD), **d** relationship between unsaturation indices and position of the =C-H stretching bond peak maxima (cm^{-1}) in FTIR spectra

3.2 Paper II: FTIR spectroscopy as a unified method for simultaneous analysis of intra- and extracellular metabolites in high-throughput screening of microbial bioprocesses

In **Paper II** we used the protocol developed in **Paper I** and we followed glucose consumption of the three fungal species and citric acid production by *Penicillium glabrum* with HTS and ATR-FTIR techniques. We compared HTS and ATR-FTIR spectroscopy techniques for the measurement of supernatant samples. Quantitative estimates of glucose and citric acid in the cultivation media were obtained by PLSR analyses. The results show a high level of correlation between the FTIR and HPLC measurements for both HTS and ATR measurements (Table 3.2). The number of components used for building glucose and citric acid HTS–FTIR vs. HPLC calibrations was lower than HTS-FTIR vs. GC analysis of fungal lipids in **Paper I**. This is logical since the chemical complexity of the cultivation media (supernatant) is relatively low when compared with the fungal biomass (Figure 3.2 c). In general, the results for HTS measurements were very similar to the results obtained with ATR methodology, with comparable RMSE values for both glucose and citric acid estimates. The main difference between the two methods are the following. First, HTS measurement of growth media often requires optimization of sample concentration, as was the case in this study where spectra were obtained from ten times diluted supernatant samples. Secondly, in ATR measurement of growth media, there is a controlled optical path length, resulting in extremely reproducible spectral measurements of technical replicates without the need of much spectral preprocessing. In contrast, HTS measurement of growth media is characterized by much larger variations between the spectra of technical replicates, due to the irreproducible film formation on the silicon microplates. For this reason in HTS method averaging of technical replicate and derivative transformation were necessary. Thirdly, since dry films are used for HTS measurements, the water signal is weak and probably a more detailed fingerprint of biomolecules can be obtained compared with ATR approach (Figure 3.2 a-b).

The RMSE values for assessment of glucose by ATR for all three fungal species (RMSE = 5–6%) are consistent with the reported values for ATR cell and probe measurements of bacterial and yeast fermentations (RMSE = 6–12%) [106, 140-142]. Likewise, the related glucose values for HTS measurement are consistent with the reported values for monitoring of mammalian cell cultures [143]. However, it should be noted that our study has covered one order of magnitude higher range of glucose concentration (up to 80 g L^{-1} glucose) compared to the one in the above-mentioned study [143]. Compared to ATR, microplate design of HTS–FTIR setup is consistent with microbioreactor plate design, and thus it is well suited for high throughput screening. Therefore, while ATR setup is probably an optimal choice for industrial scale bioprocess control, HTS setup shows a clear advantage in microbial screening studies.

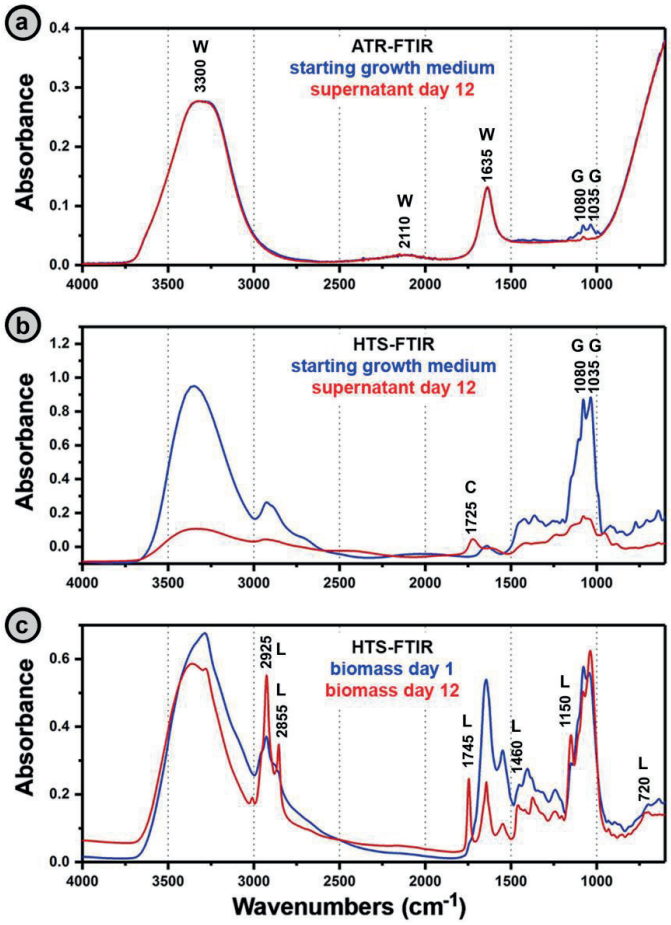

Figure 3.2 a) ATR-FTIR spectra of growth media, **b)** HTS-FTIR spectra of growth media, and **c)** HTS-FTIR spectra of biomass for *P. glabrum* cultivation at 30 °C. The marked bands are associated with molecular vibrations of (W) water, (G) glucose, (C) citric acid, and (L) lipids

Table 3.2 PLSR (test set validation) result for glucose and citric acid from fermentation supernatant between ATR/HTS-FTIR vs. HPLC measurements

technique	Glucose		Citric acid	
	R^2 (PLS factors)	RMSEP	R^2 (PLS factors)	RMSEP
ATR	0.96 (2)	4.49 (5.6%)	0.88 (4)	0.76 (8.7%)
HTS	0.95 (2)	4.98 (6.2%)	0.91 (3)	0.75 (8.6%)

3.3 Paper III: Scalability of oleaginous filamentous fungi and microalga cultivations from microtiter plate system to controlled, stirred-tank bioreactors

High-throughput screening of microorganisms and culture conditions is a pivotal step in the establishment of a cost-efficient, commercial scale bioprocess. An important criteria for such high-throughput systems is the scalability of results obtained at small scale to stirred bioreactors. In **Paper III**, we compared fermentation performance of three well-known oleaginous microorganisms, namely *Mucor circinelloides*, *Mortierella alpina* and *Crypthecodinium cohnii*, in 24-deepwell plates, benchtop (1.5 L working volume) and pre-pilot scale (25 L working volume) controlled stirred-tank bioreactors. Key fermentation physiological parameters (glucose consumption rate, biomass concentration, lipid content of the biomass, biomass and lipid yield) were comparable (max. 30% difference) for the oleaginous fungi *M. circinelloides* and *M. alpina* in Duetz-MTPS and benchtop or pre-pilot stirred-tank bioreactors (600 – 10 000 × volumetric scale factors) (Figure 3.4). The fatty acid composition of fungal and microalgal biomass from different scales also showed acceptable match. This has been achieved despite the absence of control options, such as pH and DO, in Duetz-MTPS, and the difficult fungal growth characteristics, such as severe wall growth. However, the heterotrophic microalga *C. cohnii* reached significantly higher biomass and lipid concentration in MTPS than in 1.5 L bioreactor, probably due to shear force sensitivity of this species. Application of optical online sensors in MTPS for the screening of filamentous fungi is problematic due to complex growth morphology. For these reasons at/off-line bioprocess monitoring of filamentous fungi in MTPS is a more viable approach [55]. We used the presented method in **Paper I**, namely HTS-FTIR spectroscopy to monitor lipid accumulation during cultivations, and these curves correlated well with reference curves for total lipid content of biomass, obtained by the GC analyses (Figure 3.3).

Good scalability has been reported before from state-of-the-art MTPS up to 15m^3 bioreactors, however, most of these studies have been performed with unicellular microorganisms (bacteria and yeasts) [45, 48, 49, 52, 54, 55, 88]. Scalability of filamentous fungi from MTPS to bioreactors is rarely discussed and the few studies performed to date were performed at very low substrate concentration (i.e. 5 g/L glucose) [52]. Our results demonstrated that the Duetz-MTPS can be used for the cost-efficient and scalable high-throughput screening of both single-cell, and multicellular oleaginous microorganisms.

Figure 3.3 a1-c1) FTIR spectra of *C. cohnii*, *M. circinelloides* and *M. alpina* at first and last day of cultivation **a2-c2)** Lipid accumulation based on FTIR C=O ester peak height (from pre-processed spectra) and reference GC total lipid (wt%) data

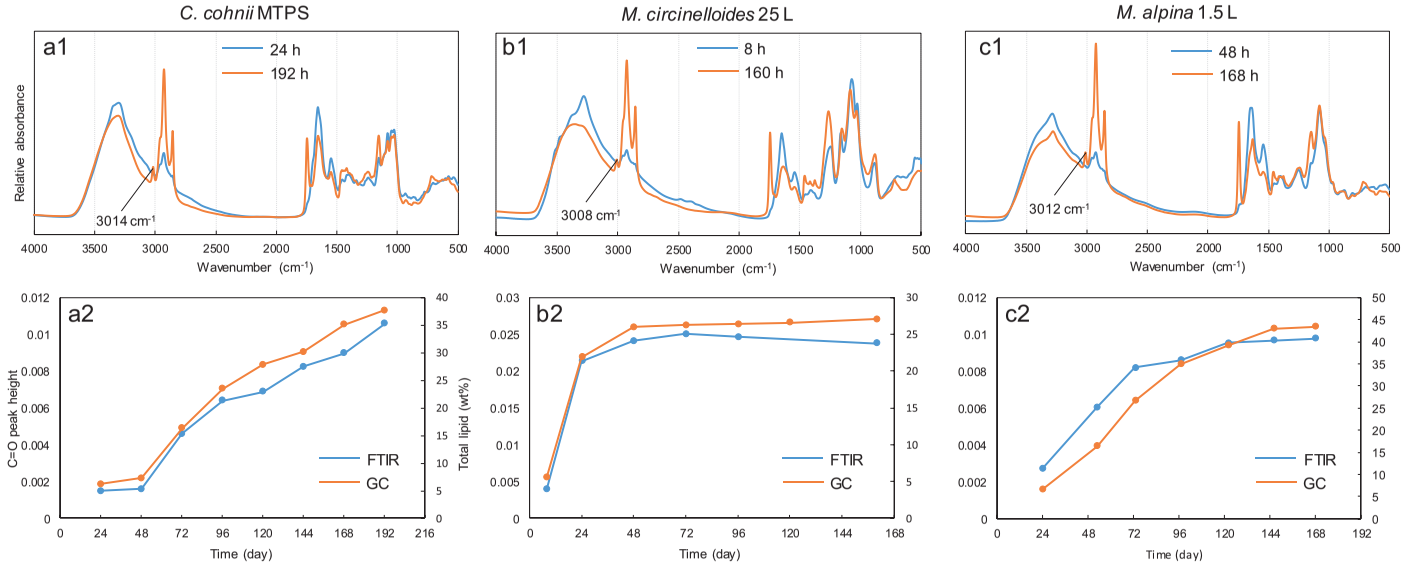

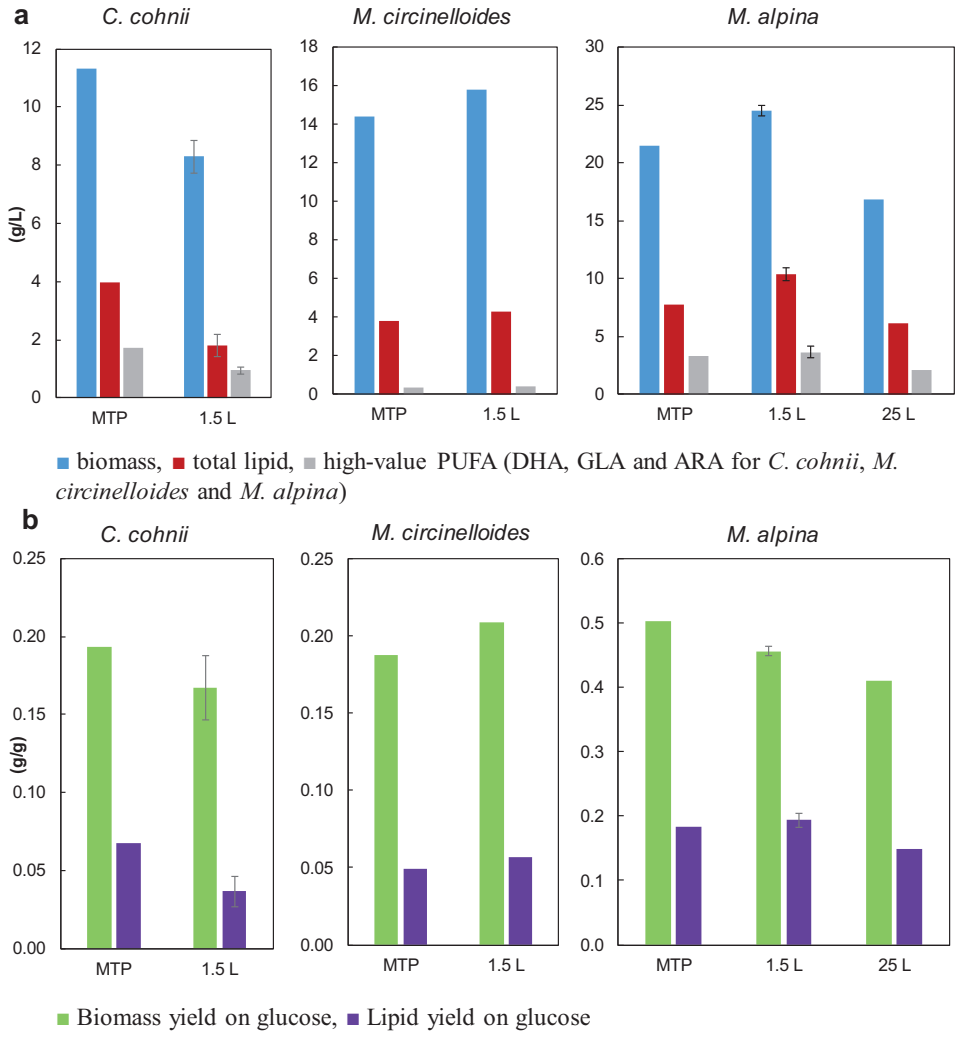

Figure 3.4 Comparison of physiological fermentation parameters of *C. cohnii*, *M. circinelloides* and *M. alpina* in Duetz-MTPS, 1.5 L and 25 L working volumes bioreactor. **a)** biomass, total lipid, high-value PUFA (g/L), **b)** biomass and lipid yield on glucose (g/g)

3.4 Paper IV: High-throughput screening of Mucoromycota fungi for the production of low-, and high-value lipids

The developed scalable and reproducible high-throughput screening system was validated in **Paper IV** by testing one hundred Mucoromycota fungi from 8 different genera: *Mucor* (42), *Amylomyces* (1), *Rhizopus* (9), *Umbelopsis* (9), *Absidia* (10), *Cunninghamella* (5), *Lichtheimia* (3) and *Mortierella* (21). Mucoromycota fungi are known as a good source of PUFA and also as promising candidates for lipid production on low-value substrates for biodiesel production. The Duetz-MTPS allowed highly reproducible cultivation of Mucoromycota fungi without compromising lipid production in the high glucose (90 g/L) medium. The top strains found in the screening for biomass, lipid content, total lipid and high-value PUFA can be seen in Table 3.3, while the fatty acid composition of the investigated fungi can be seen in Figure 3.5 a-b summarized in the PCA score and loading plots. Gamma-linolenic acid (GLA) content was the highest in *Mucor fragilis* UBOCC-A-109196 (24.5%) and in *Cunninghamella echinulata* VKM F-470 (24.0%, 1.17 g/L). For the first time, we observed concomitant alpha-linolenic (ALA) acid and GLA production in psychrophile (15 °C) *Mucor flavus* strains (max 13.0% ALA in *M. flavus* CCM 8086). Arachidonic acid (ARA) was found in all *Mortierella* strains ranging from 5.6% to 41.1% in *M. alpina* ATCC 32222 (1.48 g/L). Low cultivation temperature (15 °C) activated the temperature sensitive Δ17 desaturase enzyme in *Mortierella*, resulting in max. 11.0% eicosapentaenoic acid (EPA) production in *M. humilis* VKM F-1494 (see Figure 1.3). *Cunninghamella blakesleaana* CCM-705, *Umbelopsis vinacea* CCM F-539, UBOCC-A-101347 strains showed very good growth (more than 22 g/L dry cell weight), lipid production (7.0 - 8.3 g/L) and fatty acid composition (high palmitic, oleic acid content and low PUFA) that makes them attractive candidates for biodiesel production. Although *Absidia* spp. are not often mentioned in literature as promising oleaginous fungi, in our study several *Absidia* strains reached more than 30% lipid content. In particular, *A. glauca* CCM 451 had the highest lipid content (47.2 ± 1.8%) from all the one hundred tested strains. FTIR spectroscopy of fungal biomass was conducted as a rapid method for assessing lipid production potential (Figure 3.5 c-d). Analysis of lipid-related peaks in the FTIR spectra of fungal biomass showed only low to acceptable correlation with gas chromatography (GC) total lipid data ($0.14<R^2<0.67$). In order to predict lipid content of fungi with more precision, multivariate regression method (PLSR) was needed ($0.62<R^2<0.80$).

Many screening studies have already been performed with Mucoromycota strains focusing on the production of a particular high-value PUFA, such as GLA [6, 43] or ARA [81, 144, 145]. These studies were performed either in shake flasks [6, 40, 43, 82] or agar-based solid cultivation [81, 82, 144], often without running replicate cultures, making the results statistically questionable. Furthermore, agar-based screening results do not represent lipid production potential that can be obtained in an optimized submerged condition. In our study much higher lipid production (27% vs. 13% of dry cell weight on average for 11 strains) and higher PUFA content of the oil was achieved than in the screening study by Eroshin *et*

al. [81] on PDA medium. Several strains cultivated in the high-throughput Duetz-MTPS showed very similar fatty acid profiles to those obtained in submerged culture in SFs [6, 19, 145, 146], saving medium cost and time to perform the screening. Our results demonstrated that Duetz-MTPS is capable of the reproducible high-throughput screening of oleaginous microorganisms (Mucoromycota fungi in the present study). Several promising strains have been found for high-value PUFA and biodiesel production that will be further tested on low-value substrates, such as animal fat and lignocellulosic wastes.

Table 3.3 Top ten strains in the screening study of one hundred Mucoromycota fungi based on biomass, lipid content of biomass, total lipid, GLA and ARA content of the oil results

	Biomass (g/L)		Total lipid (wt%)
Umbelopsis vinacea UBOCC-A-101347	25.6	Absidia glauca CCM 451	47.2
Cunninghamella blakesleeana CCM F-705	22.6	Mortierella alpina ATCC 32222	44.5
Umbelopsis vinacea CCM F-539	22.6	Absidia glauca CCM 450	39.1
Cunninghamella blakesleeana VKM F-993	20.0	Cunninghamella echinulata VKM F-439	37.2
Umbelopsis isabellina VKM F-525	19.6	Cunninghamella blakesleeana CCM F-705	36.7
Lichtheimia corymbifera CCM 8077	17.8	Cunninghamella echinulata VKM F-470	36.5
Absidia coerulea CCM 8230	17.5	Absidia cylindrospora VKM F-1632	36.5
Absidia glauca CCM 450	16.6	Absidia coerulea VKM F-627	35.6
Umbelopsis ramanniana VKM F-502	15.3	Absidia glauca UBOCC-A-101330	34.8
Mucor circinelloides VI 04473	15.1	Mortierella gemmifera VKM F-1651	34.8

	GLA (% total FAs)		ARA (% total FAs)
Mucor fragilis UBOCC-A-109196	24.5	Mortierella alpina ATCC 32222	41.1
Cunninghamella echinulata VKM F-470	24.0	Mortierella hyalina VKM F-1854	26.7
Mucor mucedo UBOCC-A-101353	21.5	Mortierella alpina UBOCC-A-112046	24.6
Mucor racemosus UBOCC-A-111127	20.9	Mortierella alpina UBOCC-A-112047	20.0
Mucor flavus VKM F-1110	20.9	Mortierella gamsii VKM F-1529	18.9
Mucor lanceolatus UBOCC-A-101355	20.9	Mortierella gamsii VKM F-1641	17.9
Rhizopus stolonifer VKM F-400	20.3	Mortierella globulifera VKM F-1408	16.1
Cunninghamella echinulata VKM F-439	19.7	Mortierella gemmifera VKM F-1252	15.9
Rhizopus stolonifer CCM F-445	19.4	Mortierella gamsii VKM F-1402	15.3
Rhizopus stolonifer VKM F-399	19.0	Mortierella humilis VKM F-1494	11.3

	Total lipid (g/L)
Cunninghamella blakesleeana CCM F-705	8.3
Umbelopsis vinacea CCM F-539	7.9
Umbelopsis vinacea UBOCC-A-101347	7.0
Absidia glauca CCM 450	6.5
Absidia glauca CCM 451	6.2
Umbelopsis isabellina VKM F-525	6.0
Absidia coerulea CCM 8230	5.3
Cunninghamella blakesleeana VKM F-993	5.3
Mortierella gemmifera VKM F-1631	5.1
Cunninghamella echinulata VKM F-470	4.9

Figure 3.5 PCA scores and loadings of the one hundred Mucoromycota strains screened for single cell oil production in the Duetz-MTPS. **a-b**: GC fatty acid composition data, **c-d**: HTS-FTIR data. Strain numbers can be found in Table 4

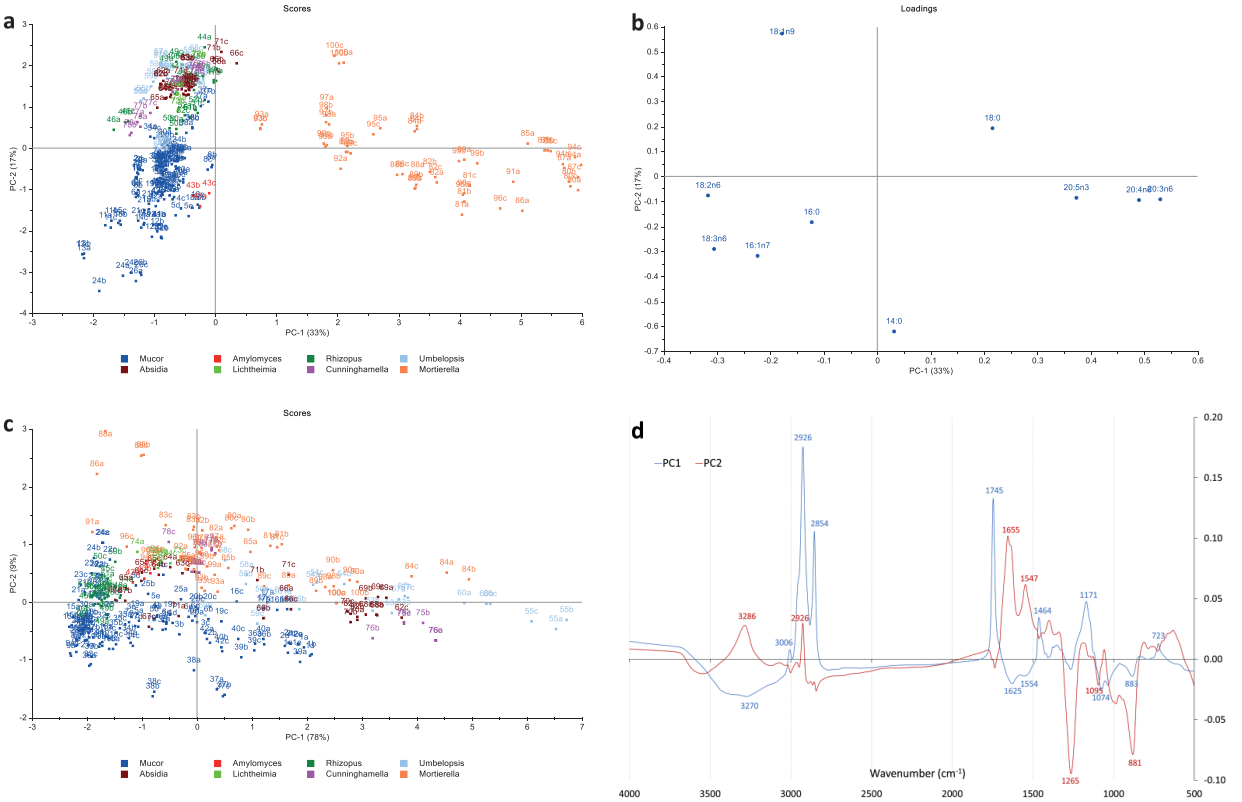

4 Conclusion and future prospects

In this PhD thesis, we studied the possibility of rapid screening of filamentous fungi for single cell oil production in the Duetz-microtiter plate system combined with high-throughput FTIR spectroscopy and multivariate data analysis. Due to advances in metabolic engineering, the throughput of traditional screening approach via shake flask cultivation is not sufficient anymore. Microtiter plates are routinely used nowadays for the screening of unicellular microorganisms such as bacteria and yeasts, since it offers very high throughput saving time and cost for the establishment of bioprocesses. Reproducible and scalable cultivation of filamentous fungi in microplate-based system, however, is a more challenging task. Complex growth morphology and lack of control options for process parameters due to adherent wall growth are the main obstacles. Quite often the overall throughput of microbial screening system is insufficient due to the laborious, analytical techniques. In single cell oil research, the traditional analysis of intracellular lipids is GC-FID or GC-MS. This procedure involves the tedious extraction and transesterification process of TAGs to FAMEs, generating a high amount of toxic waste and also a trained analyst is required. Furthermore, the GC analysis itself requires approximately half an hour to measure one sample. FTIR spectroscopy, a rapid, non-destructive analytical method is more suitable for high-throughput applications. It provides a precise biochemical fingerprint of main macromolecules, lipids, carbohydrates, and proteins in microbial biomass and can also be used for quantitative measurement of extracellular metabolites and substrates.

In **Paper I** we tested the suitability of the Duetz-microtiter plate system combined with high-throughput FTIR spectroscopy for the fast screening of three model oleaginous fungi, *M.circinelloides*, *U. isabellina* and *P. glabrum*. We showed that after optimization of culture conditions excellent reproducibility can be achieved. FTIR spectroscopy combined with chemometric techniques, such as principal components analysis and partial least squares regression, proved to be a suitable high-throughput analytical method for the screening of oleaginous microorganisms. Good prediction models have been developed for total lipid, lipid classes, and individual fatty acids. In **Paper II** we assessed high-throughput FTIR spectroscopy as a unified analytical method for the measurement of intra- and extracellular compounds in microbial screenings. We compared ATR and HTS-FTIR spectroscopy methods for the quantitative determination of glucose substrate and extracellular metabolite citric acid from *P. glabrum*. Both measurement methods resulted in almost equally good prediction models after adequate preprocessing of HTS-FTIR spectra by averaging technical replicates and applying derivative transformation. While ATR method is an established method for bioprocessing monitoring for bioreactors, HTS method is more suitable for high-throughput screening applications. We have concluded that HTS-FTIR method can be successfully applied as a multi-analyte analytical method for both intra- and extracellular metabolites and substrates in microbial screening studies. In **Paper III** we studied the scalability of microplate cultivated oleaginous filamentous fungi *M. circinelloides*, *M. alpina* and a heterotrophic microalga *C. cohnii* to controlled benchtop (1.5 L) and pre-pilot scale (25 L) stirred-tank bioreactors. Despite some differences in initial growth rate, very similar

maximal biomass, lipid yields and fatty acid composition were observed at all scales (less than 30% difference for all tested parameters) for the filamentous fungi. In case of *C. cohnii*, biomass and lipid yield were significantly higher in Duetz-MTPS than in stirred-tank bioreactor (most likely due to shear stress sensitivity of this microalga) and were in agreement with industrial requirements. In **Paper IV** the developed high-throughput cultivation analytical platform was validated by testing one hundred fungi from Mucoromycota phylum for single cell oil production. Several promising candidates have been identified by this approach for high-value PUFA and biodiesel production with very good reproducibility. FTIR spectroscopy of fungal biomass served as a rapid pre-screening analytical method for detection of promising lipid producer microorganisms, before performing the GC analysis.

The establishment of a fungal strain collection and the information obtained from the screening study (**Paper IV**) will contribute to develop processes for the production of high-value PUFAs and biodiesel from low-value animal fat ('Lipofungi' project) and lignocellulosic waste ('Bio4Fuel' projects). Another important aspect of the screening was to create a sufficiently big dataset for the robust calibration of GC fatty acid data versus FTIR spectral data of fungal biomass. We are currently examining to which extent FTIR spectroscopy can be applied for the prediction of total lipid content of the cells, summed fatty acid parameters (SAT, MUFA, PUFA, unsaturation index) and individual fatty acids. Different taxonomical levels are going to be considered from intra-species to inter-phyla. Research results are expected to be published soon.

An exciting prospect is an update of the current screening setting by the automation of sample preparation steps for FTIR measurement from Duetz-MTPS cultivation. A robotic system is being built at the RealTek/NMBU to perform biomass-liquid separation, washing of biomass, homogenization and pipetting on the silicone plates [139]. The fully automated high-throughput cultivation-analytical platform would allow even more efficient screening of microbial bioprocesses in the future.

5 Bibliography

1. Ratledge C: **Microbial production of polyunsaturated fatty acids as nutraceuticals.** *Microbial production of food ingredients, enzymes and nutraceuticals UK: Woodhead Publishing Co* 2013**:**531-558.
2. Rossi M, Amaretti A, Raimondi S, Leonardi A: **Getting lipids for biodiesel production from oleaginous fungi.** In *Biodiesel-Feedstocks and Processing Technologies.* InTech; 2011.
3. Bharathiraja B, Sridharan S, Sowmya V, Yuvaraj D, Praveenkumar R: **Microbial Oil-A Plausible Alternate Resource for Food and Fuel Application.** *Bioresource Technology* 2017.
4. Finco AMdO, Mamani LDG, Carvalho JCd, de Melo Pereira GV, Thomaz-Soccol V, Soccol CR: **Technological trends and market perspectives for production of microbial oils rich in omega-3.** *Critical reviews in biotechnology* 2017, **37:**656-671.
5. Ochsenreither K, Glück C, Stressler T, Fischer L, Syldatk C: **Production strategies and applications of microbial single cell oils.** *Frontiers in microbiology* 2016, **7**.
6. Ratledge C: **Microbial production of gamma-linolenic acid.** *Handbook of Functional Lipids edited by C Akoh, CRC Press, Boca Raton, FL, USA* 2005**:**19.
7. Papanikolaou S, Aggelis G: **Lipids of oleaginous yeasts. Part I: Biochemistry of single cell oil production.** *European Journal of Lipid Science and Technology* 2011, **113:**1031-1051.
8. Ratledge C: **Fatty acid biosynthesis in microorganisms being used for single cell oil production.** *Biochimie* 2004, **86:**807-815.
9. Hsieh C-H, Wu W-T: **Cultivation of microalgae for oil production with a cultivation strategy of urea limitation.** *Bioresource technology* 2009, **100:**3921-3926.
10. Araujo GS, Matos LJ, Gonçalves LR, Fernandes FA, Farias WR: **Bioprospecting for oil producing microalgal strains: evaluation of oil and biomass production for ten microalgal strains.** *Bioresource technology* 2011, **102:**5248-5250.
11. Gouveia L, Marques AE, Da Silva TL, Reis A: **Neochloris oleabundans UTEX# 1185: a suitable renewable lipid source for biofuel production.** *Journal of industrial microbiology & biotechnology* 2009, **36:**821-826.
12. De Swaaf M, Pronk J, Sijtsma L: **Fed-batch cultivation of the docosahexaenoic-acid-producing marine alga Crypthecodinium cohnii on ethanol.** *Applied microbiology and biotechnology* 2003, **61:**40-43.
13. Patil KP, Gogate PR: **Improved synthesis of docosahexaenoic acid (DHA) using Schizochytrium limacinum SR21 and sustainable media.** *Chemical Engineering Journal* 2015, **268:**187-196.
14. Zhao X, Kong X, Hua Y, Feng B, Zhao ZK: **Medium optimization for lipid production through co-fermentation of glucose and xylose by the oleaginous yeast Lipomyces starkeyi.** *European Journal of Lipid Science and Technology* 2008, **110:**405-412.
15. Li Y, Zhao ZK, Bai F: **High-density cultivation of oleaginous yeast Rhodosporidium toruloides Y4 in fed-batch culture.** *Enzyme and microbial technology* 2007, **41:**312-317.
16. Zhu L, Zong M, Wu H: **Efficient lipid production with Trichosporonfermentans and its use for biodiesel preparation.** *Bioresource Technology* 2008, **99:**7881-7885.
17. Meesters P, Huijberts G, Eggink G: **High-cell-density cultivation of the lipid accumulating yeast Cryptococcus curvatus using glycerol as a carbon source.** *Applied microbiology and biotechnology* 1996, **45:**575-579.
18. Papanikolaou S, Chevalot I, Galiotou-Panayotou M, Komaitis M, Marc I, Aggelis G: **Industrial derivative of tallow: a promising renewable substrate for microbial lipid, single-cell protein and lipase production by Yarrowia lipolytica.** *Electronic Journal of Biotechnology* 2007, **10:**425-435.
19. Fakas S, Papanikolaou S, Batsos A, Galiotou-Panayotou M, Mallouchos A, Aggelis G: **Evaluating renewable carbon sources as substrates for single cell oil production by**

Cunninghamella echinulata and Mortierella isabellina. *Biomass and Bioenergy* 2009, **33:**573-580.
20. Hui L, Wan C, Hai-Tao D, Xue-Jiao C, Qi-Fa Z, Yu-Hua Z: **Direct microbial conversion of wheat straw into lipid by a cellulolytic fungus of Aspergillus oryzae A-4 in solid-state fermentation.** *Bioresource technology* 2010, **101:**7556-7562.
21. Nie Z-K, Ji X-J, Shang J-S, Zhang A-H, Ren L-J, Huang H: **Arachidonic acid-rich oil production by Mortierella alpina with different gas distributors.** *Bioprocess and biosystems engineering* 2014, **37:**1127-1132.
22. Tang X, Chen H, Chen YQ, Chen W, Garre V, Song Y, Ratledge C: **Comparison of biochemical activities between high and low lipid-producing strains of Mucor circinelloides: an explanation for the high oleaginicity of strain WJ11.** *PloS one* 2015, **10:**e0128396.
23. Papanikolaou S, Komaitis M, Aggelis G: **Single cell oil (SCO) production by Mortierella isabellina grown on high-sugar content media.** *Bioresource Technology* 2004, **95:**287-291.
24. Kavadia A, Komaitis M, Chevalot I, Blanchard F, Marc I, Aggelis G: **Lipid and γ-linolenic acid accumulation in strains of Zygomycetes growing on glucose.** *Journal of the American Oil Chemists' Society* 2001, **78:**341-346.
25. Santala S, Efimova E, Kivinen V, Larjo A, Aho T, Karp M, Santala V: **Improved triacylglycerol production in Acinetobacter baylyi ADP1 by metabolic engineering.** *Microbial cell factories* 2011, **10:**36.
26. Alvarez HM, Souto MF, Viale A, Pucci OH: **Biosynthesis of fatty acids and triacylglycerols by 2, 6, 10, 14-tetramethyl pentadecane-grown cells of Nocardia globerula 432.** *FEMS microbiology letters* 2001, **200:**195-200.
27. Arabolaza A, Rodriguez E, Altabe S, Alvarez H, Gramajo H: **Multiple pathways for triacylglycerol biosynthesis in Streptomyces coelicolor.** *Applied and environmental microbiology* 2008, **74:**2573-2582.
28. Ward OP, Singh A: **Omega-3/6 fatty acids: alternative sources of production.** *Process Biochemistry* 2005, **40:**3627-3652.
29. Lee JM, Lee H, Kang S, Park WJ: **Fatty acid desaturases, polyunsaturated fatty acid regulation, and biotechnological advances.** *Nutrients* 2016, **8:**23.
30. Ruiz-López N, Sayanova O, Napier JA, Haslam RP: **Metabolic engineering of the omega-3 long chain polyunsaturated fatty acid biosynthetic pathway into transgenic plants.** *Journal of experimental botany* 2012, **63:**2397-2410.
31. **DSM in Food, Beverages & Dietary Supplements, Nutritional lipids** [https://www.dsm.com/markets/foodandbeverages/en_US/products/nutritional-lipids.html]
32. **Arachidonic Acid** [https://www.cargill.com/food-bev/na/arachidonic-acid]
33. Kyle DJ: **Arachidonic acid and methods for the production and use thereof.** Google Patents; 1997.
34. Meng X, Yang J, Xu X, Zhang L, Nie Q, Xian M: **Biodiesel production from oleaginous microorganisms.** *Renewable energy* 2009, **34:**1-5.
35. Bhuiya M, Rasul M, Khan MMK, Ashwath N, Azad AK, Hazrat M: **Second generation biodiesel: potential alternative to-edible oil-derived biodiesel.** *Energy Procedia* 2014, **61:**1969-1972.
36. Zhang J, Hu B: **Microbial biodiesel production-oil feedstocks produced from microbial cell cultivations.** In *Biodiesel-Feedstocks and Processing Technologies.* InTech; 2011.
37. Magdouli S, Yan S, Tyagi R, Surampalli R: **Heterotrophic microorganisms: a promising source for biodiesel production.** *Critical Reviews in Environmental Science and Technology* 2014, **44:**416-453.
38. Ramírez-Verduzco LF, Rodríguez-Rodríguez JE, del Rayo Jaramillo-Jacob A: **Predicting cetane number, kinematic viscosity, density and higher heating value of biodiesel from its fatty acid methyl ester composition.** *Fuel* 2012, **91:**102-111.
39. Laurens LM, Wolfrum EJ: **Feasibility of spectroscopic characterization of algal lipids: chemometric correlation of NIR and FTIR spectra with exogenous lipids in algal biomass.** *BioEnergy Research* 2011, **4:**22-35.

40. Buráňová L, Řezanka T, Jandera A: **Screening for strains of the genusMortierella, showing elevated production of highly unsaturated fatty acids.** *Folia microbiologica* 1990, **35:**578-582.
41. Chatzifragkou A, Makri A, Belka A, Bellou S, Mavrou M, Mastoridou M, Mystrioti P, Onjaro G, Aggelis G, Papanikolaou S: **Biotechnological conversions of biodiesel derived waste glycerol by yeast and fungal species.** *Energy* 2011, **36:**1097-1108.
42. Wang X-L, Han W-J, Peng K, Zhang H-Y: **Screening of Oleaginous Microorganisms from Filamentous Fungi for Microbial Lipids Production.** In *Bioinformatics and Biomedical Engineering (iCBBE), 2010 4th International Conference on*. IEEE; 2010: 1-4.
43. Weete J, Shewmaker F, Gandhi S: **γ-Linolenic acid in zygomycetous fungi: Syzygites megalocarpus.** *Journal of the American Oil Chemists' Society* 1998, **75:**1367-1372.
44. Broughton R: **Omega 3 fatty acids: identification of novel fungal and chromistal sources.** Royal Holloway, University of London2012.
45. Silk N, Denby S, Lewis G, Kuiper M, Hatton D, Field R, Baganz F, Lye GJ: **Fed-batch operation of an industrial cell culture process in shaken microwells.** *Biotechnology letters* 2010, **32:**73.
46. Knudsen PB: **Development of scalable high throughput fermentation approaches for physiological characterisation of yeast and filamentous fungi.** Technical University of Denmark2015.
47. Bills G, Platas G, Fillola A, Jimenez M, Collado J, Vicente F, Martin J, Gonzalez A, Bur-Zimmermann J, Tormo J: **Enhancement of antibiotic and secondary metabolite detection from filamentous fungi by growth on nutritional arrays.** *Journal of applied microbiology* 2008, **104:**1644-1658.
48. Lübbehüsen TL, Nielsen J, McIntyre M: **Morphology and physiology of the dimorphic fungus Mucor circinelloides (syn. M. racemosus) during anaerobic growth.** *Mycological research* 2003, **107:**223-230.
49. Long Q, Liu X, Yang Y, Li L, Harvey L, McNeil B, Bai Z: **The development and application of high throughput cultivation technology in bioprocess development.** *Journal of biotechnology* 2014, **192:**323-338.
50. Sohoni SV, Bapat PM, Lantz AE: **Robust, small-scale cultivation platform for Streptomyces coelicolor.** *Microbial cell factories* 2012, **11:**9.
51. Wu T, Zhou Y: **An intelligent automation platform for rapid bioprocess design.** *Journal of laboratory automation* 2014, **19:**381-393.
52. Knudsen PB: **Development of scalable high throughput fermentation approaches for physiological characterisation of yeast and filamentous fungi.** Technical University of Denmark2015.
53. Hegab HM, ElMekawy A, Stakenborg T: **Review of microfluidic microbioreactor technology for high-throughput submerged microbiological cultivation.** *Biomicrofluidics* 2013, **7:**021502.
54. Kensy F, Engelbrecht C, Büchs J: **Scale-up from microtiter plate to laboratory fermenter: evaluation by online monitoring techniques of growth and protein expression in Escherichia coli and Hansenula polymorpha fermentations.** *Microbial cell factories* 2009, **8:**68.
55. Posch AE, Herwig C, Spadiut O: **Science-based bioprocess design for filamentous fungi.** *Trends in biotechnology* 2013, **31:**37-44.
56. Linde T, Hansen N, Lübeck M, Lübeck PS: **Fermentation in 24-well plates is an efficient screening platform for filamentous fungi.** *Letters in applied microbiology* 2014, **59:**224-230.
57. Siebenberg S, Bapat PM, Lantz AE, Gust B, Heide L: **Reducing the variability of antibiotic production in Streptomyces by cultivation in 24-square deepwell plates.** *Journal of bioscience and bioengineering* 2010, **109:**230-234.
58. Verdoes JC, Punt PJ, Burlingame R, Bartels J, Dijk Rv, Slump E, Meens M, Joosten R, Emalfarb M: **A dedicated vector for efficient library construction and high throughput screening in the hyphal fungus Chrysosporium lucknowense.** *Industrial Biotechnology* 2007, **3:**48-57.

59. Shapaval V, Møretrø T, Suso HP, Åsli AW, Schmitt J, Lillehaug D, Martens H, Böcker U, Kohler A: **A high-throughput microcultivation protocol for FTIR spectroscopic characterization and identification of fungi.** *Journal of biophotonics* 2010, **3:**512-521.
60. Shapaval V, Møretrø T, Wold Åsli A, Suso H, Schmitt J, Lillehaug D, Kohler A: **A novel library-independent approach based on high-throughput cultivation in Bioscreen and fingerprinting by FTIR spectroscopy for microbial source tracking in food industry.** *Letters in applied microbiology* 2017.
61. Shapaval V, Schmitt J, Møretrø T, Suso H, Skaar I, Åsli A, Lillehaug D, Kohler A: **Characterization of food spoilage fungi by FTIR spectroscopy.** *Journal of applied microbiology* 2013, **114:**788-796.
62. Shapaval V, Afseth NK, Vogt G, Kohler A: **Fourier transform infrared spectroscopy for the prediction of fatty acid profiles in Mucor fungi grown in media with different carbon sources.** *Microbial cell factories* 2014, **13:**86.
63. Kensy FT: **Online Monitoring in Continuously Shaken Microtiter Plates for Scalable Upstream Bioprocessing.** *Doctoral thesis, RWTH Aachen University, Aachen, Germany, 2010*
64. Beneyton T, Wijaya IPM, Postros P, Najah M, Leblond P, Couvent A, Mayot E, Griffiths AD, Drevelle A: **High-throughput screening of filamentous fungi using nanoliter-range droplet-based microfluidics.** *Scientific reports* 2016, **6:**27223.
65. [http://www.enzyscreen.com/home.htm]
66. Chaturvedi K, Sun SY, O'Brien T, Liu YJ, Brooks JW: **Comparison of the behavior of CHO cells during cultivation in 24-square deep well microplates and conventional shake flask systems.** *Biotechnology Reports* 2014, **1:**22-26.
67. Hansen HG, Nilsson CN, Lund AM, Kol S, Grav LM, Lundqvist M, Rockberg J, Lee GM, Andersen MR, Kildegaard HF: **Versatile microscale screening platform for improving recombinant protein productivity in Chinese hamster ovary cells.** *Scientific reports* 2015, **5:**18016.
68. Haberbeck L, Oliveira R, Vivijs B, Wenseleers T, Aertsen A, Michiels C, Geeraerd A: **Variability in growth/no growth boundaries of 188 different Escherichia coli strains reveals that approximately 75% have a higher growth probability under low pH conditions than E. coli O157: H7 strain ATCC 43888.** *Food microbiology* 2015, **45:**222-230.
69. Marques MP, Carvalho F, Magalhães S, Cabral JM, Fernandes P: **Screening for suitable solvents as substrate carriers for the microbial side-chain cleavage of sitosterol using microtitre plates.** *Process Biochemistry* 2009, **44:**556-561.
70. Minas W, Bailey JE, Duetz W: **Streptomycetes in micro-cultures: Growth, production of secondary metabolites, and storage and retrieval in the 96–well format.** *Antonie Van Leeuwenhoek* 2000, **78:**297-305.
71. Morschett H, Wiechert W, Oldiges M: **Automation of a Nile red staining assay enables high throughput quantification of microalgal lipid production.** *Microbial cell factories* 2016, **15:**34.
72. Khalil ZG, Kalansuriya P, Capon RJ: **Lipopolysaccharide (LPS) stimulation of fungal secondary metabolism.** *Mycology* 2014, **5:**168-178.
73. Ami D, Posteri R, Mereghetti P, Porro D, Doglia SM, Branduardi P: **Fourier transform infrared spectroscopy as a method to study lipid accumulation in oleaginous yeasts.** *Biotechnology for biofuels* 2014, **7:**12.
74. Challagulla V, Walsh KB, Subedi P: **Microalgal fatty acid composition: rapid assessment using near-infrared spectroscopy.** *Journal of applied phycology* 2016, **28:**85-94.
75. Dean AP, Sigee DC, Estrada B, Pittman JK: **Using FTIR spectroscopy for rapid determination of lipid accumulation in response to nitrogen limitation in freshwater microalgae.** *Bioresource technology* 2010, **101:**4499-4507.
76. Liu B, Liu J, Chen T, Yang B, Jiang Y, Wei D, Chen F: **Rapid characterization of fatty acids in oleaginous microalgae by near-infrared spectroscopy.** *International journal of molecular sciences* 2015, **16:**7045-7056.

77. Peng X, Chen H: **Rapid estimation of single cell oil content of solid-state fermented mass using near-infrared spectroscopy.** *Bioresource technology* 2008, **99:**8869-8872.
78. Rumin J, Bonnefond H, Saint-Jean B, Rouxel C, Sciandra A, Bernard O, Cadoret J-P, Bougaran G: **The use of fluorescent Nile red and BODIPY for lipid measurement in microalgae.** *Biotechnology for biofuels* 2015, **8:**42.
79. Bajhaiya AK, Dean AP, Driver T, Trivedi DK, Rattray NJ, Allwood JW, Goodacre R, Pittman JK: **High-throughput metabolic screening of microalgae genetic variation in response to nutrient limitation.** *Metabolomics* 2016, **12:**9.
80. Pons M-N, Le Bonté S, Potier O: **Spectral analysis and fingerprinting for biomedia characterisation.** *Journal of Biotechnology* 2004, **113:**211-230.
81. Eroshin V, Dedyukhina E, Chistyakova T, Zhelifonova V, Kurtzman C, Bothast R: **Arachidonic-acid production by species of Mortierella.** *World Journal of Microbiology and Biotechnology* 1996, **12:**91-96.
82. Grantina-Ievina L, Berzina A, Nikolajeva V, Mekss P, Muiznieks I: **Production of fatty acids by Mortierella and Umbelopsis species isolated from temperate climate soils.** *Environ Exp Biol* 2014, **12:**15-27.
83. Yadav DR, Kim SW, Adhikari M, Um YH, Kim HS, Kim C, Lee HB, Lee YS: **Three new records of Mortierella species isolated from crop field soil in Korea.** *Mycobiology* 2015, **43:**203-209.
84. Kitcha S, Cheirsilp B: **Screening of oleaginous yeasts and optimization for lipid production using crude glycerol as a carbon source.** *Energy Procedia* 2011, **9:**274-282.
85. Tilay A, Annapure U: **Novel simplified and rapid method for screening and isolation of polyunsaturated fatty acids producing marine bacteria.** *Biotechnology research international* 2012, **2012**.
86. Isleten-Hosoglu M, Gultepe I, Elibol M: **Optimization of carbon and nitrogen sources for biomass and lipid production by Chlorella saccharophila under heterotrophic conditions and development of Nile red fluorescence based method for quantification of its neutral lipid content.** *Biochemical engineering journal* 2012, **61:**11-19.
87. Sant'Anna C, Ferreira VS, Monnerat MM, Pinto RF, de Souza W, Martins JL: **Microscopy approaches to screening oleaginous microorganisms and evaluating their potential as feedstock for biodiesel production.** *Microscopy: advances in scientific research and education* 2014, **1:**484-491.
88. Back A, Rossignol T, Krier F, Nicaud J-M, Dhulster P: **High-throughput fermentation screening for the yeast Yarrowia lipolytica with real-time monitoring of biomass and lipid production.** *Microbial cell factories* 2016, **15:**147.
89. Jape A, Harsulkar A, Sapre V: **Modified Sudan Black B staining method for rapid screening of oleaginous marine yeasts.** *International journal of current microbiology and applied sciences* 2014, **3:**41-46.
90. Kimura K, Yamaoka M, Kamisaka Y: **Rapid estimation of lipids in oleaginous fungi and yeasts using Nile red fluorescence.** *Journal of Microbiological Methods* 2004, **56:**331-338.
91. Poli JS, Dallé P, Senter L, Mendes S, Ramirez M, Vainstein MH, Valente P: **Fatty acid methyl esters produced by oleaginous yeast Yarrowia lipolytica QU21: an alternative for vegetable oils.** *Revista Brasileira de Biociências* 2013, **11**.
92. Signori L, Ami D, Posteri R, Giuzzi A, Mereghetti P, Porro D, Branduardi P: **Assessing an effective feeding strategy to optimize crude glycerol utilization as sustainable carbon source for lipid accumulation in oleaginous yeasts.** *Microbial cell factories* 2016, **15:**75.
93. Abu-Elreesh G, Abd-El-Haleem D: **Promising oleaginous filamentous fungi as biodiesel feed stocks: Screening and identification.** *European Journal of Experimental Biology* 2014, **4:**576-582.
94. de la Jara A, Mendoza H, Martel A, Molina C, Nordström L, de la Rosa V, Díaz R: **Flow cytometric determination of lipid content in a marine dinoflagellate, Crypthecodinium cohnii.** *Journal of Applied Phycology* 2003, **15:**433-438.
95. Guzmán HM, de la Jara Valido A, Duarte LC, Presmanes KF: **Estimate by means of flow cytometry of variation in composition of fatty acids from Tetraselmis suecica in response to culture conditions.** *Aquaculture international* 2010, **18:**189-199.

96. Cirulis JT, Strasser BC, Scott JA, Ross GM: **Optimization of staining conditions for microalgae with three lipophilic dyes to reduce precipitation and fluorescence variability.** *Cytometry Part A* 2012, **81:**618-626.
97. Chen W, Zhang C, Song L, Sommerfeld M, Hu Q: **A high throughput Nile red method for quantitative measurement of neutral lipids in microalgae.** *Journal of microbiological methods* 2009, **77:**41-47.
98. Nawrocka A, Lamorska J: **Determination of food quality by using spectroscopic methods.** In *Advances in agrophysical research.* InTech; 2013.
99. Santos C, Fraga ME, Kozakiewicz Z, Lima N: **Fourier transform infrared as a powerful technique for the identification and characterization of filamentous fungi and yeasts.** *Research in microbiology* 2010, **161:**168-175.
100. Ödman P: *On-line Monitoring of Microbial Cultivation Processes Using Near Infrared Spectroscopy and Multi-wavelength Fluorescence: PhD Thesis.* Center for Microbial Biotechnology, Technical University of Denmark; 2010.
101. **Infrared spectroscopy** [https://en.wikipedia.org/wiki/Infrared_spectroscopy]
102. Lecellier A, Gaydou V, Mounier J, Hermet A, Castrec L, Barbier G, Ablain W, Manfait M, Toubas D, Sockalingum G: **Implementation of an FTIR spectral library of 486 filamentous fungi strains for rapid identification of molds.** *Food microbiology* 2015, **45:**126-134.
103. Doak DL, Phillips JA: **In situ monitoring of an Escherichia coli fermentation using a diamond composition ATR probe and mid-infrared spectroscopy.** *Biotechnology progress* 1999, **15:**529-539.
104. Pollard D, Buccino R, Connors N, Kirschner T, Olewinski R, Saini K, Salmon P: **Real-time analyte monitoring of a fungal fermentation, at pilot scale, using in situ mid-infrared spectroscopy.** *Bioprocess and Biosystems Engineering* 2001, **24:**13-24.
105. Schenk J, Viscasillas C, Marison IW, von Stockar U: **On-line monitoring of nine different batch cultures of E. coli by mid-infrared spectroscopy, using a single spectra library for calibration.** *Journal of biotechnology* 2008, **134:**93-102.
106. Veale EL, Irudayaraj J, Demirci A: **An On-Line Approach To Monitor Ethanol Fermentation Using FTIR Spectroscopy.** *Biotechnology progress* 2007, **23:**494-500.
107. Wu Z, Xu E, Long J, Zhang Y, Wang F, Xu X, Jin Z, Jiao A: **Monitoring of fermentation process parameters of Chinese rice wine using attenuated total reflectance mid-infrared spectroscopy.** *Food Control* 2015, **50:**405-412.
108. Preisner O, Guiomar R, Machado J, Menezes JC, Lopes JA: **Application of Fourier transform infrared spectroscopy and chemometrics for differentiation of Salmonella enterica serovar Enteritidis phage types.** *Applied and environmental microbiology* 2010, **76:**3538-3544.
109. Rebuffo-Scheer CA, Schmitt J, Scherer S: **Differentiation of Listeria monocytogenes serovars by using artificial neural network analysis of Fourier-transformed infrared spectra.** *Applied and environmental microbiology* 2007, **73:**1036-1040.
110. Kohler A, Böcker U, Shapaval V, Forsmark A, Andersson M, Warringer J, Martens H, Omholt SW, Blomberg A: **High-throughput biochemical fingerprinting of Saccharomyces cerevisiae by Fourier transform infrared spectroscopy.** *PloS one* 2015, **10:**e0118052.
111. Ami D, Mereghetti P, Doglia SM: **Multivariate analysis for Fourier transform infrared spectra of complex biological systems and processes.** In *Multivariate Analysis in Management, Engineering and the Sciences.* InTech; 2013.
112. Vongsvivut J, Heraud P, Gupta A, Thyagarajan T, Puri M, McNaughton D, Barrow CJ: **Synchrotron-FTIR microspectroscopy enables the distinction of lipid accumulation in thraustochytrid strains through analysis of individual live cells.** *Protist* 2015, **166:**106-121.
113. Davis R, Mauer L: **Fourier transform infrared (FT-IR) spectroscopy: a rapid tool for detection and analysis of foodborne pathogenic bacteria.** *Current research, technology and education topics in applied microbiology and microbial biotechnology* 2010, **2:**1582-1594.

114. Baker MJ, Trevisan J, Bassan P, Bhargava R, Butler HJ, Dorling KM, Fielden PR, Fogarty SW, Fullwood NJ, Heys KA: **Using Fourier transform IR spectroscopy to analyze biological materials.** *Nature protocols* 2014, **9:**1771-1791.
115. Szeghalmi A, Kaminskyj S, Gough KM: **A synchrotron FTIR microspectroscopy investigation of fungal hyphae grown under optimal and stressed conditions.** *Analytical and bioanalytical chemistry* 2007, **387:**1779-1789.
116. Flåtten A, Bryhni EA, Kohler A, Egelandsdal B, Isaksson T: **Determination of C22: 5 and C22: 6 marine fatty acids in pork fat with Fourier transform mid-infrared spectroscopy.** *Meat science* 2005, **69:**433-440.
117. Guillén MD, Cabo N: **Relationships between the composition of edible oils and lard and the ratio of the absorbance of specific bands of their Fourier transform infrared spectra. Role of some bands of the fingerprint region.** *Journal of Agricultural and Food Chemistry* 1998, **46:**1788-1793.
118. Ripoche A, Guillard A: **Determination of fatty acid composition of pork fat by Fourier transform infrared spectroscopy.** *Meat Science* 2001, **58:**299-304.
119. Beekes M, Lasch P, Naumann D: **Analytical applications of Fourier transform-infrared (FT-IR) spectroscopy in microbiology and prion research.** *Veterinary microbiology* 2007, **123:**305-319.
120. Carosio F, Alongi J, Malucelli G: **Layer by layer ammonium polyphosphate-based coatings for flame retardancy of polyester–cotton blends.** *Carbohydrate Polymers* 2012, **88:**1460-1469.
121. Lü F, Shao L-M, Zhang H, Fu W-D, Feng S-J, Zhan L-T, Chen Y-M, He P-J: **Application of Advanced Techniques for the Assessment of Bio-stability of Biowaste-derived Residues: A Minireview.** *Bioresource Technology* 2017.
122. Miglio R, Palmery S, Salvalaggio M, Carnelli L, Capuano F, Borrelli R: **Microalgae triacylglycerols content by FT-IR spectroscopy.** *Journal of applied phycology* 2013, **25:**1621-1631.
123. Pistorius A, DeGrip WJ, Egorova-Zachernyuk TA: **Monitoring of biomass composition from microbiological sources by means of FT-IR spectroscopy.** *Biotechnology and bioengineering* 2009, **103:**123-129.
124. Mayers JJ, Flynn KJ, Shields RJ: **Rapid determination of bulk microalgal biochemical composition by Fourier-Transform Infrared spectroscopy.** *Bioresource technology* 2013, **148:**215-220.
125. Meng Y, Yao C, Xue S, Yang H: **Application of Fourier transform infrared (FT-IR) spectroscopy in determination of microalgal compositions.** *Bioresource technology* 2014, **151:**347-354.
126. Wold S, Esbensen K, Geladi P: **Principal component analysis.** *Chemometrics and intelligent laboratory systems* 1987, **2:**37-52.
127. Wold S, Sjöström M, Eriksson L: **PLS-regression: a basic tool of chemometrics.** *Chemometrics and intelligent laboratory systems* 2001, **58:**109-130.
128. Zimmermann B, Kohler A: **Optimizing Savitzky–Golay parameters for improving spectral resolution and quantification in infrared spectroscopy.** *Applied spectroscopy* 2013, **67:**892-902.
129. Li-Chan E, Chalmers J, Griffiths P: *Applications of vibrational spectroscopy in Food Science.* John Wiley & Sons; 2011.
130. CAMO: **The Unscrambler X, Help menu.** 10.5 edition2017.
131. Esbensen KH, Guyot D, Westad F, Houmoller LP: *Multivariate data analysis: in practice: an introduction to multivariate data analysis and experimental design.* Multivariate Data Analysis; 2002.
132. Karaman I: **Sparse Mbplsr for Metabolomics Data and Biomarker Discovery : A Study on Multi-Block Data from LC-MS and NMR Metabolomics.** Aarhus University2014.
133. Challagulla V, Walsh KB, Subedi P: **Biomass and total lipid content assessment of microalgal cultures using near and short wave infrared spectroscopy.** *Bioenergy research* 2014, **7:**306-318.

134. Sancholle M, Laruelle F, Losel DM, Muchembled J, Arora D: **Biotechnological potential of fungal lipids.** *Handbook of Fungal Biotechnology* 2003, **1:**26-31.
135. Mendes A, Reis A, Vasconcelos R, Guerra P, da Silva TL: **Crypthecodinium cohnii with emphasis on DHA production: a review.** *Journal of applied phycology* 2009, **21:**199-214.
136. Duetz WA, Rüedi L, Hermann R, O'Connor K, Büchs J, Witholt B: **Methods for intense aeration, growth, storage, and replication of bacterial strains in microtiter plates.** *Applied and environmental microbiology* 2000, **66:**2641-2646.
137. **D-Glucose Assay Kit (GOPOD Format)** [https://secure.megazyme.com/D-Glucose-Assay-Kit]
138. Suutari M: **Effect of growth temperature on lipid fatty acids of four fungi (Aspergillus niger, Neurospora crassa, Penicillium chrysogenum, andTrichoderma reesei).** *Archives of microbiology* 1995, **164:**212-216.
139. Li J, Shapaval V, Kohler A, Talintyre R, Schmitt J, Stone R, Gallant AJ, Zeze DA: **A modular liquid sample handling robot for high-throughput Fourier transform infrared spectroscopy.** In *Advances in reconfigurable mechanisms and robots II.* Springer; 2016: 769-778.
140. Dahlbacka J, Kiviharju K, Eerikäinen T, Fagervik K: **Monitoring of Streptomyces peucetius cultivations using FTIR/ATR spectroscopy and quantitative models based on library type data.** *Biotechnology letters* 2013, **35:**337-343.
141. Rhiel M, Ducommun P, Bolzonella I, Marison I, Von Stockar U: **Real-time in situ monitoring of freely suspended and immobilized cell cultures based on mid-infrared spectroscopic measurements.** *Biotechnology and bioengineering* 2002, **77:**174-185.
142. Schalk R, Geoerg D, Staubach J, Raedle M, Methner F-J, Beuermann T: **Evaluation of a newly developed mid-infrared sensor for real-time monitoring of yeast fermentations.** *Journal of bioscience and bioengineering* 2017, **123:**651-657.
143. Sellick CA, Hansen R, Jarvis RM, Maqsood AR, Stephens GM, Dickson AJ, Goodacre R: **Rapid monitoring of recombinant antibody production by mammalian cell cultures using Fourier transform infrared spectroscopy and chemometrics.** *Biotechnology and bioengineering* 2010, **106:**432-442.
144. Botha A, Paul I, Roux C, Kock JL, Coetzee DJ, Strauss T, Maree C: **An isolation procedure for arachidonic acid producing Mortierella species.** *Antonie Van Leeuwenhoek* 1999, **75:**253-256.
145. Jang H-D, Lin Y-Y, Yang S-S: **Effect of culture media and conditions on polyunsaturated fatty acids production by Mortierella alpina.** *Bioresource technology* 2005, **96:**1633-1644.
146. Huang X, Chen H, Hao G, Du K, Hao D, Song Y, Gu Z, Zhang H, Chen W, Chen YQ: **Enhance eicosapentaenoic acid production in oleaginous fungus Mortierella alpina by overexpressing ω3 fatty acid desaturase.**

6 Papers

Paper I

Kosa et al. Microb Cell Fact (2017) 16:101
DOI 10.1186/s12934-017-0716-7

Microbial Cell Factories

RESEARCH

Open Access

Microtiter plate cultivation of oleaginous fungi and monitoring of lipogenesis by high-throughput FTIR spectroscopy

Gergely Kosa[1*], Achim Kohler[1], Valeria Tafintseva[1], Boris Zimmermann[1], Kristin Forfang[1], Nils Kristian Afseth[2], Dimitrios Tzimorotas[2], Kiira S. Vuoristo[3], Svein Jarle Horn[3], Jerome Mounier[4] and Volha Shapaval[1]

Abstract

Background: Oleaginous fungi can accumulate lipids by utilizing a wide range of waste substrates. They are an important source for the industrial production of omega-6 polyunsaturated fatty acids (gamma-linolenic and arachidonic acid) and have been suggested as an alternative route for biodiesel production. Initial research steps for various applications include the screening of fungi in order to find efficient fungal producers with desired fatty acid composition. Traditional cultivation methods (shake flask) and lipid analysis (extraction-gas chromatography) are not applicable for large-scale screening due to their low throughput and time-consuming analysis. Here we present a microcultivation system combined with high-throughput Fourier transform infrared (FTIR) spectroscopy for efficient screening of oleaginous fungi.

Results: The microcultivation system enables highly reproducible fungal fermentations throughout 12 days of cultivation. Reproducibility was validated by FTIR and HPLC data. Analysis of FTIR spectral ester carbonyl peaks of fungal biomass offered a reliable high-throughput at-line method to monitor lipid accumulation. Partial least square regression between gas chromatography fatty acid data and corresponding FTIR spectral data was used to set up calibration models for the prediction of saturated fatty acids, monounsaturated fatty acids, polyunsaturated fatty acids, unsaturation index, total lipid content and main individual fatty acids. High coefficients of determination ($R^2 = 0.86$–0.96) and satisfactory residual predictive deviation of cross-validation ($RPD_{CV} = 2.6$–5.1) values demonstrated the goodness of these models.

Conclusions: We have demonstrated in this study, that the presented microcultivation system combined with rapid, high-throughput FTIR spectroscopy is a suitable screening platform for oleaginous fungi. Sample preparation for FTIR measurements can be automated to further increase throughput of the system.

Keywords: Microcultivation, Oleaginous fungi, Fatty acid analysis, GC-FID, High-throughput FTIR spectroscopy, PLS regression

Background

Generally, a microorganism is considered oleaginous if the lipid content exceeds 20% of its dry weight, while up to 70% lipid content has been reported in the literature [1]. To achieve such high lipid content, microorganisms need to be cultivated in excess of a carbon source, while other nutrients such as nitrogen should be present in limiting concentration, i.e. in a high carbon-to-nitrogen ratio. Oleaginous microorganisms respond to nitrogen depletion by accumulating carbon in the form of triacylglycerol (TAG) in distinct lipid bodies. Oleaginous species can be found among yeasts, filamentous fungi and microalgae, while bacteria usually produce polyhydroxybutyrate and polyhydroxyalkanoate as storage polymers [1].

Microbial oils or single cell oils (SCO) are important sources of high-value polyunsaturated fatty acids (PUFA)

*Correspondence: gergely.kosa@nmbu.no
[1] Faculty of Science and Technology, Norwegian University of Life Sciences, Postbox 5003, 1432 Ås, Norway
Full list of author information is available at the end of the article

for human consumption as nutraceuticals. Plants do not produce PUFA longer than C18 (trienoic acids), while fish oil has several disadvantages, such as odor, accumulated toxic compounds, and overfishing [1, 2]. The commercially produced microbial oils contain high percentage of polyunsaturated fatty acids (PUFA). For example, omega-6 PUFAs, such as gamma-linolenic acid (18:3, GLA) and arachidonic acid (20:4, ARA) have been produced by the filamentous fungi *Mucor circinelloides* and *Mortierella alpina*, respectively.

Initial steps in microbial lipid research involve the screening for efficient production strains, which are either genetically modified organisms or natural isolates, and media optimization for subsequent scale-up experiments. When a large number of strains or cultivation conditions have to be tested, a high throughput screening (HTS) system is required, which can yield reproducible and scalable results. In order to increase throughput compared to traditional shake flasks, miniaturization of cultivations by microtiter plates or microbioreactors is desired [3–5]. HTS of filamentous fungi in microtiter plates is a challenging task because (a) there is a substantial risk of cross-contamination between individual cultivations, (b) highly viscous fermentation broth can cause oxygen transfer limitation and local inhomogeneity, and (c) excessive wall growth may take place, which favors sporulation.

For the screening of oleaginous microorganisms in microplates, a rapid, accurate lipid analysis is desired. Extraction, transesterification and gas chromatography (GC) is time-consuming, expensive and requires sample preparation and analysis that creates toxic wastes [6–8]. Rapid, non-invasive methods for SCO analysis involve fluorescence based measurements, near-infrared spectroscopy (NIR), Fourier transformed infrared spectroscopy (FTIR) and Raman spectroscopy [9]. FTIR spectroscopy has been successfully applied in recent years for microbial lipid research in yeast [8, 10, 11], microalgae [7, 12–14] and filamentous fungi [15]. FTIR spectroscopy is extremely versatile since it enables the overall characterization of the biochemical composition of intact cells, including proteins, lipids, and carbohydrates [11]. For that reason, FTIR spectroscopy is widely used for the rapid differentiation and identification of microorganisms [16–19]. The main advantages of FTIR spectroscopy are that (a) several compounds can be measured simultaneously, (b) the method is rapid since little or no sample preparation is required for spectral acquisition, (c) it is chemical-free, (d) it can be used for HTS and for real-time bioprocess monitoring, (e) and even spatial information can be obtained by the use of FTIR microspectroscopy systems [20, 21]. Since infrared spectra are highly complex, with many overlapping signals, multivariate data analysis is required to gain useful information [17, 22].

The aim of this study was to introduce the Duetz microtiter plate system (Duetz-MTPS) combined with HTS-FTIR spectroscopy as a high-throughput analytical platform for screening and monitoring of oleaginous fungi. In order to demonstrate the suitability of the system, we have used three fungal species and incubated them for 12 days under different temperatures. We have monitored lipogenesis of the fungal fermentations in microplates by high-throughput FTIR spectroscopy and GC reference analysis.

Methods

Fungal strains

Three oleaginous filamentous fungi were used in this study: *Mucor circinelloides* VI 04473 (Norwegian School of Veterinary Science; Oslo, Norway), *Umbelopsis isabellina* UBOCC-A-101350 (Université de Bretagne Occidentale Culture Collection; Plouzané, France) and *Penicillium glabrum* FRR 4190 (Commonwealth Scientific and Industrial Research Organisation; North Ryde, Australia).

Media and growth conditions

Cultivation of fungi was first performed on agar media to obtain spores for the inoculation and then in nitrogen-limited liquid medium in order to stimulate lipid accumulation. For spore inoculum preparation the following agar media were used: malt extract agar (MEA) for *M. circinelloides* and *P. glabrum* and potato dextrose agar (PDA) for *U. isabellina*. MEA was prepared by dissolving 30 g malt extract (Merck, Germany), 5 g peptone (Amresco, USA) and 15 g agar powder (VWR Chemicals, Belgium) in 1 L distilled water and autoclaved at 115 °C for 10 min. PDA was prepared by dissolving 39 g potato dextrose agar (VWR Chemicals, Belgium) in 1 L distilled water and autoclaved at 121 °C for 15 min. All agar cultivations were performed for 7 days at 25 °C. Spores were harvested with a bacteriological loop from agar plates after the addition of 10 mL sterile physiologic salt solution. Spore concentrations were measured with hemocytometer (Fuchs-Rosenthal, Hausser Scientific Company, USA) and a DM6000B microscope (Leica Microsystems, Germany) and spore suspensions were diluted to 3.6×10^6 spore mL^{-1}.

The broth medium was prepared according to the protocol described in Kavadia et al. [23] with modifications (g L^{-1}): glucose 80, yeast extract (Oxoid, England) 3, KH_2PO_4 7, Na_2HPO_4 2, $MgSO_4 \cdot 7H_2O$ 1.5, $CaCl_2 \cdot 2H_2O$ 0.1, $FeCl_3 \cdot 6H_2O$ 0.008, $ZnSO_4 \cdot 7H_2O$ 0.001, $CoSO_4 \cdot 7H_2O$ 0.0001, $CuSO_4 \cdot 5H_2O$ 0.0001, $MnSO_4 \cdot 5H_2O$ 0.0001. Chemicals (except yeast extract) were purchased from Merck (Germany). Liquid medium was autoclaved for

15 min at 121 °C. The pH of the medium was 6.05 after sterilization. Cultivation in liquid medium was performed in the Duetz-MTPS (Enzyscreen, Netherlands), consisting of 24-square polypropylene deep well plates, low-evaporation sandwich covers and extra high cover clamps [24], which were mounted in two Innova 40R refrigerated desktop shakers (Eppendorf, Germany). Autoclaved and dried microtiter plates were filled with 2.5 mL of sterile liquid medium by using the Stepper 411 adjustable repeater pipette (Socorex, Switzerland). Each well was inoculated with 50 µL fungal spore suspension. Cultivations were performed for 12 days at 20 and 30 °C at 300 rpm agitation speed (circular orbit 0.75″ or 19 mm). Each day, one plate was removed from both shakers for analysis.

Experimental design

All microplates were prepared in the following scheme: the first eight wells were inoculated with *M. circinelloides*, the second eight wells with *U. isabellina* and the last eight wells with *P. glabrum*. For each strain, fungal biomass of the first three wells, considered as biological replicates (210 samples in total), was used for lipid analysis by HTS-FTIR spectroscopy. Supernatant of the same wells, as well as the starting growth medium (215 samples in total), was used for glucose and protein analyses by HPLC and colorimetric assay. Finally, the merged biomass from the other five wells (70 samples in total) was used for lipid analysis by gas chromatography (GC).

Bright-field and fluorescent microscopy

Morphology of the filamentous fungi was examined with a DM6000B microscope (Leica Microsystems, Germany). Microscopic pictures were obtained with an Evolution MP camera kit (Media Cybernetics, USA). A Nile-red staining solution was prepared by dissolving 1 mg Nile-red crystals (Sigma-Aldrich, Germany) in 1 mL ethanol. Then, 10 µL Nile-red solution was dried onto a glass side, the biomass was added and covered with a glass coverslip. Nile-red stained samples were incubated for 1 h at 4 °C in the dark and images were captured using a 490 nm excitation/530 nm emission wavelength filter cube (Leica Microsystems, Germany).

Preparation of supernatant and biomass

The supernatant was separated from the fungal biomass by transferring 2 mL fermentation broth with plastic Pasteur pipettes into Eppendorf tubes and the subsequent centrifugation at 13,000 rpm for 20 min at 4 °C. Fungal biomass from Eppendorf tubes were washed three times with cold distilled water and filtered under vacuum using a Whatman No. I filter paper (GE Whatman, USA). All samples were stored at −20 °C until analysis.

Preparation of fungal biomass for FTIR analysis

The washed fungal biomass (approx. 50 µL per sample) was homogenized in 96-square deepwell plates with 500 µL distilled water using a modular liquid handling robot [25] with integrated 2 mm single-pin Q55 sonicator (Qsonica, USA). The sonication was performed in a pulse regime with 15 s sonication time and 5 s washing time. Total sonication time for *U. isabellina*, *M. circinelloides*, and *P. glabrum* was 30 s, 1 min and 1.5 min, respectively. *P. glabrum* biomass cultivated at 20 °C was manually sonicated for 2 min, due to a rigid pellet structure, which was difficult to homogenize with the robotic system.

FTIR spectroscopy

FTIR analysis of the sonicated fungal biomass was performed using the High Throughput Screening eXTension (HTS-XT) unit coupled to the Vertex 70 FTIR spectrometer (both Bruker Optik, Germany) in transmission mode. From each suspension, 8 µL were transferred to an IR-light-transparent silicon 384-well microplate (Bruker Optik, Germany) in three technical replicates. Samples were dried at room temperature for 2 h to form films that were suitable for FTIR analysis. The spectra were recorded in the region between 4000 and 500 cm^{-1} with a spectral resolution of 6 cm^{-1} and an aperture of 5.0 mm. For each spectrum, 64 scans were averaged. Each spectrum was recorded as the ratio of the sample spectrum to the spectrum of the empty microplate. In total, 210 samples were measured and 630 FTIR spectra were obtained.

Glucose analysis

Glucose was quantified using an UltiMate 3000 UHPLC system (Thermo Scientific, USA) equipped with RFQ-Fast Acid H + 8% (100 × 7.8 mm) column (Phenomenex, USA) and coupled to a refractive index (RI) detector. Samples were diluted ten times before analysis, filter sterilized and were subsequently eluted isocratically at 0.6 mL min^{-1} flow rate in 12 min with 5 mM H_2SO_4 mobile phase at 85 °C column temperature.

Protein analysis

Protein concentration in sample of supernatants was determined with a Bradford-method based colorimetric assay (Bio-Rad Protein Assay, USA) according to the microplate protocol. Absorbance was measured at 595 nm with a SPECTROstar Nano UV/Vis microplate reader (BMG Labtech, Germany). A calibration curve was prepared with media containing different amount of yeast extract.

Preparation of fungal biomass for FAME extraction and GC analysis

The fermentation broth from the other five wells of the microplate were merged, filtered and washed as described above, frozen at −20 °C and then lyophilized for 2 days in an Alpha 1-2 LDPlus freeze-dryer (Martin Christ, Germany) at −55 °C (condenser temperature) and 0.01 mbar pressure. The dried biomass was also used to calculate the cell dry weight (CDW). In order to obtain reliable dry cell weight data, the biomass grown on the walls of the wells was also collected and measured in contrast to that, used for FTIR and GC analysis.

Lipid extraction

Direct transesterification was performed according to Lewis et al. [26] with modifications for lipid extraction from fungal biomass: 2 mL screw-cap polypropylene (PP) tubes were filled, in three technical replicates, with 30 ± 3 mg freeze dried fungal biomass, 250 ± 30 mg (710–1180 µm diameter) acid-washed glass beads (Sigma-Aldrich, USA) and 600 µL methanol. The fungal biomass was disrupted in a FastPrep-24 high-speed benchtop homogenizer (MP Biomedicals, USA) at 6.5 m s^{-1}, for 1 min cycle length and 6 cycles. The disrupted fungal biomass was transferred into glass reaction tubes by washing the PP tube with 2400 µL methanol–chloroform–hydrochloric acid solvent mixture (7.6:1:1 v/v). Twenty microliters from a 25 mg mL^{-1} tridecanoic acid (C13:0, Sigma-Aldrich, USA) internal standard solution in methanol was added to the glass reaction tubes. The reaction mixture was vortexed for 10 s and incubated at 90 °C for 1 h, followed by cooling to room temperature and addition of 1 mL distilled water. The fatty acid methyl esters (FAMEs) were extracted by the addition of 2 mL hexane–chloroform (4:1 v/v) followed by 10 s vortex mixing. The reaction tubes were centrifuged at 3000*g* for 10 min at 4 °C and the upper hexane phase was collected in glass tubes. The hexane–chloroform extraction was performed thrice. Subsequently, the solvent was evaporated under nitrogen at 60 °C and FAMEs were dissolved in 1.5 mL hexane containing 0.01% butylated hydroxytoluene (BHT, Sigma-Aldrich, USA). The extracted non-lipid cell compounds (insoluble in hexane) were removed after centrifugation in Eppendorf tubes at 15,000*g* for 5 min at 4 °C. The FAMEs dissolved in hexane were transferred to GC vials containing small amount of anhydrous sodium sulfate.

GC fatty acid analysis

Analysis of the extracted FAMEs was performed in a HP 6890 gas chromatograph (Hewlett Packard, USA) equipped with a SGE BPX70, 60.0 m × 250 µm × 0.25 µm column (SGE Analytical Science, Australia) and flame ionization detector (FID). Helium was used as a carrier gas. The runtime was 36.3 min with an initial oven temperature of 100 °C, which was increased steadily to 220 °C (4.3 min to 170 °C, then 20 min to 200 °C and 12 min to 220 °C). The injector temperature was 280 °C and 1 µL was injected in split mode (50:1 split ratio). FAMEs were identified with a C4–C24 FAME standard mixture (18919-1AMP, Supelco, USA) dissolved in hexane, and were quantified by the C13:0 internal standard and relative response factors (RRF) calculated from 5-point calibration curves of the individual FAMEs in the standard mixture.

Data analysis

The FTIR spectra of fungal biomass were preprocessed in the following way: (1) technical replicates (630 spectra in total) were averaged resulting in 210 average spectra, (2) second derivative spectra were obtained by the Savitzky–Golay algorithm [27] using windows size 9 and a second degree polynomial, (3) Extended Multiplicative Signal Correction (EMSC), an MSC model extended by a linear and quadratic component, was employed on the combined spectral range comprising of 3100–2800 and of 1800–500 cm^{-1} spectral regions [28]. These spectral regions were selected since they contain bands distinctive for fungi [18, 29].

Principal component analysis (PCA) was applied in order to evaluate the differentiation ability of FTIR analysis between fungal species, cultivation temperature and time, and to compare sample variation pattern in FTIR and GC data concerning fatty acid composition. The preprocessed FTIR spectra (2nd derivative and EMSC) were used in the 3100–2800 cm^{-1} region, while the GC fatty acid data were autoscaled.

Partial least square regression (PLSR) was used to establish calibration models for fatty acid parameters of fungal biomass. In order to establish such models a data set of GC reference measurements (responses) were used as a Y matrix, which was regressed onto an X matrix containing FTIR measurements of fungal biomass (predictors). Fatty acid parameters included total lipid content of biomass and fatty acid compositional data such as saturated fatty acids (SAT), monounsaturated fatty acids (MUFA), polyunsaturated fatty acids (PUFA), unsaturation index and relevant single fatty acids. From a total of 210 averaged FTIR spectra, nine samples belonging to early growth phase of the fungi were excluded (3 biological replicates each of *M. circinelloides* 20 °C on day 1, *P. glabrum* 20 °C on day 2, and *P. glabrum* 30 °C on day 1). The remaining 201 average FTIR spectra were used for the PLSR. Reference GC fatty acid dataset was built

on the measurement of 67 fungal samples, each of them measured in three technical replicates and then results were averaged. Therefore, one averaged GC fatty acid composition was used in the regression for three corresponding biological replicate FTIR spectra. In order to optimize the number of PLSR principal components (PCs), cross-validation (CV) was performed, where cross validation segments were defined by days. All spectra from samples obtained on the same day were removed in turn and used for validating the model established on the rest of the data. A root-mean-square error (RMSE) was calculated for models with 1–25 components. The optimal model was the one with the lowest number of PCs having insignificantly higher RMSE than the model with the minimum RMSE.

The Unscrambler, V10.3 (CAMO, Norway) and Matlab, V8.5 (The Mathworks, USA) software were used to perform the data analysis.

Results and discussion

Growth and lipid accumulation of oleaginous fungi in Duetz-MTPS

The growth of dimorphic fungus *M. circinelloides* resulted in clumped mycelium mixed with dispersed yeast-like cells, while *U. isabellina* and *P. glabrum* grew in pellets of approx. 0.5–2 mm in diameter (Fig. 1). Maximum lipid bodies' diameter were 17, 5 and 2.5 µm respectively (Fig. 1). It is worth mentioning that filling volume in the 24-well MTP should not exceed 2.5 mL at 300 rpm agitation speed in order to avoid the contact of fermentation broth with sandwich cover, which potentially leads to cross-contamination.

For all three species, initial growth rate was higher at 30 °C than at 20 °C (Fig. 2a). Final biomass concentration (18–23 g L^{-1}) was similar for the three fungi at both temperatures. The exception was *M. circinelloides* grown at 20 °C, which consumed less than half of the initial

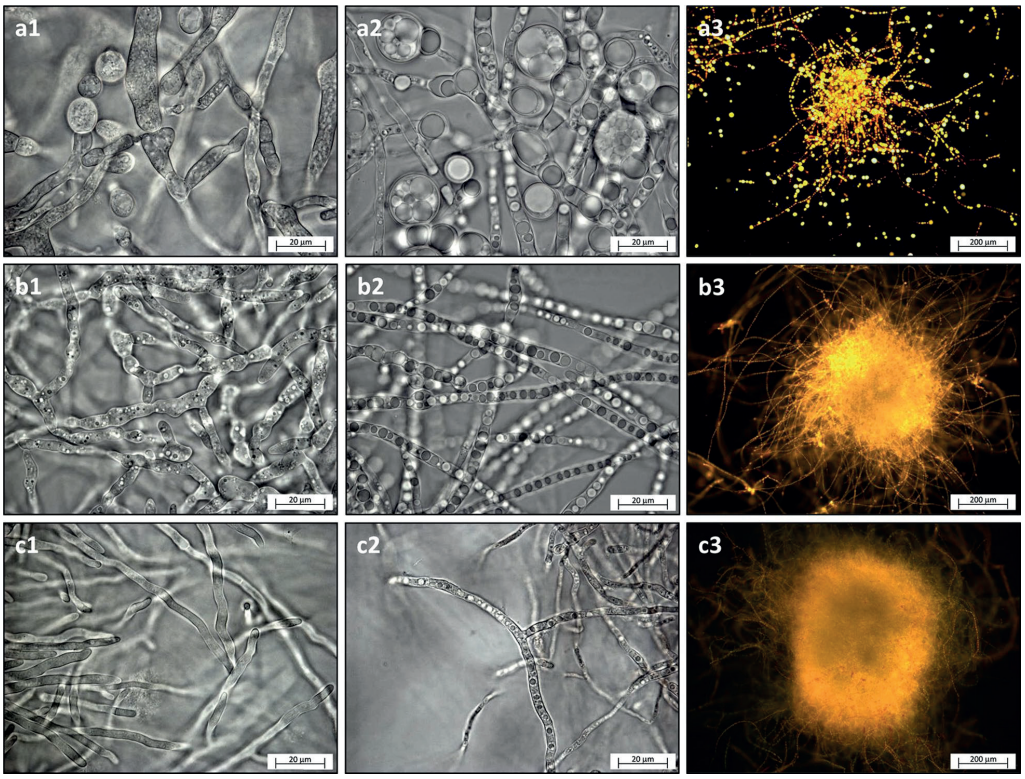

Fig. 1 Bright-field (**a1**–**c2**) and fluorescent microscopy (**a3**–**c3**) images of *M. circinelloides* (**a**), *U. isabellina* (**b**) and *P. glabrum* (**c**). Images (**a1**–**c1**) show fungal hyphae before or at the beginning of lipogenesis (day 1–2) while images (**a2**–**c3**) were captured from hyphae filled with distinct lipid bodies (day 3–6)

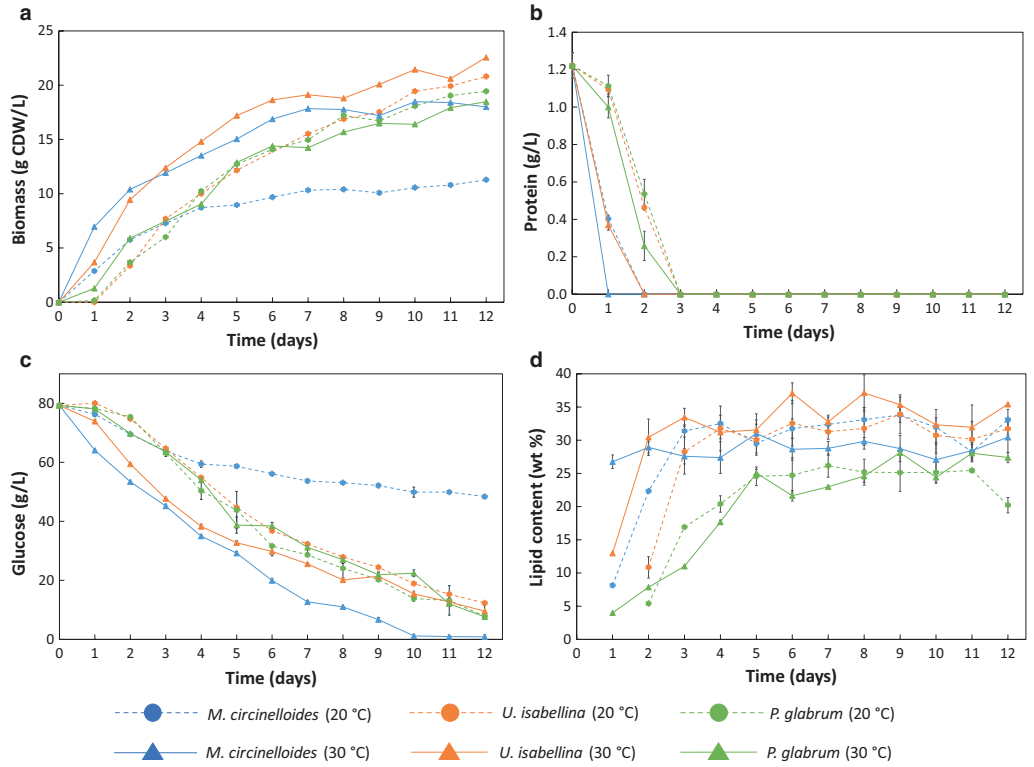

Fig. 2 Biomass (**a**), protein (**b**) and glucose (**c**) concentrations in cultivation medium and lipid content (**d**) of *M. circinelloides*, *U. isabellina* and *P. glabrum* cultivated at 20 and 30 °C in the Duetz-MTPS (n = 3, *error bars* = SD)

glucose and reached only 11 g L^{-1} biomass. However, at 30 °C, which is the optimum growth temperature for this species [30], *M. circinelloides* showed glucose depletion after 10 days of cultivation (Fig. 2c). Proteins from yeast extract were depleted within 1–3 days of cultivation for the three studied fungi (Fig. 2b), however growth continued at a reduced rate after nitrogen depletion. This result is in agreement with the study of Tang et al. [31], where the sole N-source, i.e., ammonium tartrate was depleted by *M. circinelloides* within 9–10 h, while growth continued until 60–80 h. *M. circinelloides* and *U. isabellina* reached 31–37% lipid content of the biomass, while *P. glabrum* accumulated 26–28% lipid (Fig. 2d). Further fermentation results can be found in Additional file 1: Table S1 and Figure S1.

M. circinelloides and *U. isabellina* produced unsaturated fatty acids up to 18 carbon chain length gamma-linolenic acid (C18:3n6 or GLA), while *P. glabrum* produced unsaturated fatty acids up to alpha-linolenic acid (C18:3n3 or ALA) (Fig. 3). These results are in agreement with previous studies, showing that more advanced fungi (Ascomycota and Basidiomycota) produce the n-3 isomer of the C18 trienoic fatty acid, while basal fungi (Mucoromycotina, Chytridiomycota) produce the n-6 isomer [32, 33]. After 12 days cultivation, higher content of oleic acid (C18:1n9), GLA (*M. circinelloides* and *U. isabellina*) and ALA (*P. glabrum*) was observed at 20 °C than at 30 °C, while linoleic acid (C18:2n6, LA) content was higher at 30 °C than at 20 °C for all the three studied fungi. The PUFA content in the oil, including LA, GLA and ALA rapidly decreased after the transition from exponential growth to stationary phase and remained relatively stable afterwards. In the stationary phase of *M. circinelloides* and *U. isabellina*, oleic acid content tended to increase concomitant with decrease in saturated fatty acids (C16:0, palmitic acid and C18:0, stearic acid) (Additional file 1: Figure S2).

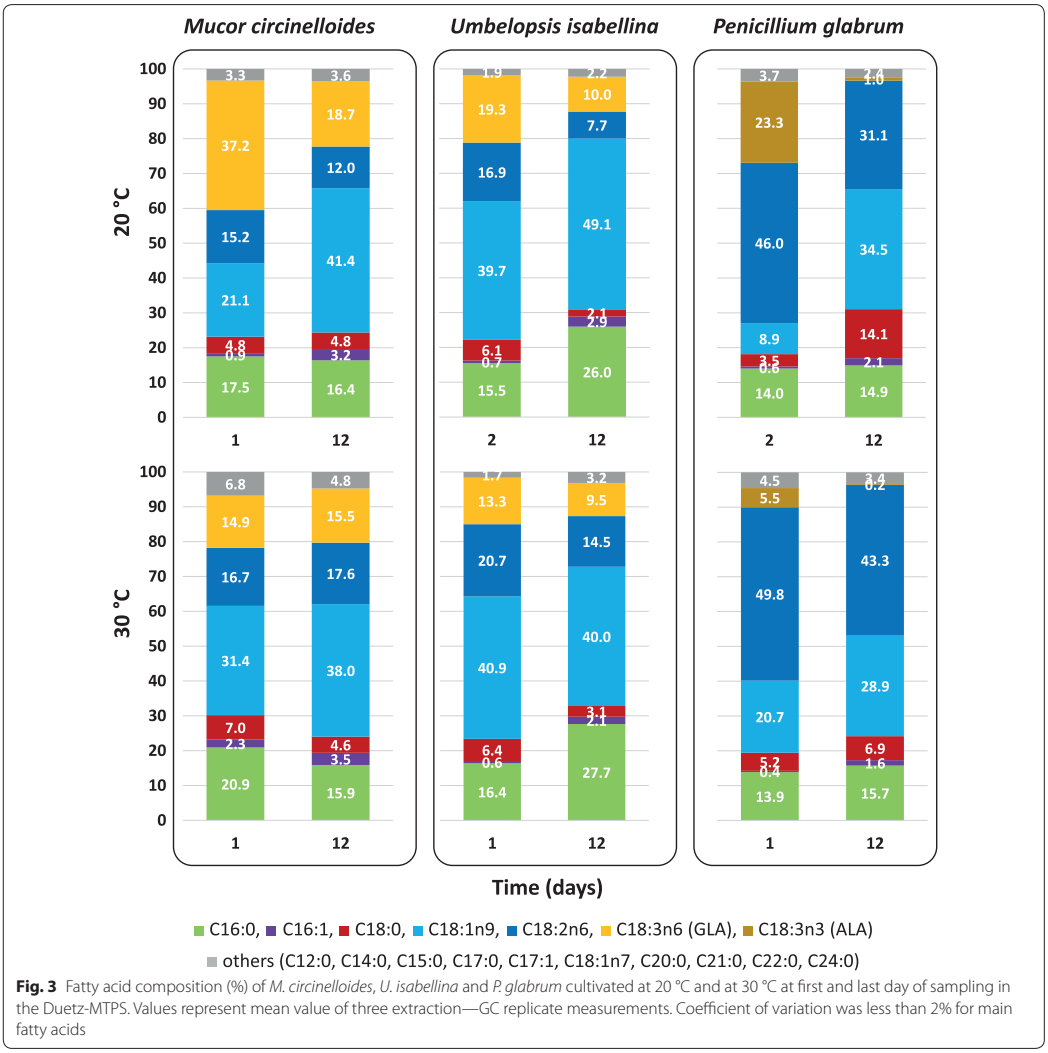

Fig. 3 Fatty acid composition (%) of *M. circinelloides*, *U. isabellina* and *P. glabrum* cultivated at 20 °C and at 30 °C at first and last day of sampling in the Duetz-MTPS. Values represent mean value of three extraction—GC replicate measurements. Coefficient of variation was less than 2% for main fatty acids

FTIR spectroscopy of oleaginous filamentous fungi

The FTIR spectra of *M. circinelloides*, *U. isabellina* and *P. glabrum* biomass after 1 and 12 days of cultivation are shown in Fig. 4. Assigned spectral bands of the FTIR spectrum and their respective functional groups are listed in Additional file 1: Table S2. In the infrared spectrum, cellular lipids were represented by several peaks, related to different lipid functional groups: (I) peaks in the regions 3050–2800 cm^{-1} (peaks N° 1–4 in Fig. 4), 1500–1300 cm^{-1} (N° 8–10) and at 725 cm^{-1} (N° 16) are related to lipid acyl chains, (II) peak around 3008 cm^{-1} (N° 1) corresponds to =C–H stretching and gives indication about the lipid unsaturation index [14, 15, 22], (III) the peak at 1745 cm^{-1} (N° 5) is related to the ester carbonyl bond, which represents the vast majority of the total lipid content in the cell [14, 22]. We observed a relative increase with the cultivation time for all lipid related bands in mid-IR spectra of all studied fungi, indicating that during cultivation in nitrogen limited medium, the main biochemical changes in fungi were related to

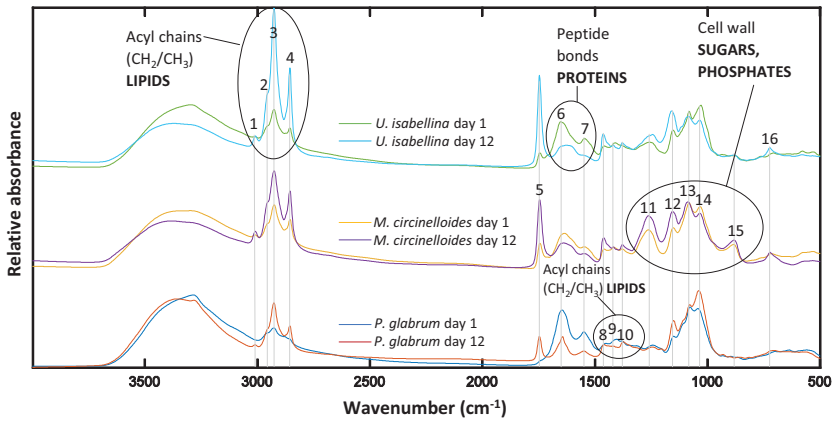

Fig. 4 FTIR spectra of *P. glabrum*, *M. circinelloides*, *U. isabellina* (30 °C) after 1 and 12 days of cultivation

intracellular lipid accumulation. As a consequence, the relative absorbance of protein-related peaks between 1690 and 1500 cm^{-1}, which are mainly influenced by the amide I (peak N° 6 in Fig. 4) and amide II bands (N° 7) [8], decreased during lipid accumulation.

Temporal-dependent changes in complex polysaccharide region (1240–900 cm^{-1}) related to phosphate groups (nucleic acids, polyphosphates, phospholipids), as well as C–O and C–O–C absorption peaks of the cell wall polysaccharides (chitin, chitosan, β-glucan, mannan, etc.), were also observed for all fungi. The appearance of the strong peaks around 1260 (peak N° 11 in Fig. 4) and 880 cm^{-1} (N° 15) in *M. circinelloides* spectra indicated an increase in polyphosphate content in its cell wall, as reported previously [34]. The *U. isabellina* IR spectra showed an absorbance increase at 1240–1250 cm^{-1}, that may also indicate a polyphosphate content increase, but this increase was less prominent than for *M. circinelloides*. Relative to amide I peak, the β (1,3)-glucan peaks (at 1150 and 1080 cm^{-1}) (peaks N° 12 and 13 in Fig. 4) and the C–O stretching peak around 1033 cm^{-1} (N° 14) increased as well with the cultivation time for all studied fungi. Such changes in the polysaccharide region of IR spectra show that the cell wall composition changes during lipid accumulation. We can hypothesize that an increase of β (1,3)-glucan peaks corresponds to an increase in the cell wall thickness which goes along with lipid accumulation. Indeed, the homogenization of lipid-rich fungal biomass used for FTIR required long time, while that used for GC analysis required the use of hydrochloric acid and harsh mechanical pretreatment (bead beating) [34]. Ami et al. [8] and Signori et al. [10] observed similar cell wall changes in FTIR spectra during oleaginous yeast lipogenesis.

PCA was performed on FTIR spectra and GC fatty acid data to evaluate temporal-, species- and cultivation temperature specific differences related to lipid production. The score plot of the first and second component of PCA of the FTIR data shows clustering according to the fungal species and cultivation temperatures (Fig. 5). The sample variation pattern in GC (Fig. 5a) and FTIR (Fig. 5b) score plots show similar tendencies and demonstrate that the main changes in fatty acid composition occur during the transition from growth phase (day 1–3) to the lipid accumulation phase (day 3–12). After 3 days of fermentation the fatty acid composition stabilizes. Furthermore, both GC and FTIR score plots indicate that reaching the stable fatty acid composition took longer for *P. glabrum* than for *M. circinelloides* and *U. isabellina* due to lower growth rate of this species. Biological replicate samples, which are marked by the same names and colors in the FTIR score plot, are close to each other. Variability between technical and biological replicates of the FTIR measurements were quantified by Pearson correlation coefficient (Additional file 1: Table S3). Technical and biological sample variability were of the same order, and two orders lower than variation between samples during the 12 days of cultivation. This demonstrates that the Duetz-system is a suitable high-throughput platform for the reproducible cultivation of filamentous fungi and that HTS-FTIR spectroscopy is a suitable high-throughput platform for the reproducible monitoring of lipogenesis of oleaginous fungi.

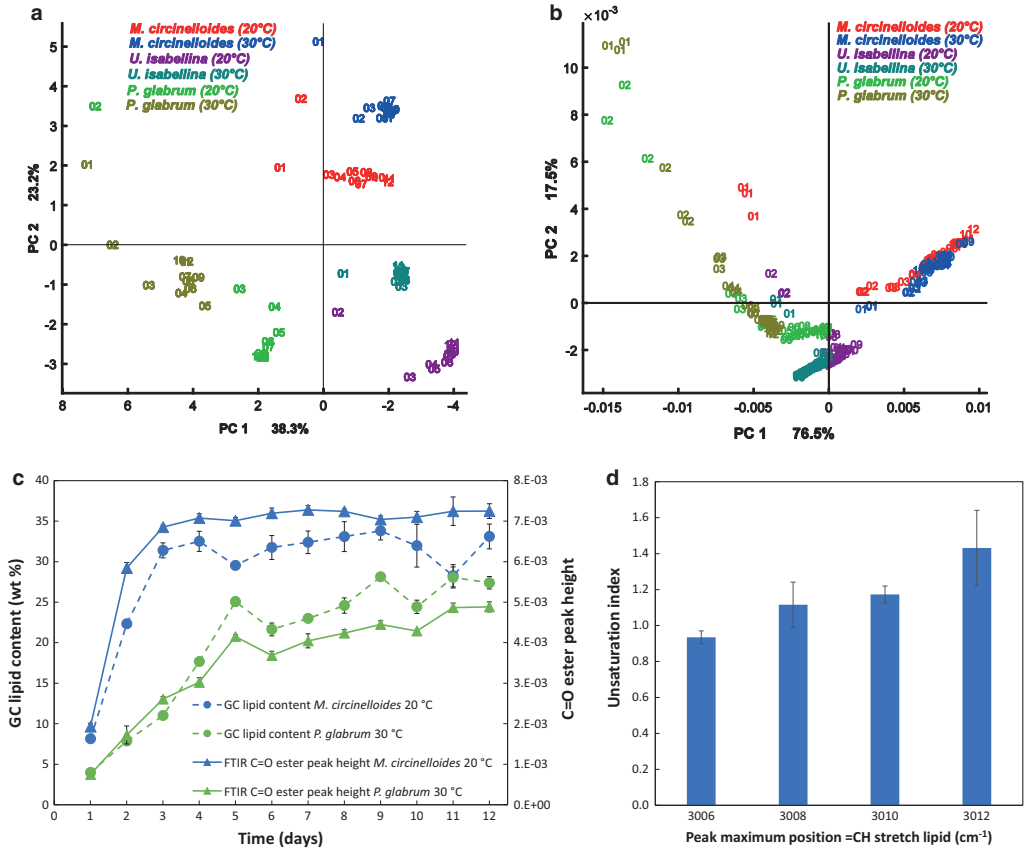

Fig. 5 Exploratory analysis of FTIR data and comparison with GC reference data. **a** First and second scores (PC1, PC2) in PCA of the auto-scaled GC fatty acid data (PC1 axis is reversed in the GC score plot). **b** First and second scores in PCA of the preprocessed FTIR spectra in the spectral range of 3100–2800 cm^{-1}. **c** Total lipid content measured by reference GC method and followed by the C=O ester peak height from the pre-processed FTIR spectra (n = 3, *error bars* = SD). **d** Relationship between unsaturation indices and position of the =C–H stretching bond peak maxima (cm^{-1}) in FTIR spectra. Unsaturation index = [Σ(% monoene + 2× % diene + 3× % triene)]/100 [35]

The total lipid content of the biomass was monitored using the C=O ester peak height (1745 cm^{-1}) of the preprocessed FTIR spectra. Total lipid trends for fungal biomass were assessed by the C=O ester peak height and compared to reference GC total lipid measurement (Additional file 1: Figure S3). For example, Fig. 5c shows that the GC and FTIR based lipid content of biomass curves for *M. circinelloides* (20 °C) and *P. glabrum* (30 °C) are well correlated. The fluctuation observed in the GC total lipid data may be due to the extraction–transesterification protocol for GC measurement, which is more prone to measurement errors than the FTIR measurement, which is done on almost intact cells. Although FTIR total lipid data cannot be used for absolute quantification without calibration to reference analysis, it provides a reliable and rapid qualitative method to monitor lipid accumulation during the cultivation of oleaginous species.

The position of the olefinic group around 3010 cm^{-1} is known to be related to the degree of unsaturation of fatty acids. It has been shown that a shift toward higher wavenumber suggests higher degree of unsaturation [14, 15]. In this study the peak position at 3006 cm^{-1} corresponded to an unsaturation index of 0.93 ± 0.04, while peak position 3012 cm^{-1} was described by an unsaturation index of 1.43 ± 0.21. Peak maxima between 3008 and 3010 cm^{-1} corresponded to an unsaturation index of 0.99–1.22 (Fig. 5d).

For the quantitative prediction of fatty acid composition and total lipid content of biomass PLSR models were established by using FTIR spectra (Additional file 2: Table S5) as X variables (or predictors) and GC fatty acid data (Additional file 3: Table S6) as Y variables (or responses). For seven of the fatty acid parameters, excellent calibration results were achieved with regression coefficients R^2 above 0.91 and for three fatty acid parameters, good models were obtained with R^2 between 0.86 and 0.89 (Table 1). Residual predictive deviation of cross-validation (RPD_{CV}) values were good to acceptable between 2.6 and 5.1. The slightly lower prediction ability for total lipid content might be due to the high variability in GC quantification (Fig. 2d). The models for MUFA and oleic acid (C18:1n9) had a high complexity involving a higher number of PLS factors compared to the other models. This high complexity may involve some degree of over-fitting. The predictions of linolenic acid and unsaturation index are shown in Additional file 1: Figure S4, where the predicted values are plotted against the measured values for both prediction and validation results. Since both prediction and validation results show the same high prediction ability, we can conclude that the calibration models are stable. Prediction result including all 210 samples can be found in Additional file 1: Table S4.

Conclusions

In this study, we have examined a high-throughput approach for the cultivation and monitoring of oleaginous fungi. For this purpose, a Duetz microtiter plate system was combined with rapid FTIR spectroscopy of fungal biomass. First, the microcultivation performance was evaluated for the studied fungi. Biological replicate cultivations in the 24 well deep well microtiter plate showed excellent reproducibility based on glucose consumption (pooled standard deviation = 1.1 g L^{-1} glucose) and FTIR spectra of biomass (average Pearson correlation coefficient = 0.9994). Fungal cultures with high biomass concentrations (up to 23 g L^{-1} CDW) and high lipid content (up to 35%) were achieved in the Duetz-MTPS.

Evaluation of the FTIR spectra of fungi during fermentation resulted in lipid accumulation curves that followed very similar trends to total lipid curves obtained by reference GC quantification. In general, the lipid accumulation curves on the basis of the FTIR C=O ester peak showed smaller day-to-day variations and thus are more plausible. For quantitative purposes, the FTIR spectral data of biomass were calibrated versus GC fatty acid data. Summed fatty acid parameters (SAT, MUFA, PUFA, total fat, unsaturation index) and main individual fatty acids were predicted with high precision (R^2 between 0.86 and 0.96, RPD_{CV} between 2.6 and 5.1). Sample preparation for HTS-FTIR measurement can be fully automated by robotics to further increase precision and throughput. We therefore conclude that HTS-FTIR spectroscopy is a simple, rapid tool for screening or at-line monitoring the cultivation of oleaginous species.

Table 1 PLS regression results between HTS-FTIR and GC fatty acid measurements (N = 201)

Fatty acid	Range	Mean	Standard deviation	R^{2a}	RMSECV[b]	RPD^{c}_{CV}	PLS factors
C16:0	13.4–31.9	20.2	6.1	0.94	1.5	4.0	6
C18:0	2.1–14.4	6.3	3.2	0.94	0.8	4.2	6
C18:1n9	25.4–49.1	37.4	5.4	0.89	1.8	3.0	21
C18:2n6	7.6–48.1	20.8	11.5	0.96	2.3	5.0	7
C18:3n6	0.0–22.3	9.1	7.2	0.96	1.4	5.1	3
SAT	22.4–39.2	29.0	4.5	0.87	1.6	2.8	6
MUFA	27.1–52.6	40.7	5.6	0.93	1.5	3.9	21
PUFA	15.9–50.5	30.3	8.1	0.93	2.2	3.7	7
Unsaturation index	0.89–1.33	1.11	0.13	0.95	0.03	4.5	9
Total lipid	7.9–37.1	27.8	6.1	0.86	2.3	2.6	4

[a] R^2, cross-validated squared correlation coefficient

[b] RMSECV, root mean square error of cross validation

[c] RPD_{CV}, residual predictive deviation of cross-validation (standard deviation/RMSECV)

Additional files

Additional file 1. Figures S1–S4, **Tables S1–S4.** Additional figures and tables.

Additional file 2: Table S5. HTS-FTIR spectra of biomass.

Additional file 3: Table S6. GC fatty acid composition.

Additional file 4: Table S7. HPLC glucose concentration.

Abbreviations
Duetz-MTPS: Duetz microtiter plate system; EMSC: extended multiplicative signal correction; HTS: high-throughput screening; FTIR: Fourier transform infrared spectroscopy; MUFA: monounsaturated fatty acids; SAT: saturated fatty acids; PUFA: polyunsaturated fatty acids; PCA: Principal Component Analysis; PLSR: partial least squares regression.

Authors' contributions
Conceived the research idea: AK, VS. Designed the experiments: GK, AK, BZ, VS. Methodology: GK, VT, BZ, KF, VS. Performed the experiments: GK. Discussed the results: GK, AK, BZ, VT, VS, NKA. Analyzed the data: GK, VT, BZ, VS. Wrote the manuscript: GK. Discussed and revised the manuscript: GK, AK, VT, BZ, KF, DM, NKA, KV, SJH, JM, VS. All authors read and approved the final manuscript.

Author details
[1] Faculty of Science and Technology, Norwegian University of Life Sciences, Postbox 5003, 1432 Ås, Norway. [2] Nofima AS, Osloveien 1, 1430 Ås, Norway. [3] Faculty of Chemistry, Biotechnology and Food Science, Norwegian University of Life Sciences, Postbox 5003, 1432 Ås, Norway. [4] Université de Brest, EA3882 Laboratoire Universitaire de Biodiversité et Ecologie Microbienne, IBSAM, ESIAB, Technopôle Brest Iroise, 29280 Plouzané, France.

Acknowledgements
The authors would like to acknowledge Sandeep Sharma and Elin Merete Wetterhus for their help with HPLC and GC measurements respectively, and Murat Bagcioglu for his help in data analysis. Wouter Duetz is also acknowledged for his valuable technical advices in microtiter plate cultivation.

Competing interests
The authors declare that they have no competing interests.

Availability of data and materials
All data generated or analysed during this study are included in this published article (and its additional files).

Funding
This work was supported by the Norwegian Research Council-BIONÆR Grant, project number: 234258/E50 and the Norwegian Research Council "Interest" Grant, project number 227356.

Publisher's Note

Received: 24 January 2017 Accepted: 5 June 2017
Published online: 09 June 2017

References

1. Ratledge C. Fatty acid biosynthesis in microorganisms being used for single cell oil production. Biochimie. 2004;86:807–15.
2. Ward OP, Singh A. Omega-3/6 fatty acids: alternative sources of production. Process Biochem. 2005;40:3627–52.
3. Linde T, Hansen NB, Lübeck M, Lübeck PS. Fermentation in 24-well plates is an efficient screening platform for filamentous fungi. Lett Appl Microbiol. 2014;59:224–30.
4. Long Q, Liu X, Yang Y, Li L, Harvey L, McNeil B, Bai Z. The development and application of high throughput cultivation technology in bioprocess development. J Biotechnol. 2014;192:323–38.
5. Meyer V, Andersen MR, Brakhage AA, et al. Current challenges of research on filamentous fungi in relation to human welfare and a sustainable bio-economy: a white paper. Fungal Biol Biotechnol. 2016;3:6.
6. Rumin J, Bonnefond H, Saint-Jean B, Rouxel C, Sciandra A, Bernard O, Cadoret JP, Bougaran G. The use of fluorescent Nile red and BODIPY for lipid measurement in microalgae. Biotechnol Biofuels. 2015;8:42.
7. Meng Y, Yao C, Xue S, Yang H. Application of Fourier transform infrared (FT-IR) spectroscopy in determination of microalgal compositions. Bioresour Technol. 2014;151:347–54.
8. Ami D, Posteri R, Mereghetti P, Porro D, Doglia SM, Branduardi P. Fourier transform infrared spectroscopy as a method to study lipid accumulation in oleaginous yeasts. Biotechnol Biofuels. 2014;7:12.
9. Münchberg U, Wagner L, Spielberg ET, Voigt K, Rösch P, Popp J. Spatially resolved investigation of the oil composition in single intact hyphae of *Mortierella* spp. with micro-Raman spectroscopy. Biochim Biophys Acta Mol Cell Biol Lipids. 2013;1831:341–9.
10. Signori L, Ami D, Posteri R, Giuzzi A, Mereghetti P, Porro D, Branduardi P. Assessing an effective feeding strategy to optimize crude glycerol utilization as sustainable carbon source for lipid accumulation in oleaginous yeasts. Microb Cell Fact. 2016;15:75.
11. Kohler A, Bocker U, Shapaval V, Forsmark A, Andersson M, Warringer J, Martens H, Omholt SW, Blomberg A. High-throughput biochemical fingerprinting of *Saccharomyces cerevisiae* by Fourier transform infrared spectroscopy. PLoS ONE. 2015;10:e0118052.
12. Dean AP, Sigee DC, Estrada B, Pittman JK. Using FTIR spectroscopy for rapid determination of lipid accumulation in response to nitrogen limitation in freshwater microalgae. Bioresour Technol. 2010;101:4499–507.
13. Jungandreas A, Costa BS, Jakob T, Von Bergen M, Baumann S, Wilhelm C. The acclimation of *Phaeodactylum tricornutum* to blue and red light does not influence the photosynthetic light reaction but strongly disturbs the carbon allocation pattern. PLoS ONE. 2014;9:e99727.
14. Vongsvivut J, Heraud P, Gupta A, Thyagarajan T, Puri M, McNaughton D, Barrow CJ. Synchrotron-FTIR microspectroscopy enables the distinction of lipid accumulation in thraustochytrid strains through analysis of individual live cells. Protist. 2015;166:106–21.
15. Shapaval V, Afseth NK, Vogt G, Kohler A. Fourier transform infrared spectroscopy for the prediction of fatty acid profiles in Mucor fungi grown in media with different carbon sources. Microb Cell Fact. 2014;13:86.
16. Janbu AO, Møretrø T, Bertrand D, Kohler A. FT-IR microspectroscopy: a promising method for the rapid identification of Listeria species. FEMS Microbiol Lett. 2008;278:164–70.
17. Santos C, Fraga ME, Kozakiewicz Z, Lima N. Fourier transform infrared as a powerful technique for the identification and characterization of filamentous fungi and yeasts. Res Microbiol. 2010;161:168–75.
18. Shapaval V, Schmitt J, Møretrø T, Suso H, Skaar I, Åsli A, Lillehaug D, Kohler A. Characterization of food spoilage fungi by FTIR spectroscopy. J Appl Microbiol. 2013;114:788–96.
19. Beekes M, Lasch P, Naumann D. Analytical applications of Fourier transform-infrared (FT-IR) spectroscopy in microbiology and prion research. Vet Microbiol. 2007;123:305–19.
20. Zimmermann B, Bagcioglu M, Sandt C, Kohler A. Vibrational microspectroscopy enables chemical characterization of single pollen grains as well as comparative analysis of plant species based on pollen ultrastructure. Planta. 2015;242:1237–50.
21. Veale EL, Irudayaraj J, Demirci A. An on-line approach to monitor ethanol fermentation using FTIR spectroscopy. Biotechnol Prog. 2007;23:494–500.
22. Ami D, Mereghetti P, Doglia SM. Multivariate analysis for Fourier transform infrared spectra of complex biological systems and processes. In: Valim de Freitas L, Barbosa Rodrigues de Freitas AP, editors. Multivariate analysis in management, engineering and the sciences. InTech; 2013. doi:10.5772/53850.
23. Kavadia A, Komaitis M, Chevalot I, Blanchard F, Marc I, Aggelis G. Lipid and gamma-linolenic acid accumulation in strains of zygomycetes growing on glucose. J Am Oil Chem Soc. 2001;78:341–6.
24. Duetz WA, Ruedi L, Hermann R, O'Connor K, Buchs J, Witholt B. Methods for intense aeration, growth, storage, and replication of bacterial strains in microtiter plates. Appl Environ Microbiol. 2000;66:2641–6.

25. Li J, Shapaval V, Kohler A, Talintyre R, Schmitt J, Stone R, Gallant AJ, Zeze DA. A modular liquid sample handling robot for high-throughput Fourier transform infrared spectroscopy. In: Ding X, Kong X, Dai SJ, editors. Advances in reconfigurable mechanisms and robots II. Cham: Springer International Publishing; 2016. p. 769–78.
26. Lewis T, Nichols PD, McMeekin TA. Evaluation of extraction methods for recovery of fatty acids from lipid-producing microheterotrophs. J Microbiol Methods. 2000;43:107–16.
27. Savitzky A, Golay MJE. Smoothing + differentiation of data by simplified least squares procedures. Anal Chem. 1964;36:1627.
28. Kohler A, Kirschner C, Oust A, Martens H. Extended multiplicative signal correction as a tool for separation and characterization of physical and chemical information in Fourier transform infrared microscopy images of cryo-sections of beef loin. Appl Spectrosc. 2005;59:707–16.
29. Shapaval V, Møretrø T, Suso HP, Åsli AW, Schmitt J, Lillehaug D, Martens H, Böcker U, Kohler A. A high-throughput microcultivation protocol for FTIR spectroscopic characterization and identification of fungi. J Biophotonics. 2010;3:512–21.
30. Michailides TJ. Characterization and comparative-studies of Mucor isolates from stone fruits from California and Chile. Plant Dis. 1991;75:373–80.
31. Tang X, Chen HQ, Chen YQ, Chen W, Garre V, Song YD, Ratledge C. Comparison of biochemical activities between high and low lipid-producing strains of *Mucor circinelloides*: an explanation for the high oleaginicity of strain WJ11. PloS ONE. 2015;10:e0128396.
32. Broughton R. Omega 3 fatty acids: identification of novel fungal and chromistal sources. London: University of London, Royal Holloway; 2012.
33. Weete JD, Shewmaker F, Gandhi SR. gamma-Linolenic acid in zygomycetous fungi: syzygites megalocarpus. J Am Oil Chem Soc. 1998;75:1367–72.
34. Forfang K, Zimmermann B, Kosa G, Kohler A, Shapaval V. FTIR spectroscopy for evaluation and monitoring of lipid extraction efficiency for oleaginous fungi. PLoS ONE. 2017;12:e0170611.
35. Suutari M. Effect of growth temperature on lipid fatty acids of four fungi (*Aspergillus niger*, *Neurospora crassa*, *Penicillium chrysogenum*, and *Trichoderma reesei*). Arch Microbiol. 1995;164:212–6.

Supplementary Material

Microtiter plate cultivation of oleaginous fungi and monitoring of lipogenesis by high-throughput FTIR spectroscopy

Gergely Kosa *,Achim Kohler, Valeria Tafintseva, Boris Zimmermann, Kristin Forfang, Nils Kristian Afseth, Dimitrios Tzimorotas, Kiira S. Vuoristo, Svein Jarle Horn, Jerome Mounier, Volha Shapaval

*Corresponding author:

Gergely Kosa
Faculty of Science and Technology
Norwegian University of Life Sciences
Postbox 5003, 1432 Ås, Norway
Email: gergely.kosa@nmbu.no

Table of contents: **Page**

Table S1 Maximum measured value of biomass concentration (CDW, g L^{-1}), lipid content of cell dry weight (wt %), total lipid concentration (g L^{-1}), and GLA concentration (mg L^{-1}) in the fermentation broth. Yield of biomass (g g^{-1}) and yield of total lipids (g g^{-1}) per glucose carbon source

Strain	Temperature (°C)	Biomass (g L^{-1})	Lipid content (wt %)	Total lipid (g L^{-1})	GLA (mg L^{-1})	Biomass/Glucose (g g^{-1})	Total lipid/Glucose (g g^{-1})
M. circinelloides VI 04473	20	11.3	34	3.7	698	0.29	0.12
	30	18.5	31	5.5	851	0.17	0.05
M. isabellina UBOCC-A-101350	20	20.8	34	6.6	662	0.29	0.09
	30	22.6	37	8.0	760	0.28	0.11
P. glabrum FRR 4190	20	19.4	26	4.9	-	0.26	0.07
	30	18.5	28	5.1	-	0.23	0.08

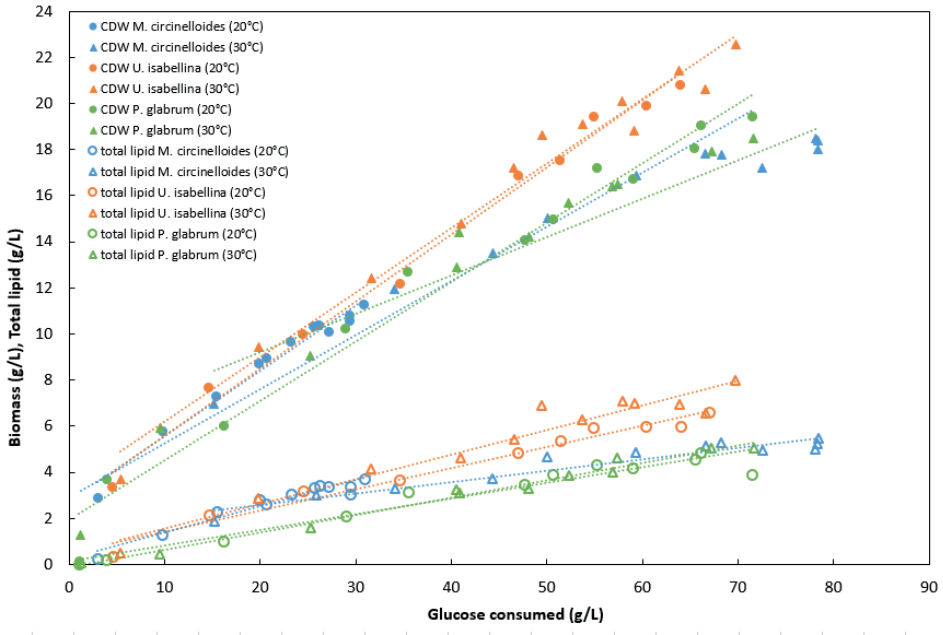

Figure S1 Biomass concentration (g L^{-1}) and total lipid content of biomass (g L^{-1}) as a function of consumed glucose (g L^{-1}). Yield of biomass (g g^{-1}) and yield of lipids (g g^{-1}) were calculated as the slope of linear regression lines of biomass and total lipid versus the amount of consumed glucose

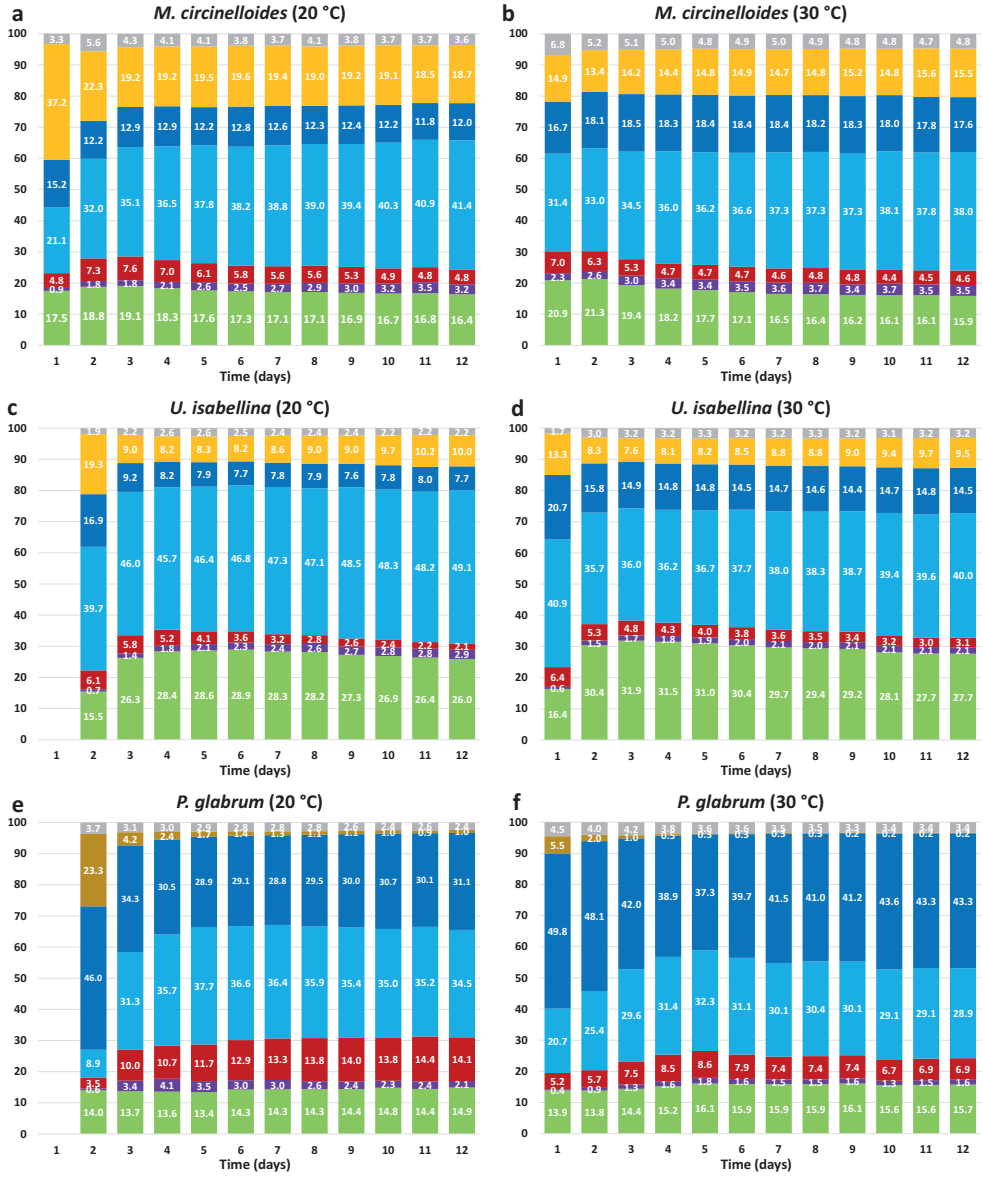

Figure S2 Fatty acid composition (%) of *M. circinelloides*, *U. isabellina* and *P. glabrum* cultivated at 20 °C and at 30 °C during cultivation for 12 days in the Duetz-MTPS. Values represent mean value of three extraction – GC replicate measurements. Coefficient of variation was less than 2 % for main fatty acids

Table S2 Peaks assignment in the FTIR spectra of microbial biomass. Peaks *1-5*, *8-10* and *16* are characteristic to lipids

Peak Nr.	Wavenumber (cm^{-1})	Peak assignment	Reference
1	*3008*	*=C-H stretching*	[1]
2	*2953*	*-C-H (CH_3) stretching (asym)*	[1]
3	*2924*	*-C-H (CH_2) stretching (asym)*	[1]
4	*2853*	*-C-H (CH_2) stretching (sym)*	[1]
5	*1745*	*-C=O (ester) stretching*	[1]
6	1695-1637	-C=O stretching, Amide I	[2]
7	1550-1520	N-H bending and C-N stretching, Amide II	[2]
8	*1465*	*-C-H (CH_2, CH_3) bending (scissoring)*	[1]
9	*1415*	*C-H rocking*	[2]
10	*1377*	*-C-H (CH_3) bending (sym)*	[1]
11	1240-1260	P=O stretching	[3]
12	1150	β (1,3)-glucans	[4]
13	1080	β (1,3)-glucans	[4]
14	1033	C-O stretching	[5]
15	880	P-O-P stretching	[6]
16	*720*	*CH_2 rocking, bending*	[1]

References:

1. Guillen MD, Cabo N: Relationships between the composition of edible oils and lard and the ratio of the absorbance of specific bands of their Fourier transform infrared spectra. Role of some bands of the fingerprint region. *Journal of Agricultural and Food Chemistry* 1998, **46:**1788-1793.
2. Kohler A, Afseth NK, Jørgensen K, Randby Å, Martens H: Quality Analysis of Milk by Vibrational Spectroscopy. In *Handbook of Vibrational Spectroscopy.* John Wiley & Sons, Ltd; 2006.
3. Davis R, Mauer L: Fourier transform infrared (FT-IR) spectroscopy: a rapid tool for detection and analysis of foodborne pathogenic bacteria. *Current research, technology and education topics in applied microbiology and microbial biotechnology* 2010, **2:**1582-1594.
4. Signori L, Ami D, Posteri R, Giuzzi A, Mereghetti P, Porro D, Branduardi P: Assessing an effective feeding strategy to optimize crude glycerol utilization as sustainable carbon source for lipid accumulation in oleaginous yeasts. *Microb Cell Fact* 2016, **15:**75.
5. Isleten-Hosoglu M, Gultepe I, Elibol M: Optimization of carbon and nitrogen sources for biomass and lipid production by Chlorella saccharophila under heterotrophic conditions and development of Nile red fluorescence based method for quantification of its neutral lipid content. *Biochemical Engineering Journal* 2012, **61:**11-19.
6. Carosio F, Alongi J, Malucelli G: Layer by Layer ammonium polyphosphate-based coatings for flame retardancy of polyester–cotton blends**.** *Carbohydrate Polymers* 2012, **88:**1460-1469.

Table S3 Variability in FTIR spectra at different levels. (1-PCC) x 10^4. PCC: Pearson Correlation Coefficient

Data set	*M. circinelloides* 20 °C	*M. circinelloides* 30 °C	*U. isabellina* 20 °C	*U. isabellina* 30 °C	*P. glabrum* 20 °C	*P. glabrum* 30 °C
Technical replicates (3 spots in 384 well HTS plate)	1.4	0.8	5.4	2.1	2.9	4.0
Biological replicates (3 wells in the 24 well microplate)	3.6	3.0	4.6	2.7	10.9	10.5
run	322.7	75.2	359.2	212.8	326.1	393.3

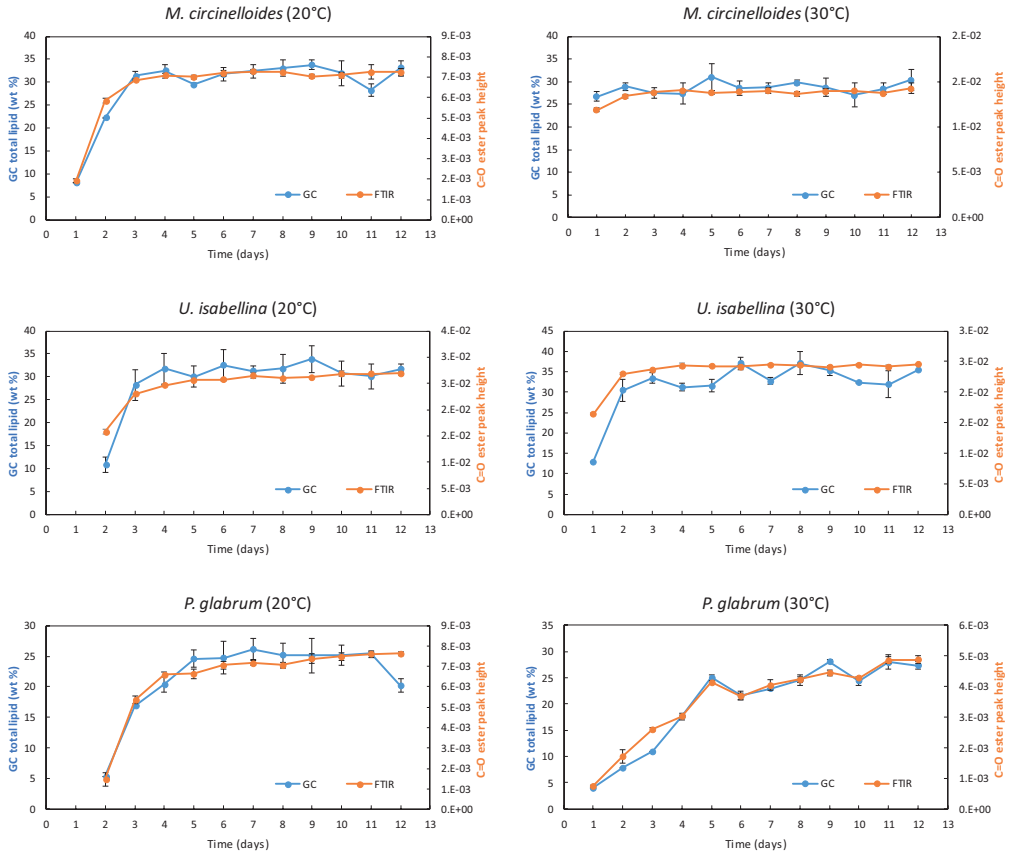

Figure S3 Total lipid content measured by reference GC method and monitored by the ester peak height of FTIR spectra (n=3, error bars = SD)

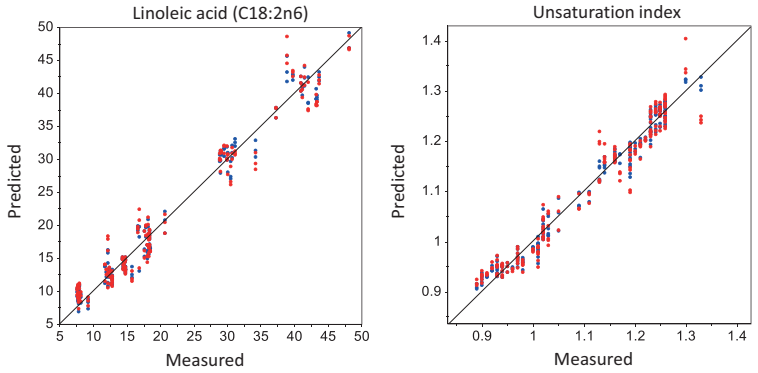

Figure S4 PLS regression results between reference GC-FID data and predicted FTIR data. **a** linoleic acid (C18:2n6c); **b** unsaturation index. Blue points represent the calibration fit obtained from the model on FTIR and GC data (closer to the target diagonal line), while red points show the predictions obtained in the more realistic cross-validation

Table S4 PLS regression results with all samples included (N=210)

Fatty acid	Range	Mean	Standard deviation	R^{2a}	RMSECV[b]	RPD_{CV}[c]	PLS factors
C16:0	13.4-31.9	19.9	6.0	0.84	2.4	2.5	3
C18:0	2.1-14.4	6.2	3.2	0.91	1.0	3.2	9
C18:1n9	8.9-49.1	36.5	6.8	0.87	2.5	2.7	17
C18:2n6	7.6-49.8	21.5	12.2	0.94	3.1	4.0	6
C18:3n6	0.0-37.2	9.2	8.0	0.95	1.7	4.7	3
SAT	20.0-39.2	28.7	4.6	0.83	1.9	2.4	6
MUFA	10.4-52.6	39.7	7.2	0.75	3.7	2.0	10
PUFA	15.9-69.5	31.5	10.0	0.93	2.7	3.7	11
unsaturation index	0.89-1.73	1.13	0.16	0.90	0.05	3.1	7
total lipid	4.0-37.1	26.8	7.5	0.86	2.8	2.6	4

[a] R^2, cross-validated squared correlation coefficient
[b] RMSECV, Root Mean Square Error of Cross Validation
[c] RPD_{CV}, Residual predictive deviation of cross-validation (standard deviation/RMSECV)

Paper II

Kosa et al. Microb Cell Fact (2017) 16:195
DOI 10.1186/s12934-017-0817-3

Microbial Cell Factories

RESEARCH

Open Access

FTIR spectroscopy as a unified method for simultaneous analysis of intra- and extracellular metabolites in high-throughput screening of microbial bioprocesses

Gergely Kosa[1,2], Volha Shapaval[1], Achim Kohler[1] and Boris Zimmermann[1*]

Abstract

Background: Analyses of substrate and metabolites are often bottleneck activities in high-throughput screening of microbial bioprocesses. We have assessed Fourier transform infrared spectroscopy (FTIR), in combination with high throughput micro-bioreactors and multivariate statistical analyses, for analysis of metabolites in high-throughput screening of microbial bioprocesses. In our previous study, we have demonstrated that high-throughput (HTS) FTIR can be used for estimating content and composition of intracellular metabolites, namely triglyceride accumulation in oleaginous filamentous fungi. As a continuation of that research, in the present study HTS FTIR was evaluated as a unified method for simultaneous quantification of intra- and extracellular metabolites and substrate consumption. As a proof of concept, a high-throughput microcultivation of oleaginous filamentous fungi was conducted in order to monitor production of citric acid (extracellular metabolite) and triglyceride lipids (intracellular metabolites), as well as consumption of glucose in the cultivation medium.

Results: HTS FTIR analyses of supernatant samples was compared with an attenuated total reflection (ATR) FTIR, which is an established method for bioprocess monitoring. Glucose and citric acid content of growth media was quantified by high performance liquid chromatography (HPLC). Partial least square regression (PLSR) between HPLC glucose and citric acid data and the corresponding FTIR spectral data was used to set up calibration models. PLSR results for HTS measurements were very similar to the results obtained with ATR methodology, with high coefficients of determination (0.91–0.98) and low error values (4.9–8.6%) for both glucose and citric acid estimates.

Conclusions: The study has demonstrated that intra- and extracellular metabolites, as well as nutrients in the cultivation medium, can be monitored by a unified approach by HTS FTIR. The proof-of-concept study has validated that HTS FTIR, in combination with Duetz microtiter plate system and chemometrics, can be used for high throughput screening of microbial bioprocesses. It can be anticipated that the approach, demonstrated here on single-cell oil production by filamentous fungi, can find general application in screening studies of microbial bioprocesses, such as production of single-cell proteins, biopolymers, polysaccharides, carboxylic acids, and other type of metabolites.

Keywords: Microcultivation, Oleaginous fungi, Citric acid, High-throughput screening, Fourier transform infrared spectroscopy, Partial least squares regression, Bioprocess monitoring, *Mucor*, *Umbelopsis*, *Penicillium*

*Correspondence: boris.zimmermann@nmbu.no
[1] Faculty of Science and Technology, Norwegian University of Life Sciences, Postbox 5003, 1432 Ås, Norway
Full list of author information is available at the end of the article

Background

Screening of a high number of candidate strains, as well as testing of different substrates and growth conditions, is a precondition for development and optimization of an efficient microbial bioprocess. Micro-bioreactors, usually in the form of multi-well microtiter plates, enable high-throughput parallel cultivation of microorganisms with culture volumes ranging from milliliter to nanoliter [1–7]. Application of such systems saves valuable time and decrease costs in the development of bioprocesses.

However, high-throughput screening can only be achieved if a high-throughput cultivation is followed by high-throughput measurement of biomass, intra- and extracellular metabolites, and substrate. Analysis is often performed by time-consuming approaches, that can involve two or more traditional analytical techniques in order to evaluate different type of analytes, thus significantly reducing the speed of the screening itself [6]. For example, screening of oleaginous microorganisms requires measurements of accumulation of intracellular lipids, as well as changes in chemical composition of the growth media. Usually this is obtained by tedious lipid extraction methods followed by gas chromatography (GC), while substrate consumption and release of extracellular metabolites is usually monitored by high performance liquid chromatography (HPLC) and by biochemical assays [1, 7, 8]. Although chromatographies are powerful methods for the analysis of metabolites, different mobile-solid phase configurations are needed for different type of analytes based on their molecular weight, solubility, polarity, and other parameters, thus often the change of a configuration or instrumentation is needed.

Over the past decade, mid-infrared (MIR) Fourier transform infrared (FTIR) spectroscopy has emerged as a powerful tool for screening, studying, and monitoring of biological processes. FTIR spectroscopy is fast and non-destructive biophysical method that detects molecular bond vibrations. Unlike traditional analytical methods, FTIR spectroscopy is not restricted to one specific cell characteristic. Given that FTIR is based on the measurement of many different spectral cell characteristics, the resulting spectrum is a precise signature of the overall chemical composition of a sample. FTIR spectra are highly reproducible and informative, and can be used both for identification purposes and for quantitative and qualitative analysis of cell's chemical constituents such as lipids, proteins, carbohydrates and biopolymers. For instance, FTIR has been used for screening of microorganisms based on their content of lipids [8–10], biopolymers [11], or general biomass composition [12, 13]. Since FTIR spectroscopy is able to perform multi-analyte analysis and provide a broad spectrum of information, it is thus considered as an alternative to traditional analytical methods in high-throughput screening. FTIR techniques, such as attenuated total reflection (ATR) cells and probes, have already been assessed for on-line monitoring of bioprocesses, including substrate consumption and extracellular metabolite formation [14–22]. A number of studies have demonstrated that infrared ATR sensors are ideal instruments for monitoring of various compounds, such as glucose [15–19], fructose [20], lactose [14], starch [16], acetate [15, 16, 20], lactate [17], lactic acid [14], ethanol [18–20], and ammonium [20]. Unfortunately, measurement of biomass in a bioreactor by ATR sensors is impractical without complex modifications of FTIR instrumentation [22, 23], and thus quantitative on-line measurements of biomass have not been conducted yet.

In addition to on-line process monitoring, FTIR also offers high-throughput analyses of microbial bioprocesses by high throughput screening (HTS) system. The analysis is usually achieved by depositing biomass samples on a multi-well IR-light-transparent microplate [7–10, 24–26]. Several studies have shown a high correlation of HTS FTIR spectroscopy with traditional analytical techniques, such as GC, HPLC, and biochemical assays, for different types of bioprocesses [7, 9, 27, 28]. However, the majority of studies have been focused on quantitative analysis of biomass, while high-throughput studies of substrates and extracellular metabolites had very limited scope [27, 28]. Thus, the application of FTIR spectroscopy in high-throughput screening of microorganisms has not been fully explored, despite the fact that it can perform high-throughput multi-analyte quantification of both intra- and extracellular metabolites and substrate consumption.

Compared with other commercial high throughput micro-bioreactors, Duetz microtiter plate system (Duetz-MTPS) is simple and cost-effective system that offers very high number of parallel cultivations [29, 30]. However, the system is usually limited only to preliminary strain screening due to lack of process information [6]. In our recent study, FTIR spectroscopy was combined with Duetz-MTPS for the screening of oleaginous filamentous fungi [7]. It has been shown that HTS FTIR spectroscopic analysis of lipids in cell biomass correlates very well with GC analysis, and can be used for the prediction of total lipid and several groups of fatty acids (saturated, monounsaturated, and polyunsaturated) in fungal cell biomass [7]. Analogous to Duetz MTPS, HTS FTIR features microplate design well suited for automation systems [31], thus it is far more suitable for high-throughput screening than probe- or cell-based ATR FTIR setting. In the present study we evaluate HTS FTIR spectroscopy as a unified method for simultaneous quantification of both intra- and extra-cellular metabolites, as well as substrate consumption in high-throughput screening of microbial

bioprocesses. Oleaginous filamentous fungi, namely *Mucor circinelloides*, *Umbelopsis isabellina* and *Penicillium glabrum*, were used as a model organisms. As previously reported, lipid production for all the studied fungal strains was relatively high, reaching 28–34% of lipid content of the biomass [7]. In addition, *Penicillium* is a good producer of organic acids [32–36].

Methods

Fungal strains

Three oleaginous filamentous fungi were used in the study: *Mucor circinelloides* VI 04473 (Norwegian School of Veterinary Science; Oslo, Norway), *Umbelopsis isabellina* UBOCC-A-101350 (Université de Bretagne Occidentale Culture Collection; Plouzané, France) and *Penicillium glabrum* FRR 4190 (Commonwealth Scientific and Industrial Research Organisation; North Ryde, Australia).

Cultivation of fungi in high-throughput Duetz-MTP screening system

Cultivation in liquid medium was performed in the Duetz-MTP screening system (Enzyscreen, Netherlands), consisting of 24-square polypropylene deep well plates, low-evaporation sandwich covers, and extra high cover clamps. Duetz plates were mounted in two Innova 40R refrigerated desktop shakers (Eppendorf, Germany). The broth medium was prepared according to the protocol described in Kavadia et al. [37] with modifications (g L^{-1}): glucose 80, yeast extract (total nitrogen 10.0–12.5%) 3, KH_2PO_4 7, Na_2HPO_4 2, $MgSO_4{\cdot}7H_2O$ 1.5, $CaCl_2{\cdot}2H_2O$ 0.1, $FeCl_3{\cdot}6H_2O$ 0.008, $ZnSO_4{\cdot}7H_2O$ 0.001, $CoSO_4{\cdot}7H_2O$ 0.0001, $CuSO_4{\cdot}5H_2O$ 0.0001, $MnSO_4{\cdot}5H_2O$ 0.0001. All chemicals were analytical grade (≥ 99%), and supplied by Merck (Germany), except yeast extract (Oxoid, England). Details of preparation of spore suspension and medium can be found in Kosa et al. [7]. In each well 2.5 mL of broth medium was inoculated with 50 µL of fungal spore suspension. Cultivations were performed for 12 days at 20 and 30 °C, at 300 rpm agitation speed (circular orbit 0.75" or 19 mm). Each day, one plate was removed from both shakers for analysis.

Experimental design

All microplates were prepared in the following way: the first eight wells were inoculated with *M. circinelloides*, the second eight wells with *U. isabellina*, and the last eight wells with *P. glabrum*. For each strain, growth medium, supernatant of fermentation broth and biomass of the first three wells, considered as biological replicates, were used for FTIR and HPLC analyses. The merged biomass from the other five wells was used for lipid analysis by gas chromatography (GC), as described in Kosa et al. [7]. In total, 216 supernatant and 6 growth media samples were measured by FTIR and HPLC. Moreover, 210 and 70 biomass samples were measured by FTIR and GC respectively; biomass of *U. isabellina* and *P. glabrum* cultivated at 20 °C were not sampled on the first day due to insufficient growth.

FTIR spectroscopy analysis

FTIR analyses of supernatant samples were conducted by both ATR and HTS accessories, while fungal biomass was analyzed by HTS only. Each sample was measured in three technical replicates, resulting in 648 spectra of supernatant and 18 spectra of growth media for both ATR and HTS, as well as 630 HTS spectra of biomass.

ATR measurement were performed using a Vertex 70 FTIR spectrometer (Bruker Optik, Germany) with the single-reflection attenuated total reflectance (SR-ATR) accessory. The ATR IR spectra were recorded with 32 scans using the horizontal SR-ATR diamond prism with 45° angle of incidence on a Specac (Slough, United Kingdom) High Temperature Golden Gate ATR Mk II. From each suspension or supernatant, 10 µL were transferred on the surface of the ATR crystal, and measured in three technical replicates. Spectra were recorded in the region between 7000 and 600 cm^{-1} with a spectral resolution of 4 cm^{-1}. Each spectrum was recorded as the ratio of the sample spectrum to the spectrum of the empty ATR plate.

HTS measurements were performed from ten times diluted supernatant samples by using the High Throughput Screening eXTension (HTS-XT) unit coupled to the Vertex 70 FTIR spectrometer (both Bruker Optik, Germany) in transmission mode. The washed fungal biomass was sonicated, in order to prepare homogeneous suspension; the detailed procedure for preparation of the biomass has been described previously [7]. From each suspension or supernatant, 8 µL were transferred to an IR-light-transparent silicon 384-well microplate (Bruker Optik, Germany) in three technical replicates. Samples were dried at room temperature for 2 h to form films that were suitable for FTIR analysis. The spectra were recorded in the region between 4000 and 500 cm^{-1} with a spectral resolution of 6 cm^{-1} and an aperture of 5.0 mm. For each spectrum, 64 scans were averaged. Each spectrum was recorded as the ratio of the sample spectrum to the spectrum of the empty microplate.

HPLC and pH analyses

Glucose and citric acid content of the starting growth media, as well as of the supernatant of fermentation broths, was quantified by an UltiMate 3000 UHPLC system (Thermo Scientific, USA), equipped with RFQ-Fast Acid H + 8% (100 × 7.8 mm) column

(Phenomenex, USA), and coupled to a refractive index (RI) detector. Samples were diluted ten times before analysis, filter sterilized, and subsequently eluted isocratically at 1.0 mL min^{-1} flow rate in 6 min with 5 mM H_2SO_4 mobile phase at 85 °C column temperature. The pH measurements of growth media were conducted by a PHM210 MeterLab electrode (Radiometer Analytical SAS, France).

Data analysis

For the analyses of ATR and HTS spectral sets of supernatant (including starting growth medium), spectral region of 1900–700 cm^{-1} was selected as this spectral region contains bands distinctive for both glucose and citric acid. ATR spectra were baseline offset corrected, and the obtained data set was used in the data analyses. HTS spectra were smoothed and transformed to second derivative form by Savitzky–Golay algorithm using a polynomial of power 2 with window size 15. Furthermore, the data set was reduced by taking an average of technical replicates, resulting in the data set with 222 spectra that was used in the data analyses. The description of the pre-processing of HTS spectra of biomass can be found in Kosa et al. [7].

Chemical similarities between samples were estimated by using principal component analysis (PCA), while partial least square regression (PLSR) was used to establish calibration models for glucose and citric acid. PLSR models were established by using a data set of HPLC reference measurements (responses) as a Y matrix, which was regressed onto an X matrix containing FTIR measurements (predictors). Optimal number of PLSR components (i.e. PLSR factors) of the calibration models (A_{Opt}), root-mean-square error (RMSE) and coefficient of determination (R^2) were calculated, and the optimal model was selected based on the lowest A_{Opt} having insignificantly higher RMSE than the model with the minimum RMSE. PLSR models for glucose prediction were based on measurements of all three fungal species, while the models for determination of citric acid were based on measurements of only *P. glabrum*. Model validation was performed using: (1) cross-validation (CV), where cross validation segments were defined per each strain, growth temperature, and day (74 segments in total, comprising either 9 spectra for ATR data set or 3 spectra for HTS set), and (2) independent test set validation (ITV), where PLSR models were built by excluding data on *P. glabrum* cultivated at 30 °C (540 and 180 spectra for determination of glucose by ATR and HTS respectively; 126 and 42 spectra for determination of citric acid by ATR and HTS respectively), and the data of *P. glabrum* 30 °C was subsequently used as an independent test set (108 and 36 spectra for ATR and HTS respectively). All pre-processing methods and data analyses were performed using The Unscrambler × 10.5 (CAMO Software, Oslo, Norway).

Results and discussion

Reference measurements of intra- and extracellular metabolites

Measurements of substrate (glucose) and extracellular metabolite (organic acids) in the growth media were performed by HPLC (Fig. 1), while lipid accumulation in the biomass was measured by GC as previously reported [7]. The pH measurements of growth media for *P. glabrum* cultivations have shown rapid drop of pH values, from pH 6 to 3 during the first 4 days of cultivation (Fig. 1a), while the pH values for growth media of *M. circinelloides* and *U. isabellina* have remained stable during the whole cultivation period. The drop of pH values was a result of simultaneous production of acids and lipids in *P. glabrum*. It has been reported previously that some oleaginous fungi can produce large amounts of organic acids, at the expenses of lipid accumulation, when grown under nitrogen-limited conditions [38].

HPLC measurements of organic acids and alcohols have shown significant citric acid production for *P. glabrum* cultivations, while productions of extracellular metabolites were negligible during the cultivation of *M. circinelloides* and *U. isabellina*. Citric acid production for *P. glabrum*, at 20 and 30 °C cultivation temperatures, has reached approx. 7.5 and 6.5 g L^{-1} respectively after 6 days of cultivation, and has remained stable for the subsequent 6 days (Fig. 1). In addition to citric acid production, the growth medium of *P. glabrum* has developed intensive yellow colour at the end of cultivation, however the chemical causing such colour change has not been identified.

FTIR spectra of growth media and fungal biomass

The FTIR spectra of growth media show wide-ranging difference between the ATR and HTS spectra. The ATR spectra (Fig. 2a) are dominated by water vibrational bands at approx. 3300 (O–H stretching), 2110 (HOH bending + libration), 1635 (HOH bending), and 580 cm^{-1} (libration). The principal glucose bands at 1200–900 cm^{-1} (C–O–C stretch, C–OH stretch, COH deformation, COC deformation, pyranose ring vibrations) are noticeable in the ATR spectrum of growth media. These bands have much narrower profiles than the broad water bands, with full width at half-maximum for glucose vibrational bands being approx. 30–40 cm^{-1}, compared to 100–400 cm^{-1} for water bands. The principal bands of citric acid, at 1725 (acid C=O stretch) and 1500–1000 cm^{-1} (C–O, C–OH, C–C vibrations) are mostly overlaid with stronger signals of either water

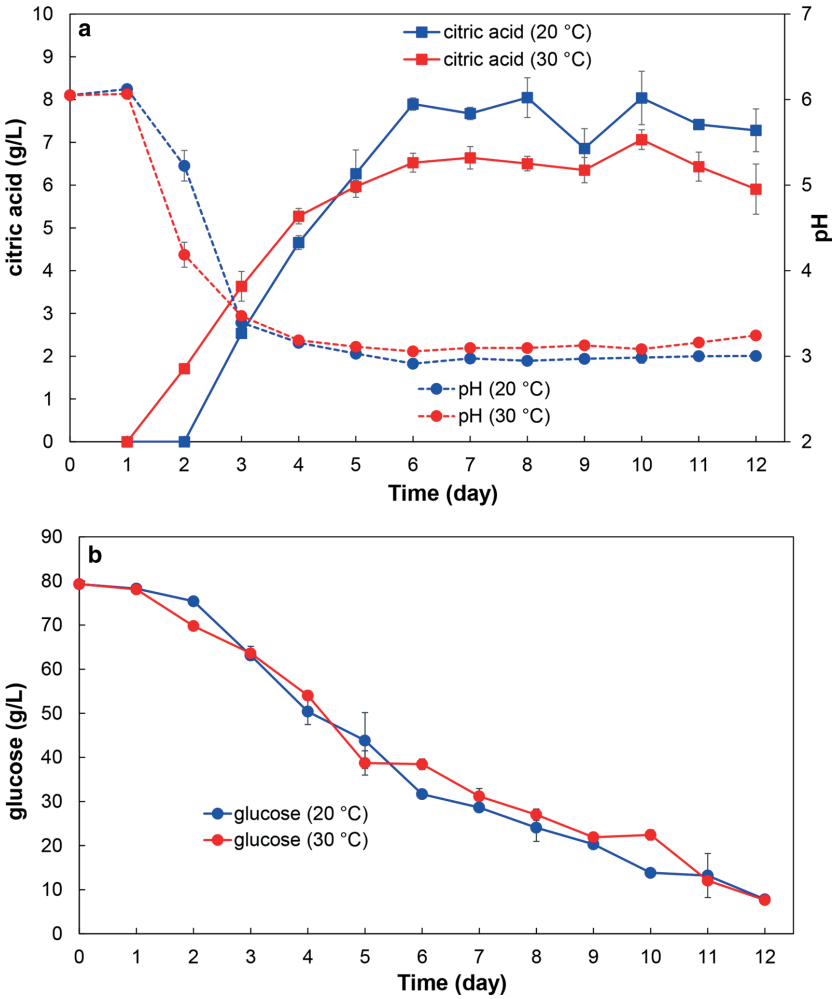

Fig. 1 **a** Progression of pH values and citric acid concentration (obtained by HPLC measurements) in cultivation medium of *P. glabrum* at 20 and 30 °C. **b** Progression of glucose concentration (obtained by HPLC measurements) in cultivation medium of *P. glabrum* at 20 and 30 °C

or glucose in the ATR spectra. Since the samples for HTS FTIR measurements were recorded as dry films, the HTS spectra are largely devoid of water bands, and clearly show principal signals of both glucose and citric acid (Fig. 2b). The concentration of citric acid in the growth media during *P. glabrum* cultivation (0–0.046 M) was several orders of magnitude lower than glucose concentration (0.042–0.444 M), reaching parity only for the end-cultivation values. This is evident in the HTS spectra of growth media on the 12th day of cultivation (Fig. 2b), where citric acid peak at 1725 cm^{-1} is of the same magnitude as glucose peak at 1035 cm^{-1}.

The development of cellular lipids can be easily detected in the biomass HTS FTIR spectra (Fig. 2c) by presence of peaks at 3050–2800 (C–H stretch), 1745 (ester C=O stretch), 1460 (CH_2 bending), 1250–1070 (C–O–C stretch and deformation) and 720 cm^{-1} (CH_2 rocking). The detailed FTIR spectral assignation of biomass for the all three fungal strains can be found in Kosa et al. [7].

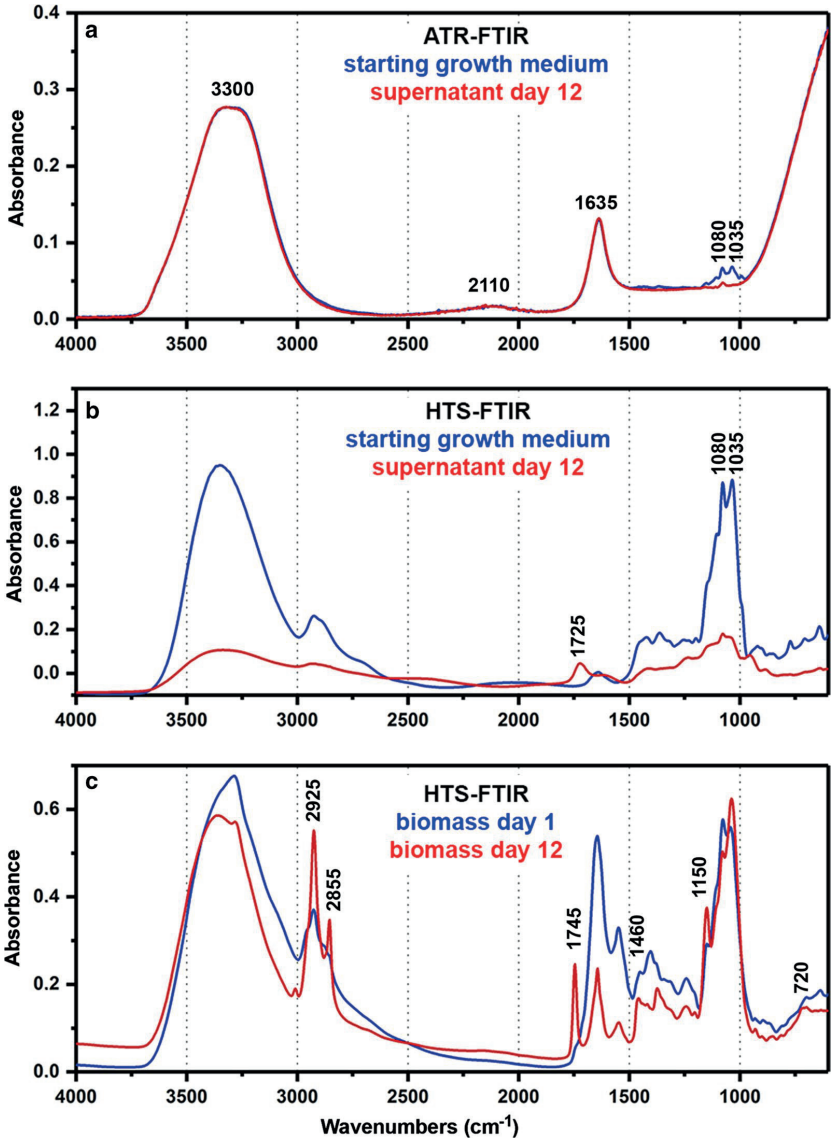

Fig. 2 **a** ATR FTIR spectra of growth media, **b** HTS FTIR spectra of growth media, and **c** HTS FTIR spectra of biomass for *P. glabrum* cultivation at 30 °C. The marked bands are associated with molecular vibrations of (W) water, (G) glucose, (C) citric acid, and (L) lipids

For both spectral data sets of growth media, the PCA results show that concentration change of glucose and citric acid during a cultivation can be monitored with great precision (Fig. 3). As can be seen in Figs. 3 and 4, for both ATR and HTS spectral data for *P. glabrum* cultivation, PC1 has high negative and high positive loadings related to glucose (1200–900 cm^{-1}) and citric acid bands (1725 cm^{-1}). Moreover, the influence of cultivation

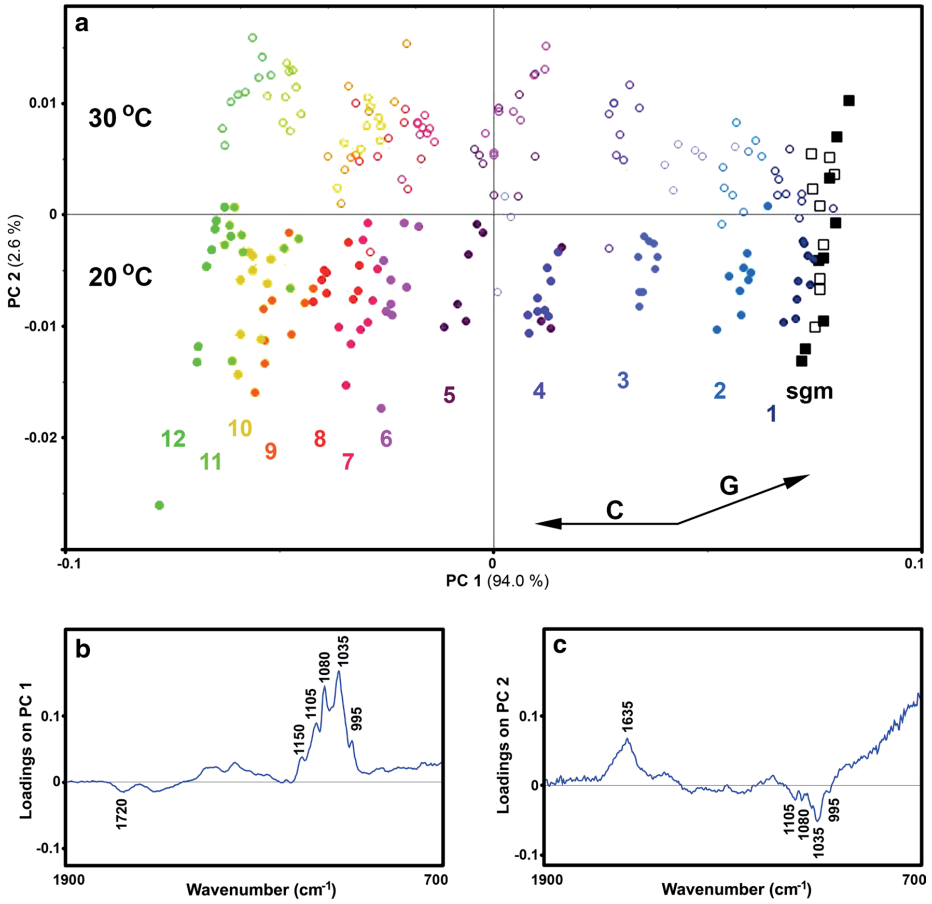

Fig. 3 **a** PCA score plot of ATR FTIR spectral data set of cultivation medium of *P. glabrum* (baseline offset corrected spectra), with depiction of starting growth media (sgm), cultivation day (1–12), and temperature (dot/block—20 °C; circle/square—30 °C). C and G vectors approximate the increase in relative amount of citric acid and glucose respectively. The percent variances for the first five PCs are 94.01, 2.59, 0.98, 0.37 and 0.16. **b** and **c** Loading plots on the first two principal components of the PCA

temperature on the chemical composition of growth media is evident even in the first couple of days of cultivation. In both data sets the score plots correctly indicate that the end-cultivation ratio of citric acid-to-glucose is higher at 20 °C than at 30 °C.

Quantitative determination of glucose and citric acid in growth medium by FTIR spectroscopy

Quantitative estimates of glucose and citric acid in the cultivation media were obtained by PLSR analyses. The results show very high level of correlation between the FTIR and HPLC measurements for both HTS and ATR measurements (Tables 1, 2). The RMSE values for assessment of glucose by ATR for all three fungal species (RMSE = 5–6%) are consistent with the reported values for ATR cell and probe measurements of bacterial and yeast fermentations (RMSE = 6–12%) [16–19]. Likewise, the related glucose values for HTS measurement are consistent with the reported values for monitoring of mammalian cell cultures [27]. However, it should be noted that our study has covered one order of magnitude higher range of glucose concentration (up to 80 g L^{-1} glucose) compared to the one in the above mentioned study [27]. The only previous reported HTS measurement of

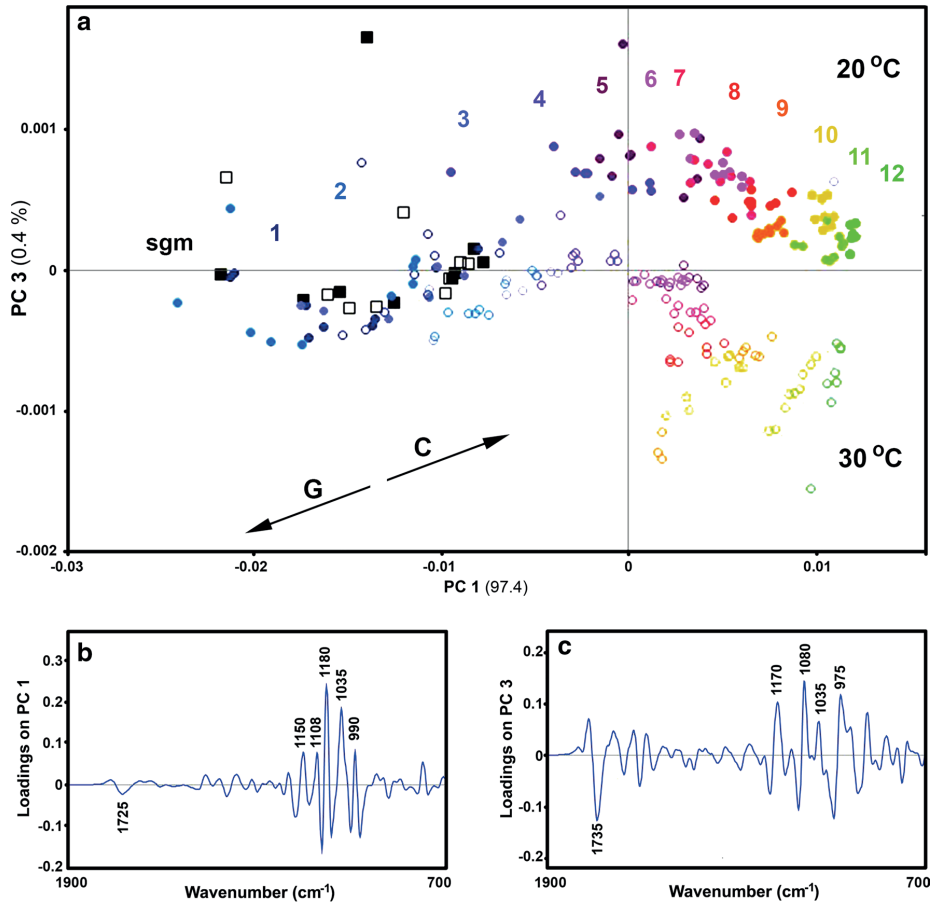

Fig. 4 **a** PCA score plot of HTS FTIR spectral data set of cultivation medium of *P. glabrum* (second derivative spectra), with depiction of starting growth media (sgm), cultivation day (1–12), and temperature (dot/block—20 °C; circle/square—30 °C). C and G vectors approximate the increase in relative amount of citric acid and glucose respectively. The percent variances for the first five PCs are 97.45, 1.69, 0.36, 0.15 and 0.13. **b** and **c** Loading plots on the first and third principal components of the PCA

Table 1 PLSR coefficients of determination (R^2) and root mean square errors (RMSE) for determination of glucose (for all three species), with the number of components in parenthesis (A_{opt}); *CV* cross validation, *ITV* independent test validation

FTIR measurement mode	CV		ITV	
	R^2 (A_{opt})	RMSE (g L^{-1} glucose)	R^2 (A_{opt})	RMSE (g L^{-1} glucose)
ATR	0.98 (1)	3.59 (4.5%)	0.96 (2)	4.49 (5.6%)
HTS	0.96 (3)	4.87 (6.1%)	0.95 (2)	4.98 (6.2%)

Table 2 PLSR coefficients of determination (R^2) and root mean square errors (RMSE) for determination of citric acid (for *P. glabrum*), with the number of components in parenthesis (A_{opt}); *CV* cross validation, *ITV* independent test validation

FTIR measurement mode	CV		ITV	
	R^2 (A_{opt})	RMSE (g L^{-1} citric acid)	R^2 (A_{opt})	RMSE (g L^{-1} citric acid)
ATR	0.97 (5)	0.51 (5.8%)	0.88 (4)	0.76 (8.7%)
HTS	0.98 (5)	0.43 (4.9%)	0.91 (3)	0.75 (8.6%)

glucose, where similarly high concentrations of glucose were measured in an artificial set of model solutions (and not an actual cultivation medium), has resulted with very large errors of prediction [28].

The number of components (PLS factors) used for building FTIR vs. HPLC calibration models for both FTIR techniques was low indicating high stability and reliability of the developed models. Moreover, the models for citric acid have low error even for independent test validation, where almost half of the data has been hold up. In addition to PLSR prediction models of the growth media, PLSR between gas chromatography fatty acid data and corresponding HTS–FTIR spectral data of biomass was used to set up models for the prediction of saturated, monounsaturated and polyunsaturated fatty acids, unsaturation index, total lipid content and principal fatty acids, and the results have been presented in Kosa et al. [7]. It has to be noted that the number of components used for building glucose and citric acid HTS–FTIR vs. HPLC calibrations was lower than FTIR–HTS vs. GC analysis of fungal lipids [7]. These results are logical since chemical complexity of the cultivation media (supernatant) is relatively low when compared with the fungal biomass.

Comparison of FTIR–HTS and FTIR–ATR measurements

In general, the results for HTS measurements were very similar to the results obtained with ATR methodology, with comparable RMSE values for both glucose and citric acid estimates (Tables 1, 2). This demonstrates that chemical analysis of both cultivation media and biomass can be performed by HTS–FTIR approach. However, the main differences between ATR and HTS approaches are worth discussing in detail. First, HTS measurement of growth media often requires optimization of sample concentration, as was the case in this study where spectra were obtained from ten times diluted supernatant samples. This requirement is often absent in ATR measurements, as demonstrated by published studies where ATR probes and cells were directly placed in the fermenters [14–22]. However, measurement of diluted samples can be an advantage of HTS approach over ATR since smaller quantities of supernatant are needed for measurement. This could be of importance in microbioreactor screening studies, where culture volumes are often extremely limited.

Secondly, in ATR measurement of growth media there is a controlled optical path length, resulting in extremely reproducible spectral measurements of technical replicates. Thus, only minimal requirements for spectral pre-processing are needed. For example, in this study, only the baseline offset correction was applied on the ATR spectral data set. In contrast, HTS measurement of growth media is characterised by much larger variations between the spectra of technical replicates, due to the irreproducible film formation on the silicon microplates. Because of morphological differences (mainly area and thickness) between the dried films, the resulting HTS spectra can have relatively large variation in absorbance values. Usually, this is not a major problem since the spectra can be normalised by applying standard normal variate or extended multiplicative signal correction, as it was the case with the HTS spectra of biomass [7]. However, such internal normalization should be applied only if the spectral set is more or less invariant regarding the total absorbance. This was not the case for the growth media, where concentration of nutrients has decreased by two orders of magnitude, resulting in large change in total absorbance and spectral profiles between the starting and final cultivation spectra (Fig. 2b). For that reason, differences in optical path length in HTS measurements were minimised by averaging individual spectra of technical replicates, as well as by converting the spectra into derivative form. The PLSR results for estimating citric acid and glucose indicate that spectral pre-processing was sufficient. However, if this is not the case, one possible solution would be an addition of an internal standard. For instance, an internal standard with a simple spectrum comprising of just a few sharp bands, such as thiocyanate salts with sharp S–C≡N stretching band at approx. 2100 cm^{-1}, could be utilized in peak normalization preprocessing [39]. In addition, we can expect that the use of a robotic system for sample preparation on silicone plates could increase the precision of HTS–FTIR measurement [31].

Thirdly, since dry films are used for HTS measurements, the water signal is weak and probably a more detailed fingerprint of biomolecules can be obtained compared with ATR approach. This could be of interest for detection and assessment of low-concentration chemicals, such as pigments. On the other hand, measurement

of dry films may prevent detection of volatile compounds in the growth media, such as low-molecular-mass organic acids and alcohols.

Finally, compared to ATR, microplate design of HTS–FTIR setup is consistent with microbioreactor plate design, and thus it is well suited for high throughput screening. Therefore, while ATR setup is probably an optimal choice for industrial scale bioprocess control, HTS setup displays clear advantage in screening studies.

Conclusions

One of the main challenge in using the high throughput micro-bioreactors has been the lack of information on cultivation parameters, including concentration profiles of reactants and products. Analyses of substrate and metabolites are often bottleneck activities, and thus can significantly hinder high throughput platforms. In our studies of lipid production of filamentous fungi, we have demonstrated that HTS FTIR, in combination with Duetz-MTPS, can be used for high throughput screening of microbial bioprocesses. Intra- and extracellular metabolites, as well as nutrients in the cultivation medium, have been monitored by a unified approach. When compared with ATR FTIR, which is an established method for bioprocess monitoring, HTS FTIR offers almost equivalent prediction of glucose and citric acid. In addition, both Duetz-MTPS and HTS FTIR have good potential for full automatization. In conclusion, it has been demonstrated that HTS FTIR spectroscopy can be used as a rapid and versatile analytical method for gaining insights on microbial bioprocesses. It can be anticipated that the approach, demonstrated here on single-cell oil production by filamentous fungi, can find general application in screening studies of microbial bioprocesses, such as production of single-cell proteins, biopolymers, polysaccharides, carboxylic acids, and other type of metabolites.

Additional file

Additional file 1. FTIR and HPLC data.

Abbreviations

ATR: attenuated total reflectance; Duetz-MTPS: Duetz microtiter plate system; HTS: high-throughput screening; FTIR: Fourier transform infrared spectroscopy; PLSR: partial least squares regression.

Authors' contributions

Conceived the research idea: BZ, VS. Designed the experiments: BZ, GK, VS. Methodology: BZ, GK. Performed the experiments: GK. Discussed the results: AK, BZ, GK, VS. Analyzed the data: BZ, GK. Wrote the manuscript: BZ, GK, VS. Discussed and revised the manuscript: AK, BZ, GK, VS. All authors read and approved the final manuscript.

Author details

[1] Faculty of Science and Technology, Norwegian University of Life Sciences, Postbox 5003, 1432 Ås, Norway. [2] Nofima AS, Osloveien 1, 1430 Ås, Norway.

Competing interests

The authors declare that they have no competing interests.

Availability of data and materials

All data generated or analyzed during this study are included in this published article and its Additional file 1.

Consent for publication

Not relevant.

Ethics approval and consent to participate

Not relevant.

Funding

This work was supported by the Research Council of Norway—BIONÆR Grant, Project Numbers 234258 and 268305.

Publisher's Note

Received: 13 September 2017 Accepted: 8 November 2017
Published online: 13 November 2017

References

1. Back A, Rossignol T, Krier F, Nicaud JM, Dhulster P. High-throughput fermentation screening for the yeast *Yarrowia lipolytica* with real-time monitoring of biomass and lipid production. Microbial Cell Factories. 2016;15:147.
2. Beneyton T, Wijaya IPM, Postros P, Najah M, Leblond P, Couvent A, Mayot E, Griffiths AD, Drevelle A. High-throughput screening of filamentous fungi using nanoliter-range droplet-based microfluidics. Sci Rep. 2016;6:27223.
3. Girard P, Jordan M, Tsao M, Wurm FM. Small-scale bioreactor system for process development and optimization. Biochem Eng J. 2001;7:117–9.
4. Kensy F, Engelbrecht C, Buchs J. Scale-up from microtiter plate to laboratory fermenter: evaluation by online monitoring techniques of growth and protein expression in *Escherichia coli* and *Hansenula polymorpha* fermentations. Microbial Cell Factories. 2009;8:68.
5. Linde T, Hansen NB, Lubeck M, Lubeck PS. Fermentation in 24-well plates is an efficient screening platform for filamentous fungi. Lett Appl Microbiol. 2014;59:224–30.
6. Long Q, Liu XX, Yang YK, Li L, Harvey L, McNeil B, Bai ZG. The development and application of high throughput cultivation technology in bioprocess development. J Biotechnol. 2014;192:323–38.
7. Kosa G, Kohler A, Tafintseva V, Zimmermann B, Forfang K, Afseth NK, Tzimorotas D, Vuoristo KS, Horn SJ, Mounier J, Shapaval V. Microtiter plate cultivation of oleaginous fungi and monitoring of lipogenesis by high-throughput FTIR spectroscopy. Microbial Cell Factories. 2017;16:101.
8. Forfang K, Zimmermann B, Kosa G, Kohler A, Shapaval V. FTIR spectroscopy for evaluation and monitoring of lipid extraction efficiency for Oleaginous fungi. Plos One. 2017;12:e0170611.
9. Shapaval V, Afseth NK, Vogt G, Kohler A. Fourier transform infrared spectroscopy for the prediction of fatty acid profiles in Mucor fungi grown in media with different carbon sources. Microbial Cell Factories. 2014;13:86.
10. Dean AP, Sigee DC, Estrada B, Pittman JK. Using FTIR spectroscopy for rapid determination of lipid accumulation in response to nitrogen limitation in freshwater microalgae. Bioresour Technol. 2010;101:4499–507.
11. Misra AK, Thakur MS, Srinivas P, Karanth NG. Screening of poly-beta-hydroxybutyrate-producing microorganisms using Fourier transform infrared spectroscopy. Biotechnol Lett. 2000;22:1217–9.
12. Kohler A, Bocker U, Shapaval V, Forsmark A, Andersson M, Warringer J, Martens H, Omholt SW, Blomberg A. High-throughput biochemical fingerprinting of *Saccharomyces cerevisiae* by Fourier transform infrared spectroscopy. Plos One. 2015;10:e0118052.
13. Feng GD, Zhang F, Cheng LH, Xu XH, Zhang L, Chen HL. Evaluation of FT-IR and Nile Red methods for microalgal lipid characterization and biomass composition determination. Bioresour Technol. 2013;128:107–12.

14. Fairbrother P, George WO, Williams JM. Whey fermentation—online analysis of lactose and lactic-acid by FT-IR spectroscopy. Appl Microbiol Biotechnol. 1991;35:301–5.
15. Doak DL, Phillips JA. In situ monitoring of an *Escherichia coli* fermentation using a diamond composition ATR probe and mid-infrared spectroscopy. Biotechnol Prog. 1999;15:529–39.
16. Dahlbacka J, Kiviharju K, Eerikainen T, Fagervik K. Monitoring of *Streptomyces peucetius* cultivations using FTIR/ATR spectroscopy and quantitative models based on library type data. Biotech Lett. 2013;35:337–43.
17. Rhiel M, Ducommun P, Bolzonella I, Marison I, von Stockar U. Real-time in situ monitoring of freely suspended and immobilized cell cultures based on mid-infrared spectroscopic measurements. Biotechnol Bioeng. 2002;77:174–85.
18. Veale EL, Irudayaraj J, Demirci A. An on-line approach to monitor ethanol fermentation using FTIR spectroscopy. Biotechnol Prog. 2007;23:494–500.
19. Schalk R, Geoerg D, Staubach J, Raedle M, Methner FJ, Beuermann T. Evaluation of a newly developed mid-infrared sensor for real-time monitoring of yeast fermentations. J Biosci Bioeng. 2017;123:651–7.
20. Kornmann H, Valentinotti S, Duboc P, Marison I, von Stockar U. Monitoring and control of *Gluconacetobacter xylinus* fed-batch cultures using in situ mid-IR spectroscopy. J Biotechnol. 2004;113:231–45.
21. Koch C, Posch AE, Goicoechea HC, Herwig C, Lendl B. Multi-analyte quantification in bioprocesses by Fourier-transform-infrared spectroscopy by partial least squares regression and multivariate curve resolution. Anal Chim Acta. 2014;807:103–10.
22. Koch C, Brandstetter M, Wechselberger P, Lorantfy B, Plata MR, Radel S, Herwig C, Lendl B. Ultrasound-enhanced attenuated total reflection mid-infrared spectroscopy in-line probe: acquisition of cell spectra in a bioreactor. Anal Chem. 2015;87:2314–20.
23. Jarute G, Kainz A, Schroll G, Baena JR, Lendl B. On-line determination of the intracellular poly(beta-hydroxybutyric acid) content in transformed *Escherichia coli* and glucose during PHB production using stopped-flow attenuated total reflection FT-IR Spectrometry. Anal Chem. 2004;76:6353–8.
24. Scholz T, Lopes VV, Calado CRC. High-throughput analysis of the plasmid bioproduction process in *Escherichia coli* by FTIR spectroscopy. Biotechnol Bioeng. 2012;109:2279–85.
25. Shapaval V, Schmitt J, Moretro T, Suso HP, Skaar I, Asli AW, Lillehaug D, Kohler A. Characterization of food spoilage fungi by FTIR spectroscopy. J Appl Microbiol. 2013;114:788–96.
26. Shapaval V, Moretro T, Suso HP, Asli AW, Schmitt J, Lillehaug D, Martens H, Bocker U, Kohler A. A high-throughput microcultivation protocol for FTIR spectroscopic characterization and identification of fungi. J Biophotonics. 2010;3:512–21.
27. Sellick CA, Hansen R, Jarvis RM, Maqsood AR, Stephens GM, Dickson AJ, Goodacre R. Rapid monitoring of recombinant antibody production by mammalian cell cultures using Fourier transform infrared spectroscopy and chemometrics. Biotechnol Bioeng. 2010;106:432–42.
28. Leon ES, Coat R, Moutel B, Pruvost J, Legrand J, Goncalves O. Influence of physical and chemical properties of HTSXT–FTIR samples on the quality of prediction models developed to determine absolute concentrations of total proteins, carbohydrates and triglycerides: a preliminary study on the determination of their absolute concentrations in fresh microalgal biomass. Bioprocess Biosyst Eng. 2014;37:2371–80.
29. Duetz WA. Microtiter plates as mini-bioreactors: miniaturization of fermentation methods. Trends Microbiol. 2007;15:469–75.
30. Duetz WA, Witholt B. Oxygen transfer by orbital shaking of square vessels and deepwell microtiter plates of various dimensions. Biochem Eng J. 2004;17:181–5.
31. Li J, Shapaval V, Kohler A, Talintyre R, Schmitt J, Stone R, Gallant AJ, Zeze DA. A modular liquid sample handling robot for high-throughput Fourier transform infrared spectroscopy. In: Ding X, Kong X, Dai SJ, editors. Advances in reconfigurable mechanisms and robots II. Cham: Springer; 2016. p. 769–78.
32. Okerentugba PO, Anyanwu VE. Evaluation of citric acid production by *Penicillium* sp. ZE-19 and its improved UV-7 strain. Res J Microbiol. 2014;9:208–15.
33. Magnuson JK, Lasure LL. Organic acid production by filamentous fungi. In: Tkacz JS, Lange L, editors. Advances in fungal biotechnology for industry, agriculture, and medicine. Boston: Springer; 2004. p. 307–40.
34. Tang X, Chen HQ, Chen YQ, Chen W, Garre V, Song YD, Ratledge C. Comparison of biochemical activities between high and low lipid-producing strains of *Mucor circinelloides*: an explanation for the high oleaginicity of strain WJ11. Plos One. 2015;10:e0128396.
35. Papanikolaou S, Komaitis M, Aggelis G. Single cell oil (SCO) production by *Mortierella isabellina* grown on high-sugar content media. Biores Technol. 2004;95:287–91.
36. Thevenieau F, Nicaud J-M. Microorganisms as sources of oils. OCL. 2013;20:D603.
37. Kavadia A, Komaitis M, Chevalot I, Blanchard F, Marc I, Aggelis G. Lipid and gamma-linolenic acid accumulation in strains of zygomycetes growing on glucose. J Am Oil Chem Soc. 2001;78:341–6.
38. Levinson WE, Kurtzman CP, Kuo TM. Characterization of *Yarrowia lipolytica* and related species for citric acid production from glycerol. Enzyme Microbial Technol. 2007;41:292–5.
39. Furlan P, Servey J, Scott S, Peaslee M. FTIR analysis of mouse urine urea using IR cards. Spectrosc Lett. 2004;37:311–8.

Paper III

Scalability of oleaginous filamentous fungi and microalga cultivations from microtiter plate system to controlled stirred-tank bioreactors

Gergely Kosa[1,*] (gergely.kosa@nmbu.no), Kiira S. Vuoristo[2] (kiira.vuoristo@nmbu.no), Svein Jarle Horn[2] (svein.horn@nmbu.no), Boris Zimmermann[1] (boris.zimmermann@nmbu.no), Nils Kristian Afseth[3] (nils.kristian.afseth@nofima.no), Achim Kohler[1] (achim.kohler@nmbu.no), Volha Shapaval[1] (volha.shapaval@nmbu.no)

(1) Faculty of Science and Technology, Norwegian University of Life Sciences, Postbox 5003, 1432 Ås, Norway

(2) Faculty of Chemistry, Biotechnology and Food Science, Norwegian University of Life Sciences, Postbox 5003, 1432 Ås, Norway

(3) Nofima AS, Osloveien 1, NO-1433 Ås, Norway

Phone number and ORCID ID of corresponding author: +47-454-46857; 0000-0001-7031-1152

Abstract

Recent developments in molecular biology and metabolic engineering have resulted in a large increase in the number of strains that need to be tested, positioning high-throughput screening of microorganisms as an important step in bioprocess development. Scalability is crucial for performing reliable screening of microorganisms. Most of the scalability studies from microplate screening systems to controlled stirred-tank bioreactors have been performed so far with unicellular microorganisms. We have studied scalability of industrially relevant oleaginous filamentous fungi and microalga from Duetz-microtiter plate system to benchtop and pre-pilot bioreactors. Maximal glucose consumption rate, biomass concentration, lipid content of the biomass, biomass and lipid yield values showed good scalability for *Mucor circinelloides* (less than 20% differences) and *Mortierella alpina* (less than 30% differences) filamentous fungi. Maximal glucose consumption and biomass production rates were identical for *Crypthecodinium cohnii* in microtiter plate and benchtop bioreactor. Most likely due to shear stress sensitivity of this microalga in stirred bioreactor, biomass concentration and lipid content of biomass were significantly higher in microtiter plate system than in benchtop bioreactor. Still, fermentation results obtained in Duetz-microtiter plate system for *Crypthecodinium cohnii* are encouraging compared to what has been reported in literature. Good reproducibility (coefficient of variation less than 15% for biomass growth, glucose consumption, lipid content and pH) were achieved in the Duetz-microtiter plate system for *Mucor circinelloides* and *Crypthecodinium cohnii*. *Mortierella alpina* cultivation reproducibility might be improved with inoculation optimization. In conclusion, we have presented suitability of the Duetz-microtiter plate system for the reproducible, scalable and cost-efficient high-throughput screening of oleaginous microorganisms.

Keywords: Duetz-microtiter plate system, high-throughput screening, oleaginous microorganism, scalability, bioreactors

Introduction

High-throughput screening (HTS) of microorganisms and cell cultures is an important step in the development of sustainable bioprocesses. Shake flasks have been the standard for screening of microbes, substrates and growth conditions for a long time. Due to advances in metabolic engineering the number of strains to be tested have increased significantly, making the throughput capacity of the shake flask cultures insufficient (Knudsen 2015a; Silk et al. 2010). Recent developments in the miniaturization of fermentation systems have opened new opportunities in HTS, saving time and cost for bioprocess- and product development (Lübbehüsen et al. 2003). Microtiter plates based systems (MTPS), with either 24, 48 or 96 well plates, are the most commonly used initial screening platform in biotechnology due to their simplicity, high throughput, good reproducibility and automation possibilities (Long et al. 2014; Sohoni et al. 2012; Wu and Zhou 2014). It has been reported that variability of extracellular metabolite production by filamentous microorganisms in MTPS is significantly lower than is shake flasks (Linde et al. 2014; Siebenberg et al. 2010; Sohoni et al. 2012). Commercial HTS microtiter plate systems differ by monitoring and control options of process parameters (pH, DO, feeding, metabolites), throughput, instrument and running cost (Long et al. 2014). Sophisticated, state-of-the-art MTPS with built-in optical sensors aim to mimic bioreactor cultivation environment. Good scalability has been reported in these system up to 15m^3 bioreactors, however, most of these studies have been performed with unicellular microorganisms (bacteria and yeasts) (Back et al. 2016; Kensy et al. 2009; Knudsen 2015b; Long et al. 2014; Lübbehüsen et al. 2003; Posch et al. 2013; Silk et al. 2010). Scalability of filamentous fungi from MTPS to bioreactors is rarely discussed and the few studies performed to date, were performed at very low substrate concentration (i.e. 5 g/L glucose) (Knudsen 2015b). Application of optical online sensors in MTPS for the screening of filamentous fungi is problematic due to adherent wall growth and complex growth morphology. For these reasons at/off-line bioprocess monitoring of filamentous fungi in MTPS is a more viable approach (Posch et al. 2013).

Duetz-MTPS is a simple and low-cost HTS system that consist of standard microplates (24, 48 or 96 wells) combined with a plate cover that enables sufficient gas transfer and prohibit extensive evaporation and cross-contamination of strains during cultivations (Duetz et al. 2000). The system offers very high throughput since MTPs can be stacked in a shaker. However, the system is considered less scalable due to lack of control options and is therefore mainly used for initial strain selection based on end-point productivities (Long et al. 2014; Sohoni et al. 2012). In a recent study we have evaluated the cultivation of *Mucor circinelloides*, *Umbelopsis isabellina* and *Penicillium glabrum* oleaginous filamentous fungi in the Duetz-MTPS, resulting in good reproducibility and kinetics (Kosa et al. 2017). The aim of the current study is to evaluate scalability of filamentous fungi and microalga cultivations from Duetz-MTPS to controlled stirred-tank bioreactors. For this purpose, we selected the following oleaginous microorganisms: filamentous fungi *Mucor circinelloides* and *Mortierella alpina*, and heterotrophic microalga (marine dinoflagellate) *Crypthecodinium cohnii.* The selected microorganisms are producers of high-value polyunsaturated fatty acids (PUFAs), such as gamma-linolenic acid (GLA, C18:3n6), arachidonic acid (ARA, C20:4n6) and docosahexaenoic acid (DHA, C22:6n3) and have been used worldwide in nutraceutical products (Ratledge 2013). According to our knowledge, this is the first study on the scalability of oleaginous filamentous fungi and microalgae from Duetz-MTPS to controlled stirred-tank bioreactors. We also show how Fourier-transform infrared (FTIR) spectroscopy can be used

in combination with the Duetz-MTPS for high-throughput characterization of oleaginous filamentous fungi and microalgae.

Materials and methods

Microorganisms

Mucor circinelloides VI 04473 was obtained from Norwegian School of Veterinary Science (Oslo, Norway), while *Mortierella alpina* ATCC 32222 and *Crypthecodinium cohnii* ATCC 40750 were obtained from American Type Culture Collection (Manassas, USA).

Media and growth conditions

For inoculum preparation, filamentous fungi *M. circinelloides* and *M. alpina* were first cultivated on malt extract and potato dextrose agar, while dinoflagellate *C. cohnii* was maintained statically on ATCC 2076 medium consisting of 4 g/L yeast extract (YE, Oxoid, Hampshire, England), 12 g/L glucose and 25 g/L sea salts (Sigma-Aldrich, St Louis, USA). All cultures were incubated at 25 °C for seven days. Inoculum medium for bioreactor experiments contained 40 g/L glucose - 10 g/L YE for *M. circinelloides*, 20 g/L glucose - 10 g/L YE for *M. alpina* and ATCC 2076 medium for *C. cohnii*. 0.5 and 2 L shake flasks (baffled for fungi) were filled in with 150 and 625 mL inoculum media, respectively. Flasks were inoculated with fungal spores from Petri-dishes or with 10 v/v% 7 days old *C. cohnii* seed culture and were grown at 25 °C for 2-4 days at shaking speed 100-150 rpm.

The lipid production media for *M. circinelloides* contained 80 g/L glucose and 3 g/L YE, for *M. alpina* it contained 60 g/L glucose and 10 g/L YE, while for *C. cohnii* it consisted of 60 g/L glucose, 5 g/L YE and 25 g/L sea salts. Fungal lipid production media also contained (g/L): KH_2PO_4 7, Na_2HPO_4 2, $MgSO_4.7H_2O$ 1.5, $CaCl_2.2H_2O$ 0.1, (from 1000x concentrated stock solution): $FeCl_3.6H_2O$ 0.008, $ZnSO_4.7H_2O$ 0.001, $CoSO_4.7H_2O$ 0.0001, $CuSO_4.5H_2O$ 0.0001, $MnSO_4.5H_2O$ 0.0001 (Kavadia et al. 2001). Chemicals except YE were bought from Merck (Darmstadt, Germany). In case of *M. alpina* 3.5 g/L KH_2PO_4 and 1 g/L Na_2HPO_4 were used. The chemical composition of lipid production media was the same for all tested cultivation scales (Duetz-MTPS – 2.5 mL, benchtop fermenter – 1.5 L and pilot scale fermenter – 25 L). Demineralized water was used for media preparation in Duetz-MTPS and benchtop bioreactor, while tap water was used in the pre-pilot scale bioreactor. pH of production media after autoclaving were 6.6, 6.1, and 6.3 for *C. cohnii*, *M. circinelloides* and *M. alpina* respectively and pH was only controlled in bioreactors.

Cultivations in Duetz-MTPS were performed in autoclaved 24-square polypropylene deep well MTPs (total volume per well: 11 mL) with low evaporation version sandwich cover (Enzyscreen, Heemstede, Netherlands). All wells were filled in with sterile lipid production medium and were incubated with 10 - 250 μL fungal spore or microalga suspensions, resulting in 2.5 mL final volume. The final concentrations were $5 \cdot 10^8$ and $5 \cdot 10^7$ of spores /mL for *M. circinelloides* and *M. alpina*, respectively. For *C. cohnii* the final concentration was $5 \cdot 10^6$ cells/mL. MTPS were incubated at 28 °C at 300 rpm (circular orbit 0.75" or 19 mm) in an Innova 40R refrigerated desktop shaker (Eppendorf, Hamburg, Germany) for 7-8 days and each day one plate was removed for the analysis of biomass and

supernatant. For scalability study, the merged content of the wells were used, while reproducibility in MTPS were tested by measuring three individual wells.

The bioreactor cultivations were performed in 2.5 L total volume glass fermenter (Minifors, Infors, Bottmingen, Switzerland) and 42 L total volume stainless steel in-situ sterilizable fermenter (Techfors-S, Infors) with working volumes of 1.5 L and 25 L, respectively (working volumes are used for referring to benchtop and pre-pilot scale fermentations in the following). Autoclaved and in-situ sterilized media were inoculated with 10 and 4 v/v% (in benchtop and pre-pilot bioreactors, respectively) of the above mentioned shake flask inoculums. Glucose and trace element solutions were sterilized separately from the YE-salts solution and combined afterwards (same procedure in Duetz-MTPS).

For mixing, the benchtop and pilot fermenter were equipped with two and three 6-blade Rushton turbines respectively. Temperature for all cultivations was 28 °C. pH was monitored with a pH probe (Mettler Toledo, Greifensee, Switzerland) and was kept at 6.0 for *M. circinelloides*, *M. alpina* and 6.5 for *C. cohnii* with the automatic addition of 1 M NaOH and 1 M H_2SO_4 (for fungi) or 1 M HCl (for microalga). Dissolved oxygen (DO) was monitored with Hamilton (Bonaduz, Switzerland) and Mettler-Toledo polarographic oxygen sensors (in 1.5 L and 25 L bioreactors) and was maintained above 20% of the saturation with the automatic control of stirrer speed (300-600 rpm or 100-600 rpm for microalga). Off-gas analysis was performed with a FerMac 368 (Electrolab Biotech, Tewkesbury, UK) and Infors gas analyzers connected to the off-gas condenser of the glass and stainless steel fermenters, respectively. Cultures were aerated through a sparger at 0.5 VVM for fungi (0.75 and 12.5 L/min) and 1.0 VVM (1.5 L/min) for the microalga. Foam was controlled via a foam sensor with five times diluted Glanapon DB 870 antifoam (Busetti, Vienna, Austria).

M. alpina and *C. cohnii* had two parallel runs in the glass fermenters, while in case of *M. circinelloides* only single run was performed in 1.5 L bioreactor due to technical problems. The cultivation of microalga *C. cohnii* was performed in MTPS and glass bioreactors, but not in the pre-pilot bioreactor due to the corrosive nature of ATCC 2076 medium for stainless steel (Behrens et al. 2010; Hillig et al. 2013).

Microscopy

Micrographs were recorded with a DM6000B microscope (Leica Microsystems, Wetzlar, Germany) in bright-field and fluorescence mode after Nile-red staining according to the previously described protocol (Kosa et al. 2017).

Optical density measurement

Optical density of *C. cohnii* was measured (after proper dilution) at 600 nm with a SPECTROstar Nano UV/Vis microplate reader (BMG Labtech, Ortenberg, Germany).

Preparation of fungal biomass for FTIR analysis and lipid extraction for GC fatty acid analysis

Fungal biomass from MTPS and 1.5 L cultivations were filtered through a Whatman No. I filter paper in a vacuum setup (GE Whatman, Maidstone, UK), while in case of the 25 L cultivations a 75 μm aperture test sieve was used

(Endecotts, London, UK) for biomass separation. After filtration, the fungal biomass was washed thoroughly with distilled water. In case of microalga *C. cohnii*, the biomass was separated from medium by centrifugation at 3000 rpm and it was washed once with distilled water. In the next step, the fungal and algal biomass was frozen at -20 °C and then was lyophilized overnight in an Alpha 1-2 LDPlus freeze-dryer (Martin Christ, Osterode am Harz, Germany) at -55 °C and 0.01 mbar pressure. The freeze-dried biomass was also used to calculate cell dry weight (CDW, g/L). Approximately 10 mg of freeze-dried biomass was transferred into 2 mL screw-cap tubes containing 500 µL distilled water and 250 ± 30 mg acid-washed glass beads (800 µm, OPS Diagnostics, Lebanon, USA). Biomass was then homogenized for 1-2 min in a FastPrep-24 high-speed benchtop homogenizer (MP Biomedicals, USA) at 6.5 m s^{-1}. This homogenized fungal suspension was used for HTS-FTIR analysis. Lipid extraction protocol was performed according to previously described protocol (Kosa et al. 2017).

Fourier transform infrared (FTIR) spectroscopy

FTIR analysis of freeze-dried and homogenized fungal biomass was performed with the High Throughput Screening eXTension (HTS-XT) unit coupled to the Vertex 70 FTIR spectrometer (both Bruker Optik, Germany) in transmission mode (Kosa et al. 2017). Technical replicate spectra were averaged and then EMSC corrected (Kohler et al. 2005). For peak height determination second derivative (Savitzky-Golay, 2nd degree polynomial, 9 windows size) and EMSC correction were applied (Zimmermann and Kohler 2013). All pre-processing methods were performed using The Unscrambler X 10.5 (CAMO Software, Oslo, Norway).

GC-FID fatty acid analysis

Determination of total lipid content of fungal biomass (FAME content) and fatty acid composition analysis were performed with a HP 6890 gas chromatograph (Hewlett Packard, Palo Alto, USA) equipped with an SGE BPX70, 60.0 m × 250 µm × 0.25 µm column (SGE Analytical Science, Ringwood, Australia) and flame ionization detector (FID) (Kosa et al. 2017). For identification and quantification of fatty acids the C4-C24 FAME mixture (Supelco, St. Louis, USA), C13:0 tridecanoic acid (Sigma-Aldrich) and C23:0 tricosanoic acid (Larodan, Solna, Sweden) internal standards were used.

HPLC analysis

Glucose in the fermentation supernatant was quantified by using an UltiMate 3000 UHPLC system (Thermo Scientific, Waltham, USA) equipped with RFQ-Fast Acid H+8 % (100 × 7.8 mm) column (Phenomenex, Torrance, USA) and coupled to a refractive index (RI) detector. Samples were filter sterilized and subsequently eluted using isocratic method at 1.0 mL min^{-1} flow rate in 6 min with 5 mM H_2SO_4 mobile phase at 85 °C column temperature.

Data analysis

Biochemical similarities between biomass samples were estimated using principal component analysis (PCA) of either GC or FTIR data. PCA data analysis was performed using The Unscrambler X 10.5 (CAMO Software, Oslo, Norway).

Results

Scalability of the cultivation of the three oleaginous model organisms, *C. cohnii*, *M. circinelloides* and *M. alpina* from Duetz-MTPS to controlled stirred-tank bioreactors were evaluated based on the following characteristics: (a) cell morphology, (b) growth and substrate consumption rates, (c) biomass concentration and lipid content of biomass, and (d) fatty acid composition. The biochemical composition of cells were also measured by FTIR spectroscopy. In addition to scalability, the reproducibility of cultivations in Duetz-MTPS was investigated.

Morphology

The morphology of *C. cohnii* was similar in MTPS and in 1.5 L bioreactor: a combination of motile cells with two flagella and bigger static cells (Mendes et al. 2009) (Additional file 1, Figure S1 a-b). The cells had a high number of oval starch granules (Deschamps et al. 2008), and towards the end of the fermentation circular lipid bodies (Figure 1 a1-a2). Micrographs of *C. cohnii* show that algal cells are sensitive to shear stress, resulting in cell bursting (Additional file 1, Figure S1 c). *M. circinelloides* is a dimorphic fungus capable of growing both in filaments and yeast like single cells, depending on environmental conditions (Lübbehüsen et al. 2003). In stirred bioreactors, the single cell form was more pronounced than in MTPS, probably caused by higher shear forces in the bioreactors (Additional file 1, Figure S2). The predominant filamentous form looked similar at all tested scales, with different size (up to 15 μm) of lipid bodies in the hyphae (Figure 1, b1-b2). *M. alpina* also had similar morphology at all tested scales: fluffy pellets with a high number of small lipid bodies in the hyphae (max diameter 3 μm) (Figure 1 c1-c2).

Glucose consumption and biomass production rates

Maximal glucose consumption rate was highest in the 1.5 L scale for the filamentous fungi (0.86 and 0.54 g/L/h for *M. circinelloides* and *M. alpina*, respectively) (Figure 2). Maximal glucose consumption rate was the same in MTPS and 25 L bioreactor for *M. circinelloides* (0.72 g/L/h), while in case of *M. alpina* it was higher in MTPS than in 25 L bioreactor with 0.47 g/L/h – 0.39 g/L/h. The dinoflagellate *C. cohnii* reached the same maximal glucose consumption rate in MTPS and 1.5 L bioreactor (0.50 g/L/h). Comparison of biomass production rates between MTPS and bioreactors was only possible for *C. cohnii* due to significant wall growth of filamentous fungi *M. circinelloides* and *M. alpina* at all tested scales (Additional file 1, Figure S5). Therefore, only end-point biomass concentration of the fungi was measured from the bioreactor cultures. *C. cohnii* had the same maximal biomass production rate (0.11 g/L/h) in MTPS and in 1.5 L fermenter. The CO_2 off-gas data from the bioreactor cultivations (Figure 2 b2-c2) show that after an exponential growth phase (10 h for *M. circinelloides* and 30 h for *M. alpina*), the cells entered into the stationary growth (i.e. lipid accumulation) phase. This is caused by the nitrogen depletion (approximately 1.5 and 5 g/L) from yeast extract. It is also visible from the growth and substrate consumption curves, that *M. alpina* had one day longer lag phase in MTPS than in the stirred bioreactors.

Biomass concentration and lipid content of biomass

Due to the long lag phase observed in the 1.5 L bioreactor runs with *C. cohnii*, the maximal biomass concentration was higher in the MTPS than in the glass bioreactor: 11.3 vs. 8.7 g/L (Figure 3a). *M. circinelloides* reached comparable

(14.4 and 15.8 g/L) end-point biomass concentration in MTPS and in the 1.5 L bioreactor (it was not measured at 25 L fermentation). End-point biomass concentration of *M. alpina* in MTPS was higher than in 25 L bioreactor, but lower than in 1.5 L bioreactor: 21.5 – 24.5 ± 0 .5 – 16.9 g/L. Lipid content of *C. cohnii* increased during cultivations until glucose depletion, and reached significantly higher level in MTPS than in the glass bioreactor: 35.0 vs. 21.8 ± 3.0 %. Oil content of *M. circinelloides* was above 20% already within the first 24-48 h in all tested scales (nitrogen source depleted at 10 h), and then it increased only moderately in the following days with maximal values of 29.9 – 27.3 – 27.0 % in MTPS, 1.5 and 25 L bioreactor runs, respectively. *M. alpina* started to accumulate lipids later than *M. circinelloides* due to the longer growth phase and higher nitrogen level in the medium (initial YE level was 10 g/L instead of 3 g/L). Maximal lipid content values of *M. alpina* were comparable across the tested scales: 36.4 – 42.4 ± 0.4 – 36.4 % in MTPS, 1.5 and 25 L bioreactors.

Fatty acid composition of single cell oil

The fatty acid composition of *C. cohnii*, *M. circinelloides*, and *M. alpina* biomass is summarized in the PCA scores plot of the GC data (Additional file 1, Figure S6). *C. cohnii* is characterized by high content of C12:0, C14:0, C16:0 and C22:6n3 (DHA) and separated from the fungal oils on PC1 axis, while PC2 separates *M. circinelloides* from *M. alpina*. The separation of fungal oil composition is based on the presence/absence of C20 fatty acids (C20:3n6 DGLA and C20:4 ARA) and the relative amount of monounsaturated fatty acids (C16:1n7, C18:1n9c) in the oil. Maximum DHA content of the oil in *C. cohnii* microalga cells was 52.6 ± 4.3% in the bioreactor and 46.3% in MTPS (it increased from 42.9% after glucose depletion) (Table 1). It has been shown that *C. cohnii* has high oxygen demand for growth and synthesis of highly unsaturated PUFA such as DHA (Hillig 2014). This is in agreement with our results since the oil of the microalga grown in the bioreactor – where the aeration is more effective than in Duetz-MTPS - contained more unsaturated fatty acids, (C18:1n9, C22:6n3 DHA) and less C14:0. In case of *M. circinelloides* the FA composition of the fungal oil matched very good in MTPS and 1.5 L bioreactor, while in 25 L bioreactor the GLA content of oil was found to be higher (15.0 % vs. 10.0 %) (Table 2). Lipid content and fatty acid composition of the wall grown fungi from the 1.5 L bioreactors was investigated, and it was found to be very similar to the submerged biomass (Additional file 1. Table S2). The ARA content in *M. alpina* oil (42.0 – 35.3 ± 3.0 – 34.4 %) showed good match at different scales (Table 3), however major differences were found in the oleic acid (C18:1n9) content between scales (11.7 – 24.8 ± 3.7 – 17.3 %). Similar to *M. circinelloides*, the lipid content and composition of the wall grown *M. alpina* biomass was very similar to the submerged biomass (Additional file 1. Table S3).

FTIR analysis of *C. cohnii*, *M. circinelloides* and *M. alpina* biomass

Microalgal and fungal biomass were also analyzed by high-throughput FTIR spectroscopy. The most obvious change in mid-IR spectra of microalga and filamentous fungi during the bioprocesses was the increase of lipid-related peak intensities (Figure 4). The C=O ester peak height at 1745 cm^{-1} in the mid-IR spectra was used to monitor lipid accumulation during cultivations, and these curves correlated well with reference curves for total lipid content of biomass, obtained by the GC analyses. It is worth mentioning that the peak at approximately 3010 cm^{-1}, which is related to =C-H stretching, correlates with the unsaturation level of single cell oil. The peak position was at 3014 cm^{-1} for *C. cohnii* (unsaturation index, UI = 2.86), 3012 cm^{-1} for *M. alpina* (UI = 1.93), and 3008 cm^{-1} for *M. circinelloides*

(UI = 1.24). PCA results of FTIR data (Additional file 1, Figure S7) confirm that biomass composition correlated well between different scales in case of *M. circinelloides* and *M. alpina*, while *C. cohnii* cultivation was less scalable from MTP to 1.5 L bioreactor.

Reproducibility in Duetz-MTPS

The reproducibility of *C. cohnii*, *M. circinelloides* and *M. alpina* cultivations in MTPS were evaluated based on the fermentation results achieved in three individual wells of the same MTP (Table 4). *C. cohnii* and *M. circinelloides* showed good reproducibility after 8 and 7 days of cultivations with less than 15 % coefficient of variation for all measured parameters (glucose consumption, fatty acid composition, pH, biomass concentration and total lipid content of the biomass), while in case of *M. alpina* the variations were higher.

Discussion

C. cohnii had a much shorter lag phase in MTPS than in the bioreactor (Figure 2a) and it reached substantially higher biomass concentration and lipid content than in the stirred-tank bioreactor. Since inoculation ratio was same at both scale (10 v/v%, OD_{600nm} = 4) this might be the consequence of high shear stress in the bioreactor, caused by the agitation on the cells (stirrer speed maximum was 530 rpm). Nonetheless, different inoculums were used for MTP and the bioreactor; therefore no clear conclusion can be drawn. Hillig et al. cultivated *C. cohnii* in 24 deepwell plate together with perfluorodecalin (PFD) in order to avoid (reduce) oxygen limitation. An OD (optical density) value of 17 with PFD compared to 13 without PFD was measured, while in our study and OD of 31.6 was reached. Moreover, in the study by Hillig et al. addition of water to deepwell plates had to be applied during the long cultivation of *C. cohnii*, in order to compensate for the severe evaporation loss. In Duetz-MTPS the evaporation rate is very low (16 µl/well/day at 30ºC, 50% humidity) (Enzyscreen) therefore addition of water was not necessary in our study. The values achieved in the Duetz-MTPS with *C. cohnii* are promising in comparison with industrial requirements (CDW > 10 g/L, DHA in oil > 20%, total DHA > 1.5 g/L) (Kyle et al. 1998).

In general, a better comparison of fermentation physiological parameters of filamentous fungi between MTPS and bioreactors could have been achieved with unified inoculation approach (i.e. inoculation with spores and same final spores concentration).

The reproducibility results in the Duetz-MTPS can be explained by the difference in morphology between strains. Cell and spore suspension inoculums were homogenous and easy to pipette in case of *C. cohnii* and *M. circinelloides*, while *M. alpina* inoculum in addition to spores also contained mycelium that made it difficult to transfer inoculum equally into each well. It is likely that separation (filtration) of mycelium fragments from spores or fragmentation of mycelium for *M. alpina* inoculation can decrease the observed variability in Duetz-MTPS cultivation (Knudsen 2015a; Sohoni et al. 2012). In addition, the growth morphology of *M. alpina* is in the form of fluffy pellets of different size, and this can negatively affect the reproducibility in Duetz-MTPS. In order to reduce this effect, glass beads can be added to the cultivation. For example, Sohoni et al. observed for *Streptomyces coelicor* that the addition of 3 mm glass beads prevented both pellet morphology and wall growth, improving reproducibility and scalability from MTP to benchtop bioreactor (Sohoni et al. 2012). Another strategy to induce dispersed growth of filamentous fungi is the addition of

carboxypolymethylene, an anionic polymeric additive to the medium (Knudsen 2015a). Despite these issues, the fatty acid composition of all the tested microorganisms showed excellent reproducibility in the Duetz-MTPS. (Additional file 1, Table S1-S3).

In conclusion, key fermentation physiological parameters (glucose consumption rate, biomass concentration, lipid content of the biomass, biomass and lipid yield) were comparable (max 30% difference) for the oleaginous fungi *M. circinelloides* and *M. alpina* in Duetz-MTPS and benchtop or pre-pilot stirred-tank bioreactors (600 – 10 000 × volumetric scale factors). This has been achieved despite the absence of control options, such as pH and DO, in Duetz-MTPS, and the difficult fungal growth characteristics, such as severe wall growth. However, the heterotrophic microalga *C. cohnii* reached significantly higher biomass and lipid concentration in MTPS than in 1.5 L bioreactor, probably due to shear force sensitivity of this species. It is worth mentioning that the screening throughput of oleaginous microorganisms in the Duetz-MTPS can be increased by combining at-line FTIR spectroscopy and the automation of the cultivation-analytical system (Li et al. 2016). Reproducibility and scalability results demonstrated that the Duetz-MTPS can be used for the cost-efficient, high-throughput screening of both single cell and multicellular oleaginous microorganisms.

Authors' contributions

Conceived the research idea: BZ. Designed the experiments: GK. Methodology: GK. Performed the experiments: GK, KV. Discussed the results: GK, BZ, KV, SJH, VS, NKA, AK. Analyzed the data: GK. Wrote the manuscript: GK. Discussed and revised the manuscript: GK, BZ, KV, SJH, VS, NKA, AK. All authors read and approved the final manuscript.

Funding

This work was supported by the Norwegian Research Council-BIONÆR Grant "Single Cell Oil", project number: 234258/E50, Norwegian Research Council-BIONÆR Grant "Lipofungi", project number: 268305 and the Norwegian Research Council Grant "Interest", project number 227356.

Acknowledgements

The authors would like to acknowledge Line Degn Hansen for help in performing the 25 L fermentations.

Compliance with ethical standards

Conflict of interest

The authors declare that they have no conflict of interest.

Ethical statement

This article does not contain any studies with human participants or animals performed by any of the authors.

References

Back A, Rossignol T, Krier F, Nicaud J-M, Dhulster P (2016) High-throughput fermentation screening for the yeast Yarrowia lipolytica with real-time monitoring of biomass and lipid production. Microbial cell factories 15(1):147

Behrens PW, Thompson JM, Apt K, Pfeifer JW, Wynn JP, Lippmeier JC, Fichtali J, Hansen J (2010) Method to reduce corrosion during fermentation of microalgae. Google Patents

Deschamps P, Guillebeault D, Devassine J, Dauvillée D, Haebel S, Steup M, Buléon A, Putaux J-L, Slomianny M-C, Colleoni C (2008) The heterotrophic dinoflagellate Crypthecodinium cohnii defines a model genetic system to investigate cytoplasmic starch synthesis. Eukaryotic cell 7(5):872-880

Duetz WA, Rüedi L, Hermann R, O'Connor K, Büchs J, Witholt B (2000) Methods for intense aeration, growth, storage, and replication of bacterial strains in microtiter plates. Applied and environmental microbiology 66(6):2641-2646

Enzyscreen List sandwich covers for 24 well MTPs. PUblisher. http://www.enzyscreen.com/sandwich_covers_24_mtps.htm Accessed 10.10.2017

Hillig F (2014) Impact of cultivation conditions and bioreactor design on docosahexaenoic acid production by a heterotrophic marine microalga—A scale up study. TU Berlin

Hillig F, Annemüller S, Chmielewska M, Pilarek M, Junne S, Neubauer P (2013) Bioprocess Development in Single-Use Systems for Heterotrophic Marine Microalgae. Chemie Ingenieur Technik 85(1-2):153-161

Kavadia A, Komaitis M, Chevalot I, Blanchard F, Marc I, Aggelis G (2001) Lipid and γ-linolenic acid accumulation in strains of Zygomycetes growing on glucose. Journal of the American Oil Chemists' Society 78(4):341-346

Kensy F, Engelbrecht C, Büchs J (2009) Scale-up from microtiter plate to laboratory fermenter: evaluation by online monitoring techniques of growth and protein expression in Escherichia coli and Hansenula polymorpha fermentations. Microbial cell factories 8(1):68

Knudsen PB (2015a) Development of scalable high throughput fermentation approaches for physiological characterisation of yeast and filamentous fungi. Technical University of Denmark

Knudsen PB (2015b) Development of scalable high throughput fermentation approaches for physiological characterisation of yeast and filamentous fungi. Technical University of Denmark

Kohler A, Kirschner C, Oust A, Martens H (2005) Extended multiplicative signal correction as a tool for separation and characterization of physical and chemical information in Fourier transform infrared microscopy images of cryo-sections of beef loin. Applied spectroscopy 59(6):707-716

Kosa G, Kohler A, Tafintseva V, Zimmermann B, Forfang K, Afseth NK, Tzimorotas D, Vuoristo KS, Horn SJ, Mounier J (2017) Microtiter plate cultivation of oleaginous fungi and monitoring of lipogenesis by high-throughput FTIR spectroscopy. Microbial cell factories 16(1):101

Kyle DJ, Reeb SE, Sicotte VJ (1998) Dinoflagellate biomass, methods for its production, and compositions containing the same. Google Patents

Li J, Shapaval V, Kohler A, Talintyre R, Schmitt J, Stone R, Gallant AJ, Zeze DA (2016) A Modular Liquid Sample Handling Robot for High-Throughput Fourier Transform Infrared Spectroscopy Advances in Reconfigurable Mechanisms and Robots II. Springer, pp 769-778

Linde T, Hansen N, Lübeck M, Lübeck PS (2014) Fermentation in 24-well plates is an efficient screening platform for filamentous fungi. Letters in applied microbiology 59(2):224-230

Long Q, Liu X, Yang Y, Li L, Harvey L, McNeil B, Bai Z (2014) The development and application of high throughput cultivation technology in bioprocess development. Journal of biotechnology 192:323-338

Lübbehüsen TL, Nielsen J, McIntyre M (2003) Morphology and physiology of the dimorphic fungus Mucor circinelloides (syn. M. racemosus) during anaerobic growth. Mycological research 107(2):223-230

Mendes A, Reis A, Vasconcelos R, Guerra P, da Silva TL (2009) Crypthecodinium cohnii with emphasis on DHA production: a review. Journal of applied phycology 21(2):199-214

Posch AE, Herwig C, Spadiut O (2013) Science-based bioprocess design for filamentous fungi. Trends in biotechnology 31(1):37-44

Ratledge C (2013) Microbial production of polyunsaturated fatty acids as nutraceuticals. Microbial production of food ingredients, enzymes and nutraceuticals UK: Woodhead Publishing Co:531-558

Siebenberg S, Bapat PM, Lantz AE, Gust B, Heide L (2010) Reducing the variability of antibiotic production in Streptomyces by cultivation in 24-square deepwell plates. Journal of bioscience and bioengineering 109(3):230-234

Silk N, Denby S, Lewis G, Kuiper M, Hatton D, Field R, Baganz F, Lye GJ (2010) Fed-batch operation of an industrial cell culture process in shaken microwells. Biotechnology letters 32(1):73

Sohoni SV, Bapat PM, Lantz AE (2012) Robust, small-scale cultivation platform for Streptomyces coelicolor. Microbial cell factories 11(1):9

Wu T, Zhou Y (2014) An intelligent automation platform for rapid bioprocess design. Journal of laboratory automation 19(4):381-393

Zimmermann B, Kohler A (2013) Optimizing Savitzky–Golay parameters for improving spectral resolution and quantification in infrared spectroscopy. Applied spectroscopy 67(8):892-902

List of figures

Fig. 1 Morphology of oleaginous microalga and fungi **a** *C. cohnii* (Duetz-MTPS, 120h). **b** *M. circinelloides* (Duetz-MTPS, 168 h). **c** *M. alpina* (25 L bioreactor, 145 h) in bright-field (1) and fluorescence mode after Nile-red staining (2)

Fig. 2 a1-c1 Fermentation characteristics of *C. cohnii* (a), *M. circinelloides* (b) and *M. alpina* (c) in Duetz-MTPS, 1.5 L and 25 L bioreactors. **b2-c2** CO_2 (%) in the exhaust gas during bioreactor cultivations

Fig. 3 Comparison of physiological fermentation parameters of *C. cohnii*, *M. circinelloides* and *M. alpina* in Duetz-MTPS, 1.5 L bioreactor and 25 L bioreactor. **a** biomass, total lipid, total high-value PUFA (DHA, GLA and ARA for *C. cohnii*, *M. circinelloides* and *M. alpina*) [g/L]. **b** Biomass yield on glucose, lipid yield on glucose [g/g]

Fig. 4 a1-c1 FTIR spectra of *C. cohnii*, *M. circinelloides* and *M. alpina* at first and last day of cultivation. **a2-c2** Lipid accumulation based on FTIR C=O ester peak height (from pre-processed spectra) and reference GC total lipid (wt%) data

Table 1. Fatty acid composition (%), lipid content of biomass (wt %) of *C.cohnii* ATCC 40750 in Duetz-MTPS and in 1.5 L benchtop bioreactors at 168 h (MTPS) – 198 h (bioreactor)

	C12:0	C14:0	C16:0	C18:0	C18:1n9	C22:6n3	Lipid content (wt %)
2.5 mL	3.3	21.0	22.5	2.8	5.9	42.9	35.0
1.5 L	1.5±0.5	11.6±3.0	19.7±1.3	2.5±0.9	9.6±1.0	52.6±4.3	21.8±3.0

Table 2. Fatty acid composition (%), lipid content of biomass (wt %) of *M. circinelloides* VI 04473 in Duetz-MPTS, 1.5 L benchtop bioreactor and in 25 L pre-pilot bioreactor at 160-168 h

	C14:0	C16:0	C16:1	C18:0	C18:1n9	C18:2n6	C18:3n6	Lipid content (wt %)
2.5 mL	3.2	15.7	4.2	8.8	35.6	13.5	10.0	26.4
1.5 L	2.3	15.2	5.2	4.6	40.7	15.3	10.3	27.3
25 L	1.6	16.3	3.1	4.4	36.7	17.6	15.0	27.0

Table 3. Fatty acid composition (%), lipid content of biomass (wt%) of *M. alpina* ATCC 32222 in Duetz-MTPS, 1.5 L benchtop bioreactors and 25 L pre-pilot bioreactor at 168h

	C16:0	C18:0	C18:1n9	C18:2n6	C18:3n6	C20:3n6	C20:4n6	Lipid content (wt %)
2.5 mL	12.3	11.1	11.7	8.2	4.6	4.1	42.0	36.4
1.5 L	11.0±0.2	9.6±0.1	24.8±3.7	4.3±1.2	3.3±0.2	2.3±0.4	35.3±3.0	42.4±1.4
25 L	13.1	11.7	17.3	7.8	4.7	3.3	34.4	36.4

Table 4. Well-to-well reproducibility of oleaginous microorganisms in 24-deepwell microtiter plates in the Duetz-system based on biomass production (cell dry weight, CDW, g/L), lipid content of the biomass (wt %), glucose consumption (g/L) and pH. Fermentation broth from three individual wells were analyzed from each MTP. AVG = average, CV% = coefficient of variation

	CDW (g/L)		lipid content (wt%)		glucose consumed (g/L)		pH	
	AVG	CV%	AVG	CV%	AVG	CV%	AVG	CV%
C. cohnii (t=192h)	9.5	4.1	34.0	7.9	58.9	0.03	6.9	2.3
M. circinelloides (t=168h)	13.3	2.3	29.5	13.6	76.1	1.3	5.0	1.7
M. alpina (t=168h)	20.6	8.0	36.5	17.7	40.2	20.6	6.6	0.2

Fig1

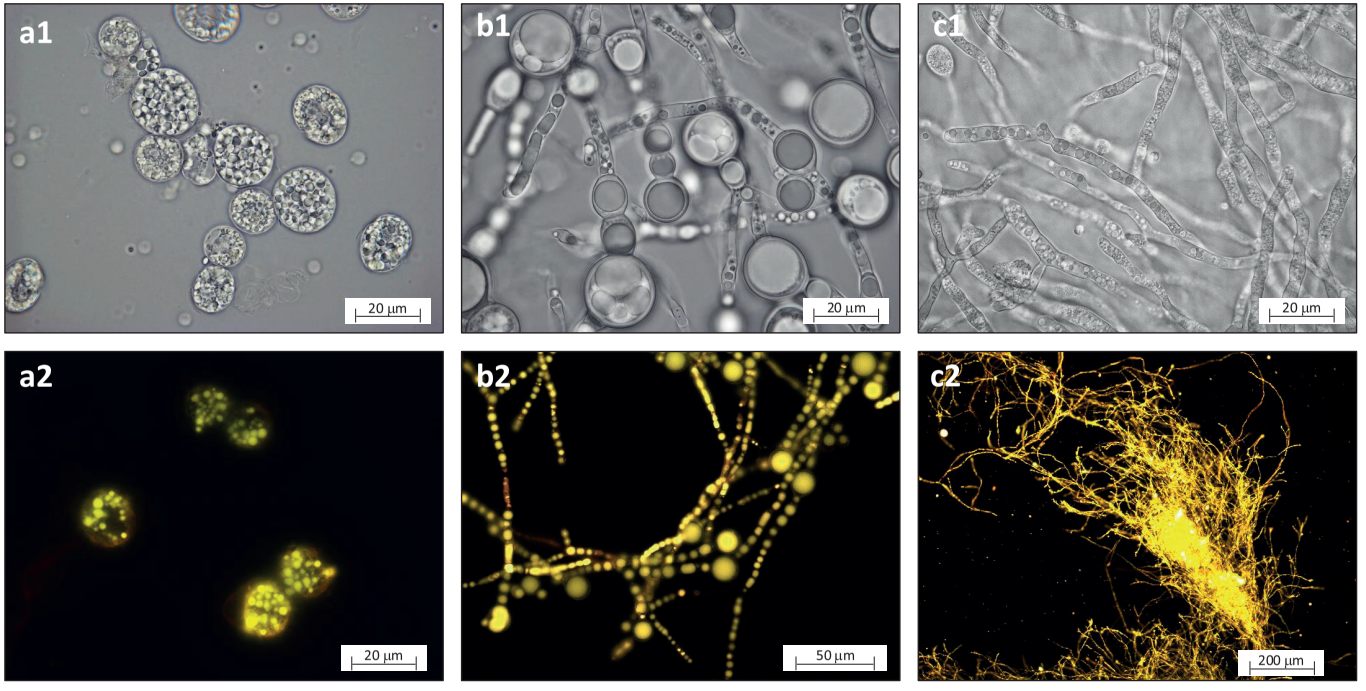

Fig2

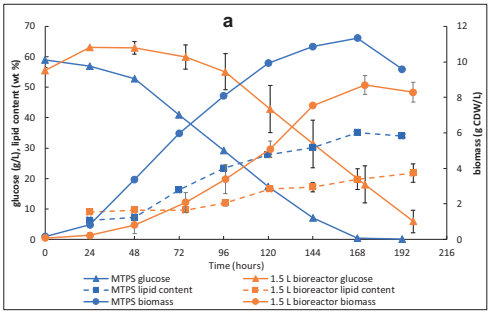
a
glucose (g/L), lipid content (wt %)
biomass (g CDW/L)
Time (hours)
MTPS glucose
MTPS lipid content
MTPS biomass
1.5 L bioreactor glucose
1.5 L bioreactor lipid content
1.5 L bioreactor biomass

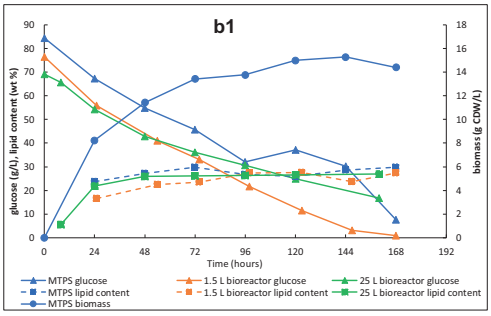
b1
glucose (g/L), lipid content (wt %)
biomass (g CDW/L)
Time (hours)
MTPS glucose
MTPS lipid content
MTPS biomass
1.5 L bioreactor glucose
1.5 L bioreactor lipid content
25 L bioreactor glucose
25 L bioreactor lipid content

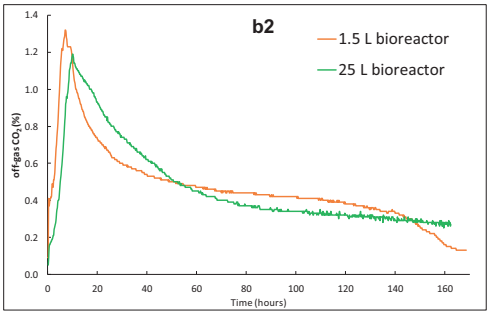
b2
1.5 L bioreactor
25 L bioreactor
off-gas CO2 (%)
Time (hours)

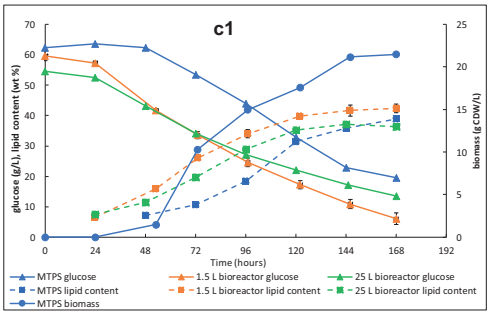
c1
glucose (g/L), lipid content (wt %)
biomass (g CDW/L)
Time (hours)
MTPS glucose
MTPS lipid content
MTPS biomass
1.5 L bioreactor glucose
1.5 L bioreactor lipid content
25 L bioreactor glucose
25 L bioreactor lipid content

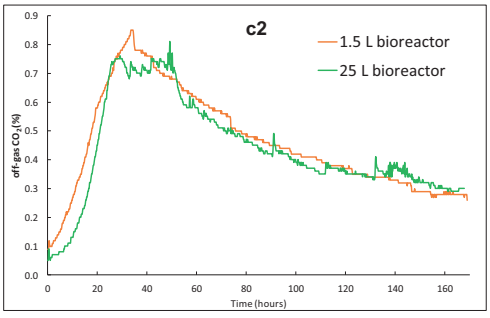
c2
1.5 L bioreactor
25 L bioreactor
off-gas CO2 (%)
Time (hours)

Fig3

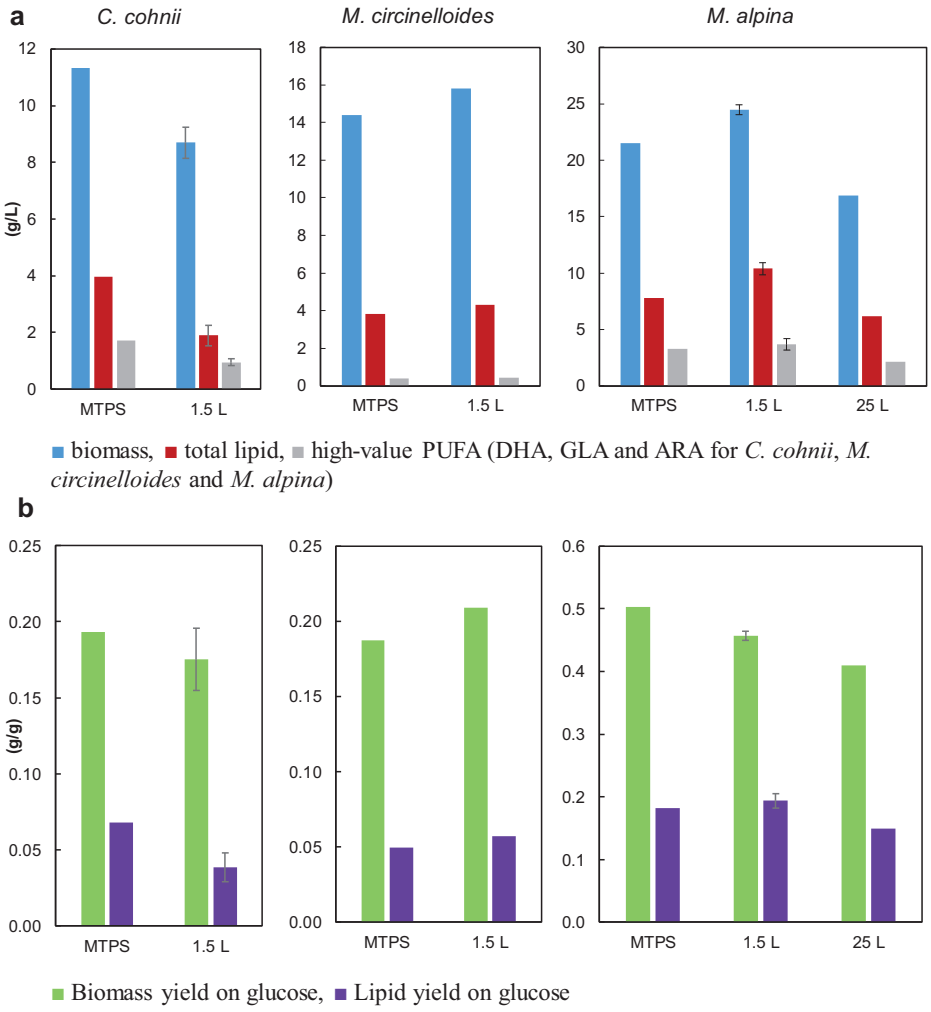
a
C. cohnii
M. circinelloides
M. alpina
(g/L)
MTPS
1.5 L
25 L
biomass, total lipid, high-value PUFA (DHA, GLA and ARA for C. cohnii, M. circinelloides and M. alpina)
b
(g/g)
Biomass yield on glucose, Lipid yield on glucose

Fig4

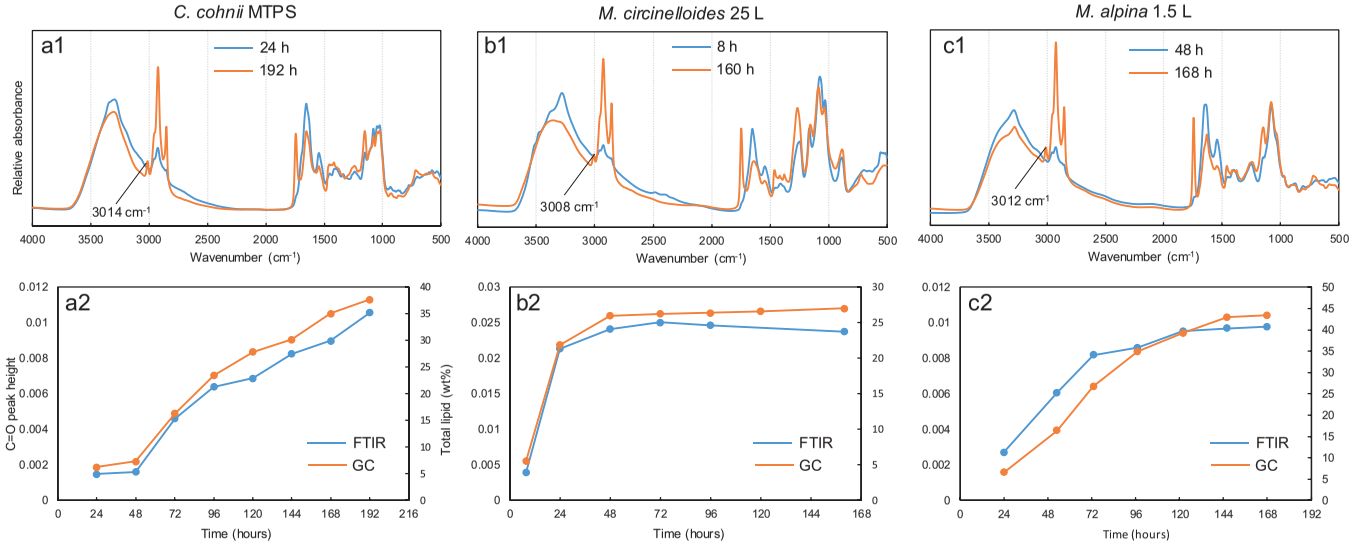
C. cohnii MTPS
M. circinelloides 25 L
M. alpina 1.5 L
a1
b1
c1
24 h
192 h
8 h
160 h
48 h
168 h
Relative absorbance
3014 cm-1
3008 cm-1
3012 cm-1
Wavenumber (cm-1)
a2
b2
c2
C=O peak height
Total lipid (wt%)
FTIR
GC
Time (hours)

Applied Microbiology and Biotechnology

Scalability of oleaginous filamentous fungi and microalga cultivations from microtiter plate system to controlled stirred-tank bioreactors

Supplementary material

Gergely Kosa[1,*], Kiira S. Vuoristo[2], Svein Jarle Horn[2], Boris Zimmermann[1], Nils Kristian Afseth[3], Achim Kohler[1], Volha Shapaval[1]

(1) Faculty of Science and Technology, Norwegian University of Life Sciences, Postbox 5003, 1432 Ås, Norway

(2) Faculty of Chemistry, Biotechnology and Food Science, Norwegian University of Life Sciences, Postbox 5003, 1432 Ås, Norway

(3) Nofima AS, Osloveien 1, NO-1433 Ås, Norway

Phone number and e-mail address of the corresponding author: +47-454-46857, gergely.kosa@nmbu.no

Table of contents: **Page**

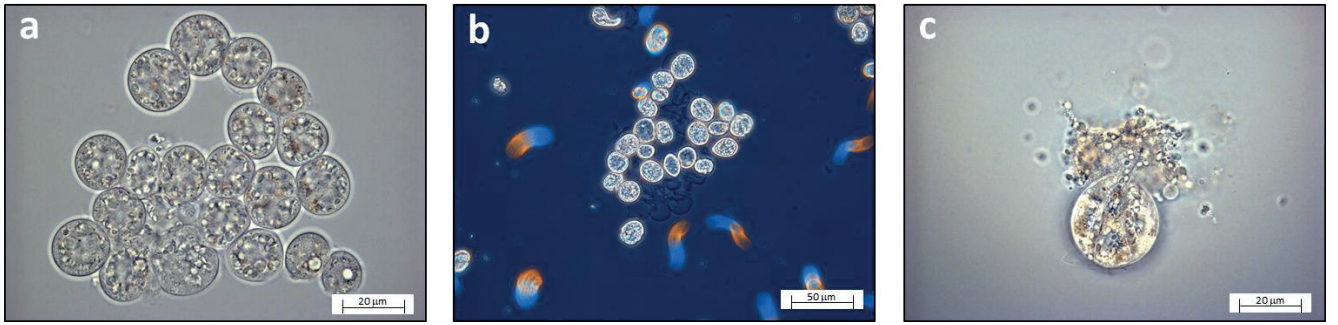

Fig. S1 Micrographs of *C. cohnii* ATCC 40750 in 1.5 L working volume benchtop bioreactor: **a)** cells contain high number of oval starch granules (48 h), **b)** phase-contrast image of moving cells and cysts (121 h), and **c)** bursting cell (76 h)

Fig. S2 Yeast-like form of the dimorphic fungus *Mucor circinelloides* (1.5 L working volume benchtop bioreactor, t = 12 h)

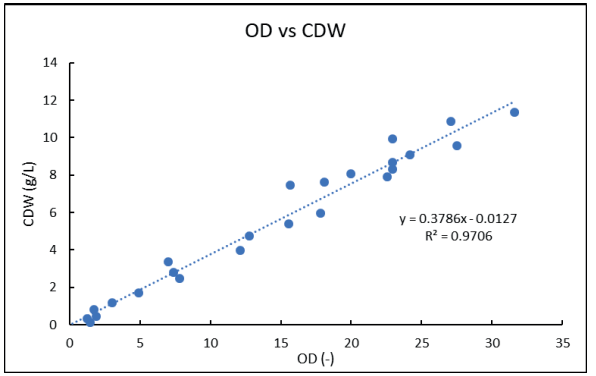

Fig. S3 Optical density (600 nm) and cell dry weight (CDW) calibration for *C. cohnii* ATCC 40750 (Data combined from Duetz-MTPS and 1.5 L working volume bioreactor cultivations)

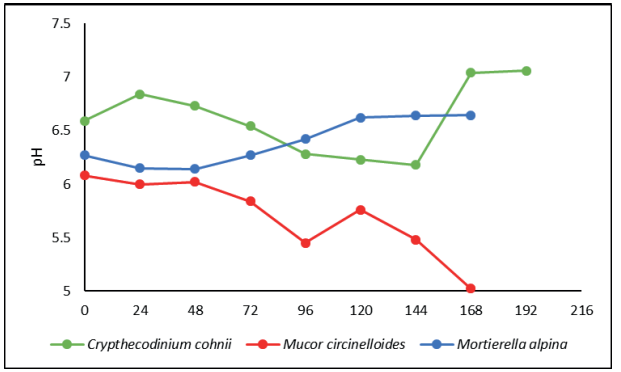

Fig. S4 Development of broth pH in Duetz-MTPS of *C. cohnii*, *M. circinelloides* and *M. alpina*. Media were not buffered.

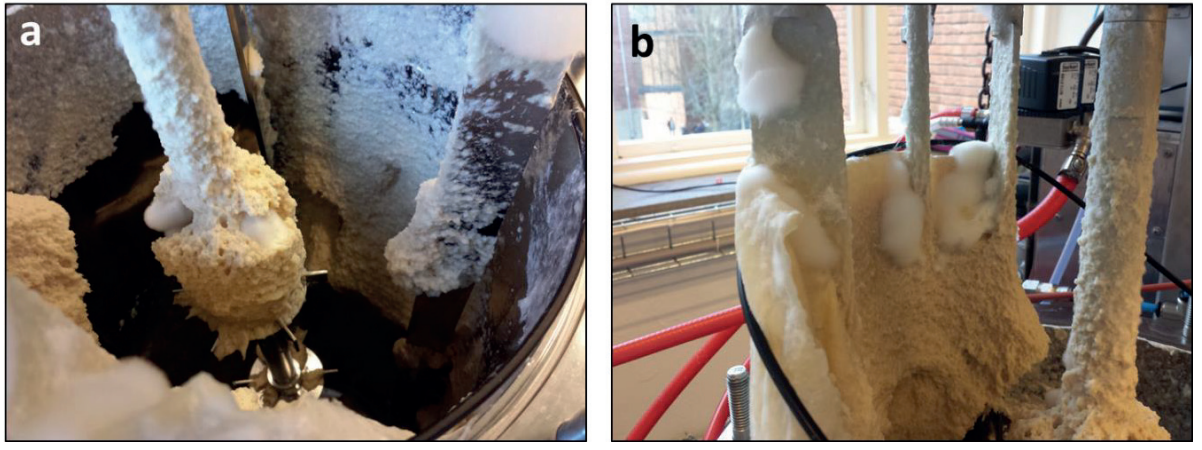

Fig. S5 *Mortierella alpina* ATCC 32222 grown on impellers, baffles and wall of the 42 L total volume pre.pilot bioreactor. Aerial mycelium started to grow on baffles.

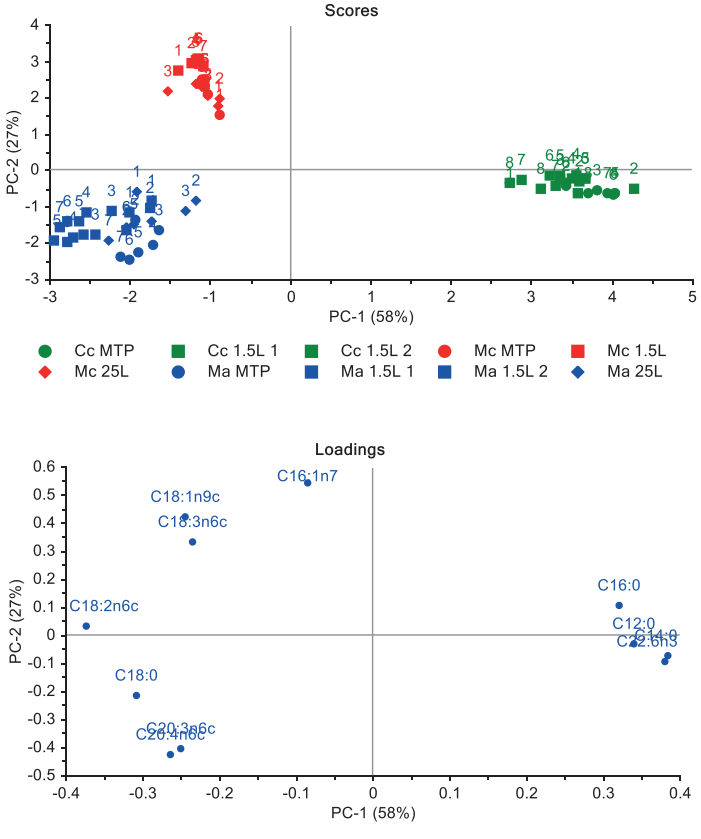

Fig. S6 a PCA scores (samples) and **b** loadings (fatty acids) of the fatty acid composition from *C. cohnii*, *M. circinelloides* and *M. alpina* cultured in Duetz-MTPS, 1.5 L benchtop and 25 L pre-pilot bioreactors. Numbers in the score plot indicate fermentation time in days.

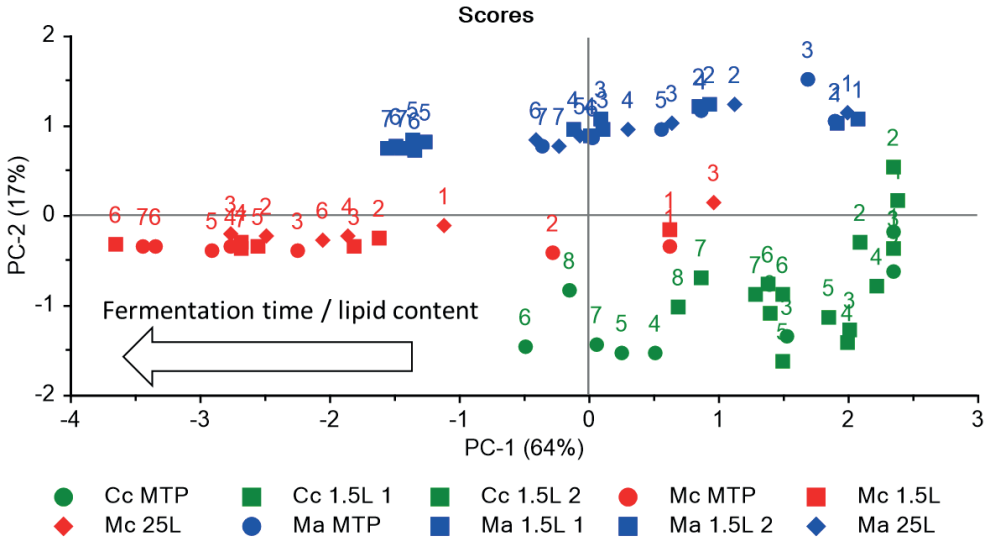

Fig. S7 PCA score plot of the (pre-processed) FTIR spectra of biomass (Cc = *C. cohnii*, Mc = *M. circinelloides*, Ma = *M. alpina*) at different cultivation scales. Numbers in the score plot indicate cultivation time in days.

Table S1 Fatty acid composition and total lipid content (FAME, weight% of biomass) of *C. cohnii* ATCC 40750 in Duetz-MTPS, 1.5 L working volume benchtop bioreactor. Fatty acid composition results are average of three technical replicate extraction – GC measurements (if there was enough biomass). From Duetz-MTPS, three individual wells were also measured at 192 h for reproducibility test.

scale	time (h)	C12:0	C14:0	C16:0	C16:1n7c	C18:0	C18:1n9c	C20:0	C22:6n3	unsat. index	total lipid (wt%)
MTPS	24	0.7	10.8	17.8	0.4	1.4	10.3	0.0	58.3	3.61	6.2 ± 0.5
	48	1.6	14.7	21.5	0.2	1.2	7.3	0.0	51.2	3.19	7.3 ± 0.1
	72	3.0	19.4	22.0	0.2	2.1	6.8	0.1	44.6	2.78	16.3 ± 0.5
	96	3.7	21.3	22.2	0.1	2.3	6.1	0.2	42.6	2.64	23.4 ± 1.4
	120	3.7	21.5	22.5	0.1	2.7	5.9	0.2	42.0	2.60	27.8 ± 0.9
	144	3.7	21.4	22.0	0.1	2.6	5.7	0.2	43.1	2.66	30.2 ± 0.9
	168	3.3	21.0	22.5	0.1	2.8	5.9	0.2	42.9	2.65	35.0 ± 1.1
	192	2.6	18.9	21.8	0.1	2.6	6.0	0.2	46.3	2.86	34.0 ± 2.7
	192 well I	2.9	19.9	21.8	0.1	2.4	6.0	0.2	45.4	2.88	30.9
	192 well II	2.5	19.0	21.8	0.1	2.6	5.9	0.2	46.7	2.89	35.9
	192 well III	2.4	18.7	21.8	0.1	2.6	6.0	0.2	46.8	2.86	35.2
1.5 L WV bioreactor I	48	6.6	14.6	15.1	0.9	1.4	12.6	0.0	47.3	2.97	10.0
	76	3.8	14.5	17.9	0.8	1.4	10.9	0.0	49.0	3.08	9.1 ± 0.1
	97	3.5	14.8	19.6	0.7	1.0	10.4	0.0	48.6	3.04	11.4 ± 0.1
	121	3.6	15.4	21.3	0.5	1.0	10.7	0.1	45.8	2.87	16.3 ± 0.2
	144	2.9	14.5	20.6	0.4	1.7	9.8	0.2	47.9	3.01	17.1 ± 0.0
	172	2.3	14.8	21.4	0.3	2.8	9.4	0.2	47.2	2.95	22.2 ± 0.4
	198	1.9	13.7	20.6	0.2	3.1	8.8	0.3	49.5	3.29	23.9 ± 0.3
1.5 L WV bioreactor II	24	5.2	15.4	16.1	0.0	1.5	10.7	0.0	50.1	3.11	8.9
	48	8.1	16.3	17.7	0.6	1.3	8.7	0.0	45.3	2.82	9.1
	76	4.0	15.1	20.5	0.8	1.2	10.1	0.0	47.1	2.95	10.1 ± 0.0
	97	3.0	14.5	21.8	0.8	1.0	10.9	0.0	46.9	2.94	12.6 ± 0.2
	121	2.3	13.5	21.6	0.7	1.1	10.9	0.1	48.5	3.04	16.9 ± 0.1
	144	1.9	13.1	22.4	0.6	1.8	11.4	0.2	46.0	2.93	14.9 ± 0.5
	172	1.2	11.0	20.0	0.5	1.9	10.6	0.2	52.6	3.30	17.4 ± 0.1
	198	1.1	9.4	18.8	0.4	1.9	10.3	0.2	55.6	3.48	19.7 ± 0.0

Table S2 Fatty acid composition and total lipid content (FAME, weight% of biomass) of *Mucor circinelloides* VI 04473 in Duetz-MTPS, 1.5 L working volume benchtop bioreactor and 25 L working volume pre-pilot bioreactor. Fatty acid composition results are average of three technical replicate extraction – GC measurements (if there was enough biomass). From Duetz-MTPS three individual wells were also measured at 168 h for reproducibility test.

scale	time (h)	C10:0	C12:0	C14:0	C15:0	C16:0	C16:1n5	C16:1n7	C17:0	C17:1	C18:0	C18:1n9t	C18:1n9c	C18:1n7c	C18:2n9t	C18:2n6c	C18:3n6c	C20:0	C20:1n9c	C20:2	C22:0	C24:0	unsat. index	total lipid (wt%)
MTPS	24	0.1	0.2	1.2	0.6	19.7	0.1	1.2	3.7	1.0	7.6	0.1	30.0	0.3	0.3	14.8	16.5	0.3	0.3	0.2	0.3	0.6	1.15	23.7 ± 1.3
	48	0.2	0.3	1.5	0.5	17.7	0.2	2.7	2.5	0.9	6.0	0.1	34.0	0.5	0.4	15.7	15.1	0.2	0.3	0.2	0.2	0.3	1.17	27.1 ± 0.4
	72	0.2	0.3	1.7	0.4	16.3	0.3	3.5	2.1	0.8	5.1	0.1	35.9	0.7	0.4	16.3	14.3	0.2	0.3	0.2	0.1	0.3	1.19	29.9 ± 0.4
	96	0.5	0.5	2.0	0.4	16.1	0.3	3.9	1.7	0.7	5.1	0.1	36.5	0.7	0.5	16.0	13.5	0.2	0.3	0.2	0.1	0.2	1.17	26.7 ± 0.6
	120	0.2	0.3	1.9	0.3	16.6	0.4	3.7	1.5	0.6	4.6	0.1	37.4	0.7	0.6	16.1	13.7	0.1	0.2	0.2	0.1	0.2	1.19	25.9 ± 1.1
	144	0.4	0.5	2.1	0.3	16.2	0.4	3.9	1.4	0.6	5.0	0.1	37.9	0.8	0.6	15.6	12.9	0.1	0.3	0.2	0.1	0.2	1.16	28.7 ± 1.1
	168	1.2	1.2	2.8	0.3	15.2	0.3	4.5	1.2	0.7	7.5	0.1	37.1	1.0	0.7	14.2	10.4	0.2	0.2	0.1	0.2	0.4	1.06	29.9 ± 3.4
	168 well I	1.0	1.2	2.8	0.3	14.9	0.3	4.6	1.2	0.7	7.3	0.1	37.6	1.1	0.7	14.4	10.4	0.2	0.2	0.1	0.1	0.3	1.06	31.0
	168 well II	0.9	1.1	2.6	0.3	15.0	0.3	4.6	1.3	0.7	6.9	0.1	37.9	1.0	0.7	14.5	10.6	0.2	0.3	0.1	0.2	0.3	1.08	34.0
	168 well III	1.2	1.1	2.7	0.3	15.2	0.3	4.5	1.2	0.6	7.0	0.1	37.4	1.0	0.7	14.4	10.8	0.2	0.2	0.1	0.2	0.3	1.07	28.0
1.5 L WV bioreactor	25	0.3	0.4	1.6	0.4	13.7	0.1	4.7	1.7	1.1	4.5	0.1	36.5	1.2	0.6	17.2	14.0	0.2	0.3	0.2	0.1	0.3	1.23	16.5 ± 0.9
	54	0.3	0.4	1.8	0.4	14.9	0.1	5.4	1.3	0.8	3.8	0.1	38.2	1.2	0.6	17.7	11.5	0.1	0.3	0.2	0.1	0.2	1.19	22.5 ± 1.2
	74	0.3	0.4	1.9	0.3	15.0	0.2	5.4	1.2	0.7	3.5	0.1	39.1	1.1	0.7	17.4	11.3	0.1	0.3	0.2	0.1	0.1	1.18	23.6 ± 0.5
	98	0.2	0.3	1.9	0.3	15.1	0.3	5.3	1.1	0.7	3.3	0.1	40.4	1.1	0.7	16.9	11.0	0.1	0.3	0.2	0.1	0.1	1.18	27.3 ± 2.5
	123	0.2	0.3	1.9	0.3	15.1	0.3	5.3	1.0	0.6	3.2	0.1	41.3	1.1	0.8	16.5	10.9	0.1	0.3	0.2	0.0	0.1	1.17	27.5 ± 1.4
	144	0.3	0.4	2.0	0.2	15.0	0.3	5.3	0.9	0.6	3.2	0.1	41.6	1.1	0.9	16.2	10.8	0.1	0.3	0.2	0.0	0.1	1.17	23.8 ± 1.5
	168	0.5	0.7	2.3	0.2	15.2	0.3	5.2	0.9	0.6	4.6	0.1	40.7	1.1	0.9	15.3	10.3	0.1	0.3	0.2	0.0	0.1	1.13	27.3 ± 1.0
	168 wall	0.6	0.8	2.4	0.2	15.1	0.2	5.2	0.9	0.6	6.1	0.1	39.6	1.2	0.9	14.8	9.9	0.2	0.3	0.2	0.1	0.2	1.09	29.5 ± 1.3
25 L WV bioreactor	8	0.0	0.3	1.6	0.6	15.3	0.0	2.0	1.2	0.4	6.0	0.0	21.6	0.4	1.6	15.7	31.2	0.0	0.0	0.2	0.4	1.3	1.53	4.51 ± 0.1
	24	0.1	0.2	1.3	0.6	19.7	0.1	2.4	2.9	0.9	7.5	0.1	31.0	0.5	0.4	17.0	13.0	0.3	0.3	0.2	0.2	0.5	1.10	21.8
	48	0.1	0.2	1.5	0.5	19.6	0.1	2.8	2.2	0.8	6.6	0.1	32.6	0.6	0.5	17.5	12.4	0.2	0.2	0.2	0.2	0.4	1.11	26.0
	72	0.1	0.2	1.5	0.4	18.4	0.2	2.8	1.8	0.7	5.9	0.1	33.3	0.6	0.4	18.2	13.7	0.2	0.2	0.2	0.2	0.3	1.17	26.2
	96	0.1	0.2	1.6	0.3	17.5	0.3	3.1	1.5	0.6	5.0	0.1	35.1	0.6	0.5	17.9	14.0	0.2	0.2	0.2	0.1	0.3	1.20	26.4
	120	0.1	0.2	1.6	0.3	17.0	0.4	3.0	1.4	0.6	4.7	0.1	35.6	0.6	0.5	17.8	14.6	0.1	0.2	0.2	0.1	0.3	1.22	26.6
	160	0.1	0.2	1.6	0.3	16.3	0.5	3.1	1.2	0.5	4.4	0.1	36.7	0.7	0.6	17.6	15.0	0.1	0.2	0.2	0.1	0.2	1.24	27.0

Table S3 Fatty acid composition and total lipid content (FAME, weight% of biomass) of *Mortierella alpina* ATCC 32222 in Duetz-MTPS, 1.5 L working volume benchtop bioreactor and 25 L working volume pre-pilot bioreactor. Fatty acid composition results are average of three technical replicate extraction – GC measurements (if there was enough biomass). From Duetz-MTPS three individual wells were also measured at 168 h for reproducibility test.

scale	time (h)	C14:0	C15:0	C16:0	C16:1n7c	C17:0	C17:1	C18:0	C18:1n9c	C18:1n7c	C18:2n6c	C18:3n6c	C20:0	C20:1n9c	C20:2	C20:3n6c	C20:4n6c	C22:0	C24:0	unsat. index	total lipid (wt%)
MTPS	48	0.9	1.0	12.0	0.4	1.6	0.8	5.0	11.8	0.3	10.4	15.0	0.3	0.3	0.3	5.0	30.3	0.7	1.1	2.23	7.1 ± 0.2
	72	1.4	1.0	16.3	0.3	2.1	0.7	6.0	14.3	0.3	7.2	9.2	0.4	0.2	0.2	5.6	30.6	0.7	1.1	2.02	10.7 ± 0.3
	96	1.7	0.4	16.5	0.2	1.0	0.3	9.6	13.8	0.2	7.1	5.6	0.6	0.3	0.3	4.9	34.3	0.9	0.9	2.01	18.4 ± 1.1
	120	1.4	0.2	14.5	0.1	0.6	0.1	11.0	12.4	0.2	8.2	4.9	0.6	0.4	0.4	4.2	38.0	0.9	0.7	2.13	31.4 ± 1.1
	144	1.1	0.2	12.9	0.1	0.5	0.1	10.9	10.6	0.2	8.1	5.1	0.6	0.4	0.4	4.2	42.2	0.8	0.6	2.28	35.8 ± 1.6
	168	0.9	0.2	12.4	0.1	0.5	0.1	11.1	12.2	0.2	8.7	4.6	0.6	0.5	0.5	4.0	40.7	0.9	0.6	2.23	38.9 ± 2.2
	168 well I	1.0	0.2	12.7	0.1	0.5	0.1	11.3	12.7	0.2	8.9	4.5	0.6	0.5	0.5	4.0	39.4	0.9	0.5	2.23	40.4
	168 well II	0.9	0.2	12.3	0.1	0.5	0.1	11.0	12.2	0.2	9.0	4.5	0.6	0.5	0.5	3.8	40.7	0.9	0.6	2.11	40.0
	168 well III	1.5	0.0	15.9	0.2	0.4	0.1	10.1	14.1	0.2	6.0	5.1	0.6	0.5	0.3	4.9	37.9	0.9	0.6	2.27	29.0
1.5 L WV bioreactor I	24	0.7	2.7	9.1	0.3	4.9	2.9	1.5	12.9	0.6	8.3	16.2	0.0	0.3	0.3	4.4	29.3	0.3	1.2	2.22	6.6 ± 0.2
	53	1.5	0.9	16.8	0.2	2.2	0.9	7.6	21.5	0.3	5.8	5.7	0.5	0.4	0.3	3.7	26.6	0.9	1.2	1.76	16.4 ± 0.1
	73	1.2	0.4	15.1	0.2	1.3	0.4	9.6	23.7	0.3	5.3	4.1	0.7	0.7	0.3	3.0	29.2	1.1	1.1	1.79	26.7 ± 0.3
	97	0.9	0.3	13.0	0.1	0.9	0.3	10.5	24.6	0.2	4.9	3.6	0.7	0.9	0.3	2.7	31.4	1.2	1.1	1.86	34.9 ± 0.8
	122	0.7	0.2	12.1	0.1	0.8	0.2	10.4	26.2	0.2	4.3	3.4	0.7	1.1	0.3	2.4	31.8	1.2	1.1	1.88	39.2 ± 2.2
	146	0.5	0.2	11.5	0.1	0.6	0.2	10.2	23.3	0.2	5.0	3.4	0.7	1.0	0.3	2.6	35.2	1.2	1.0	2.00	43.0 ± 0.8
	168	0.5	0.1	10.9	0.1	0.6	0.1	9.6	22.2	0.2	5.2	3.4	0.7	1.0	0.4	2.6	37.4	1.2	1.1	2.08	43.4 ± 0.4
1.5 L WV bioreactor II	24	0.6	2.9	8.7	0.3	5.1	3.1	1.5	11.9	0.3	8.2	15.7	0.1	0.2	0.3	4.4	29.8	0.2	1.3	2.23	6.7 ± 0.1
	53	1.5	1.0	16.2	0.2	2.4	1.0	7.2	22.0	0.3	5.4	6.4	0.5	0.5	0.3	3.6	25.9	0.9	1.3	1.75	15.4 ± 0.0
	73	1.2	0.5	14.8	0.2	1.4	0.5	9.2	25.8	0.3	4.5	4.2	0.7	0.8	0.2	2.8	27.4	1.1	1.2	1.74	25.5 ± 0.4
	97	0.9	0.3	13.0	0.1	1.0	0.3	10.1	27.8	0.2	4.0	3.6	0.7	1.1	0.2	2.4	29.0	1.2	1.1	1.78	33.1 ± 0.3
	122	0.7	0.2	12.1	0.1	0.8	0.2	10.3	26.2	0.2	4.3	3.4	0.7	1.1	0.3	2.4	31.7	1.2	1.1	1.88	40.4 ± 2.1
	146	0.6	0.2	11.5	0.1	0.7	0.2	9.8	28.0	0.2	3.5	3.2	0.7	1.2	0.2	2.1	31.7	1.2	1.2	1.88	40.4 ± 0.0
	168	0.5	0.2	11.1	0.1	0.6	0.2	9.5	27.4	0.2	3.5	3.2	0.7	1.2	0.2	2.0	33.2	1.2	1.1	1.93	41.4 ± 0.3
25 L WV bioreactor	24	0.7	2.3	10.7	0.2	5.1	1.8	2.8	14.3	0.2	8.1	19.3	0.0	0.3	0.3	4.8	24.4	0.4	1.3	2.08	7.5 ± 0.9
	48	1.5	2.4	15.4	0.3	5.1	1.9	4.2	14.1	0.2	5.6	10.4	0.3	0.2	0.3	4.9	28.2	0.6	1.3	1.94	11.5 ± 0.3
	72	1.7	0.9	18.0	0.2	2.3	0.7	8.6	16.8	0.2	6.5	6.3	0.6	0.4	0.3	4.5	28.4	1.0	1.2	1.81	19.8 ± 0.2
	96	1.2	0.5	15.8	0.2	1.5	0.4	10.5	17.4	0.2	7.1	5.3	0.7	0.5	0.3	3.9	30.9	1.1	1.0	1.88	28.9 ± 0.3

	120	0.8	0.3	14.2	0.1	1.2	0.3	11.5	17.7	0.2	7.4	4.9	0.8	0.6	0.4	3.5	32.3	1.2	1.0	1.92	35.2 ± 1.0
	144	0.7	0.3	13.5	0.1	1.1	0.3	11.8	17.4	0.2	7.6	4.8	0.8	0.7	0.4	3.4	33.3	1.1	0.9	1.96	37.1 ± 2.4
	168	0.6	0.3	13.1	0.1	1.0	0.2	11.7	17.3	0.2	7.8	4.7	0.7	0.7	0.4	3.3	34.4	1.1	0.8	2.00	36.4 ± 0.7
	168 wall	0.8	0.6	13.2	0.1	1.7	0.5	10.3	16.3	0.2	6.9	5.5	0.7	0.6	0.4	3.7	34.1	1.2	1.1	2.00	35.2 ± 0.4

Table S4 Fermentation results of *C. cohnii* (168 – 192 h), *M. circinelloides* (168 h) and *M. alpina* (160-168 h) cultivated in Duetz-MTPS, 1.5 L and 25 L working volume bioreactors. Yx/s: biomass yield on glucose, Yp/s: lipid yield on glucose, Qp: overall lipid production rate, Qx: overall biomass production rate, Qs: overall substrate consumption rate, qP: overall specific lipid production rate, qS: overall specific substrate consumption rate.

C. cohnii	Biomass (g CDW/L)	Total lipid (g/L)	DHA (g/L)	Glu consumed (g/L)	Yx/s (g/g)	Yp/s (g/g)	Qp (g/L/day)	Qx (g/L/day)	Qs (g/L/day)	qP (g/g/day)	qS (g/g/day)
MTPS	11.3	4.0	1.70	58.6	0.193	0.068	0.57	1.62	8.4	0.050	0.739
1.5 L	8.3±0.6	1.8±0.4	0.9±0.1	49.6±2.8	0.167±0.021	0.036±0.009	0.219±0.045	1.005±0.067	6.0±0.3	0.026±0.004	0.726±0.09

M. circinelloides	Biomass (g CDW/L)	Total lipid (g/L)	GLA (g/L)	Glu consumed (g/L)	Yx/s (g/g)	Yp/s (g/g)	Qp (g/L/day)	Qx (g/L/day)	Qs (g/L/day)	qP (g/g/day)	qS (g/g/day)
MTPS	14.4	3.8	0.38	76.8	0.188	0.050	0.543	2.056	11.0	0.038	0.762
1.5 L	15.8	4.3	0.45	75.7	0.209	0.057	0.617	2.261	10.8	0.039	0.683
25 L	-	-	-	52.3	-	-	-	-	-	-	-

M. alpina	Biomass (g CDW/L)	Total lipid (g/L)	GLA (g/L)	ARA (g/L)	Glu consumed (g/L)	Yx/s (g/g)	Yp/s (g/g)	Qp (g/L/day)	Qx (g/L/day)	Qs (g/L/day)	qP (g/g/day)	qS (g/g/day)
MTPS	21.5	7.8	0.36	3.3	42.8	0.502	0.183	1.12	3.07	6.1	0.052	0.284
1.5 L	24.5±0.5	10.4±0.5	0.34±0.03	3.7±0.5	53.6±1.9	0.46±0.01	0.194±0.011	1.48±0.08	3.5±0.03	7.7±0.3	0.061±0.003	0.313±0.005
25 L	16.9	6.1	0.29	2.1	41.1	0.410	0.149	0.92	2.5	5.9	0.055	0.366

Paper IV

High-throughput screening of Mucoromycota fungi for the production of low-, and high-value lipids

Gergely Kosa[1*] (gergely.kosa@nmbu.no), Boris Zimmermann[1] (boris.zimmermann@nmbu.no), Achim Kohler[1] (achim.kohler@nmbu.no), Dag Ekeberg[2] (dag.ekeberg@nmbu.no), Nils Kristian Afseth[3] (nils.kristian.afseth@nofima.no), Jerome Mounier[4] (jerome.mounier@univ-brest.fr), Volha Shapaval[1] (volha.shapaval@nmbu.no)

(1)Faculty of Science and Technology, Norwegian University of Life Sciences, Postbox 5003, 1432 Ås, Norway

(2) Faculty of Chemistry, Biotechnology and Food Science, Norwegian University of Life Sciences, Postbox 5003, 1432 Ås, Norway

(3) Nofima AS, Osloveien 1, N-1430 Ås, Norway

(4) Université de Brest, EA3882 Laboratoire Universitaire de Biodiversité et Ecologie Microbienne, IBSAM, ESIAB, Technopôle Brest Iroise, 29280 Plouzané, France

Correspondence address: Faculty of Science and Technology, Norwegian University of Life Sciences, Postbox 5003, 1432 Ås, Norway

Abstract

Background: Mucoromycota fungi are important sources of low- and high-value fatty acids. Several oleaginous Mucoromycota fungi are considered as promising candidates for the production of biodiesel, while *Mortierella alpina* fungus is already used for commercial scale arachidonic acid production. An important research objective is the selection of suitable strains for the production of lipids for different applications. In this study, the aim was to use the Duetz-microtiter plate system (Duetz-MTPS) combined

with Fourier transform infrared (FTIR) spectroscopy for high-throughput screening of one hundred Mucoromycota fungi for the production of low- and high-value lipids.

Results: The reproducible, high-throughput cultivation of Mucoromycota fungi in the Duetz-MTPS allowed finding several promising strains for high-value PUFA and biodiesel purposes. Gamma-linolenic acid (C18:3n6, GLA) content was the highest in *Mucor fragilis* UBOCC-A-109196 (24.5%), and in *Cunninghamella echinulata* VKM F-470 (24.0%, 1.17 g/L medium). For the first time, we observed concomitant alpha-linolenic (C18:3n3, ALA) acid and GLA production in psychrophilic *Mucor flavus* strains (max 13.0% ALA in *M. flavus* CCM 8086). Arachidonic acid (C20:4n6, ARA) was found in all *Mortierella* strains ranging from 5.6% to 41.1% in *M. alpina* ATCC 32222 (1.48 g/L). Dihomo-gamma-linolenic acid (C20:3n6, DGLA) was also present in all *Mortierella* fungi up to 6.5% of total fatty acids. Low cultivation temperature (15 °C) activated the temperature sensitive Δ17 desaturase enzyme in *Mortierella,* resulting in max. 11.0% eicosapentaenoic acid (EPA) production in *M. humilis* VKM F-1494. *Cunninghamella blakesleeana* CCM-705, *Umbelopsis vinacea* CCM F-539, UBOCC-A-101347 strains showed very good growth (more than 22 g/L dry cell weight), lipid production (7.0 - 8.3 g/L) and fatty acid composition (high palmitic, oleic acid content and low PUFA) that makes them attractive candidates for biodiesel production. While *Absidia* spp. are not often mentioned in literature as promising oleaginous fungi, in our study several *Absidia* strains reached more than 30% lipid content. In particular, *A. glauca* CCM 451 had the highest lipid content (47.2% ± 1.8%) from all 100 tested strains. We also demonstrated FTIR spectroscopy as a rapid, high-throughput method for pre-screening promising oleaginous fungi before detailed gas-chromatography fatty acid analysis.

Conclusions: High-throughput screening of Mucoromycota fungi in the Duetz-MTPS, combined with fast HTS-FTIR spectroscopy and multivariate analysis, is a feasible approach. Several promising strains have been identified by this method for the production of high-value PUFA and biodiesel.

Keywords: High-throughput screening, Mucoromycota, filamentous fungi, single cell oil, PUFA, biodiesel, FTIR

Background

Oleaginous microorganism have been considered, for nearly a century, as an alternative source for the production of low- and high-value lipids -single cell oils- but only in the past two or three decades they have started to be used commercially [1]. Fungal oil, especially in filamentous fungi contains remarkable amount of omega-6 polyunsaturated fatty acids (PUFAs), such as GLA, DGLA and ARA. ARA produced by *Mortierella alpina* is included in infant formulas worldwide. ARA is necessary for the proper brain and eye development of babies and ARA also prevents the undesirable retro-conversion of DHA to EPA in these formulas [2]. DGLA was reported to possess antitumor properties [3], while GLA has been used to alleviate premenstrual tension and for the improvement of various skin conditions [2, 4]. Recently, microbial lipids (yeasts, filamentous fungi and microalgae) have been considered as possible alternative raw materials for biodiesel production, since they can potentially contain high amounts of saturated (SAT) and monounsaturated fatty acids (MUFA) and can grow rapidly in a controlled environment. The commercially produced single cell oil contains high amount of PUFA, and the process is based on heterotrophic cultivation, where the most often used substrate is glucose [1, 5]. However, for low-value biodiesel application, low cost substrates, such as food rest materials, waste glycerol, lignocellulosic materials are being tested for economical sustainability. Fungi (yeast and molds) are able to grow and accumulate lipids in such substrates [6-9].

Many members of Mucoromycota fungi have been reported as oleaginous [6, 10, 11]. Ratledge performed extensive screening of more than 300 Mucoromycota fungi (13 genera) based on several criteria in order to find the best producer for GLA production. A *Mucor circinelloides* strain was identified and the industrial production of GLA has started in 1985 [5]. Similarly, Weete *et al.* screened more than 150 Mucoromycota strains to find the fungus with the highest content of GLA in the oil. *Syzygites megalocarpus* accumulating 62% GLA was selected [12]. Eroshin *et al.* [13] and Botha *et al.*[14] performed screening of *Mortierella* strains (87 and 61 respectively) on a solid agar medium (MEG or PDA) in order to find the best producer of ARA, where *Mortierella alpina* was selected as the best species. The previously performed

screenings were specifically focused on the production of high-value fatty acids and in most of the cases on a single high-value PUFA. The extensive evaluation of Mucoromycota fungi for the production of a broad spectrum of low- and high-value lipids for different applications has not been performed so far. In addition, all the performed screenings were done in a shake flask/bioreactor/agar plate set-up, often without statistically relevant number of replicates [12, 13, 15-18].

Miniaturization of fermentation technologies enables the screening of a high number of strains under controlled conditions [19, 20]. Recently, we have demonstrated in Duetz-microtiter plate system the reproducible and scalable high-throughput cultivation of oleaginous filamentous fungi [21, 22]. In addition, we have shown that Fourier transform (FTIR) spectroscopy combined with multivariate analyses, is a powerful high-throughput analytical approach for the quantitative and qualitative assessment of total lipid content, lipid classes and individual fatty acids in the fungal biomass [22, 23]. It also enables precise quantitative measurement of extracellular metabolites and nutrients in the cultivation medium [21]. Thus, we suggested using of Duetz-microtiter plate system together with FTIR spectroscopy for high-throughput screenings of filamentous fungi for lipid production.

The aim of this study was to perform high-throughput screening of Mucoromycota fungi for low and high-value lipid production by combining cultivation in Duetz-microtiter plate system with FTIR analysis of fungal biomass. The study has covered 100 strains of Mucoromycota, including *Amylomyces*, *Mucor*, *Rhizopus*, *Umbelopsis*, *Absidia*, *Lichtheimia*, *Cunninghamella*, and *Mortierella* species.

Methods

Fungal strains

One hundred Mucoromycota fungal strains from eight different genera *Mucor*, *Amylomyces*, *Rhizopus*, *Umbelopsis*, *Absidia*, *Cunninghamella*, *Lichtheimia* and *Mortierella* were used in this study (Table 1). The phylogenetic tree of the investigated Mucoromycota fungi is shown in Figure 1. Fungi were obtained in living or lyophilized form from the Czech Collection of Microorganisms (CCM; Brno, Czech Republic), the Food Fungal Culture Collection (FRR; Common wealth Scientific and Industrial Research

Organisation, North Ryde, Australia), the Norwegian School of Veterinary Science (VI; Oslo, Norway), the Université de Bretagne Occidentale Culture Collection (UBOCC; Brest, France), the All-Russian Collection of Microorganisms (VKM; Moscow, Russia) and the American Type Culture Collection (ATCC; VA, USA).

Media and growth conditions

Mucoromycota fungi were cultivated first on malt extract (MEA) or potato dextrose agar (PDA) for seven days at 15 - 25 °C. The type of agar medium was in most cases interchangeable, but for instance, *Cunninghamella blakesleeana* CCM F-705 did not grow on PDA, only on MEA (in contrast to the culture collection's recommendation). The majority of the one hundred tested fungi were mesophilic and grew well at room temperature (20-25 °C) with some exceptions (e.g. *Mucor flavus* CCM 8086). Spores from the agar cultures were harvested by using sterile saline solution.

A liquid medium was prepared according to the protocol described by Kavadia et al. [24] with the following modifications (g L^{-1}): glucose 90, yeast extract 5, KH_2PO_4 7, Na_2HPO_4 2, $MgSO_4 \cdot 7H_2O$ 1.5, $CaCl_2 \cdot 2H_2O$ 0.1, $FeCl_3 \cdot 6H_2O$ 0.008, $ZnSO_4 \cdot 7H_2O$ 0.001, $CoSO_4 \cdot 7H_2O$ 0.0001, $CuSO_4 \cdot 5H_2O$ 0.0001, $MnSO_4 \cdot 5H_2O$ 0.0001. All chemicals were obtained from Merck (Darmstadt, Germany), except yeast extract (Oxoid, Basingstoke, England). The pH of the medium was 6.05 after sterilization. Spore suspensions (10-100 μL, depending on sporulation strength) were transferred to 2.5 ml liquid medium in 24-square polypropylene deep well plates using the Duetz-microtiter plate system (Duetz-MTPS; Enzyscreen, Heemstede, Netherlands) [22]. Inoculated microtiter plates (MTPs) were mounted on an Innova 40R refrigerated desktop shaker (Eppendorf, Hamburg, Germany) by using the clamp system and were cultivated with a shaking rate of 300 rpm (circular orbit 0.75") for 5-7 days at 15 - 28 °C. Three strains (*Mortierella gamsii* VKM F-1529, *Mortierella globulifera* VKM F-1408 and *Mortierella globulifera* VKM F-1448) failed to grow in the Duetz-MTPS and were grown for 9 days at 15°C in 500 mL baffled shake flasks (SFs) filled with 100 mL of the above-described medium.

Experimental design

For each strain, three biological replicates were prepared. Each biological replicate was represented by the spore suspension prepared from the separate Petri-dishes. For *Mucor circinelloides* strains, five biological replicates were prepared. The *M. gamsii* and *M. globulifera* strains in SFs were run without replicates. In order to have enough biomass for GC analysis, three wells in the MTP were inoculated for each strain and each biological replicate (i.e. eight strains per MTP). For every biological replicate, microcultivations were performed in a separate MTP. Biomass from the three wells of each MTP plate were merged and used for GC-FID. GC-MS fatty acid analysis and FTIR spectroscopy. The supernatant of the fermentation broth and initial growth medium was used for high-performance liquid chromatography (HPLC) glucose analysis.

Microscopy

Micrographs were prepared from fresh biomass according to Kosa et al. [22] in bright-field and fluorescence mode after Nile-red staining with a DM6000B microscope (Leica Microsystems, Wetzlar, Germany).

Preparation of fungal biomass for HTS-FTIR analysis

Fermentation broth was vacuum filtered on Whatman No. I filter paper (GE Whatman, Maidstone, UK) and the fungal biomass was washed thoroughly with distilled water. Approximately 10 mg of the washed biomass was transferred into 2 mL screw-cap tube, 500 µL distilled water and 250 ± 30 mg acid-washed glass beads (800 µm, OPS Diagnostics, NJ, USA) were added, then the biomass was homogenized for 1-2 min in a FastPrep-24 high-speed benchtop homogenizer (MP Biomedicals, USA) at 6.5 m s^{-1}. This homogenized fungal suspension was used for FTIR analysis.

FTIR spectroscopy

FTIR analysis of homogenized fungal biomass was performed with the High Throughput Screening eXTension (HTS-XT) unit coupled to the Vertex 70 FTIR spectrometer (both Bruker Optik, Ettlingen, Germany) in transmission mode [22]. The FTIR system was equipped with a globar mid-IR source and a DTGS detector. The spectra were recorded on 384-well silicon microplates in transmission mode, with a spectral resolution of 4 cm^{-1} and digital spacing of 1.928 cm^{-1}. Background (reference) spectra of an empty microplate well was recorded before each sample well measurement. The spectra were collected in the 4000-500 cm^{-1} spectral range, with 64 scans for both background and sample spectra, and using an aperture of 5.0 mm. Measurements were controlled by the OPUS 7.5 software (Bruker Optik, Ettlingen, Germany).

Lipid extraction from the fungal biomass

Washed fungal biomass was frozen at -20 °C and then lyophilized overnight in an Alpha 1-2 LDPlus freeze-dryer (Martin Christ, Germany) at -55 °C and 0.01 mbar pressure. Freeze-dried biomass was used to determine cell dry weight. Lipid extraction from freeze-dried fungal biomass was based on a cell disruption step with glass beads followed by a direct transesterification-extraction procedure. The details of the method can be found in [22].

GC-FID fatty acid analysis

Determination of total lipid content of fungal biomass (FAME content) and fatty acid composition analysis were performed with a HP 6890 gas chromatograph (Hewlett Packard, Palo Alto, USA) equipped with an SGE BPX70, 60.0 m × 250 μm × 0.25 μm column (SGE Analytical Science, Ringwood, Australia) and flame ionization detector (FID). For identification and quantification of fatty acids, the C4-C24 FAME mixture (Supelco, St. Louis, USA) and C13:0 tridecanoic acid internal standard (Sigma-Aldrich, St Louis, USA) standards were used.

GC-MS fatty acid analysis

Identification and quantification of peaks, which were present in GC-FID chromatogram, but not present in the external FAME mixture, were performed by GC-MS. The analysis were carried out on an Agilent 6890 Series gas chromatograph (GC; Agilent, Wilmington, DE, USA) in combination with an Autospec Ultima mass spectrometer (MS; Micromass, Manchester, England) using an EI ion source. The GC was equipped with a CTC PAL Auto sampler (CTC Analytics, Zwingen, Switzerland). Separation was carried out on a 60 m Restek column (Rtx®-2330) with 0.25 mm I.D. and a 0.2 µm film thickness of fused silica 90% biscyanopropyl/10% pylphenylcyanoprol polysiloxane stationary phase (Restek, Bellefonte, PA, USA). For carrier gas, helium was used at 1.0 mL/min constant flow. The EI ion source was used in positive mode, producing 70 eV electrons at 250 °C. The MS was scanned in the range 40–600 m/z with 0.3 s scan time, 0.2 s inter scan delay, and 0.5 s cycle time. The transfer line temperature was set to 270 °C. The resolution was 1200. A split ratio of 1/10 was used with injections of 1.0 µL sample volume. Identification of fatty acids was performed by comparing retention times with standards as well as MS library searches. The MassLynx version 4.0 (Waters, Milford, MA, USA) and the NIST 2014 Mass Spectral Library (Gaithersburg, MD, USA) was used. The GC oven had a start temperature of 65 °C, which was held for 3 min, before the temperature was raised to 150 °C (40 °C/min), held for 13 min, and again increased to 151 °C (2 °C/min), held for 20 min, followed by a slow increase to 230 °C (2 °C/min), held for another 10 min, before finally increasing to end temperature of 240 °C (50 °C/min), which was held for 3.7 min.

HPLC glucose analysis

Glucose was quantified using an UltiMate 3000 UHPLC system (Thermo Scientific, Waltham, USA) equipped with RFQ-Fast Acid H+8 % (100 x 7.8 mm) column (Phenomenex, Torrance, USA) and coupled to a refractive index (RI) detector. Samples were diluted ten times before analysis, then filter sterilized and subsequently eluted isocratically at 1.0 mL min^{-1} flow rate in 6 min with 5 mM H_2SO_4 mobile phase at 85 °C column temperature.

Data analysis

FTIR spectra (4000-500 cm^{-1}) were preprocessed by transforming to 2nd derivative form with the Savitzky-Golay (S-G) method (2nd degree polynomial, 9 or 15 windows size), followed by Extended Multiplicative Scatter Correction (EMSC) with linear and quadratic components [25]. Principal component analysis (PCA) of the EMSC corrected FTIR data and auto-scaled GC fatty acid data was performed in The Unscrambler X, V10.5 (CAMO, Oslo, Norway). Partial Least Squares Regression (PLSR) between FTIR data (S-G and EMSC) and GC fatty acid data was performed with a leave-one-biological replicate-out cross validation scheme, and with limiting the maximum number of PLS factors to ten.

Results

Diversity of macro- and microscopic morphology of Mucoromycota fungi grown in the Duetz-MTPS

A variety of macroscopic growth characteristics were observed during the cultivation of Mucoromycota fungi under lipid accumulation conditions in the Duetz-MTPS (Figure 2 a-b). Forty-nine strains, mainly from *Mucor* and *Rhizopus* genera, grew in a dispersed hyphal form, forty-two strains from genera *Umbelopsis*, *Absidia*, *Cunninghamella*, *Lichtheimia*, *Mortierella* grew in the form of different size pellets, while the remaining strains showed mixed macroscopic morphology. Wall growth was observed in several strains (especially in *Mucor*, *Rhizopus* and *Mortierella* genera, because dispersed mycelium and fluffy pellets were more prone to attach to the wall than globular pellets), which resulted in the presence of sporulation. In this study, only the submerged fungi was used for biomass determination, GC and FTIR analyses. Majority of the fungal biomass had white color with the exception of some *Mucor* strains which had pale yellow (*M. circinelloides* FRR 5020, FRR 5021, FRR 4846, *M. mucedo* UBOCC-A-101361), intense yellow (*M. hiemalis* UBOCC-A-101359, 101360, 111119, 112185) or dark green color (*M. mucedo* UBOCC-A-101353, 101362), due to the production of carotenoids and other pigments (Figure 2 c-d).

All studied Mucoromycota fungi grew in a filamentous form, while in case of *Mucor*, filamentous and single cell yeast-like form were both observed (dimorphism) (Figure 3b). Lipid bodies (LBs) of *Mucor*

reached in some cases 20 μm in diameter (Figure 3a). *M. hiemalis* strains showed yellow-colored LBs due to the presence of lipophilic carotenoids (Figure 3c). Strains of *Rhizopus* sp. displayed branched mycelium with a limited amount of LBs (Figure 3d). Hyphae of *Umbelopsis*, *Cunninghamella*, *Lichtheimia* and *Mortierella* were filled with 2-5 μm LBs (Figure 3e-l). The mycelium of *Mortierella zonata* UBOCC-A-101348 had swollen hyphal tips, which were completely filled with LBs (Figure 3k). Extracellular LBs were observed for fungi with high lipid content (*Absidia*, *Umbelopsis* and *Cunninghamella*) probably due to the applied pressure during micrograph preparation (Figure 3i-j). Yellow-gold fluorescence of the Nile-red stained samples confirmed the presence of TAGs in intra- and extracellular LBs (Figure 3e, g, j, l).

Biomass concentration and lipid content of Mucoromycota fungi

The (submerged) biomass concentration and total lipid content is reported in Figure 6b (*Mucor* strains and *Amylomyces rouxii*), Figure 7b1-7b4 (*Rhizopus*, *Umbelopsis*, *Absidia*, *Lichtheimia* and *Cunninghamella*) and Figure 8b (*Mortierella*). The best ten oleaginous Mucoromycota fungi according to biomass concentration (g/L CDW), total lipid content in biomass (wt%) and total lipid concentration (g/L medium) are reported in Table 2. The summary of the results is presented for each genus in Figure 4.

Umbelopsis (11-26, average 16 g/L CDW) and *Cunninghamella* (13-23, average 16.6 g/L CDW) strains reached the highest biomass concentration; *U. vinacea* UBOCC-A-101347, *Cunninghamella blakesleeana* CCM-705 and *Umbelopsis vinacea* CCM F-539 produced the most biomass: 25.6 - 22.6 g/L. All other Mucoromycota fungi showed typically lower biomass concentration in the range of 2 to 18 g/L. *Rhizopus* strains grew poorly (5-10, average 7.2 g/L) despite of the high glucose consumption (average 68 g/L). *Rhizopus spp*. acidified the liquid medium, indicating acid production, which might negatively affected the growth. *Mortierella*, in general, grew slowly in the Duetz-MTPS; some strains did not grow properly in the standard conditions (90 g/L glucose, 28 °C), therefore glucose concentration and temperature had to be lowered (See Table 1). *M. globulifera* VKM F-1408 (2 g/L), VKM F-1448 (6 g/L) and *M. gamsii* VKM F-1529 (9 g/L) did not grow in the Duetz-MTPS, and reached low biomass

concentration in the shake flask as well. From *Mucor* genus, the biomass concentration was the highest in *M. circinelloides* species: five strains reached 15-12 g/L.

All studied strains of *Umbelopsis*, *Absidia*, *Lichtheimia* and *Cunninghamella* were characterized as oleaginous with a total lipid content from 26% to 47%. *Absidia* strains, except *A. cylindrospora* CMM F-52T, accumulated more than 30% of lipids (Figure 7b3) and the highest lipid content among all the one hundred tested fungi, 47.2% ± 1.8%, was observed in *Absidia glauca* CCM 451. Among *Umbelopsis* and *Cunninghamella* strains, the highest lipid content was between 35% and 37% in *U. vinacea* CCM F-539, *C. blakesleeana* CMM F-705, *C. echinulata* VKMF-439, and *C. echinulata* VKM F-470. The lipid content in *Mucor* spp. varied between 8% and 32%, showing large diversity within species as well (e.g. 12% in *M. hiemalis* FRR 5101 and 32% in *M. hiemalis* UBOCC-A-101359). The best lipid producers were found within *M. hiemalis*, where four species reached 30% - 32%. All *M. circinelloides* strains were oleaginous with a lipid content of 22% - 27%. The lipid content of *Rhizopus* spp. was moderate, with highest value of 23% in *Rhizopus stolonifer* CCM F-445. Most Mortierella strains were oleaginous and half of strains reached more than 30% lipid content in their biomass. *M. alpina* ATCC 32222 had the second highest lipid content from all tested fungi (44.5% ± 0.3%).

Fatty acid profile of Mucoromycota fungi

The FA profile of the hundred fungi was analyzed by PCA. PCA score and loading plots are shown in Figure 5 a-b. PC1 separates Mortierella and Mucorales orders primarily based on the presence or absence of C20 FAs (DGLA, ARA and EPA). PC2 separates Mucorales order into two clusters: *Mucor* and *Amylomyces* genera are characterized by high myristic acid (C14:0), palmitoleic acid (C16:1n7) and GLA content, while *Rhizopus*, *Umbelopsis*, *Absidia*, *Lichtheimia*, *Cunninghamella* genera are characterized by high oleic acid (C18:1n9, OA) content.

Production of high-value PUFA in Mucoromycota fungi

Main fatty acids profile of *Mucor*, *Amylomyces rouxii* can be seen in Figure 6a. The FA profile of *Rhizopus*, *Umbelopsis*, *Absidia*, *Lichtheimia*, and *Cunninghamella* is shown in Figure 7a1-a4, while for *Mortierella* strains it is presented in Figure 8a. The ten best strain for GLA and ARA production are presented in Table 3.

In Mucor the most abundant FA was OA, except in *M. fragilis* UBOCC-A-109196, *M. mucedo* UBOCC-A-101362 and 101363 where both linoleic acid (C18:2n6, LA) and γ-linolenic acid (C18:3n6, GLA) content was higher than OA. Among all studied Mucoromycota fungi, *M. fragilis* UBOCC-A-109196 produced the highest percentage of GLA: 24.5% ± 0.3%. Two additional strains, *M. flavus* VKM F-1110 and *M. racemosus* UBOCC-111127 strains also produced more than 20% GLA, but only the latter one was oleaginous (23% total lipid content). Two of *M. flavus* strains CCM 8086 and VKM F-1003, in addition to 9.1% – 11.1% GLA content, also produced 13.0% and 9.0% α-linolenic acid (C18:3n4, ALA), respectively. Both strains were grown at low temperature (15 °C and 20 °C) that induced the expression of Δ15-desaturase enzyme (ω3 desaturase), resulting in α-linolenic acid (C18:3n4, ALA) production. ALA was further desaturated by Δ6-desaturase leading to the 3.0% - 1.8% stearidonic acid (C18:4n3, SDA) and elongated to 0.9% - 0.5% eicosatrienoic acid (C20:3n3, ETE). Interestingly, the expression of Δ15-desaturase enzyme was much weaker in *M. flavus* VKM-1097 grown at 20 °C, where only 0.4% ALA was produced along with only 1.3% SDA and no ETE detected, while in *M. racemosus* UBOCC-A 111127 the low temperature cultivation temperature did not lead to ALA, SDA or ETE production. In *Rhizopus* fungi the GLA content varied between 5.5% - 20.3%. *R. stolonifer* strains produced the highest amount of GLA (19.0% - 20.3%), while its content varied greatly in *R. microsporus*. (6.0% - 18.8%), and the lowest content of GLA was in *R. oryzae* strains (5.5% - 9.4%). GLA content was low, between 5% and 9% in *Umbelopsis* strains. In case of *Absidia* and *Lichtheimia* fungi, the GLA content was lowest in *L. corymbifera* strains (4.0% - 7.0%) and highest in *A. cylindrospora* strains (13.5% - 16.9%). In the genus *Cunninghamella, C. echinulata* strains produced much higher level of GLA (16.0% - 24.0%) than *C. blakesleeana* strains (5.6%

- 6.1%). *C. echinulata* VKM F-470 showed the second highest GLA content from the tested one hundred Mucoromycota strains: 24.0% ± 1.1%.

Mortierella fungi produced significant amounts of C20 PUFAs, mainly dihomo-γ-linolenic acid (C20:3n6, DGLA), ARA and EPA. The average unsaturation index (calculated based on Suutari *et. al* [26]) was higher in *Mortierella* genus (1.50 combined and 1.40 for 28 °C cultivation only) than in the other genera (0.98 - 1.20) (Figure 4g). The *Mortierella* strains, which were cultivated at 15 °C produced higher content of omega-3 FAs, indicating the expression of ω3-desaturase (Δ15, Δ17) genes. Comparing the fungal oil of *Mortierella* at low (15 °C) and high (28 °C) cultivation temperatures, the ALA content was on average 0.53% (max. 0.8%) and 0.08%, while the SDA content was 0.9% (max. 1.4%) and 0.1%. The eicosatetraenoic acid (C20:4n3, ETA) content was 1.2% (max. 2.1%) and 0.1%, while EPA was found to be 6.6 (max. 10.8%) and 0.5%, respectively. In some species that were cultivated at 28 °C, close to 2% EPA was found in the oil (*M. elongata* VKM-F524 and *M. globulifera* VKM F-1448), indicating a lower activity of ω3-desaturase at room temperature. DGLA was found in the highest percentage in *M. gamsii* strains (15 °C): 5.1% - 6.5%. The industrially relevant *M. alpina* ATCC 32222 (28 °C) strain produced the highest amount of ARA (41.1% ± 0.8%, unsaturation index: 2.25), followed by *M. hyalina* VKM F-1854 (26.7% ± 1.2%) and *M. alpina* UBOCC-A-112046 (24.6% ± 1.2%). *M. globulifera* VKM F-1408 (15 °C) produced various PUFA at high level (unsaturation index: 2.16): GLA (11.5% ± 1.1%), DGLA: 4.9% ± 0.1%, ARA: 16.1% ± 0.6%, EPA: 8.0% ± 1.1%. The highest EPA content was achieved in *M. humilis* VKM F-1494 (15 °C): 10.8% ± 0.3%.

In addition to the above described FAs, Mucoromycota fungi also produced odd chain-number FAs in smaller quantitites, amongst others: pentadecylic acid (C15:0, average 0.3%, max. 1.5%), margaric acid (C17:0, average 0.6%, max 3.0%), heptadecenoic acid (C17:1n7, average 0.3%, max. 1.3%). The cis-vaccenic acid (C18:1n7, average 0.4%, max. 1.3%) was observed in the majority of fungi. Further, lignoceric acid (C24:0, average 0.8%, max. 3.0%) and nervonic acid (C24:1n9 average 0.2%, max. 1.8%)

were abundant. From the trans FAs, the fatty acid C18:2n9 occurred most frequently and in highest amount (average 0.5%, max. 2.4%).

Low value fatty acids in Mucoromycota fungi for biodiesel production

The screened Mucoromycota fungi were also analysed for their suitability for biodiesel production. The two most important properties of FAs that affect the fuel properties are the length of the carbon chain and the number of double bonds [27]. The ideal fatty acid composition for good oxidative stability of biodiesel is a ratio of C16:1, C18:1, C14:0 fatty acid 5:4:1 [28, 29]. The EN14214 standard for biodiesel describes the required specifications of biodiesel (FAME): the cetane number (CN) should be higher than 51 (the higher the better), the density at 15°C should be between 860-900 $kg \cdot m^{-3}$, and the iodine value (IV, g I_2/100g) less than 120. The GLA content should be less than 12%, and the PUFA content with four or more double bonds less than 1%. CN, density, IV and the higher heating value (HHV, $MJ \cdot kg^{-3}$) biodiesel properties were predicted according to Ramírez-Verduzco *et al.* [29].

Based on these calculations, forty-two strains met the requirement of EN14214 standard: 17 *Mucor* strains, 5 *Rhizopus*, all *Umbelopsis*, 6 *Absidia*, all *Lichtheimia* and 2 *Cunninghamella.* Strains with high ALA/GLA and C20 PUFA content (e.g. *Mucor* spp. with more than 12% GLA, *R. stolonifer*, *A. cylindrospora*, *C. echinulata* and *Mortierella* spp.) were not suitable for biodiesel production. The ten best biodiesel producers based on their lipid content (wt%), lipid concentration (g/L) and cetane number can be seein in Table 4. *U. vinacae* CCM F-539 and UBOCC-A-101347 had the best biodiesel characteristics based on the highest CN value (62.8 - 62.3), lowest iodine value (70.6 - 71.7), and amongst the highest HHV values (39.75-39.81 $MJ \cdot kg^{-1}$).

FTIR spectroscopy

Fungal biomass was also measured by high-throughput FTIR spectroscopy as a rapid method for the screening of Mucoromycota fungi for single cell oil production. FTIR spectra of three Mucoromycota fungi

with very different lipid content can be seen in Figure 9. The most important peaks were assigned in Table 5. We observe that the lipid related FTIR peaks change according to the lipid content of fungi.

In Figure 10 the PCA analysis of the EMSC corrected FTIR spectra is shown for the spectral region 4000-500 cm^{-1}. Biological replicates (labelled by a-c or a-e) are located close to each other in the scores plot confirming good cultivation reproducibility in the Duetz-MTPS. The main separation of fungi is based on lipid content of the biomass (PC1, 78% variance) demonstrated by lipid specific peaks (2-6, 9, 13, 17) in the loading plot. PC2 explains 9% of the variance. The ratio of protein (7, 8) and phosphate (12, 14, 16) is responsible for the separation of strains in PC2. *Mucor* species have predominantly negative PC2 scores, which can be explained by their very high polyphospate content [30]. The FTIR data indicate that *Mucor*/*Amylomyces* and *Rhizopus* have lower total lipid content on average than *Absidia*, *Umbelopsis*, *Cunninghamella* and *Mortierella* genera, which is in accordance with the GC measurement results (see Figure 4).

FTIR spectra of Mucoromycota fungi were used to estimate the lipid content in the mycelium (measured by GC-FID analysis). Several previously published univariate methods were tested for the whole set of studied strains, and individually for each genus, and were compared to the multivariate method (PLSR). The univariate methods were based on: peak height of C=O ester peak (1745 cm^{-1}), area of C-H stretching region (3040-2780 cm^{-1}), ratio of C=O ester peak height and amide I peak height (1655 cm^{-1}), ratio of C-H stretching area and amide I area (1724-1585 cm^{-1}), ratio of C=O ester or C-H stretching area and the combined amide I+II area (1790-1480 cm^{-1}) [31-37]. Best result of these analyses are listed in Table 6. Univariate regression results are only acceptable in case of *Mucor*/*Amylomyces*, *Rhizopus*, *Absidia*/*Lichheimia* and *Mortierella* genera, and were clearly outperformed by the PLSR method.

Discussion

It is known, that reproducible cultivation of filamentous fungi is a challenging task due to varying morphology and adherent wall growth [20, 38]. Despite of this fact, in many previous shake flask-based

single cell oil screening studies [12, 15, 16] there were no biological replicates involved, either due to time (cultivation, extraction) and/or space (shaker) limitations, making the reproducibility of the experiments difficult to judge. The Duetz-MPTS enabled good reproducibility of biological replicate cultivations: the pooled coefficients of variation (average of all data) for total lipid content of fungi, biomass concentration, and consumed glucose were 6.1%, 12.1% and 5.5 %, respectively. The variation between biological replicates is very small, given the fact that spores originated from different Petri-dishes, thus potentially having different spore concentration. In our previous study we showed good reproducibility of the cultivation of filamentous fungi and microalga in individual wells in the Duetz-MTPS ('Scalability of oleaginous filamentous fungi and microalga cultivations from microtiter plate system to controlled stirred-tank bioreactors', submitted manuscript and Kosa *et al.*, 2017 [22]). Similarly, other studies have shown that microtiter plate cultivation can offer very good, (sometimes better) reproducibility for filamentous fungi, bacteria [39-41] and yeast [42] than SF based cultivation. Nevertheless, wall growth was also an issue in the current study, especially with fungi with dispersed mycelium or fluffy pellet morphology (mainly *Mucor*, *Rhizopus* and *Mortierella* spp.). Wall grown biomass weight can exceed the weight of the submerged biomass weight ('Scalability of oleaginous filamentous fungi and microalga cultivations from microtiter plate system to controlled stirred-tank bioreactors', submitted manuscript and Kosa et al. 2017 [22]). In the current study the wall-grown biomass was not collected, therefore the reported biomass concentration should be considered as the submerged biomass concentration or a 'minimum' value. In some cases the reported biomass values are therefore severely underestimated, affecting also other reported fermentation parameters (total lipid (g/L), yield values etc.). In order to solve wall growth of filamentous organisms in MTPS, addition of glass beads or carboxypolymethylene to the medium, and mutation to pellet morphology have been succesfully applied [40, 41, 43, 44].

Reproducibility of total lipid measurement (wt%) was estimated by performing the extraction-transesterification - GC-FID procedure three times on a *Mucor flavus* CCM 8086 and *Absidia glauca* CCM 451 biomass samples (i.e. three technical replicates). The coefficient of variation for the total lipid content

was very low for both *Mucor flavus* CCM 8086 and *Absidia glauca* CCM 451 samples (0.9% and 5.3%, respectively) indicating the reliability of the procedure.

We have confirmed the potential of several already well-known species for high value PUFA (*Mucor* spp., *Cunninghamella echinulata*, *Rhizopus stolonifer, M. alpina*) and biodiesel (*Umbelopsis* spp., *Cunninghamella blakesleeana* etc.) production [5, 13, 14, 18, 45, 46]. Since Duetz-MTPS offers much higher throughput (enabling to run sufficient amount of replicates), requires lower space and medium cost, therefore our method is the preferred one for screening purpose. In addition, we found much higher total lipid content (27% vs. 13% on average) and high-value PUFA (e.g. in *M. elongata* VKM F-524 we found 3.0% DGLA and 1.9% EPA) content in eleven *Mortierella* strains (VKM F-525, F-1611, F-1408, F-1448, F-1495, F-1631, F-1252, F-524, F-1614, F-1402, F-1529) that were also screened by Eroshin *et al.* [13] in an agar-based medium. This can be explained by the differences in cultivation mode and medium composition, i.e. submerged cultivation in a high carbon-to-nitrogen medium allows to reach higher lipid content in the fungi.

Absidia species are rarely mentioned in literature as oleaginous fungi. According to our results, fungi from the genus *Absidia* deserve more attention as excellent lipid producers. The only report that we found was from Puttalingamma [47], who screened 11 *Absidia/Lichtheimia* strains in different carbon sources and reached high biomass and lipid yield (up to 43.6 g/L with *L. corymbifera* MTCC 1549 and 51.4% in *A. repenses* MTCC 1327). However, in the study of Puttalingamma gravimetric lipid yield is reported, which often severely overestimates the lipid content [48], and it is not as reliable method as transesterification to FAME employing an internal standard. The benefit of the transesterification to FAME is that it represent directly the biodiesel potential. Moreover in our study detailed fatty acid profile of 12 *Absidia*/*Lichtheimia* is presented in contrast to [47].

An interesting finding of our study was the unusual concomitant production of comparable amount of α-linolenic acid and γ-linolenic acid in *M. flavus* CCM 8086 (15°C cultivation) and VKM F-1003 (20°C). It is well known, that cold temperature activate the ω3 desaturase enzymes in fungi, leading to omega-3

fatty acid production [14, 15, 49-51]. It was also observed in in this study with *Mortierella* spp., where the production of EPA increased at 15 °C compared to 28°C. Nonetheless, according to our knowledge ALA production has not yet been reported in *Mucor* fungi.

In the current study, we investigated FTIR spectroscopy for the prediction of total lipid content in the biomass as a rapid analytical method for single cell oil screening. On the other hand it is known that FTIR spectroscopy can be used for the prediction of fatty acid composition as well [22]. In addition, FTIR spectroscopy is a well-established high-throughput method for the classification of microorganisms, due to its ability to provide highly reproducible spectral fingerprints [52]. The estimation of fatty acid composition by calibrating FTIR spectra to fatty acid profiles obtained by reference methods will be investigated in a follow-up article.

Conclusions

We showed in this study that the Duetz-microtiter plate system is suitable for the reproducible cultivation of a large variety of Mucoromycota fungi, while revealing details about lipid production potential. We have found several promising candidates for PUFA and biodiesel production purposes with this method. The benefit of the microtiter plate cultivation is the very high throughput (plates can be stacked in a shaker) and the possibility to automate the system. Currently in our lab, a robotic system is under development allowing biomass-liquid separation, washing of biomass, homogenization and pipetting on the HTS-FTIR silicone plates [53]. The fully automated high-throughput cultivation-analytical platform may allow even more efficient screening of microbial bioprocesses in the future. Wall-growth of fungi can hinder automation of the system, therefore it should be prevented in the future. Furthermore, we showed the potential of high-throughput FTIR spectroscopy, as a rapid analytical method for the detection of high lipid producers, before performing the detailed fatty acid analysis by gas chromatography.

Declarations

Authors' contributions

Conceived the research idea: AK, VS. Designed the experiments: GK. Methodology: GK. Performed the experiment: GK. Discussed the results: BZ, DE, GK, VS. Analyzed the data: BZ, GK. Wrote the manuscript: GK. Discussed and revised the manuscript: AK, BZ, DE, GK, JM, NKA, VS. All authors read and approved the final manuscript.

Funding

This work was supported by the Research Council of Norway - BIONÆR Grant, project numbers 234258 and 268305.

Acknowledgements

The authors would like to acknowledge Elin Merete Wetterhus for help troubleshooting the GC-FID.

Competing interests

The authors declare that they have no competing interests.

Ethics approval and consent to participate

Not applicable

References

1. Ochsenreither K, Glück C, Stressler T, Fischer L, Syldatk C: **Production strategies and applications of microbial single cell oils.** *Frontiers in microbiology* 2016, **7**.
2. Ratledge C: **Microbial production of polyunsaturated fatty acids as nutraceuticals.** *Microbial production of food ingredients, enzymes and nutraceuticals UK: Woodhead Publishing Co* 2013**:**531-558.
3. Wang X, Lin H, Gu Y: **Multiple roles of dihomo-γ-linolenic acid against proliferation diseases.** *Lipids in health and disease* 2012, **11:**25.
4. Finco AMdO, Mamani LDG, Carvalho JCd, de Melo Pereira GV, Thomaz-Soccol V, Soccol CR: **Technological trends and market perspectives for production of microbial oils rich in omega-3.** *Critical reviews in biotechnology* 2017, **37:**656-671.

5. Ratledge C: **Microbial production of gamma-linolenic acid.** *Handbook of Functional Lipids edited by C Akoh, CRC Press, Boca Raton, FL, USA* 2005**:**19.
6. Magdouli S, Yan S, Tyagi R, Surampalli R: **Heterotrophic microorganisms: a promising source for biodiesel production.** *Critical Reviews in Environmental Science and Technology* 2014, **44:**416-453.
7. Meng X, Yang J, Xu X, Zhang L, Nie Q, Xian M: **Biodiesel production from oleaginous microorganisms.** *Renewable energy* 2009, **34:**1-5.
8. Rossi M, Amaretti A, Raimondi S, Leonardi A: **Getting lipids for biodiesel production from oleaginous fungi.** In *Biodiesel-Feedstocks and Processing Technologies.* InTech; 2011.
9. Zhang J, Hu B: **Microbial biodiesel production-oil feedstocks produced from microbial cell cultivations.** In *Biodiesel-Feedstocks and Processing Technologies.* InTech; 2011.
10. Bharathiraja B, Sridharan S, Sowmya V, Yuvaraj D, Praveenkumar R: **Microbial Oil-A Plausible Alternate Resource for Food and Fuel Application.** *Bioresource Technology* 2017.
11. Kosa M, Ragauskas AJ: **Lipids from heterotrophic microbes: advances in metabolism research.** *Trends in biotechnology* 2011, **29:**53-61.
12. Weete J, Shewmaker F, Gandhi S: **γ-Linolenic acid in zygomycetous fungi: Syzygites megalocarpus.** *Journal of the American Oil Chemists' Society* 1998, **75:**1367-1372.
13. Eroshin V, Dedyukhina E, Chistyakova T, Zhelifonova V, Kurtzman C, Bothast R: **Arachidonic-acid production by species of Mortierella.** *World Journal of Microbiology and Biotechnology* 1996, **12:**91-96.
14. Botha A, Paul I, Roux C, Kock JL, Coetzee DJ, Strauss T, Maree C: **An isolation procedure for arachidonic acid producing Mortierella species.** *Antonie Van Leeuwenhoek* 1999, **75:**253-256.
15. Broughton R: **Omega 3 fatty acids: identification of novel fungal and chromistal sources.** Royal Holloway, University of London2012.
16. Buráňová L, Řezanka T, Jandera A: **Screening for strains of the genusMortierella, showing elevated production of highly unsaturated fatty acids.** *Folia microbiologica* 1990, **35:**578-582.
17. Chatzifragkou A, Makri A, Belka A, Bellou S, Mavrou M, Mastoridou M, Mystrioti P, Onjaro G, Aggelis G, Papanikolaou S: **Biotechnological conversions of biodiesel derived waste glycerol by yeast and fungal species.** *Energy* 2011, **36:**1097-1108.
18. Grantina-Ievina L, Berzina A, Nikolajeva V, Mekss P, Muiznieks I: **Production of fatty acids by Mortierella and Umbelopsis species isolated from temperate climate soils.** *Environ Exp Biol* 2014, **12:**15-27.
19. Bills G, Platas G, Fillola A, Jimenez M, Collado J, Vicente F, Martin J, Gonzalez A, Bur-Zimmermann J, Tormo J: **Enhancement of antibiotic and secondary metabolite detection from filamentous fungi by growth on nutritional arrays.** *Journal of applied microbiology* 2008, **104:**1644-1658.
20. Lübbehüsen TL, Nielsen J, McIntyre M: **Morphology and physiology of the dimorphic fungus Mucor circinelloides (syn. M. racemosus) during anaerobic growth.** *Mycological research* 2003, **107:**223-230.
21. Kosa G, Shapaval V, Kohler A, Zimmermann B: **FTIR spectroscopy as a unified method for simultaneous analysis of intra-and extracellular metabolites in high-throughput screening of microbial bioprocesses.** *Microbial cell factories* 2017, **16:**195.
22. Kosa G, Kohler A, Tafintseva V, Zimmermann B, Forfang K, Afseth NK, Tzimorotas D, Vuoristo KS, Horn SJ, Mounier J: **Microtiter plate cultivation of oleaginous fungi and monitoring of lipogenesis by high-throughput FTIR spectroscopy.** *Microbial cell factories* 2017, **16:**101.
23. Shapaval V, Afseth NK, Vogt G, Kohler A: **Fourier transform infrared spectroscopy for the prediction of fatty acid profiles in Mucor fungi grown in media with different carbon sources.** *Microbial cell factories* 2014, **13:**86.

24. Kavadia A, Komaitis M, Chevalot I, Blanchard F, Marc I, Aggelis G: **Lipid and γ-linolenic acid accumulation in strains of Zygomycetes growing on glucose.** *Journal of the American Oil Chemists' Society* 2001, **78:**341-346.
25. Zimmermann B, Kohler A: **Optimizing Savitzky–Golay parameters for improving spectral resolution and quantification in infrared spectroscopy.** *Applied spectroscopy* 2013, **67:**892-902.
26. Suutari M: **Effect of growth temperature on lipid fatty acids of four fungi (Aspergillus niger, Neurospora crassa, Penicillium chrysogenum, andTrichoderma reesei).** *Archives of microbiology* 1995, **164:**212-216.
27. Stansell GR, Gray VM, Sym SD: **Microalgal fatty acid composition: implications for biodiesel quality.** *Journal of Applied Phycology* 2012, **24:**791-801.
28. Islam MA, Magnusson M, Brown RJ, Ayoko GA, Nabi MN, Heimann K: **Microalgal species selection for biodiesel production based on fuel properties derived from fatty acid profiles.** *Energies* 2013, **6:**5676-5702.
29. Ramírez-Verduzco LF, Rodríguez-Rodríguez JE, del Rayo Jaramillo-Jacob A: **Predicting cetane number, kinematic viscosity, density and higher heating value of biodiesel from its fatty acid methyl ester composition.** *Fuel* 2012, **91:**102-111.
30. Orlowski M: **Mucor dimorphism.** *Microbiological reviews* 1991, **55:**234-258.
31. Bajhaiya AK, Dean AP, Driver T, Trivedi DK, Rattray NJ, Allwood JW, Goodacre R, Pittman JK: **High-throughput metabolic screening of microalgae genetic variation in response to nutrient limitation.** *Metabolomics* 2016, **12:**9.
32. Dean AP, Sigee DC, Estrada B, Pittman JK: **Using FTIR spectroscopy for rapid determination of lipid accumulation in response to nitrogen limitation in freshwater microalgae.** *Bioresource technology* 2010, **101:**4499-4507.
33. Laurens LM, Wolfrum EJ: **Feasibility of spectroscopic characterization of algal lipids: chemometric correlation of NIR and FTIR spectra with exogenous lipids in algal biomass.** *BioEnergy Research* 2011, **4:**22-35.
34. Mayers JJ, Flynn KJ, Shields RJ: **Rapid determination of bulk microalgal biochemical composition by Fourier-Transform Infrared spectroscopy.** *Bioresource technology* 2013, **148:**215-220.
35. Meng Y, Yao C, Xue S, Yang H: **Application of Fourier transform infrared (FT-IR) spectroscopy in determination of microalgal compositions.** *Bioresource technology* 2014, **151:**347-354.
36. Miglio R, Palmery S, Salvalaggio M, Carnelli L, Capuano F, Borrelli R: **Microalgae triacylglycerols content by FT-IR spectroscopy.** *Journal of applied phycology* 2013, **25:**1621-1631.
37. Pistorius A, DeGrip WJ, Egorova-Zachernyuk TA: **Monitoring of biomass composition from microbiological sources by means of FT-IR spectroscopy.** *Biotechnology and bioengineering* 2009, **103:**123-129.
38. Posch AE, Herwig C, Spadiut O: **Science-based bioprocess design for filamentous fungi.** *Trends in biotechnology* 2013, **31:**37-44.
39. Linde T, Hansen N, Lübeck M, Lübeck PS: **Fermentation in 24-well plates is an efficient screening platform for filamentous fungi.** *Letters in applied microbiology* 2014, **59:**224-230.
40. Siebenberg S, Bapat PM, Lantz AE, Gust B, Heide L: **Reducing the variability of antibiotic production in Streptomyces by cultivation in 24-square deepwell plates.** *Journal of bioscience and bioengineering* 2010, **109:**230-234.
41. Sohoni SV, Bapat PM, Lantz AE: **Robust, small-scale cultivation platform for Streptomyces coelicolor.** *Microbial cell factories* 2012, **11:**9.
42. Kohler A, Böcker U, Shapaval V, Forsmark A, Andersson M, Warringer J, Martens H, Omholt SW, Blomberg A: **High-throughput biochemical fingerprinting of Saccharomyces cerevisiae by Fourier transform infrared spectroscopy.** *PloS one* 2015, **10:**e0118052.

43. Knudsen PB: **Development of scalable high throughput fermentation approaches for physiological characterisation of yeast and filamentous fungi.** Technical University of Denmark2015.
44. Verdoes JC, Punt PJ, Burlingame R, Bartels J, Dijk Rv, Slump E, Meens M, Joosten R, Emalfarb M: **A dedicated vector for efficient library construction and high throughput screening in the hyphal fungus Chrysosporium lucknowense.** *Industrial Biotechnology* 2007, **3:**48-57.
45. Fakas S, Papanikolaou S, Batsos A, Galiotou-Panayotou M, Mallouchos A, Aggelis G: **Evaluating renewable carbon sources as substrates for single cell oil production by Cunninghamella echinulata and Mortierella isabellina.** *Biomass and Bioenergy* 2009, **33:**573-580.
46. Jang H-D, Lin Y-Y, Yang S-S: **Effect of culture media and conditions on polyunsaturated fatty acids production by Mortierella alpina.** *Bioresource technology* 2005, **96:**1633-1644.
47. .V P: **Lipid profile from Absidia spp.** *International Journal of Advanced Research* 2015, **3:**616-620.
48. McNichol J, MacDougall KM, Melanson JE, McGinn PJ: **Suitability of soxhlet extraction to quantify microalgal fatty acids as determined by comparison with in situ transesterification.** *Lipids* 2012, **47:**195-207.
49. Huang X, Chen H, Hao G, Du K, Hao D, Song Y, Gu Z, Zhang H, Chen W, Chen YQ: **Enhance eicosapentaenoic acid production in oleaginous fungus Mortierella alpina by overexpressing ω3 fatty acid desaturase.**
50. Okuda T, Ando A, Negoro H, Kikukawa H, Sakamoto T, Sakuradani E, Shimizu S, Ogawa J: **Omega-3 eicosatetraenoic acid production by molecular breeding of the mutant strain S14 derived from Mortierella alpina 1S-4.** *Journal of bioscience and bioengineering* 2015, **120:**299-304.
51. Okuda T, Ando A, Negoro H, Muratsubaki T, Kikukawa H, Sakamoto T, Sakuradani E, Shimizu S, Ogawa J: **Eicosapentaenoic acid (EPA) production by an oleaginous fungus Mortierella alpina expressing heterologous the Δ17-desaturase gene under ordinary temperature.** *European journal of lipid science and technology* 2015, **117:**1919-1927.
52. Lecellier A, Gaydou V, Mounier J, Hermet A, Castrec L, Barbier G, Ablain W, Manfait M, Toubas D, Sockalingum G: **Implementation of an FTIR spectral library of 486 filamentous fungi strains for rapid identification of molds.** *Food microbiology* 2015, **45:**126-134.
53. Li J, Shapaval V, Kohler A, Talintyre R, Schmitt J, Stone R, Gallant AJ, Zeze DA: **A Modular Liquid Sample Handling Robot for High-Throughput Fourier Transform Infrared Spectroscopy.** In *Advances in Reconfigurable Mechanisms and Robots II.* Springer; 2016: 769-778.
54. [http://www.mycobank.org/]
55. Ami D, Posteri R, Mereghetti P, Porro D, Doglia SM, Branduardi P: **Fourier transform infrared spectroscopy as a method to study lipid accumulation in oleaginous yeasts.** *Biotechnology for biofuels* 2014, **7:**12.
56. Beekes M, Lasch P, Naumann D: **Analytical applications of Fourier transform-infrared (FT-IR) spectroscopy in microbiology and prion research.** *Veterinary microbiology* 2007, **123:**305-319.
57. Carosio F, Alongi J, Malucelli G: **Layer by layer ammonium polyphosphate-based coatings for flame retardancy of polyester–cotton blends.** *Carbohydrate Polymers* 2012, **88:**1460-1469.
58. Guillén MD, Cabo N: **Relationships between the composition of edible oils and lard and the ratio of the absorbance of specific bands of their Fourier transform infrared spectra. Role of some bands of the fingerprint region.** *Journal of Agricultural and Food Chemistry* 1998, **46:**1788-1793.
59. Lü F, Shao L-M, Zhang H, Fu W-D, Feng S-J, Zhan L-T, Chen Y-M, He P-J: **Application of Advanced Techniques for the Assessment of Bio-stability of Biowaste-derived Residues: A Minireview.** *Bioresource Technology* 2017.
60. Szeghalmi A, Kaminskyj S, Gough KM: **A synchrotron FTIR microspectroscopy investigation of fungal hyphae grown under optimal and stressed conditions.** *Analytical and bioanalytical chemistry* 2007, **387:**1779-1789.

606 **List of figures**

607 **Fig. 1** Phylogenetic tree of Mucoromycota fungi used in the study (according to Westerdijk Fungal
608 Biodiversity Institute [54])

609 **Fig. 2 a-b)** Variety of Mucoromycota fungi morphologies grown under lipid accumulation conditions in
610 Duetz-MTPS (small-big pellets, dispersed, wall-growth), **c)** *Mucor mucedo* UBOCC-A-101353**, d)** *Mucor*
611 *hiemalis* UBOCC-A-101359

612 **Fig. 3** Different microscopic morphologies of oleaginous mycelium of Mucoromycota fungi. **a)** *Mucor*
613 *racemosus* FRR 3336, **b)** *Mucor circinelloides* CCM 8328 (single cell form), **c)** *Mucor hiemalis* UBOCC-
614 A-101359, **d)** *Rhizopus oryzae* CCM 8075, **e)** *Umbelopsis isabellina* UBOCC-A-101350, **f)** *Umbelopsis*
615 *ramanniana* CCM F-622, **g)** *Umbelopsis vinacea* UBOCC-A-101347, **h)** *Umbelopsis vinacea* CCM F-539,
616 **i)** *Absidia coerulea* CCM 8230, **j)** *Cunninghamella blakesleeana* VKM F-993, **k)** *Mortierella zonata*
617 UBOCC-A-101348, **l)** *Mortierella hyalina* VKM F-1854

618 **Fig. 4** Box-and-whisker plots of biomass concentration (g/L CDW) **(a)**, glucose consumption (g(L) **(b)**,
619 lipid content of biomass (wt%) **(c)**, lipid concentration (g/L medium) **(d)**, biomass- **(e)** and lipid yield on
620 glucose (g/g) **(f)**, unsaturation indeces(-) for the tested Mucoromycota genera.

621 **Fig. 5 a)** Scores plot of GC fatty acid data. Numbers in the scores plot refer to strains in Table 1, while
622 letters refer to biological replicates (3 biological replicates:a, b, c or 5 biological replicates: a, b, c, d, e for
623 *M. circinelloides* strains) **b)** Loading plot of GC fatty acid data. Fatty acid data was autoscaled before PCA

624 **Fig. 6 a)** Fatty acid profile (%), **b)** total lipid content (wt%) and biomass concentration (g/L) of *Amylomyces*
625 *rouxii* and *Mucor* fungi

626 **Fig. 7 a)** Fatty acid composition (%), **b)** total lipid content (wt%) and biomass concentration (g/L) of
627 *Rhizopus* **(1)**, *Umbelopsis* **(2)**, *Absidia/Lichtheimia* **(3)**, *Cunninghamella* **(4)** fungi

628

Fig. 8 a) Fatty acid composition (%), **b)** total lipid content (wt%) and biomass concentration (g/L) of *Mortierella* fungi

Fig. 9 (EMSC corrected) FTIR spectra of Mucoromycota fungi with low (*Rhizopus microsporus* VKM-1091, 13.0 wt%), intermediate (*Mortierella humilis* VKM F-1528, 27.2 wt%) and high total lipid content (*Absidia glauca* CCM 451, 45.9 wt%)

Fig. 10 a) Scores and **b)** loadings (PC1-2) plots of FTIR data (EMSC corrected). The explained variances for the first five PCs are 78%, 9%, 5%, 3%, and 2%. Numbers in the scores plot refers to strains in Table 1, while letters refer to biological replicates (3 biological replicates:a, b, c or 5 biological replicates: a, b, c, d, e for *M. circinelloides* strains). Peak assignments can be found in Table 5

Table 1 List of Mucoromycota fungi used in the screening. Unless stated otherwise, standard cultivation conditions were used: 28 °C, 90 g/l glucose, 5 days, Duetz-MTPS. Non-standard cultivation conditions: I: 20 °C, II: 15 °C, III: 15 °C, 7 days, IV: 50 g/L glucose, V: 15 °C, 50 g/L glucose, 9 days, shake flask

No.	Strains	No.	Strains
1	*Mucor circinelloides* VI 04473	51	*Rhizopus stolonifer* VKM F-399
2	*Mucor circinelloides* CCM 8328	52	*Rhizopus stolonifer* VKM F-400
3	*Mucor circinelloides* FRR 4846	53	*Umbelopsis isabellina* UBOCC-A-101350
4	*Mucor circinelloides* FRR 5020	54	*Umbelopsis isabellina* UBOCC-A-101351
5	*Mucor circinelloides* FRR 5021	55	*Umbelopsis isabellina* VKM F-525
6	*Mucor circinelloides* UBOCC-A-102010	56	*Umbelopsis ramanniana* CCM F-622
7	*Mucor circinelloides* UBOCC-A-105017	57	*Umbelopsis ramanniana* VKM F-502
8 (II)	*Mucor flavus* CCM 8086	58	*Umbelopsis vinacea* CCM 8333
9 (I)	*Mucor flavus* VKM F-1003	59 (I)	*Umbelopsis vinacea* CCM F-513
10 (I)	*Mucor flavus* VKM F-1097	60	*Umbelopsis vinacea* CCM F-539
11	*Mucor flavus* VKM F-1110	61	*Umbelopsis vinacea* UBOCC-A-101347
12	*Mucor fragilis* CCM F-236	62	*Absidia coerulea* CCM 8230
13	*Mucor fragilis* UBOCC-A-109196	63	*Absidia coerulea* VKM F-627
14	*Mucor fragilis* UBOCC-A-113030	64	*Absidia coerulea* VKM F-833
15	*Mucor hiemalis* FRR 5101	65	*Absidia cylindrospora* CCM F-52T
16	*Mucor hiemalis* UBOCC-A-101359	66	*Absidia cylindrospora* VKM F-1632
17	*Mucor hiemalis* UBOCC-A-101360	67	*Absidia cylindrospora* VKM F-2428
18	*Mucor hiemalis* UBOCC-A-109197	68	*Absidia glauca* CCM 450
19	*Mucor hiemalis* UBOCC-A-111119	69	*Absidia glauca* CCM 451
20	*Mucor hiemalis* UBOCC-A-112185	70	*Absidia glauca* CCM F-444
21	*Mucor lanceolatus* UBOCC-A-101355	71	*Absidia glauca* UBOCC-A-101330
22	*Mucor lanceolatus* UBOCC-A-109193	72	*Lichtheimia corymbifera* CCM 8077
23	*Mucor lanceolatus* UBOCC-A-110148	73	*Lichtheimia corymbifera* VKM F-507
24	*Mucor mucedo* UBOCC-A-101353	74	*Lichtheimia corymbifera* VKM F-513
25	*Mucor mucedo* UBOCC-A-101361	75	*Cunninghamella blakesleeana* CCM F-705
26	*Mucor mucedo* UBOCC-A-101362	76	*Cunninghamella blakesleeana* VKM F-993
27	*Mucor plumbeus* CCM F-443	77	*Cunninghamella echinulata* VKM F-439
28	*Mucor plumbeus* FRR 2412	78	*Cunninghamella echinulata* VKM F-470
29	*Mucor plumbeus* FRR 4804	79	*Cunninghamella echinulata* VKM F-531
30	*Mucor plumbeus* UBOCC-A-109204	80	*Mortierella alpina* ATCC 32222
31	*Mucor plumbeus* UBOCC-A-109208	81	*Mortierella alpina* UBOCC-A-112046
32	*Mucor plumbeus* UBOCC-A-109210	82	*Mortierella alpina* UBOCC-A-112047
33	*Mucor plumbeus* UBOCC-A-111125	83 (IV)	*Mortierella elongata* VKM F-1614
34	*Mucor plumbeus* UBOCC-A-111128	84	*Mortierella elongata* VKM F-524
35	*Mucor plumbeus* UBOCC-A-111132	85 (III)	*Mortierella gamsii* VKM F-1402
36	*Mucor racemosus* CCM 8190	86 (V)	*Mortierella gamsii* VKM F-1529
37	*Mucor racemosus* FRR 3336	87 (III)	*Mortierella gamsii* VKM F-1641
38	*Mucor racemosus* FRR 3337	88 (IV)	*Mortierella gemmifera* VKM F-1252
39	*Mucor racemosus* UBOCC-A-102007	89 (III)	*Mortierella gemmifera* VKM F-1631
40	*Mucor racemosus* UBOCC-A-109211	90	*Mortierella gemmifera* VKM F-1651
41 (II)	*Mucor racemosus* UBOCC-A-111127	91 (V)	*Mortierella globulifera* VKM F-1408
42	*Mucor racemosus* UBOCC-A-111130	92 (V)	*Mortierella globulifera* VKM F-1448
43	*Amylomyces rouxii* CCM F-220	93	*Mortierella globulifera* VKM F-1495
44	*Rhizopus microsporus* CCM F-718	94 (III)	*Mortierella humilis* VKM F-1494
45	*Rhizopus microsporus* CCM F-792	95	*Mortierella humilis* VKM F-1528
46	*Rhizopus microsporus* VKM F-1091	96 (III)	*Mortierella humilis* VKM F-1611
47	*Rhizopus oryzae* CCM 8075	97	*Mortierella hyalina* UBOCC-A-101349
48	*Rhizopus oryzae* CCM 8076	98	*Mortierella hyalina* VKM F-1629
49	*Rhizopus oryzae* CCM 8116	99	*Mortierella hyalina* VKM F-1854
50	*Rhizopus stolonifer* CCM F-445	100	*Mortierella zonata* UBOCC-A-101348

Table 2 The ten best Mucoromycota strains based on biomass concentration (g/L), total lipid content of the biomass (wt%), and total lipid concentration (g/L medium)

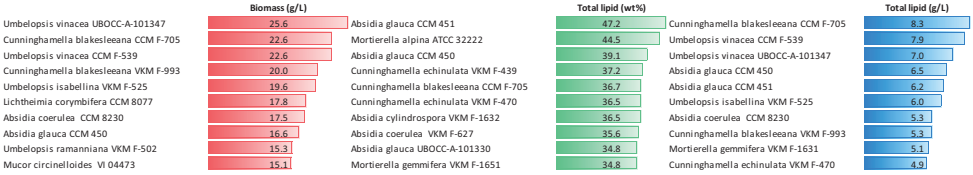

Table 3 The ten best Mucoromycota fungi identified for the production of GLA and ARA in wt% of total fatty acids and g/L in medium

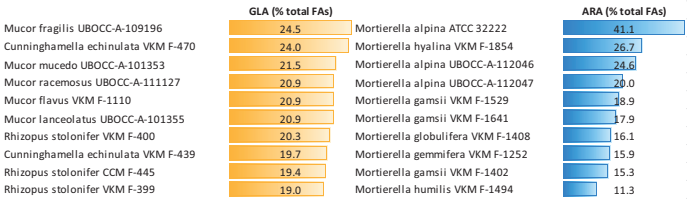

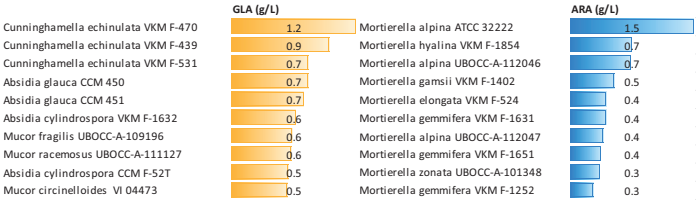

Table 4 The ten best Mucoromycota strains for biodiesel production based on their total lipid content (wt%), total lipid concentration (g/L medium) and calculated cetane number (Ramírez-Verduzco *et al.* [29])

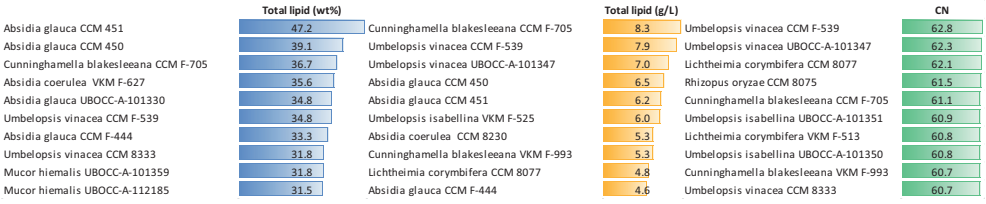

664 **Table 5** Tentative peak assignment of spectral bands in FTIR spectra of filamentous fungi. Abbreviations:

665 asym, antisymmetric; sym, symmetric; str, stretching; def, deformation [36, 55-60]

No.	Frequency (cm^{-1})	Assignment	Main biomolecules
1	~3300	N-H str (amide A), O-H str	Protein, Carbohydrate
2	3010	=C-H str	Lipid
3	2955	C-H str (asym) of $-CH_3$	Lipid
4	2925	str of $>CH_2$ of acyl chains (asym)	Lipid
5	2850	str of CH_2 of acyl chains (sym)	Lipid
6	1745	C=O str.	Lipid
7	1680-1640	Amide I band (C=O str)	Protein
8	1580-1520	Amide II (CONH bending)	Protein
9	1465	CH_2 def	Lipid
10	1410	Amide III band (C-N str)	Protein
11	1380	CH_3 bending	Lipid
12	1265	P=O str (asym) of $>PO_2$ phosphodiesters	Polyphosphate, Phospholipid
13	1155	C-O-C stretch	Lipid
14	1080	P O str (sym) of $>PO_2$	Polyphosphate, Phospholipid
15	900-1200	C-O str, C-C str., C-O-H def. C-O-C def.	Carbohydrate
16	875	P-O-P stretching	Polyphosphate, Phospholipid
17	725	CH_2 def	Lipid

666

667

668

669

670

671

672

673

674

675

676

Table 6 Prediction of total lipid content in fungal biomass from differently preprocessed FTIR spectra for all the strains together and for the six genera separately (*Amylomyces* and *Lichtheimia* were treated together with *Mucor* and *Absidia*, respectively)

R^2 between GC total lipid and FTIR data	Peak height [a] 1745 cm^{-1},	Peak height [b] 1745 cm^{-1}	Peak height ratio[b] 1745/1655 cm^{-1}	PLSR [c] (factors/RMSECV)
All (100)	0.41	**0.48**	0.14	0.72 (3/4.20)
***Mucor*/*Amylomyces* (43)**	0.36	0.44	**0.52**	0.80 (6/2.72)
***Rhizopus* (9)**	0.31	**0.54**	0.50	0.73 (2/1.80)
***Umbelopsis* (9)**	0.04	**0.06**	0.00	0.43 (8/2.60)
***Absidia/Lichtheimia* (13)**	**0.45**	0.20	0.11	0.62 (9/3.75)
***Cunninghamella* (5)**	**0.14**	0.00	0.00	0.77 (5/2.27)
***Mortierella* (21)**	0.45	**0.67**	0.05	0.78 (10/3.45)

a EMSC correction with linear and quadratic component were used in the full spectral range (4000-500 cm^{-1})

b second derivative spectra were obtained by the Savitzky–Golay (S-G) algorithm using windows size (ws) 9 and a second degree polynomial in the full spectral range (4000-500 cm^{-1}) followed by EMSC.

c Spectra were prepocessed with (S-G) algorithm (ws 15, 2nd degree polynomial) followed by EMSC and cross-validation with leave-one-biological replicate-out method. The maximum amount of PLSR components was 10. RMSECV: Root Mean Square Error of Cross Validation

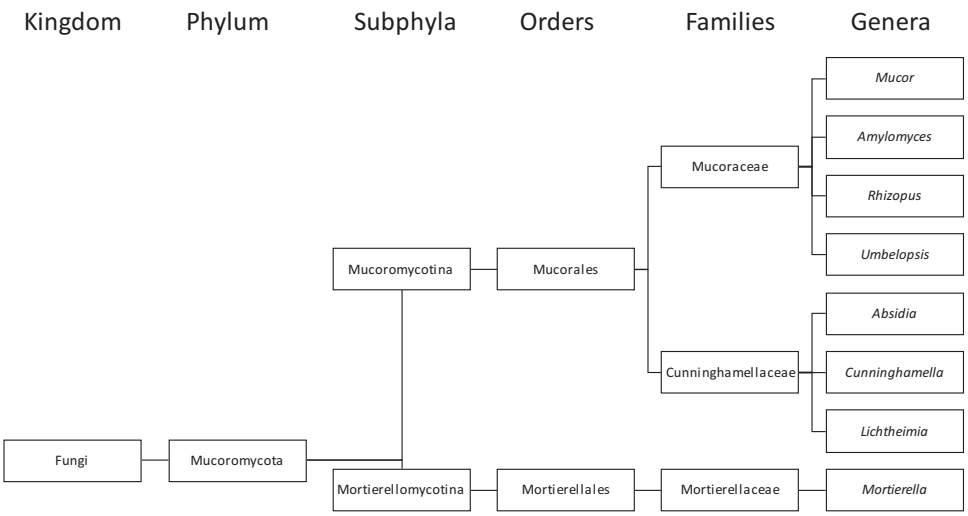

691

692 **Fig. 1** Phylogenetic tree of Mucoromycota fungi used in the study (according to Westerdijk Fungal
693 Biodiversity Institute [54])

694

695

696

697

698

699

700

701

702

703

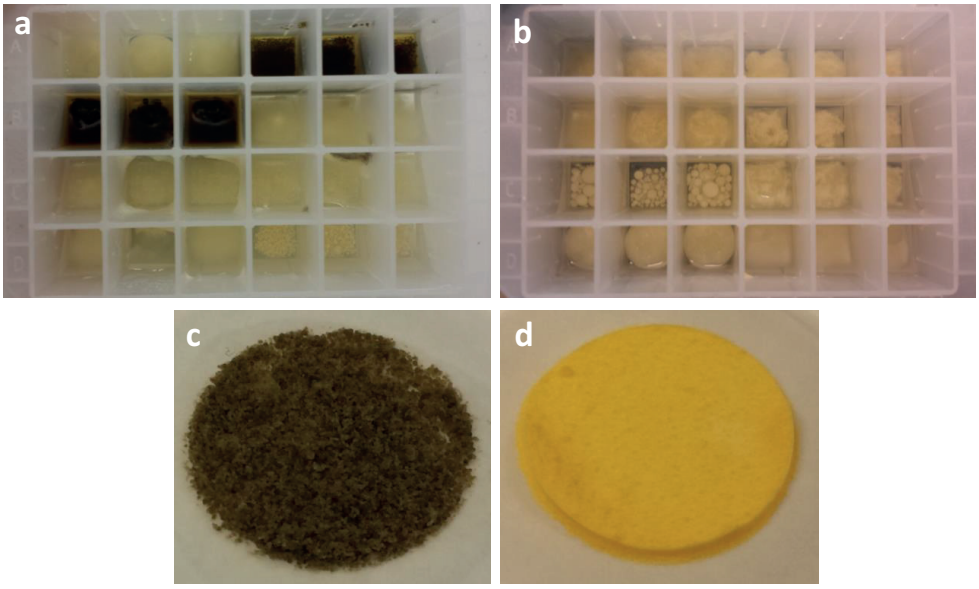

704

705 **Fig. 2 a-b)** Variety of Mucoromycota fungi morphologies grown under lipid accumulation conditions in

706 Duetz-MTPS (small-big pellets, dispersed, wall-growth), **c)** *Mucor mucedo* UBOCC-A-101353**, d)** *Mucor*

707 *hiemalis* UBOCC-A-101359

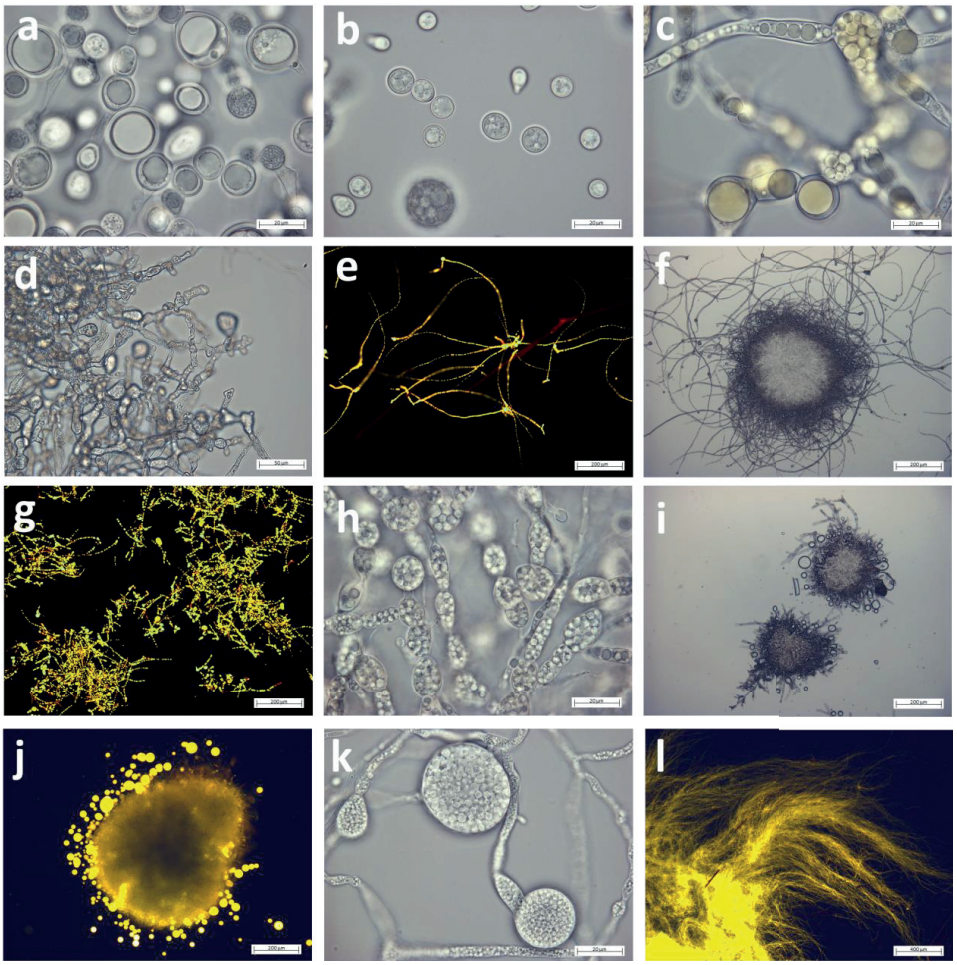

Fig. 3 Different microscopic morphologies of oleaginous mycelium of Mucoromycota fungi. **a)** *Mucor racemosus* FRR 3336, **b)** *Mucor circinelloides* CCM 8328 (single cell form), **c)** *Mucor hiemalis* UBOCC-A-101359, **d)** *Rhizopus oryzae* CCM 8075, **e)** *Umbelopsis isabellina* UBOCC-A-101350, **f)** *Umbelopsis ramanniana* CCM F-622, **g)** *Umbelopsis vinacea* UBOCC-A-101347, **h)** *Umbelopsis vinacea* CCM F-539, **i)** *Absidia coerulea* CCM 8230, **j)** *Cunninghamella blakesleeana* VKM F-993, **k)** *Mortierella zonata* UBOCC-A-101348, **l)** *Mortierella hyalina* VKM F-1854

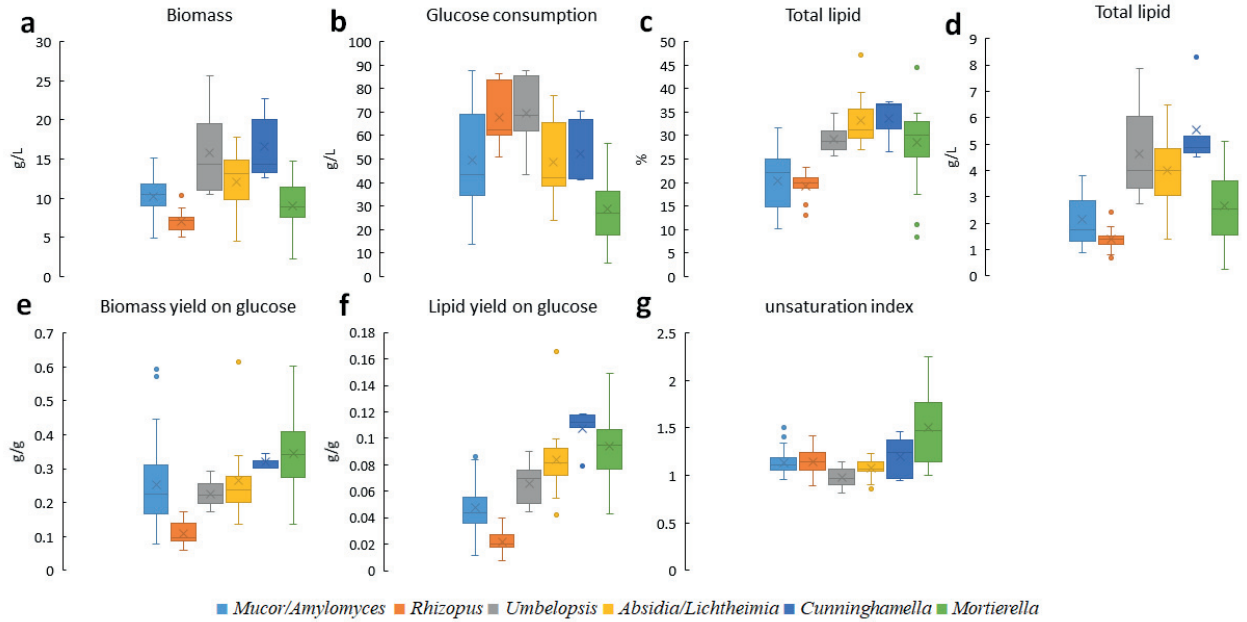

Fig. 4 Box-and-whisker plots of **a)** biomass concentration (g/L CDW), **b)** glucose consumption (g/L), **c)** lipid content of biomass (wt%), **d)** lipid concentration (g/L medium), **e)** biomass- and **f)** lipid yield on glucose (g/g), **g)** unsaturation index for the tested Mucoromycota genera

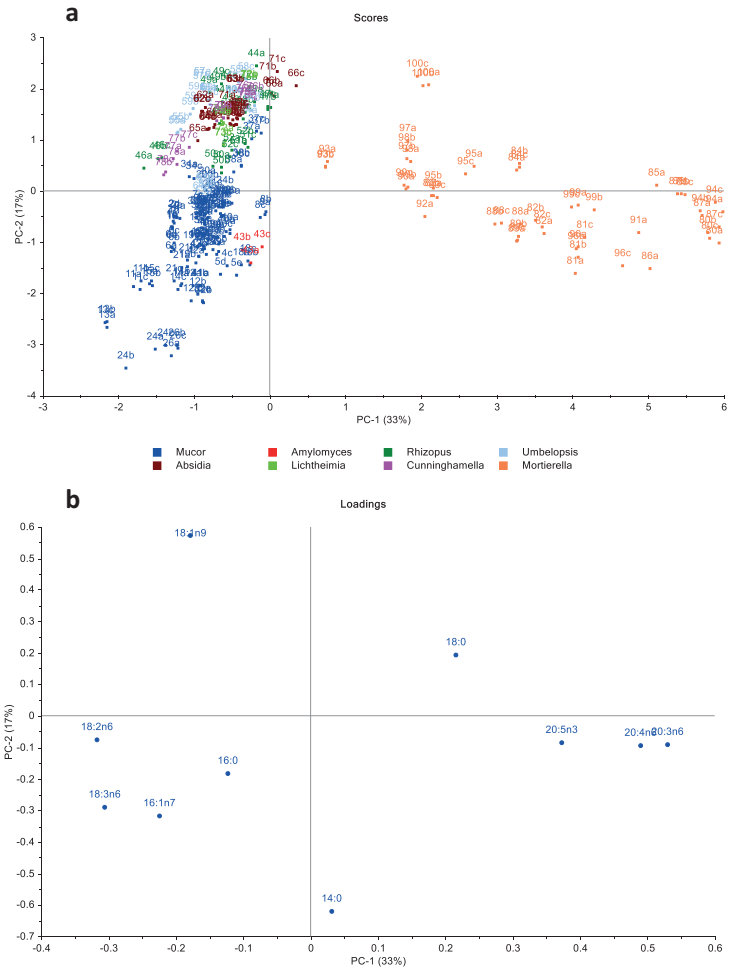

716

717 **Fig. 5 a)** Scores plot of GC fatty acid data. Numbers in the scores plot refer to strains in Table 1, while
718 letters refer to biological replicates (3 biological replicates:a, b, c or 5 biological replicates: a, b, c, d, e for
719 *M. circinelloides* strains) **b)** Loading plot of GC fatty acid data. Fatty acid data was autoscaled before PCA

720

721

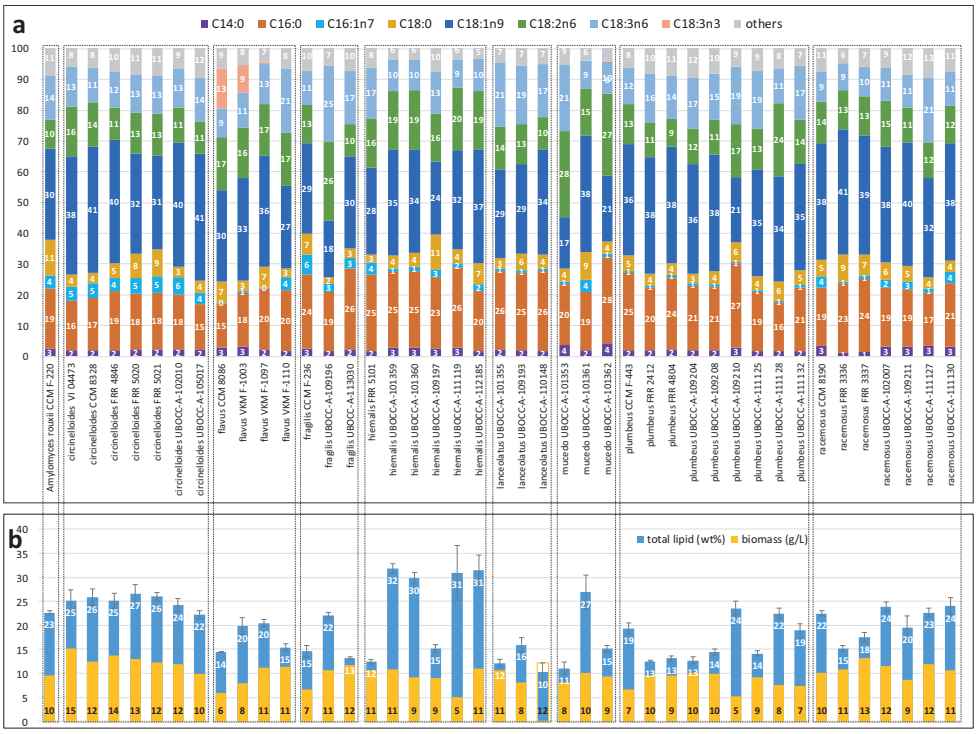

722

723 **Fig. 6 a)** Fatty acid profile (%), **b)** total lipid content (wt%) and biomass concentration (g/L) of *Amylomyces*

724 *rouxii* and *Mucor* fungi

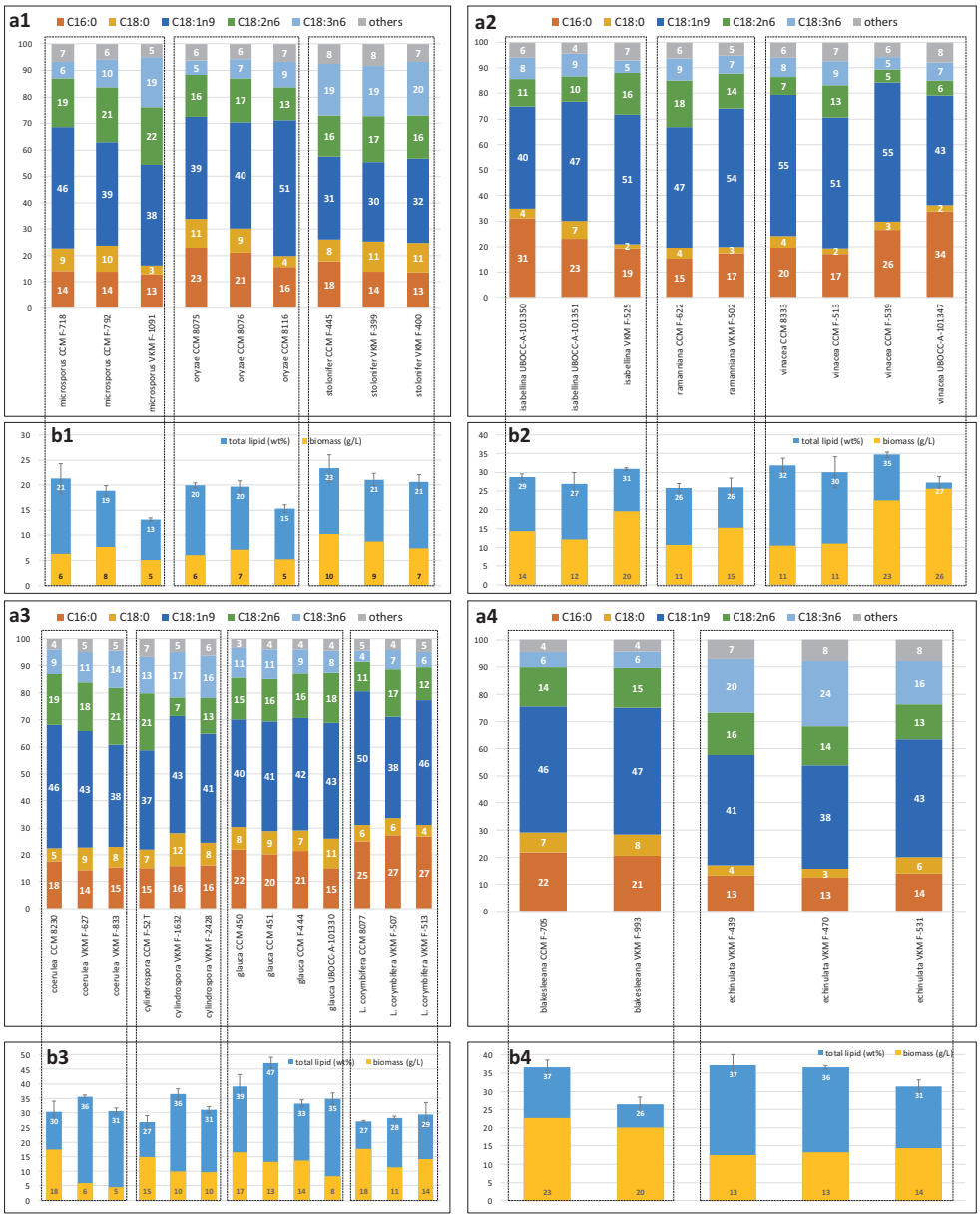

725

726 **Fig. 7. a)** Fatty acid composition (%), **b)** total lipid content (wt%) and biomass concentration (g/L) of

727 *Rhizopus* **(1)**, *Umbelopsis* **(2)**, *Absidia/Lichtheimia* **(3)**, *Cunninghamella* **(4)** fungi

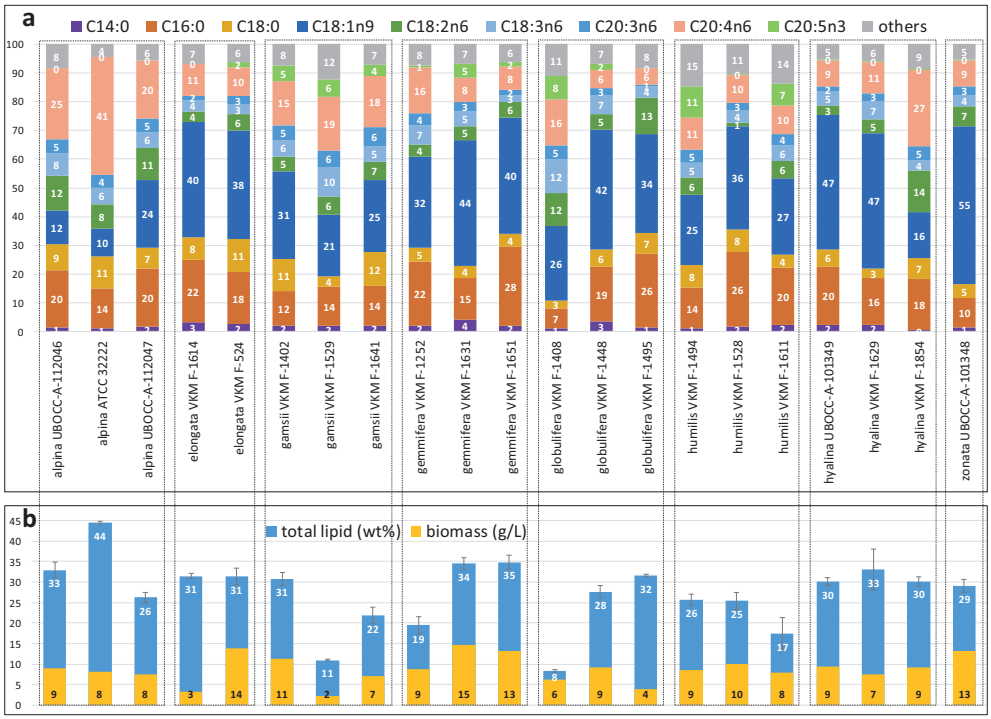

728

729 **Fig. 8 a)** Fatty acid composition (%), **b)** total lipid content (wt%) and biomass concentration (g/L) of

730 *Mortierella* fungi

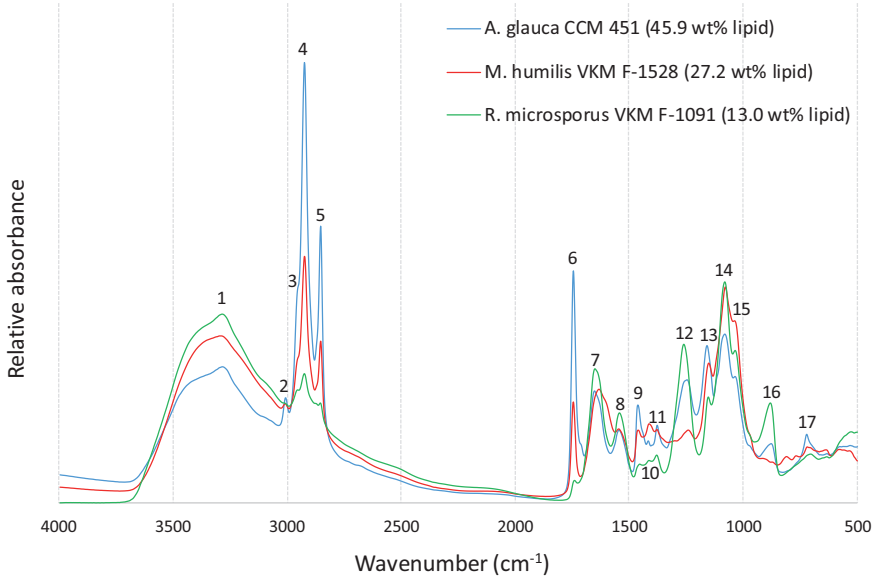

731

732 **Fig. 9** (EMSC corrected) FTIR spectra of Mucoromycota fungi with low (*Rhizopus microsporus* VKM-

733 1091, 13.0 wt%), intermediate (*Mortierella humilis* VKM F-1528, 27.2 wt%) and high total lipid content

734 (*Absidia glauca* CCM 451, 45.9 wt%)

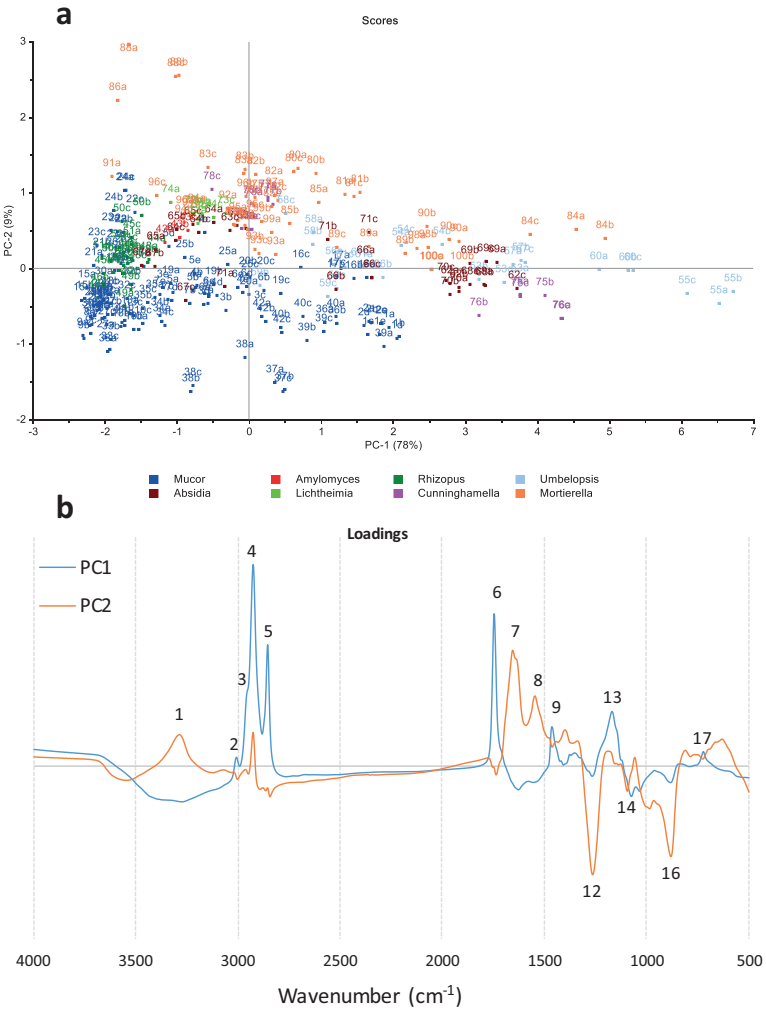

735

736 **Fig. 10 a)** Scores and **b)** loadings (PC1-2) plots of FTIR data (EMSC corrected). The explained variances
737 for the first five PCs are 78%, 9%, 5%, 3%, and 2%. Numbers in the scores plot refers to strains in Table
738 1, while letters refer to biological replicates (3 biological replicates:a, b, c or 5 biological replicates: a, b, c,
739 d, e for *M. circinelloides* strains). Peak assignments can be found in Table 5

Errata Sheet

Page number	Paragraph	Change from	Change to
ix	Presentations 2017	BioTech 2017 and 7th Czech-Swiss Symposium, 13-17th April 2017, Prague, Czech Republic	BioTech 2017 and 7th Czech-Swiss Symposium, 13-17th June 2017, Prague, Czech Republic
3	Figure 1.1	Figure 1.1 Time course of batch fermentation in microbial production of lipids	Figure 1.1 Time course of batch fermentation in microbial production of lipids (data is derived from **Paper III** in this thesis)
5	The biochemistry of lipid accumulation in oleaginous microorganisms	'hydrophilic'	'hydrophobic'
50	**Paper I**	Table 3.1	Units needs to be added. C16:0, C18:0, C18:1n9, C18:2n6, C18:3n6, SAT, MUFA, PUFA (wt% of total fatty acids); total lipid (wt% of biomass)
5 in **Paper IV**	Fungal strains	Abbreviation for 'All-Russian Collection of Microorganisms (Moscow, Russia)' is missing	All-Russian Collection of Microorganisms (VKM; Moscow, Russia)
12 in **Paper IV**	Production of high-value PUFA in Mucoromycota fungi	Four more strains produced more than 20% GLA of the oil, but only M. racemosus UBOCC-A-111127 was oleaginous (23% total lipid)	Two additional strains, *M. flavus* VKM F-1110 and *M. racemosus* UBOCC-111127 strains also produced more than 20% GLA, but only the latter one was oleaginous (23% total lipid content)
12 in **Paper IV**	Production of high-value PUFA in Mucoromycota fungi	'Interestingly, the expression of Δ6-desaturase enzyme…'	'Interestingly, the expression of Δ15-desaturase enzyme…'
32 in **Paper IV**	Fig 4.	Version without outlier points shown	Version with outlier points shown

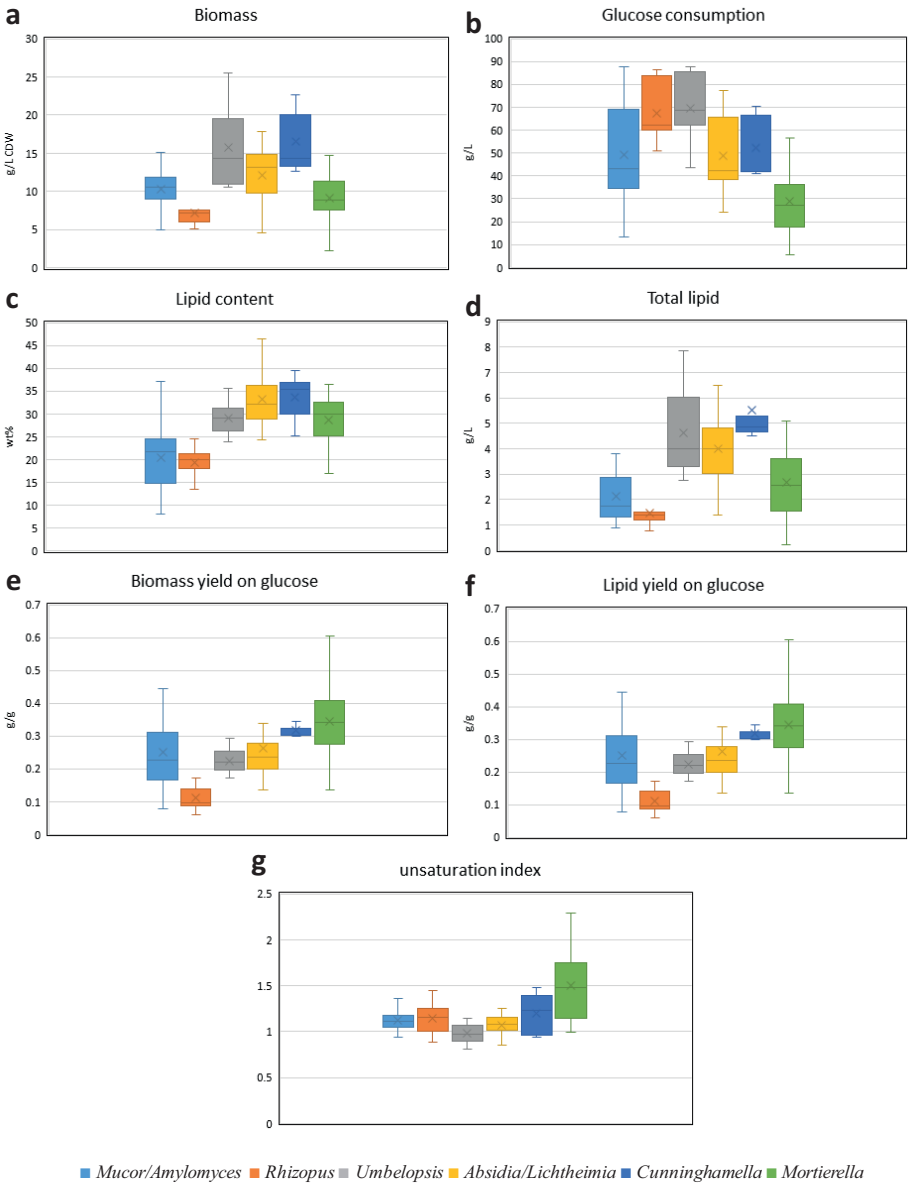

Paper IV Fig. 4 (original version, without outliers shown) Box-and-whisker plots of **a)** biomass concentration (g/L CDW), **b)** glucose consumption (g/L), **c)** lipid content of biomass (wt%), **d)** lipid concentration (g/L medium), **e)** biomass- and **f)** lipid yield on glucose (g/g), **g)** unsaturation index for the tested Mucoromycota genera

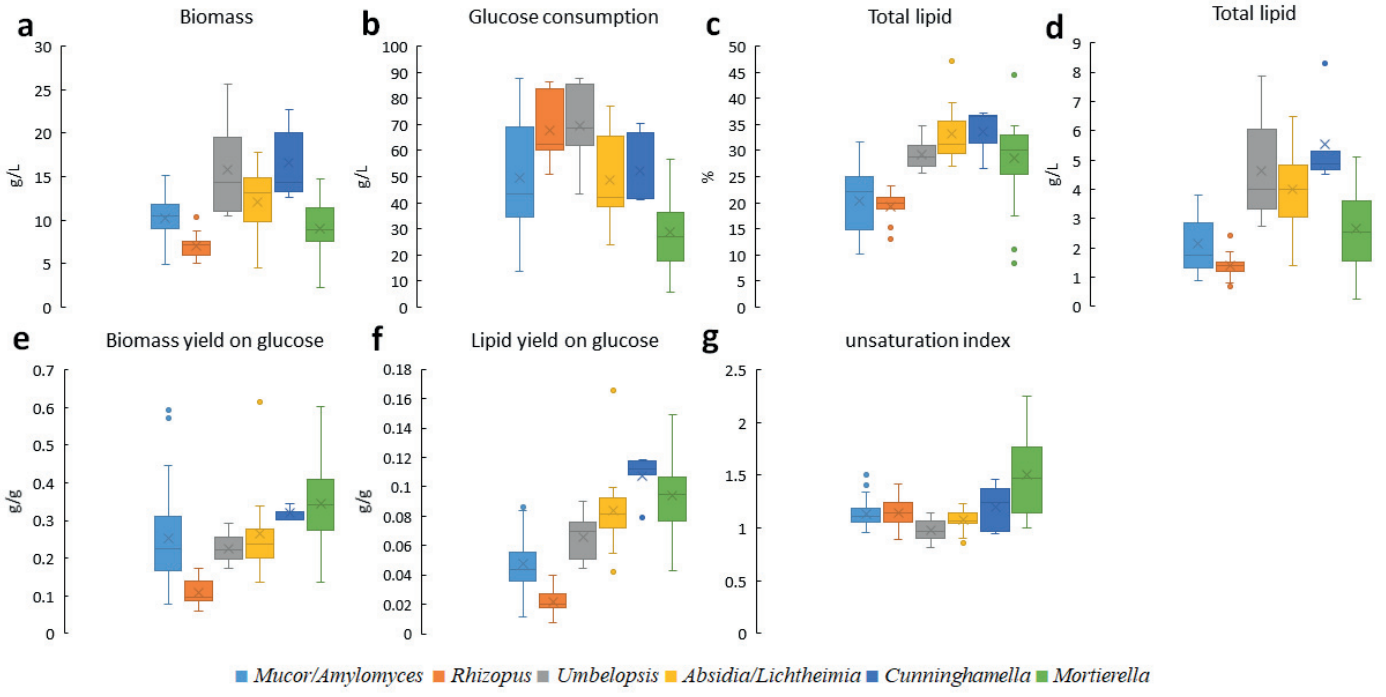

Paper IV Fig. 4 (revised version, with outliers shown) Box-and-whisker plots of **a)** biomass concentration (g/L CDW), **b)** glucose consumption (g/L), **c)** lipid content of biomass (wt%), **d)** lipid concentration (g/L medium), **e)** biomass- and **f)** lipid yield on glucose (g/g), **g)** unsaturation index for the tested Mucoromycota genera

ISBN: 978-82-575-1500-3
ISSN: 1894-6402

Norwegian University
of Life Sciences

Postboks 5003
NO-1432 Ås, Norway
+47 67 23 00 00
www.nmbu.no

97286 / ANDVORDGRAFISK.NO